Results: Strictures were characterized by a mean 2.3-fold increase in overall mural thickness and by 2.6- and 1.8-fold increases in the areas occupied by smooth muscle and collagen, respectively. Approximately half the increase in wall thickness was attributable to a mean 22-fold expansion of the muscularis mucosae (MM) from 2.2±1.6% to 16.5±10.1% of the total mural thickness and the remainder of the increase to expansions of the internal layer of muscularis propria (MP-I) and submucosa (SM). The external layer of the muscularis propria was similar in thickness and composition to controls. Microscopically, the expanded MM featured (1) architectural disarray, (2) myocyte hyperplasia and (3) pericellular collagen fibers. In contrast, the thickened MP-I featured (1) preserved muscular architecture, (2) no pericellular collagen fibers, and (3) widened intramuscular septa with increased collagen. The SM exhibited fibrosis in continuity with the intramuscular septa. Additionally, submucosal arteries and veins frequently exhibited eccentric fibromuscular hyperplasia which was polarized toward the mucosa.
Conclusions: Stricturing Crohn's ileitis is characterized by distinctive fibromuscular alterations in the individual intestinal wall layers. These alterations may reflect differential mesenchymal responses to luminal-based and transmural inflammatory stimuli. The implications for stricture pathogenesis may help guide progress toward prevention and therapy.

844 Constrictive Strictures in Crohn's Ileitis

Xiaofei Zhang, Huai-Bin Mabel Ko, Zhenjian Cai, Hongfa Zhu, Alexandros D Polydorides, Noam Harpaz. Icahn School of Medicine at Mount Sinai, New York, NY.
Background: Ileal strictures in Crohn's disease (CD) classically present as segmental regions of mural thickening, "rubber-hose" rigidity and luminal narrowing, features that correspond microscopically to fibromuscular, lymphoid or neural hypertrophy and distorted mural architecture. We describe a subset of ileal CD strictures in which these features are relatively inconspicuous and where luminal narrowing results mostly from contracture of the intestinal wall.
Design: In a prospective study, resected ileal strictures of 26 CD patients were serially cross-sectioned along with the adjoining non-strictured bowel. Evaluation of H&E-stained slides revealed a subset of strictures with reduced external circumference. For morphometric analysis we selected a specimen that contained 5 separate strictures yielding a total of 79 cross-sections (Figure). H&E and smooth muscle actin-stained slides were digitally scanned at 20X and evaluated morphometrically via Halo software (Indica Labs).
Results: The outer circumferences of the intestinal wall in strictured segments at their narrowest points measured 58.1, 72.1, 63.0, 69.4 and 66.2% of controls. The walls of the strictured segments and individual muscular layers were thickened compared to control sections (mean 6.4±2.2 vs 3.6±0.9mm, respectively, p=0.004) but there were no significant differences in the areas of the muscularis mucosae (11.3±2.0 vs. 14.3±7.2mm^2, respectively, p=0.77) or muscularis propria (75.1±10.0 vs. 65.1±1.7mm^2, respectively, p=0.69), suggesting a net conservation of muscle mass. There was no histological evidence of architectural distortion of the mural layers or substantial neural or lymphoid hyperplasia. The maximal proportions of outer circumferences covered by mesenteric fat in the strictured and non-strictured areas were 79.8±5.6% vs. 42.5±4.9%, respectively (p=0.004).

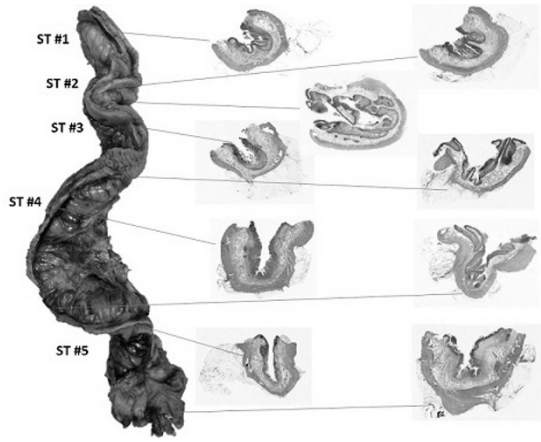

Conclusions: A subset of "constrictive" ileal strictures in CD is characterized by contracture, preserved mural architecture and near-encasement by mesenteric fat. We hypothesize that such strictures result from compression by hypertrophic mesentery, but cannot exclude a role for unidentified physiologic interactions between the mesentery and intestinal wall. These findings support recent hypotheses regarding a primary role for the mesentery in the pathogenesis of CD.

Genitourinary Pathology (including Renal tumors)

845 PTEN and p27 Loss Differ Among Morphologic Patterns of Prostate Cancer

Daniel W Abbott, Shira Ronen, Amrou Abdelkader, Anjishnu Banerjee, Yayun Xu, Oleksandr Kravtsov, Ken A Iczkowski. Medical College of Wisconsin, Milwaukee, WI.
Background: The presence and amount of cribriform prostate cancer (Cribr.) versus other Gleason 4 cancer are associated with increased recurrence (PMID:21685037) and cancer death (PMID:25189638). PTEN loss inactivates cell cycle inhibitor p27/Kip1 (PMID:11175795): both prognostically adverse events, whose correlation with morphology has not been studied in detail.
Design: Selected whole slides from 46 cancer specimens with Cribr. were immunostained (IHC) for PTEN or p27. A subset of 15 cases was studied by chromogenic in situ hybridization (ISH, RNAscope®, Advanced Cell Diag.) using probe to PTEN or CDKN1B (to detect p27). To analyze both IHC and ISH, for each Gleason (Gl.) morphologic subtype, 2-3 JPG 400x images were captured, and (after editing out stroma) the fraction of tumor epithelium positive was digitally assessed using Axiovision Release 4.7.1. For IHC, 0-0.1 was assigned 0, >0.1-0.4 was 1+, >0.4-0.7 was 2+, >0.7 was 3+. Statistical analysis for IHC used the Kolmogorov-Smirnov test (10 comparisons, significant if p<0.005). ISH used fixed effects for morphology and random effects for each patient (significant: p<0.05).
Results: IHC:

Acini	Mean PTEN IHC (0-3+)	p
Benign	2.52	ref
Gl. 3	1.88	.07
Gl. 4- Fused	1.50	.0012
Gl. 4 Cribr- peripheral cells	1.48	.01 (borderline)
Gl. 4 Cribr- central cells	0.90	<.0001
Gl. 4 Cribr- small size like benign	1.22	.0003
Gl. 5	0.80	<.0001

p27 loss compared to benign acini (mean 2.5+) was significant only for Cribr- peripheral (mean 1.5+, p=.0029); Fused was (p=.0075).
ISH: With PTEN, significant loss normalized to benign acini was observed for cribriform cancer (p<0.02), but not for fused small acini or Gleason 3/separate acini.

Acini	Mean PTEN ISH*	p
Benign	7.9	ref
Gl. 3	7.2	.582
Gl. 4- Fused	5.9	.159
Gl. 4- Cribr (peripheral and central)	5.0	.019
*100x (Pixels of epithelium with signal/Total pixels of epithelium)		

With CDKN1B, the degree of signal loss in these 3 cancer morphologies was not significant.
Conclusions: The uniquely adverse outcome of cribriform cancer is mirrored by greater molecular changes than in other morphologies.
Cribriform structures' peripheral cells have higher proliferation index according to prior work. PTEN loss predominates in central cells and p27 loss peripherally, suggesting that a biphenotypic population plays a role in generating cribriform growth. For PTEN loss as a prognostic factor, cribriform structures demand separate assessment in peripheral vs. central populations.

846 Non-Tumoral Parenchymal Changes in Renal Cell Carcinoma Cases

Behnoush Abedi-Ardekani, Lars Egevad, Roz Banks, James D McKay, Paul Brennan, Ghislaine Scelo. International Agency for Research on Cancer, Lyon, France; Karolinska Institute, Stockholm, Sweden; University of Leeds, Leeds, United Kingdom.
Background: Large, unexplained geographical variations in renal cell carcinoma (RCC) incidence rates have been observed, with the highest rates observed in the Czech Republic (CR). We explored chronic pathological changes in the non-tumoral renal cortex (CPCRC) of RCC cases from five European countries involved in the Cancer Genomic of the Kidney (CAGEKID) study, and their possible relationship with tumorigenesis.
Design: Scanned images of 626 frozen normal tissue samples distant from the tumor in conventional RCC cases from CR, Romania, Serbia, United Kingdom (UK) and Russia were read twice by one pathologist who evaluated the degrees of interstitial inflammation and fibrosis, tubular atrophy, golomerulosclerosis and arterial wall thickening. In the CAGEKID project, an independent systematic review of normal tissues was conducted by another pathologist to assess the level of inflammation and fibrosis with additional comments for any other specific features such as glomerulosclerosis. The agreement between these two independent observations was 89%. We used logistic regressions to analyze the association of these pathologies with clinico-pathological variables and country of residence.
Results: CPCRC were observed in 116 (18.5%) of samples. Higher age was the strongest predictor (OR=1.06 for 1-year increment, 95% CI: 1.04-1.08). After adjusting for age, country was significantly associated with the presence of CPCRC. Compared to Russia, CPCRC were more common in CR (OR=2.04, 1.15-3.61) and in Romania (OR=3.56, 1.80-7.07), while no significant difference was observed with the UK and Serbia. To assess potential confounders of the association with country and sampling method, we

additionally adjusted for hypertension, presence of medulla, and type of nephrectomy (partial or radical), which only marginally affected the risk estimates. Restricting the analysis to cases with total absence of medulla reduced the risk estimates to 1.44 (0.77-2.70) and 3.09 (1.33-7.15) in CR and Romania, respectively. In univariate analysis, tumor size was not associated with CPCRC.

Conclusions: The frequency of CPCRC in RCC cases varies across countries and this is unlikely to be due to sampling method or pressure effect of the tumor alone. These changes were more frequent in CR (with the highest incidence rates of RCC) and in Romania (where RCC cases were shown to be exposed to aristolochic acid). Our findings suggest that CPCRC, possibly linked to environmental exposures, may be relevant to renal tumorigenesis in these countries.

847 Granulocytic Sarcoma of the Testis in Children: Histology, Immunohistochemistry, and Molecular Studies of 5 Cases of This Very Rare Location

Kristen Adams, Xinchun Zhou, Hend Abulsayen, Siraj M El Jamal, Ali G Saad. University of Mississippi Medical Center, Jackson, MS.

Background: Granulocytic sarcoma (GS) is a tumor mass of myeloblasts or immature myeloid cells in an extramedullary site or in the bone. The tumor can involve any organs but testicular involvement is exceedingly rare particularly in children. Here we report the clinical, molecular and immunophenotype of 5 cases of testicular GS with emphasis on the frequent negativity of myeloperoxidase (MPO) and CD34, a potential cause of diagnostic pitfalls.

Design: Electronic records were searched for pediatric patients with GS of the testis. All slides were reviewed and a representative block is selected and immunostained with antibodies against CD34, CD68, MPO, CD117, CD79a, TdT, CD10, CD4, CD20, CD3 and lysozyme. In addition, FISH analysis for *MLL* rearrangement is performed in all cases. Demographic data and clinical findings were retrieved from the patients' medical records.

Results: The search yielded 5 cases (average age: 12.6 years; range: 7-14.5 years). Three patients presented with testicular enlargement and 2 patients presented with testicular pain. In all patients, testicular ultrasound (US) showed largely similar findings including testicular enlargement with an ill-defined hypoechoic mass. The masses ranged in size from 0.9 to 2.5 cm (average: 1.8 cm). *MLL* rearrangement was identified in all 5 cases. In addition, immunohistochemistry showed the tumor cells to be positive for lysozyme, CD68, and CD4 confirming a monocytic lineage. The tumor cells were negative for CD34 and MPO. They were also negative for CD117, CD79a, CD3, CD20, CD10, and TdT. Clinical follow-up, available in only 3 cases, showed that all 3 patients received chemotherapy and are still alive at least 19 months after diagnosis.

Conclusions: Herein, we describe five cases of testicular GS in pediatrics patients. We report that all cases show *MLL* rearrangement which may explain the monocytic differentiation in all of them. Moreover, CD34 and MPO, two of the most common markers used for cases of acute myeloid leukemia and granulocytic sarcoma, are negative in all 5 cases. This brings the importance of using a broader antibody panel when cases of pediatrics GS are suspected, especially in the testis.

848 SWI/SNF Complex Alterations Are Uncommon in Fumarate Hydratase-Deficient Renal Cell Carcinoma: Immunohistochemical Analysis of 27 Tumors

Abbas Agaimy, Mahul B Amin, Anthony J Gill, Daniel Berney, Cristina Magi-Galluzzi, Mathilde Sibony, Steven C Smith, Saul Suster, Kiril Trpkov, Ondřej Hes, Arndt Hartmann. University Hospital of Erlangen, Erlangen, Germany.

Background: Fumarate hydratase-deficient renal cell carcinoma (FH-RCC) is a rare, aggressive renal cell neoplasm, originally defined in the setting of hereditary leiomyomatosis and renal cell carcinoma (HLRCC) syndrome. Recently, the term "FH-deficient RCC" has been proposed for cases with equivocal or undocumented clinical and/or genetic features of HLRCC syndrome. The Switch/Sucrose non-fermentable (SWI/SNF) complex is a multi-subunit protein complex with tumor suppressor properties involved in chromatin remodelling and regulation of gene expression. SWI/SNF loss is observed in a subset of dedifferentiated RCC of different types. FH-deficient RCC share some general features with SWI/SNF-deficient malignancies, including anaplastic nuclear features, foci of dedifferentiation, and a highly aggressive clinical course.

Design: We analysed 27 FH-deficient RCCs from 26 patients (all 16 cases with conclusive genetic data had a confirmed FH gene mutation) using 6 commercially available SWI/SNF antibodies (SMARCB1/INI1, SMARCA2, SMARCA4, SMARCC1, SMARCC2 and ARID1A) on conventional slides.

Results: Complete loss of SMARCB1 and ARID1A was observed in 1 of 26 (3.8%) and 1 of 27 (3.7%) evaluable cases (total 7.5%), respectively. Both tumors showed prominent papillary growth, but no undifferentiated or solid foci. Another case with confirmed FH gene mutation showed partial loss of ARID1A in 40% of tumor cells, imparting a hybrid pattern (FH mutation results on the SMARCB1-deficient case are pending). Expression of SMARCA2 (21/21), SMARCA4 (27/27), SMARCC1 (25/25) and SMARCC2 (27/27) was intact in all cases with evaluable results.

Conclusions: A small subset of FH-deficient RCC shows loss of SWI/SNF complex components, likely occurring as secondary genetic events. However, this uncommon feature should not be mistaken for SWI/SNF-deficient dedifferentiated RCC of other common types. Our results point to the relevance of including IHC evaluation of both FH and SWI/SNF pathways in aggressive and poorly differentiated RCC with features suggestive of deficiency of either marker sets. The prognostic implications of combined FH- and SWI/SNF-deficiency (double deficient tumors) as well as the genetic backgrounds remain to be further studies.

849 Programmed Death-1 (PD-1) Receptor/PD-1 Ligand (PD-L1) Expression in Fumarate Hydratase-Deficient Renal Cell Carcinoma

Reza Alaghehbandan, Jan Stehlik, Kiril Trpkov, Cristina Magi-Galluzzi, Maria Pane Foix, Daniel Berney, Mathilde Sibony, Saul Suster, Abbas Agaimy, Delia Perez Montiel, Kristyna Pivovarcikova, Kvetoslava Michalova, Ondrej Daum, Ondrej Ondic, Pavla Rotterova, Michal Michal, Ondrej Hes. University of British Columbia, Vancouver, Canada; Charles University, University Hospital, Plzen, Czech Republic; University of Calgary, Calgary, Canada; Robert J. Tomsich Pathology Institute, Cleveland Clinic, Cleveland, OH; Bellvitge University Hospital, Barcelona, Spain; Bart´s Cancer Center, London, United Kingdom; Hospital Cochin, Paris, France; Medical Colledge Wisconsin, Milwaukee, WI; University of Erlangen, Erlangen, Germany; Institute Nacional de Cancerologia, Mexico City, Mexico.

Background: Fumarate hydratase-deficient renal cell carcinoma (FHD-RCC) is a rare, aggressive tumor affecting younger patients, whichalso occurs in HLRCC syndrome. This is the first study to assess the PD-1 receptor and PD-1 ligand in FHD-RCC.

Design: FFPE samples from 13 FHD-RCC,confirmed for *FH* mutation,, were evaluated by immunohistochemistry (IHC) for PD-1/PD-L1 reactivity in tumor cells and tumor infiltrating lymphocytes (TILs). Moderate/strong (2/3+) staining in >5% tumour cells was 'positive', 1-5% positive cells (any intensity) was 'weak positive', and no staining was 'negative'. PD1/PD-L1 expression in tissue blocks was alsoevaluated by qPCR.

Results: Mean age was 50.8 years (range 24-65 y);8 males and 5 females. Mean tumor size was 9.6 cm (range 0.9-18). PD1 was positive in tumor cells in 1/13, weak positive in 1/13, and negative in 11/13 cases, respectively. PD-L1 was positive in tumor cells in 2/13 cases, weak positive in 8/13, and negative in 3/13 cases, respectively. TILs were foundin peri and intratumoral fashion in 10/13 cases. In TILs, PD1 was positive in 1/13, weak positive in 3/13, and negative in 9/13 cases. In TILs, PD-L1 was positive in 1/13, weak positive in 5/13, and negative in 7/13 cases, respectively. qPCR confirmed the 1 IHC positive PD1 sample, and 2/3 weak positive samples (no mRNA detected in the third). In 9 IHC negative PD1 samples, qPCR confirmed lackof PD1 expression in 6, while 3 showed weak PD1 mRNA. Of 11 IHC weak positive samples overall, PDL1 mRNA was found in 8; 2 PDL-1 negative samples were confirmed by qPCR. No specific morphology was found in PD1/PDL1 positive cases, and no association between PD1/PDL1 positivity was found in tumor cells and TILs.

Conclusions: Majority of FHD-RCCs did not express PD1/PD-L1 by IHC neither in the tumor cells nor in the TILs, which was confirmed by molecular analysis. Targeted-therapies may be beneficial in rare positive PD1/PD-L1 FHD-RCC cases, provided the expression is confirmed by IHC and molecular testing.

850 Comparison of Genomic Alterations in Urothelial Carcinoma (UC) with and without *TERT* Promoter Mutation Using a Next-Generation Sequencing (NGS) Assay

Hikmat Al-Ahmadie, Isharwal Sumit, François Audenet, Eugene J Pietzak, Eugene K Cha, Anuradha Gopalan, Ying-Bei Chen, Joseph S Sirintrapun, Samson W Fine, Satish K Tickoo, Victor E Reuter, Jonathan E Rosenberg, Bernard H Bochner, Dean F Bajorin, Ahmet Zehir, Barry S Taylor, Michael F Berger, Gopa Iyer, David Solit. Memorial Sloan Kettering Cancer Center, New York, NY.

Background: Telomerase reverse transcriptase (*TERT*) is the most frequently altered gene in UC, detected across all grades and stages of disease. We sought to characterize *TERT* alterations within a prospective cohort of UC treated at our institute and compare the frequency of genomic alterations in *TERT* promoter mutant vs wild-type UC specimens.

Design: Patients diagnosed with bladder urothelial tumors were enrolled onto an institutional review board approved prospective sequencing protocol. Tumor and matched germline DNA were analyzed for somatic point mutations, truncations, copy number alterations, and insertions/deletions using the MSK-IMPACT NGS assay that detects alterations in all exons and select introns of 410 oncogenes and tumor suppressor genes as well as the entire *TERT* promoter region.

Results: 329 UC were sequenced of which 236 (71.7%) harbored *TERT* mutations, the majority being promoter region hotspots (chr5: 1295228 G>A [81%] and chr5:1295250 G>A [16%]). Patients with *TERT* promoter mutations were significantly older than those without (69.01 ± 10.70 years vs. 65.44 ± 11.78 years, p=0.0317). UC with *TERT* promoter mutations had significantly higher mutation count [median 10 (range: 2-76) vs median 5 (range: 0-119)] as well as copy number alterations [median 0.11 (range: 0-0.68) vs median 0.047 (range: 0-0.65)]. In non-invasive papillary carcinoma, *TERT* promoter mutations were identified in 14 of 23 low grade (61%) and in 26 of 30 high grade (87%) tumors. Between UC with and without *TERT* promoter mutations, there was a significant difference in mutation frequencies in many genes that are relevant in bladder cancer including *ARID1A*(33% vs 11%), *PIK3CA*(28% vs 13%), *FGFR3*(32% vs 16%), *CREBBP*(19% vs 4%), *CDKN1A*(17% vs 2%), *ERBB2*(26% vs 9%), *ERCC2*(15% vs 3%), *TSC1*(11% vs 0%), *PTPRT* (12% vs 2%), *KMT2C*(17% vs 9%), *RB1*(19% vs 9%), *SPEN* (10% vs 2%), *NF1* (10% vs 3%), *ANKRD11* (6% vs 0%), *IKZF1* (6% vs 0%), *CDK12* (11% vs 2%), and *ATRX* (3% vs 9%) (all with $p \leq 0.05$).

Conclusions: *TERT* is the most frequently altered gene in bladder cancer with the majority of *TERT* alterations comprised of two hotspot mutations. UC with *TERT* promoter mutations tend to occur in older patients and are associated with overall higher mutation count and copy number alterations. A number of genes are differentially mutated in UC with and without *TERT* promoter mutations and may suggest a link between *TERT* promoter mutations and distinct mutations profiles in UC.

851 Cyclin D1 Immunoexpression in Urinary Bladder Carcinoma Is Associated with Stage, Grade and Survival

Basim J Al-Maghrabi, Mohamad N Khabaz, Taoufik Nedjadi, Jaudah A Al-Maghrabi. King Fahd Medical Research Centre, King Abdulaziz University, Jeddah, Saudi Arabia; Faculty of Medicine, King Abdulaziz University, Jeddah, Saudi Arabia; Rabigh Faculty of Medicine, King Abdulaziz University, Jeddah, Saudi Arabia.

Background: Cyclin D1 regulates the G0-G1 succession as well as promotes cell growth. Inconsistent information on the significance of this protein have been stated in the subject of bladder cancer This study investigates the association between cyclin D1 immunohistochemical phenotype and the clinicopathological findings in bladder cancer.

Design: 128 cases of previously diagnosed bladder cancer and 24 tissue samples of normal bladder were utilized for cyclin D1 expression detection using tissue microarrays and immunohistochemistry.

Results: High grading score of nuclear cyclin D1 immunoexpression has been found in 66 (51.6%) bladder cancer cases, while 12 (50%) control cases showed cyclin D1 immunoreactivity. Strong cyclin D1 immunohistochemical staining has been significantly linked with low grades (P=0.001), low stages (P=0.005), while low scores of cyclin D1 immunostaining were associated with muscularis propria invasion (P=0.003), lymph node invasion (P=0.024), and vascular invasion (P=0.010). Furthermore, histotype of bladder cancer slightly associated with cyclin D1 immunostaining (P=0.049), all of the squamous cell carcinoma cases showed low level of cyclin D1 immunostaining, while 55.4% of urothelial carcinoma cases revealed strong cyclin D1 immunostaining. Significant different survival distributions have been observed with cyclin D1 staining of transformed epithelium (P=0.026). High cyclin D1 staining of transformed epithelial cells is positively associated with poor survival.

Conclusions: Our results confirm the great values of cyclin D1 in the prognosis of bladder cancer. These preliminary findings recommend that cyclin D1 may be a valuable tissue biomarker for presaging grade, stage, and poor prognosis in bladder cancer.

852 Primary Renal Soft Tissue Neoplasms in Nephrectomy Specimens Evaluated at a Single Institution

Fatimah I Alruwaii, Muhammad Idrees, Shaoxiong Chen. Indiana University School of Medicine, Indianapolis, IN.

Background: Primary renal soft tissue neoplasms are rare but diverse. Several different neoplasms of mesenchymal derivation can arise as primary renal masses; however, occasional incidental tumors are identified in nephrectomies performed for end stage renal disease. The rarity of these tumors poses diagnostic challenges for the general pathologists, unfamiliar with many of these entities. Herein, we document their frequencies with demographic information in nephrectomy specimens.

Design: we retrospectively searched our database for nephrectomy specimens from year 2000 to 2016. Total 5128 cases were identified and reports were reviewed. Clinical data was obtained from clinical notes.

Results: 218 total and partial nephrectomies performed for neoplastic or non-neoplastic kidney disease contained mesenchymal neoplasms. 197 (90%) neoplasms were benign and the remaining neoplasms were malignant. The mean age of presentation for benign and malignant neoplasms was 54 and 44 years respectively. The results are shown in the table.

Table: Renal soft tissue neoplasms

Diagnosis	Mean ages (years)	Number of cases (%)
Benign	**54**	**197 (90)**
Angiomyolipoma	56	133 (61)
Medullary fibroma	58	39 (18)
Mesoblastic nephroma	9 weeks	5 (2)
IMT	49	4 (2)
Leiomyoma	55	3 (1)
Solitary fibrous tumor	53	3 (1)
Glomus tumor	37	2 (1)
Hemangioma	28	2 (1)
Lymphangioma	57	2 (1)
Schwannoma	45	2 (1)
Malignant	**44**	**21 (10)**
Synovial sarcoma	38	9 (4)
Ewing sarcoma	40	6 (3)
Leiomyosarcoma	54	2 (1)
UPS	73	2 (1)
Pleomorphic liposarcoma	68	1 (0.5)
Malignant glomus tumor	60	1 (0.5)

IMT: inflammatory myofibroblastic tumor
UPS: undifferentiated pleomorphic sarcoma

Conclusions: The incidence of soft tissue neoplasms in nephrectomy specimens is 4.3% in our institution. The majority of soft tissue neoplasms are benign with angiomyolipoma being the most common followed by incidental medullary fibroma. The most common malignant tumors are synovial and Ewing sarcomas, presenting at a relatively younger age groups under 40 years old.

853 MYC Drives Overexpression of Telomerase RNA (hTR/TERC) in Prostate Cancer

Javier A Baena Del Valle, Qizhi Zheng, David Esopi, Michael Rubenstein, Gretchen K Hubbard, Maria C Moncaliano, Andrew Hruszkewycz, Ajay Vaghasia, Srinivasan Yegnasubramanian, Sarah J Wheelan, Alan Meeker, Christopher M Heaphy, Angelo M De Marzo. The Johns Hopkins University School of Medicine, Baltimore, MD; Fundacion Santa Fe De Bogota, Bogota DC, Colombia; University of Maryland, Baltimore County, Baltimore, MD; National Cancer Institute, Bethesda, MD.

Background: Telomerase consists of at least two essential elements, an RNA component hTR or TERC that contains the template for telomere DNA addition, and a catalytic reverse transcriptase (TERT). While expression of TERT has been considered the key rate limiting component for telomerase activity, increasing evidence suggests an important role for the regulation of TERC in telomere maintenance and perhaps other functions in human cancer

Design: We developed and validated a novel branched DNA based in situ hybridization assay to comprehensively study TERC expression during disease progression in clinical samples from various stages of prostate cancer (PCa) progression. We further explored MYC regulation of TERC in PCa and examined cell proliferation and apoptosis in TERC-depleted PCa cell lines.

Results: By 3 orthogonal methods including RNAseq, qRT-PCR, and an analytically validated chromogenic RNA in situ hybridization assay, we report consistent TERC overexpression in PCa. This overexpression occurs at the precursor stage (e.g. high grade prostatic intraepithelial neoplasia), and persists throughout all stages of disease progression. Levels of TERC correlate with levels of MYC in clinical samples and we also show the following: forced reductions of MYC result in decreased TERC levels in 8 cancer cell lines (prostate, lung, breast, and colorectal); forced overexpression of MYC in PCa cell lines, and in the mouse prostate, results in increased TERC levels; human TERC promoter activity is decreased after MYC silencing; and MYC occupies the TERC locus by chromatin immunoprecipitation (ChIP). Finally, we show that knockdown of TERC by siRNA results in reduced proliferation of prostate cancer cell lines without increased apoptosis.

Conclusions: These studies indicate that TERC is consistently overexpressed in all stages of PCa, and its expression is regulated by MYC. These finding nominate TERC as a novel PCa biomarker and therapeutic target.

854 Neurovascular Structure-Adjacent Frozen-Section Examination (NeuroSAFE) of Radical Prostatectomies Improves Negative Surgical Margin Rates

Samuel J Ballentine, G Kenneth Haines, Hinaben J Panchal, Avinash K Reddy, Ash Tewari, Qiusheng Si. Icahn School of Medicine at Mount Sinai, New York, NY.

Background: Neurovascular Structure-Adjacent Frozen-section Examination (NeuroSAFE) is a recent surgical method utilizing frozen section assessment of margins as a means to improve nerve sparing prostatectomies while maintaining a sound oncologic surgical procedure. Little is known about how the histopathological characteristics of prostatic adenocarcinoma influence the surgical margin status in these cases.

Design: From 9/9/2014 to 6/17/2015, 276 radical prostatectomies (RPs) were performed using NeuroSAFE protocols at our hospital. 69 RPs performed without NeuroSAFE protocols from 10/21/2013 to 8/12/2016, were used for comparison. The original NeuroSAFE protocol involved removing the right and left posterior-lateral aspects of the prostate, serially sectioning and evaluating these perpendicular margins. We modified this technique to also include the apical margin. Resection data were analyzed for the influence of histopathological parameters such as TNM stage, Gleason grade groups, frozen section and final margin status, tumor burden (% tumor x prostate weight), and rate of extra-prostatic extension on NeuroSAFE RPs surgical margin status.

Results: Positive final surgical margins were detected in 19 of 276 (6.9%) NeuroSAFE RPs compared to 18 of 69 (26.1%) non-NeuroSAFE RPs (P = <0.001). Of NeuroSAFE RPs with positive final margins, 18 of 19 (94.7%) were due to tumor extension to margins not evaluated at frozen analysis. Of NeuroSAFE RPs, resections with positive final surgical margins had larger tumor burden (13.7g vs 5.5g; p = <0.001), and higher frequency of extraprostatic extension (EPE) (52.6% vs 20.2%; p = 0.003). These findings were also significant in non-NeuroSAFE RPs; Tumor burden (12.7g vs 5.0g; p = <0.001) and EPE (33.3% vs 9.8%; p = 0.049). NeuroSAFE RPs showed no statistically significant difference in surgical margin status when lower Gleason prognostic grade groups were compared to higher Gleason prognostic grade groups (Groups 1-2: 5% vs Groups 3-5: 11.8%; p = 0.08).

Conclusions: RPs performed by NeuroSAFE protocols had significantly lower positive final surgical margin rates than traditional RP. This technique can be adapted in standard pathology laboratories. Larger tumor burdens and EPE remain risk factors for positive final surgical margins.

855 Predicting High Risk Pathologic Features at Prostatectomy Using Multiparametric MRI

Heather S Barker, Brittaney E O'Bryan, Houda Alatassi, Alberic Rogman, Albert Seow, Jamie Messer. University of Louisville, Louisville, KY.

Background: Prostate Cancer patients with adverse pathologic features have an increased risk of biochemical recurrence and the development of metastatic disease. Multiparametric MRI (MP MRI) has shown the potential to accurately assess for high risk features based on biopsy results, however few studies have examined the concordance of MP MRI with prostatectomy specimens.

Design: Between January 2014 and July 2016 a total of 45 prostatectomies were performed by a single surgeon, with 30 having a preoperative 3T MP MRI available for evaluation. We retrospectively reviewed the preoperative assessment of high risk

pathologic features (extracapsular extension/ECE, seminal vesicle invasion/SVI, lymph node involvement/LNI and high Gleason score) compared to postoperative pathologic staging. A single Genitourinary pathologist reviewed all surgical specimens, and all of the MRIs were reviewed with consensus of dedicated MRI radiologists.

Results: From the 30 available prostatectomies with a median age of 62.5 and a median preoperative PSA of 8.5 (IQR 6.2 to 13.9); 17 patients had ECE, 5 had SVI, 5 had LNI, and 15 had high risk Gleason score (4+3, tertiary pattern 5, 4+4 or higher). The distribution of the Gleason scores were 3+3 (5), 3+4 (10), 4+3 (4), tertiary 5 (4), 4+4 or greater (7). Surgical margins were positive in 4 patients. The sensitivity, specificity, PPV and NPV of MP-MRI for ECE is 64.71 (95%CI 38.33 - 65.79), 92.31 (95% CI 63.97 - 99.81), 91.67 (95% CI 61.52 - 99.79), 66.67 (95% CI 40.89 - 86.96) respectively. For the detection of SVI on MP MRI the sensitivity, specificity, PPV, and NPV were 60 (95% CI 14.66 - 94.73), 96 (95% CI 76.95 - 99.90), 75 (95% CI 19.41 - 99.37), and 92.31 (95% CI 74.87 - 99.05). For the evaluation of LNI sensitivity was 100 (95% CI 47.82 - 100), specificity was 96 (95% CI 79.65 - 99.90), PPV was 83.33 (95% CI 35.88 - 99.58), NPV was 100 (95% CI85.75 - 100). With regards to evaluation of high risk Gleason score was sensitivity was 94.44 (95% CI 72.71 - 99.86), Specificity was 66.67 (95% CI 34.89 - 90.08), PPV was 80.95 (95% CI 58.09 - 94.55), NPV was 88.89 (95% CI 51.75 - 99.72).

Conclusions: MP MRI has a reasonable sensitivity and specificity for the preoperative detection of high risk features at prostatectomy, as well as a NPV. This could provide assistance in the selection of patients appropriate for Active Surveillance as well as in the preoperative counseling regarding multimodality treatment.

856 Clinical Significance of Tertiary Pattern 4 in Gleason 3+3=6 Adenocarcinoma of the Prostate

Nicholas Barna, Mark Ettel, Fei Chen, Peng Lee, Hongying Huang, Jonathan Melamed, Ming Zhou, Fang-Ming Deng. New York University Langone Medical Center, New York, NY.

Background: Tertiary Gleason score (GS) patterns in adenocarcinoma of the prostate at radical prostatectomy (RP) have been scrutinized in the context of the group grade (GG) system. Some recommend GS 3+3=6 with tertiary 4 (GS6t4) be reported as "GS 3+4=7 (GG2) with <5% pattern 4." Others have shown that GS6t4 is not significantly different than GS6 or represents an intermediate category between GS6 (GG1) and GS 3+4=7 (GG2) based on biochemical recurrence (BCR) after RP. Few long term studies have examined the prognostic implications of GS6t4; thus we seek to characterize its significance with long term follow-up in a large cohort of RP cases.

Design: Cases of GS6, GS6t4 and GS 3+4=7 were analyzed among patients who underwent RP from 1998–2008 at three tertiary care institutions. BCR-free survival (BFS) was evaluated by Kaplan-Meier analysis and multivariate Cox proportional hazards regression including the following factors: pT stage, surgical margin involvement, PSA and age. Pathologic characteristics were assessed for all tumors (chi-squared, *t*-test).

Results:

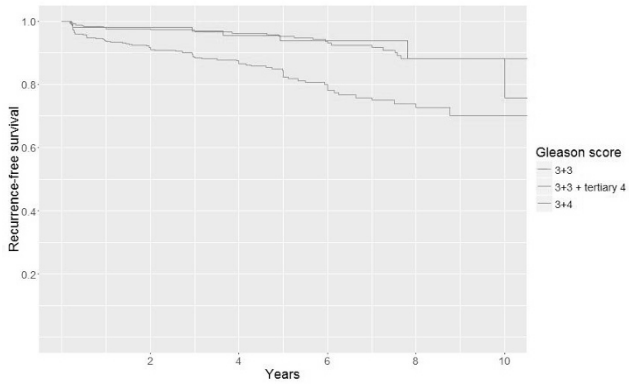

Of 866 evaluated cases, 349 (40.3%) were GS6, 100 (11.5%) were GS6t4 and 417 (48.2%) were GS 3+4=7. Median follow-up time was 5.01 years. By univariate analysis, BFS for GS6t4 was not significantly different from GS6 (p=0.833) but was significantly different from GS 3+4=7 (p=0.009). By multivariate analysis, BFS for GS6t4 was not significantly different from either GS6 (p=0.734) or GS 3+4=7 (p=0.120). Characteristics of GS6t4 prostate cancer were intermediate between those of GS6 and GS3+4=7 prostate cancer, although more similar to GS6 cancer. Compared to GS6 tumors, GS6t4 tumors were no different in PSA (p=0.373) and surgical margin positivity (p=0.162) but were more likely to have advanced pT stage (p=0.002). However, mean pre-operative PSA was increased (p<0.001) and pT stage was higher (p<0.001) in GS3+4=7 cancer compared to GS6t4 tumors with no difference in surgical margin positivity (p=0.417).

Conclusions: Gleason score 6 with tertiary pattern 4 adenocarcinoma of the prostate has behavior and characteristics more similar to GS6 as compared to GS 3+4=7. The findings suggest GS6t4 is a relatively indolent subset and may better fit group grade 1 as opposed to group grade 2.

857 Morphologic and Clinical Comparison of *BRCA*+ and *BRCA*- Prostate Carcinoma

Amanda Barrett, Lauren E Schwartz. The Hospital of the University of Pennsylvania, Philadelphia, PA.

Background: Many *BRCA* mutated (*BRCA*+) carcinomas have been identified including high grade serous carcinomas (HGSC) and prostate carcinoma (PCa). In contrast to *BRCA*+ HGSCs, which have been found to exhibit similar morphologic features, few *BRCA*+ PCa have been morphologically compared. The primary aims of this study are to describe the clinical and pathologic features associated with *BRCA*+ PCa, and to identify potential morphologic patterns that are characteristic of *BRCA*+ PCa.

Design: Twelve patients with PCa and either somatic or germline *BRCA* testing were identified via search of pathology reports and clinical records at our institution. All available histological material was reviewed and a retrospective analysis of the clinical features at the time of presentation was conducted. The patient's age, presenting PSA, disease extent at diagnosis, Gleason grade/score, and the presence of distinctive morphologic features were analyzed for each tumor.

Results: Of the 12 patients identified with PCa and *BRCA* test results, 7/12 (58%) were positive for a *BRCA* mutation (6 for *BRCA2* and 1 for *BRCA1*). The age at diagnosis was similar for both groups (*BRCA*+ average 64 (range 53-72) and *BRCA*- average 62 (range 56-72. *BRCA*+ presented more frequently with metastatic disease (71%) compared to *BRCA*- (20%), and higher PSA values (median 42.98 and 5.72 ng/mL, respectively). The Gleason score/grade groups assigned histologically were similar for both groups, with the majority of patients (86% *BRCA*+, 80% *BRCA*-) being assigned a component of Gleason pattern 5/grade group 5. Morphologic features characteristic of the *BRCA*+ tumors included: various patterns of Gleason grade 5 and 4 with little to no pattern 3 identified. Patterns of 5 included variably sized nests and cords, rather than sheets and individual cells. Necrosis was present in 1 case. *BRCA*- cases were morphologically more variable with 2 cases showing necrosis. Finally, *BRCA* mutated carcinomas were associated with more aggressive clinical course, which resulted in the death of 2 patients 1 year after diagnosis, and 1 patient 4 years after diagnosis.

Conclusions: Our results suggest that there are features of PCa that may correlate with *BRCA*+ disease including: higher grade morphology, metastasis at presentation, higher PSA at diagnosis, and aggressive clinical course. Although, our study did not identify a distinct morphologic pattern associated with *BRCA*+ prostate cancer as seen in *BRCA*+ HGSC, our sample size was small and we plan to continue our study as more patients are molecularly tested.

858 Disappearing Prostate Cancer on Template Biopsy. A Pathological and Radiological Study

Luis Beltran, Yen Zhi Tang, Francis Chinegwundoh, Daniel Berney. Barts Health, London, United Kingdom.

Background: Transperineal template biopsies (TPTB) are increasingly used in the UK to assess eligibility for Active Surveillance (AS) protocols in men with prostate cancer (PC), for diagnosis in patients with previous negative transrectal ultrasound guided biopsies (TRUS) and to correlate with multiparametric (mp) MRI imaging. The incidence and pathological and radiological findings in negative TPTB after PC diagnosis on TRUS are unknown.

Design: We identified all TPTBs performed in Barts Health between 2014-2016 and reviewed all cases with a previous positive TRUS. Cases were divided into two cohorts: 1. Negative TPTBs and matching TRUS and 2. Positive TPTBs and matching TRUS. The following variables have been compared: No of cores in TPTB, No of cores in TRUS, No of cores involved in TRUS, % cores involved in TRUS, Gleason in TRUS, total cancer length in TRUS, bilateral tumour in TRUS, prostate volume, presence of potential tumour on mpMRI and No of TPTB cores/prostate volume.

Results: There were 232 TPTBs over 2 years of which 35 had a previous positive TRUS. Of these, the TPTB was negative in 11 (31%). A negative TPTB significantly correlated with a lower TRUS cancer length (p=0.0041), lower % of TRUS cores involved (p=0.035), no visible tumour on mpMRI (p=0.0214) and lower No of TPTB cores/prostate volume (p=0.0214) using Fisher exact test.

	Negative TPTB (n=11)	Positive TPTB (n=24)
Mean core No TPTB (range)	39.36 (31-48)	45.2 (18-87)
Mean PSA (range)	8.1 (5.8-8.8)	10.01 (4.2-25)
Mean core No involved TRUS (range)	1.45 (1-2)	2.29 (1-6)
Mean core No examined TRUS (range)	13 (12-16)	13.45 (12-17)
% cores involved TRUS (range)	11% (7%-25%)	17% (7%-35%)
Mean Grade Group (range)	1.27 (1-3)	1.33 (1-3)
Mean total cancer length (mm) TRUS (range)	2.31 (0.5-6)	5.29 (1-16)
Bilateral involvement in TRUS	18%	37%
Mean prostate volume (cc) (range)	76.7 (39-143)	51.52 (31-98)
Tumour seen on mpMRI	30%	76%
Mean No cores TPTB/prostate volume (range)	0.56 (0.38-0.76)	0.92 (0.41-1.56)

Conclusions: False negative TPTBs are strongly associated with mpMRI undetectable small volume tumours and lower disease volume on multiple parameters as well as less intense sampling. Correlation with imaging and clinical is vital before TPTB as this may be avoided in selected cases.

859 PTEN Loss in Gleason Score 3+4=7 Prostate Biopsies Is Associated with Non-Organ Confined Disease at Radical Prostatectomy

Liana Benevides Guedes, Jeff Tosoian, Jessica Hicks, Ashley E Ross, Tamara L Lotan. Johns Hopkins University School of Medicine, Baltimore, MD.

Background: Men with intermediate risk prostate cancer have widely variable outcomes, with some suggesting that active surveillance or less invasive therapies (brachytherapy or focal therapy) may be appropriate for some men with Gleason Score 3+4=7 disease. Molecular markers may help further distinguish prostate cancers with aggressive behavior. Here, we tested whether loss of the PTEN tumor suppressor, an immunohistochemestry assay highly correlated with genomic deletions of the *PTEN* gene, in Gleason 3+4=7 tumor biopsies is associated with adverse pathology at prostatectomy.

Design: We queried prostate needle biopsies from 2000-2014 with a maximum Gleason score of 3+4=7 followed by prostatectomy. A total of 260 cases had PTEN status evaluable by clinical-grade immunohistochemistry. Biopsy PTEN status was correlated with pre- and post-operative clinical-pathologic parameters.

Results: PTEN loss was detected in 27% of Gleason 3+4=7 biopsies. Loss of PTEN was less common in tumors of African-American compared to European-American men (9% vs. 31%; p=0.002). Among metrics of tumor volume, cases with PTEN loss were more likely to have at least one core in the case showing >50% involvement by tumor (p=0.01). PTEN loss was more common among men with higher clinical stage and age, though differences were not statistically significant (p=0.067 and 0.10 respectively), however it was not significantly associated with pre-operative PSA level, number or proportion of cores involved by tumor or bilateral involvement of tumor on core biopsies. At prostatectomy, tumors with PTEN loss were more likely to be upgraded at RP to GS 4+3=7 and above (26% vs 14%; p=0.023) and to show non-organ confined disease (52% vs 27%; p<0.001) compared to those with PTEN intact. In logistic regression models including age, race, PSA, clinical stage and biopsy tumor involvement, PTEN loss at biopsy remained significantly associated with increased risk of non-organ confined disease (HR=2.46; 95% CI: 1.34-4.49; p=0.004). In ROC analysis for non-organ confined disease, the AUC for models including PSA and clinical stage was increased from 0.61 to 0.67 upon inclusion of PTEN status.

Conclusions: PTEN loss in Gleason score 3+4=7 biopsy is independently associated with increased risk of non-organ confined disease at prostatectomy and adds to pre-operative parameters commonly used to predict pathologic stage.

860 Validation of p53 Immunohistochemistry for Sensitive and Specific Detection of *TP53* Mutation in Prostate Cancer

Liana Benevides Guedes, Fawaz Almutairi, Michael C Haffner, Gaurav Rajoria, Zach Liu, Szczepan Klimek, Roberto Zoino, Kasra Yousefi, Angelo M De Marzo, William Isaacs, Edward M Schaeffer, Ashley E Ross, Tamara L Lotan. Johns Hopkins University School of Medicine, Baltimore, MD; Pathline Emerge Pathology Services, Ramsey, NJ; GenomeDx Biosciences, Vancouver, BC, Canada.

Background: *TP53* missense mutations occur in less than 5% of primary prostate cancers (PCa) and over 20% of castrate resistant prostate cancer (CRPC), suggesting that they are highly enriched in lethal PCa. Thus, identifying primary tumors with *TP53* mutations may help to identify PCa with lethal potential. Here, we pre-analytically, analytically and clinically validated a robust immunohistochemistry (IHC) assay to detect deleterious *TP53* missense mutations in PCa.

Design: A p53 IHC assay was developed in a CLIA-accredited laboratory using the BP53-11 monoclonal antibody on the Ventana Benchmark immunostaining system. Benign prostate was entirely negative for p53 protein expression. For analytic validation, 56 FFPE cell lines from the NCI-60 panel and 47 FFPE PCa tissues with known *TP53* mutation status were studied. Mouse xenograft tumors of DU145 and VCaP cell lines were subjected to different pre-analytic variables to evaluate the effects on immunostaining results. Clinical validation was performed in two partially overlapping cohorts of men undergoing radical prostatectomy (RP) with a median of 10 years of follow-up, including one cohort of men with intermediate/high risk PCa (n=322) and one of men with biochemical recurrence (BCR) (n=195).

Results: p53 protein over-expression was 97% sensitive for detection of deleterious *TP53* missense mutations in the NCI-60 cell line panel (29/30 missense mutations correctly identified). Lack of over-expression was 96% (25/26) specific for absence of *TP53* missense mutation. In FFPE prostate tumors, the positive predictive value (PPV) of p53 protein over-expression for underlying missense mutation was 90% (28/31), while the negative predictive value (NPV) was 94% (15/16). In a cohort of men with intermediate or high risk PCa at RP (including 30 tumors with known *TP53* mutation status as described above), the univariate hazard ratio for metastasis among cases with p53 over-expression compared to those without was 4.84 (95% CI: 2.44 -9.61). In a partially over-lapping cohort of men who underwent RP followed by BCR, the univariate hazard ratio for metastasis among cases with p53 over-expression compared to those without was 4.14 (95% CI: 2.41-7.11).

Conclusions: These studies validate a simple method to assess the presence of deleterious *TP53* missense mutations in PCa in clinical specimens and support the utility of this tissue marker as a prognosticator for aggressive disease.

861 Should Reporting of Peri-Neural Invasion and Extra-Capsular Extension Be Mandatory in Prostate Cancer BiopsieS? Correlation with Outcome in 988 Cases Treated Conservatively

Daniel Berney, Amar Ahmad, Vishnu Parameshwaran, Peter Scardino, Henrik Moller, Jack Cuzick, Luis Beltran. Memorial Sloan Kettering Cancer Center, New York, NY; Queen Mary University of London, London, United Kingdom; Kings College London, London, United Kingdom.

Background: The identification of peri-neural invasion (PNI) and extra capsular extension (ECE) in prostate cancer (PC) biopsies is time consuming and can be difficult. Although this is required information in most datasets, there is little evidence on their effect on outcome in patients treated conservatively.

Design: Cases of PC were identified from three cancer registries in the UK from men with clinically localized prostate cancer diagnosed by needle biopsy from 1990-2003. The endpoint was prostate cancer death (DOD). Clinical variables included PSA, age and clinical stage. Patients treated radically within 6 months, those with objective evidence of metastases or who had prior hormone therapy were excluded. Follow up was through cancer registries up until 2012. Deaths were divided into those from PC and those from other causes, according to WHO criteria. 988 biopsy cases (6522 biopsy cores) were centrally reviewed by two uropathologists and assigned a Gleason score and Grade Group (GG). The presence of both PNI and ECE was recorded

Results: Of 988 patients, PNI was present in 284 and ECE in 29. Both were highly associated with GG ($p=2.2x10^{-16}$ & $p=1.071x10^{-8}$) respectively and strongly associated with each other ($p=6.39x10^{-9}$). On univariate analysis PNI was highly significantly associated with DOD (HR 2.54, CI 1.77 – 3.63, $p< 0.58x\ 10^{-7}$), but ECE was not (p= 0.333). On multivariate analysis with GG, serum PSA, clinical stage and extent of disease, PNI lost significance (HR 1.38, CI 0.93 – 2.04, p<0.112). Further examination of cases which may have been entered for active surveillance in GGs 1 and 2 revealed 11/290 cases from GG1 with PNI and 43/258 from GG2. A total of 8/54 men of GG1-2 with PNI died from prostate cancer, compared with 46/494 men of GG1-2 without PNI. Although these differences were not significant, use of a Cox regression model with PSA and GG1-2 allowed construction of a highly significant prognostic index (PI) (HR=2.99 SI 2.00-4.49, $p=1.09x10^{-7}$) This PI was significantly higher in cases with PNI whether alive (p=0.003) or DOD(p=0.006)

Conclusions: The utility of routinely examining prostate biopsies for ECE and PNI is doubtful, although there may be some utility in identification of PNI in GGs 1 and 2 as it may be indicative of higher grade/stage disease. We recommend that datasets should be amended so that PNI reporting is required only in GGs 1 and 2.

862 Acquired Cystic Kidney Disease and/or Kidney Transplantation Associated Genitourinary Tumors: Report of 37 Tumors

Athanase Billis, Leandro LL Freitas, Larissa BE Costa, Marcel A Asato, Karina S Araujo, Daniele M Losada, Amanda P Herculiani, Livia LA Azevedo, Gabriel VBS Tabosa, Bruna C Zaidan, Gabriel LP Oliveira, Lucas QA Bastos, Ruana M Rocha. School of Medical Sciences, State University of Campinas (Unicamp), Campinas, Sao Paulo, Brazil.

Background: Renal transplant recipients and dialysis patients, especially those with acquired cystic kidney disease, are at increased risk of malignancies. The aim of our study was to analyze the types of malignancies in the genitourinary tract and determine the frequency of new entities included in the 2016 book of the "WHO classification of tumours of the urinary system and male genital organs".

Design: We studied the histologic type of 37 genitourinary tumors from 21 patients in dialysis and/or submitted to renal transplant.

Results: The mean age of the 21 patients was 55 years (range 40-78 years); 61% males and 39% females. From the total of 37 tumors: 34 were from native end-stage kidneys, 1 from the pelvis of the transplant kidney, and 2 from the urinary bladder. The latter 3 tumors were high-grade urothelial carcinomas: stage pT3 from the pelvis, stage pT1 with micro-papillary features in one, and stage pT2 in the other tumor from the urinary bladder. The 2 patients with urothelial carcinoma of the urinary bladder had polyomavirus infection. One of these 2 patients had concomitantly one acquired cystic disease-associated renal cell carcinoma in one of the native kidneys. The frequency of the histologic type in 34 tumors from native kidneys was: 1. Papillary carcinoma 13/34 (38.2%) (type1: 23.1%; type 2: 76.9%); 2. Papillary adenoma 9/34 (26.5%); 3. Acquired cystic disease-associated renal cell carcinoma 4/34 (11.8%); 4. Oncocytoma 3/34 (8.8%); 5. Conventional clear cell renal cell carcinoma 3/34 (8.8%); and, 6. Clear cell papillary (tubulopapillary) renal cell carcinoma 2/34 (5.34%). Papillary adenoma was multiple in 2 patients, and papillary carcinoma multiple in 4 patients. All other histologic types were single tumors.

Conclusions: The frequency of two new entities included in the 2016 book of the "WHO classification of tumours of the urinary system and male genital organs" was 11.8% and 5.9% for acquired cystic disease-associated renal cell carcinoma and clear cell papillary (tubulopapillary) renal cell carcinoma, respectively. No tumor was chromophobe renal cell carcinoma. It is noteworthy the high-grade urothelial carcinomas from the urinary bladder in two patients with polyomavirus infection supporting its oncogenic potential for the urothelium. In patients with polyomavirus infection the routine screening for malignancy should include the native kidneys as well as the transplanted kidney and the urinary bladder.

863 Prognostic Value of Gleason Grade 4 and Its Architectural Patterns at Prostate Biopsy on Predicting Biochemical Recurrence Following Radical Prostatectomy

Athanase Billis, Leandro LL Freitas, Larissa BE Costa, Ruana M Rocha, Lucas QA Bastos, Gabriel LP Oliveira, Amanda P Herculiani, Karina S Araujo, Marcel A Asato, Daniele M Losada, Livia LA Azevedo, Gabriel VBS Tabosa, Bruna C Zaidan. School of Medical Sciences, State University of Campinas (Unicamp), Campinas, Sao Paulo, Brazil.

Background: It has been shown that men with a post-2005 grade of Gleason score 3+4=7 have a better prognosis than those graded prior to 2005. Percent pattern 4 in cases with Gleason score 7 on biopsy may be an additional criterium in the selection of men for active surveillance. Furthermore, grade 4 has a heterogeneous set of architetural patterns, each of which may reflect a distinct prognostic value. We aimed a novel approach of Gleason grade 4 at prostate biopsy. We studied the number of sections with Gleason grade 4 regardless of percentage or linear extent and its architectural patterns.
Design: We analyzed the needle biopsies of 148 consecutive patients submitted to radical prostatectomy. All biopsies were extended (mean 13 sections, range 12-20 sections). Gleason grade 4 was diagnosed according to 4 patterns: "fused glands", "cribriform glands", "glomeruloid glands", and "ill-defined glands with poorly formed glandular lumina". Biochemical recurrence (BCR) following surgery was considered as PSA $\geq$ 0.2 ng/mL. Time to BCR was studied using the Kaplan-Meier product-limit analysis.
Results: From a total of 148 patients, 27/148 (18.2%) patients had Gleason grade 4 in only one core of the biopsy (Group 1) associated with no cancer in other cores (11.1% biopsies) or Gleason score 3+3=6 varying from 1 to 5 in the other cores (88,9% biopsies); 29/148 (19.6%) patients had Gleason grade 4 in $\geq$ 2 cores (Group 2) associated with no cancer in other cores (24.1%) or Gleason score 3+3=6 varying from 1 to 5 in the other cores (75.9% biopsies); and, 92/148 (62.2%) patients had only Gleason grade 3+3=6 on biopsy (Group 3) with cancer varying from 1 to 10 cores in the biopsy. In all biopsies in Group 1, Gleason grade 4 was pattern "fused glands" but in group 2 all patterns could be seen, and in most of the biopsies $\geq$ 2 patterns were present. Comparing time to BCR after surgery, there was a significant difference between Group 1 vs Group 2 (log rank, p=0.049) but no difference between Group 1 vs Group 3 (log-rank, p=0.720).
Conclusions: Our study showed that the number of cores with Gleason grade 4 on a biopsy regardless of percentage and extent has predictive value for time to BCR after surgery. An important finding was the favorable predictive value of Gleason grade 4 in only one core of a biopsy and with only pattern "fused glands". In the heterogeneous Gleason grade 4, pattern "fused glands" seems to have a less biologic potential.

864 Clinicopathologic Features of Patients without Biochemical Recurrence More Than 5 Years Following Radical Prostatectomy with Limited Tumor, pT2, and Negative Margins: Comparison of Tumors with Gleason Score 3+3=6 vs 3+4=7 in the Surgical Specimen

Athanase Billis, Maisa M Quintal, Leandro LL Freitas, Larissa BE Costa, Bruna C Zaidan, Gabriel VBS Tabosa, Livia LA Azevedo, Amanda P Herculiani, Daniele M Losada, Karina S Araujo, Marcel A Asato, Gabriel LP Oliveira, Lucas QA Bastos, Ruana M Rocha. School of Medical Sciences, State University of Campinas (Unicamp), Campinas, Sao Paulo, Brazil.

Background: It has been questioned the biologic potential of Gleason grade 4 in biopsy or surgical specimen depending on extent, percentage or pattern. We aimed to find clinicopathologic differences comparing patients with Gleason 3+3=6 vs Gleason 3+4=7 in the surgical specimen with limited tumor, pT2, negative surgical margins, and long time without biochemical recurrence (BCR).
Design: Surgical specimens were completely step sectioned. Tumor extent was evaluated by a semiquantitative point-count method. Gleason grade 4 was diagnosed according to 4 patterns: "fused glands", "cribriform glands", "glomeruloid glands", and "ill-defined glands with poorly formed glandular lumina". BCR was considered as PSA $\geq$ 0.2 ng/mL.
Results: In a cohort of 401 consecutive patients submitted to surgery, 43/401 (10.7%) patients had no BCR more than 5 years after surgery (mean 8 years, range 5-14 years), limited tumor, pT2, and negative margins. In 33/43 (76.7%) patients (Group 1) Gleason score in the specimen was 3+3=6; in 10/43 (23.3%) patients (Group 2) Gleason score was 3+4=7 with no tertiary grade. In Group 2 the predominant and more extensive Gleason grade 4 pattern was "fused glands"; in 3 patients isolated small foci of "cribriform glands" were seen only associated with mucin in 3 patients and with collagenous nodules in 1 patient. Both groups had Gleason score 3+3=6 in the needle biopsy, therefore Gleason score 3+3=6 was upgraded to 3+4=7 in 10 patients. Comparing the clinicopathologic features of the groups there was no significant difference related to: age (p=0.555), race (p=0.172), preoperative PSA (p=0.437), prostate weight (p=0.107), PSA density (p=0.893), presence of nodular hyperplasia (p=0.656), total biopsy cores (p=0.841), number of cores with cancer (p=0.656), percentage of cancer in a single core (p=0.244), and mm of cancer in a single core (p=0.679).
Conclusions: It seems that Gleason score 3+3=6 in biopsy upgraded to 3+4=7 in surgical specimen, is not an adverse finding in patients with limited tumor, pT2, and negative surgical margins comparing to patients with these same findings but Gleason 3+3=6 in both biopsy and surgical specimen. In Group 2 the predominant and more extensive Gleason grade 4 pattern was "fused glands"; "cribriform glands" were seen only in isolated small foci associated with mucin or collagenous nodules.

865 Immunohistochemical Differentiation of Plasmacytoid Urothelial Carcinoma (UC) from Secondary Involvement of the Bladder by Adenocarcinoma of the Breast or Gastrointestinal (GI) Tract

Walaa Borhan, Jonathan I Epstein. Johns Hopkins Hospital, Baltimore, MD; Taibah University, Medina, Saudi Arabia.

Background: Plasmacytoid UC is a rare variant, with infiltrating loosely cohesive individual cells with plasmacytoid cytoplasm often co-existing with cells with rhabdoid, signet-ring, and bland cells with centrally located nuclei resembling lobular carcinoma of the breast or signet ring cell adenocarcinoma from the GI tract. It also difficult to exclude metastatic lobular carcinoma of the breast as both lesions are positive for GATA3 and show a loss of Ecadherin.
Design: We performed a panel of six antibodies in 45 cases of plasmacytoid UC.

Antibody	Positve Cases(%)	Extent of Positivity
PR	6/45 (13.3%)	2 Diffuse/4 Focal
ER	0/45 (0%)	-
GCDFP-15	11/45 (24.4%)	3 Diffuse/8 Focal
Mammaglobin	0/45 (0%)	-
P-CEA	22/45 (48.8%)	7 Diffuse/15 Focal
CDX2	8/45 (17.7%)	3 Diffuse/5 Focal

37 (82.2%) were male, and 8 (17.7%) female. Positive staining was considered if there was moderate or strong staining. Weak immunoreactivity was considered negative. Secondary carcinoma involving the bladder was excluded clinically and/or histologically by the concurrence of usual in-situ or invasive UC.
Results: All cases of plasmacytoid variant of UC failed to express estrogen receptors (ER) and mammaglobin. Immunoreactivity for gross cystic disease fluid protein 15 (GCDFP-15), progesterone receptors (PR), CDX2 and P-CEA showed staining in 11(24.4%), 6(13.3%), 8(17.7%) and 22(48.8%) of cases, respectively. GCDFP-15 was positive in 4 out of 8 female cases included in the study. One of them also focally expressed PR.
Conclusions: In the bladder, where there is the differential diagnosis of plasmacytoid UC vs. metastatic breast carcinoma, positivity for ER and mammaglobin strongly supports the diagnosis of metastatic breast carcinoma. Mammaglobin and ER are positive in approximately 70% and >95% of infiltrating lobular breast carcinomas, respectively, such that negative staining for mammaglobin favors and negative staining for ER strongly supports plasmacytoid UC over metastatic lobular carcinoma. In our series, all cases of plasmacytoid UC were negative for mammaglobin and ER. In contrast, GCDFP-15 and PR expression can be expressed in both plasmacytoid UC and lobular carcinoma. CDX2 and P-CEA are not useful to exclude secondary involvement of the bladder by tumors from the GI tract; GATA3 positivity strongly favors plasmacytoid UC, although rare adenocarcinomas from the GI tract can express GATA3.

866 Lymphoepithelioma-Like Carcinoma of the Bladder: Analysis of Mismatch Repair Proteins and PD-L1 by Immunohistochemistry

Cori Breslauer, William Kim, Jonathan I Epstein, Sara E Wobker. University of North Carolina, Chapel Hill, NC; Johns Hopkins Medical Institutions, Baltimore, MD.

Background: Lymphoepithelioma-like carcinoma (LELC) of the bladder is a rare subtype of urothelial carcinoma consisting of undifferentiated epithelial cells within a dense lymphocytic infiltrate. Pure/predominant LELC appears to demonstrate better response to chemotherapy with better overall survival, but the mechanism for this finding is not yet understood. The interaction of programmed death-1 (PD-1) and programmed death-ligand 1 (PD-L1) inhibits T cell activation, and thus prevents tumor cell death. PD-L1 overexpression has been shown to independently predict worse outcomes in urothelial carcinoma, but its role in LELC - a subtype defined by its immune infiltrate - is not well understood. In the colon, medullary phenotype which mimics the morphology of LELC, is associated with microsatellite instability. We sought to evaluate the mismatch repair (MMR) protein and PD-L1 staining behavior in this rare variant of bladder carcinoma.
Design: A retrospective search of the pathology electronic medical record was performed for cases containining "bladder" and "lymphoepithelioma-like carcinoma" diagnosed between 2000 and 2016. Ten cases were identified in the initial search, 8 cases had sufficient archival tissue for analysis. Hematoxylin and eosin stained slides of each case were reviewed to confirm this diagnosis and additional unstained sections were obtained for IHC. Tissue sections were stained for the mismatch repair proteins (MSH2, MSH6, MLH1 and PMS2) as well as PD-L1 22C3. PD-L1 positivity was defined as either low (>1-49%) or high (>50%) expression in tumor cells.
Results: Of 8 cases of bladder LELC, 7 (88%) demonstrated PD-L1 positivity. Staining intensity was variable, with 4/7 demonstrating high expression and 3/7 demonstrating low expression. All 8 cases of LELC uniformly retained MMR protein expression, the only exception being isolated loss of MSH6 in a single case.
Conclusions: LELC of the bladder demonstrates reliable expression of PD-L1. Despite the finding that PD-L1 overexpression confers a poor prognosis in conventional urothelial carcinoma, the role of the dense immune infiltrate in LELC may be related to its superior response to chemotherapy. Further study will include IHC assessment of infiltrating T cells for PD-1 and RNA sequencing of these tumors.

867 Pathologic Prognostic Factors in Radical Cystectomy Post-Neodjuvant Chemotherapy

Fadi Brimo, Kiril Trpkov, Daniel Athanazio, Asli Yilmaz, Michelle Downes, Elan Hahn, Shraddha Solanki, Tamara Jamaspishvili, Wassim Kassouf, David Berman. McGill University Health Center, Montreal, QC, Canada; Calgary Laboratory Services and University of Calgary, Calgary, AB, Canada; Sunnybrook Health Sciences Center, Toronto, ON, Canada; Queen's University, Kingston, ON, Canada.

Background: Traditional pathologic parameters and additional morphologic changes may be important in prognosticating patients treated with neoadjuvant chemotherapy (NAC) and radical cystectomy (RC). Recently, the prognostic value of tumor regression grade (TRG) was also described *(AJSP 2014, 38 (3): 325-332)*.

Design: We evaluated 121 patients from a multi-institutional cohort treated with NAC for urothelial carcinoma (UC).We recorded the following data: pT and pN stage, surgical margins (SM), lymphovascular invasion (LVI), variant histology, TRG, and the presence and extent of stromal and nuclear changes. We systematically evaluated the following stromal changes: fibroblastic reaction, severe inflammation, hyalinization of bladder wall, calcifications, necrosis, hemorrhage, regressive lymph node changes, foreign body giant cells, necrosis, and foamy macrophages. The evaluated NAC-related nuclear changes included: pyknosis, intranuclear inclusions, smudgy chromatin, and vacuolated cytoplasm. The follow-up included recurrence and death of disease (DOD) as clinical end-points.

Results: Mean patient age was 65 y. The distribution of TRG1, 2 and 3 was 22%, 18%, and 60%, respectively. No residual invasive or metastatic UC (<pT1+pN0) was found in 23 cases (19%). Any therapy-related nuclear changes were found in 32% patients, but they were only prominent in 17%. Mean follow-up was 18 months. Recurrence and DOD occurred in 61(50.4%) and 40 (33%) patients, respectively.

Recurrence: On univariate analysis, >pT1(p=0.0001), >pN0 (p<0.0001), LVI (p<0.0001), and TRG3 (p=0.027) all significantly correlated with recurrence. The only variables to preserve their association in a multivariate model were >pT1 and >pN0.

Death: On univariate analysis significant association with DOD was found for >pT1(p=0.002), >pN0 (p=0.0002), positive SM (p=0.0026), LVI (p=0.0002), TRG3 (p=0.02) . On multivariate analysis, only >pN0 (p=0.003) and positive SM (p=0.01) were found significant.

Conclusions: Neither TRG nor any of the chemotherapy-related stromal or nuclear changes correlated with recurrence or survival in patients treated with NAC and RC. Pathologic stage and SM status were the two most important pathologic predictors of outcome. The continuous growth of this unique cohort through multi-institutional collaboration will help further evaluate these findings and will serve as a platform to test molecular prognosticators.

868 Comparative Study of *TERT* Promoter Mutation Status in Urothelial Carcinomas with Divergent Differentiation

Noah Brown, Madelyn Lew, Helmut Weigelin, Bryan Betz, Rohit Mehra. University of Michigan, Ann Arbor, MI.

Background: *TERT* promoter mutations resulting in increased expression of TERT are known to occur in the majority of urothelial carcinomas (UCC). The most frequent known mutations are c.-146C>T (Chr.5:1295250C>T), c.-124C>T (Chr.5:1295228C>T), c.-138_139CC>TT (Chr.5:1295242_1295243CC>TT) and c.-124_125CC>TT (Chr.5:1295228_1295229CC>TT). There is increasing use of *TERT* promoter testing for the detection of recurrent UCC in urine samples. However, this testing will only be of value for *TERT*-mutated UCC. Tumor heterogeneity could complicate the assessment of *TERT* status within the primary tumor if morphologically divergent components differ in *TERT* mutation status. To our knowledge, no previous study has compared *TERT* promoter genotypes within the divergent components.

Design: Using a clinical grade allele-specific PCR assay targeting the four mutations listed above, we evaluated formalin-fixed paraffin-embedded tissues from 14 patients with invasive high-grade UCC and 4 patients with non-invasive, high-grade UCC. The age range of the patients in this cohort was 59 to 86 years, with majority of the patients demonstrating pathologic stage pT2b to pT4 at the time of cystectomy. Among the invasive cases were 9 UCC with divergent differentiation including sarcomatoid, nested and tubular, micropapillary and glandular. For these cases, DNA was extracted from separately microdissected divergent and the associated conventional UCC components.

Results: Overall, *TERT* promoter mutations (including -124 and -146) were identified in 71.4% (10/14) invasive high-grade UCC and 50% (2/4) non-invasive high-grade UCC, similar to frequencies described in previous studies. Identical *TERT* promoter genotypes were observed within conventional and divergent components from each of the 9 cases of UCC with divergent differentiation.

Conclusions: Our preliminary findings suggest that *TERT* mutation status does not vary among morphologically distinct components of UCC within a given patient, which may suggest a clonal relationship of divergent components to associated UCC with conventional morphology.

869 Analytical and Interpretative Phases of Molecular Diagnostics of MiTF Family Translocation Renal Cell Carcinoma

Matteo Brunelli, Serena Pedron, Anna Calìò, Stefano Gobbo, Guido Martignoni. University of Verona, Verona, Italy.

Background: MiTF family translocation renal cell carcinomas (tRCCs) show a variety of morphological aspects, in part reflecting cytogenetic differences. The cut-offs for appropriate diagnostic interpretation of Xp11-TFE3 translocation RCCs and t(6;11)-TFEB tRCCs are not well established and still lack consensus. We sought to investigate both the analytical and interpretative phases of such a molecular diagnostics.

Design: 22 renal neoplasia including 17 tRCCs and 5 angiomyolipomas were recruited and arrayed. Xp11 break-apart, dual fusion ASPS-TFE3 and TFEB break-apart probes were used. Count of single orange, single green, adjacent/fused orange-green signals were tabulated. Cathepsin-k and PAX-8 were also performed.

Results: Five tRCCs and one melanotic Xp11 tRCC showed Xp11 riarrangements. Two Xp11 tRCCs showed additional fusion for ASPC-TFE3 genes (cathepsin-k positive in one case). Five t(6;11)-TFEB RCCs showed break-apart TFEB riarrangements. One case showed dual-fusion ASPS-TFE tRCCs without Xp break-apart riarrangement. Among males, a mean of 50% of nuclei showed split signals, 20% wild-fusion and 10% one orange and green signals. Among females, a mean of 50% wild-fused, 30% split signals and 20% of single orange, green signals were registered. tRCCs with dual fusion ASPS-TFE3 showed fused signals in >30% of nuclei. Normal adjacent parenchyma showed split or fused signals in up to 14% of nuclei (range 8% to 16%). TFEB break-apart signals were registered in at least 60% of nuclei among three t(6;11)-TFEB RCCs. Angiomyolipomas showed from 3 to 5% split or fused signals. Cathepsin-k was always positive except for two ASPS-TFE3 tRCCs.

Conclusions: 1) The analytical and interpretative phases of molecular diagnostics of tRCCS have a two steps recognition; 2) the analytical phase need to be corrected by findings from adjacent normal parenchyma; 3) to avoid erroneous interpretation during the interpretative phase when borderline cut-off is observed; 4) TFE3/NONO or inv(X)(p11.1;q12) may be in the cohort of negative cathepsin-k cases or when discordances are observed between break-apart vs dual fusion Xp probes at the analytical phase; 4) TFEB tRCCs have less variability in findings split signals.

870 Continuous versus Discontinuous Tumor Involvement: A Dilemma in the Quantitation on Prostate Biopsy

Caroline Bsirini, Alexandra Danakas, Hiroshi Miyamoto. University of Rochester, Rochester, NY.

Background: The extent of prostatic adenocarcinoma involvement in a needle core biopsy is one of the most critical parameters to guide treatment options including determination of eligibility for active surveillance. However, no consensus has been reached for an optimal method of quantifying discontinuous tumor foci separated by intervening benign tissue. Indeed, there are two methods used in estimating tumor involvement in a prostate core biopsy (PBx): additive and linear quantifications, by subtracting and including the intervening tissue, respectively. The current study aims to investigate the relationship between the tumor extent on PBx and radical prostatectomy (RP) findings.

Design: In a retrospective, blinded manner, we examined sets of PBx and RP performed at our institution between 2008 and 2011. Forty-nine cases met the inclusion criteria of only one core involvement of Gleason score 6 cancer on PBx and were then divided into three groups based on the linear length of tumor involvement with (*i.e.* discontinuous) and without (*i.e.* continuous) intervening benign tissue: Group 1 (G1, n=38): <3 mm in tumor length (continuous or discontinuous); Group 2 (G2, n=4): ≥3 mm in tumor length (continuous); and Group 3 (G3, n=7): ≥3 mm in tumor length (discontinuous).

Results: The lengths (mm, mean ± SD) of tumor involvement excluding the intervening tissue on PBx were: 1.21 ± 0.69 (G1); 3.63 ± 0.95 (G2); and 2.21 ± 0.99 (G3). In the RP specimens, there were no statistically significant differences in the rate of up-grading (*i.e.* Gleason score ≥7) between the groups (G1: 21%; G2: 50%; G3: 14%). However, the rates of extraprostatic extension and positive surgical margin were considerably lower in G1 (13% and 8%) than in G3 (43%, *P*=0.064 and 43%, *P*=0.039), but not in G2 (0%, *P*=1.000 and 0%, *P*=1.000), respectively. Estimated cancer volumes (cc, mean ± SD) on RP were: 1.82 ± 1.48 (G1); 2.46 ± 1.58 (G2); and 2.74 ± 1.92 (G3). Kaplan-Meier analysis revealed no significant differences in the risk of biochemical recurrence after RP between the groups.

Conclusions: Discontinuous (≥3 mm) involvement of Gleason score 6 cancer on PBx was found to correlate with the risks of extraprostatic extension and positive surgical margin on RP. It also appeared to correlate with larger tumor volume compared to cases with <3 mm cancer, but with similar tumor volume compared to cases with continuous ≥3 mm cancer. Thus, linear quantitation including intervening benign tissue on PBx may more precisely predict the actual tumor extent.

871 Temporal Trends in Prostatic Carcinoma Staging in a 23-Year Cohort of Men Treated with Radical Prostatectomy

Allen P Burke, William R Gesztes, Inger L Rosner, Stephen Brassell, Kevin R Rice, Shiv K Srivastava, Jennifer Cullen, Huai-Ching Kuo, Isabell Sesterhenn. Joint Pathology Center (JPC), Silver Spring, MD; Walter Reed National Military Medical Center (WRNMMC), Bethesda, MD; Center for Prostate Disease Research (CPDR), Rockville, MD; Saint Lukes Clinic Mountain States, Boise, ID.

Background: Recently, there has been a decrease in routine PSA screening and a trend towards active surveillance for selected patients with prostatic carcinoma (PCa). The objective of this retrospective study was to examine a cohort of 1870 prostatic carcinomas treated by radical RP for prostatic carcinoma between 1993 through 2016, comparing three time periods: before routine screening, during routine screening, and after the initiation of optional screening and active surveillance.

Design: Whole mounts of serial slices of 1870 prostates were evaluated, with largest tumor size, grade, extraprostatic extension (EPE), margins, seminal vesicle invasion (SVI) evaluated uniformly. Tumor grade was re-evaluated for conformity to the 2016 WHO grade group system (GG). Pathologic variables were compared among 3 time periods: A: 1993-2000; B: 2003-2012; and C: 2013-2016.

Results: Comparing a plateau between 2003 and 2016 (period B), both periods before and after (A and C, respectively) showed increased rates of EPE and SVI, higher GG, and larger tumors (all p <0.0001).

Conclusions: The stage and grade of tumors in this cohort was significantly lower during the phase of routine surveillance compared to before and after. The reason for this difference needs to be explored, by considering surgical variables and screening information on individual patients.

872 Should Tertiary Grades Be Assessed on Radical Prostatectomy Specimens Using the WHO 2016 Grade Group System?

Allen P Burke, William R Gesztes, Huai-Ching Kuo, Inger L Rosner, Shiv K Srivastava, Isabell Sesterhenn. Joint Pathology Center, Silver Spring, MD; Center for Prostatic Disease Research, Rockville, MD.

Background: The use of tertiary (tert) grades in the WHO 2016 grade group (GG) system has not been addressed, applied to radical prostatectomies.

Design: We retrospectively graded a series of 1761 prostatectomies using the WHO 2016 GG system, in which there is no % minimum for tert Gleason pattern 5, and a 5% maximum of Gleason pattern 3 for Grade Group 5. We modified the system in order to provide tert subgroups (≤5% and >5%) including Gleason 3 + 3 tertiary 5; Gleason score 7 tert 5; and Gleason score 9 with tert 3 (>5%). Outcome using both systems was determined by biochemical recurrence (BCR) and development of metastasis (mets).

Results: Median follow-up was 8.4 years. There was a step-wise increase in mets from WHO 2016 GG1-3, GG4, to GG5 (p<.0001). There was a increase in the rate of BCR from GG 1-2, GG 3-4, and GG5 (p<.0001). Tert subgroups demonstrated that Gleason 3 + 3 with tert 5 behave similar to GG1; Gleason 3 + 4 with tert 5 >5% behave similar to GG3; Gleason 4 + 3 tert 5 > 5% behave similar to GG4; and that Gleason [4 + 5] tert 3 >5% behave similar to GG5. Using these cutoffs, there was a stepwise increase in mets and BCR from GG1 - GG5 (both p<.0001), providing better separation than WHO 2016 GG.

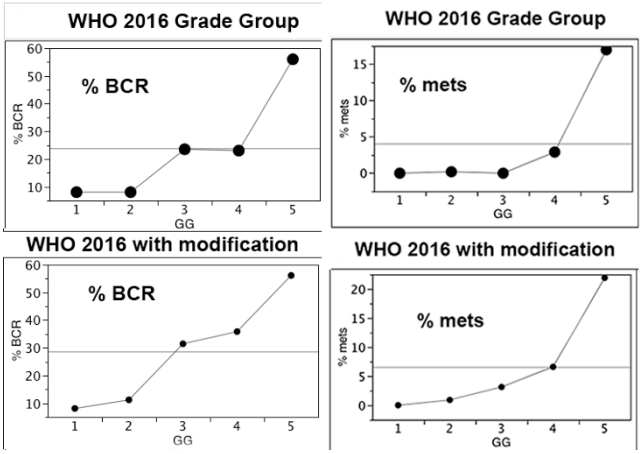

Conclusions: In prostatectomies, a tert pattern 5 should be ignored in GG1 tumors; and GG5 should include tumors with tert 3 >5%. For Gleason score 7 (GG2 and GG3), the % of tert pattern 5 should be reported, as the extent appears to correlate with prognosis.

873 Effect of Neoadjuvant Intense Androgen Deprivation Therapy in PD-L1 Expression in Prostate Cancer

Carla Calagua, Kristin Shaw, Joshua Russo, Rachel Schaefer, Rosina Lis, Zhenwei Zhang, Massimo Loda, Mary-Ellen Taplin, Steven P Balk, Yue Sun, Huihui Ye. Beth Israel Deaconess Medical Center, Boston, MA; Dana-Farber Cancer Institute, Boston, MA; Memorial Sloan-Kettering Cancer Center, New York, NY.

Background: Although prostate cancer (PCa) is thought to be resistant to PD-1/PD-L1 immunotherapies, recent studies reported that Enzalutimide treatment induced PD-L1 expression in PCa and anti-PD-1 antibody pembrolizumab showed anti-tumor efficacy in a subset of patients with Enzalutimide-resistant PCa. It is not clear if intense androgen deprivation therapy (IADT) has a similar immune modulation effect. In this study, we examined PD-L1 expression in residual tumors post neoadjuvant treatment with leuprolide with abiraterone acetate plus prednisone in a phase II clinical trial.

Design: Representative tumor sections from 43 trial cases and 53 grade- and stage-matched untreated control radical prostatectomy cases were subject to immunohistochemistry to evaluate PD-L1 expression. Additional immunostains were performed on all cases to examine tumor *ERG* and *PTEN* status and extent of neuroendocrine differentiation, to investigate potential mechanisms of PD-L1 expression. PD-L1-positive tumors were also stained for CD3 and PD-1 to characterize tumor-associated immune cells.

Results: Surprisingly, IADT-treated tumors showed a trend of reduced PD-L1 expression compared to untreated tumors. 7.0% of treated and 9.4% of untreated cases showed PD-L1 expression in >5% of tumor cells, respectively (p=0.73). 11.6% of treated and 24.5% of untreated cases showed PD-L1 expression in >1% of tumor cells, respectively (p=0.12). In addition, tumor PD-L1 expression had no significant association with *PTEN* deletion, *ERG* fusion status, or immunopositivity for chromogranin and synaptophysin. PD-L1-positive tumor cells were closely associated with CD3- and PD-1-positive immune cells, independent of treatment status.

Conclusions: Neoadjuvant IADT using leuprolide with abiraterone acetate plus prednisone reduces PD-L1 expression in PCa, indicating the addition of PD-1/PD-L1 immunotherapies to IADT may not increase the therapeutic effect in the neoadjuvant setting. PD-L1 expression in PCa is likely to be an adaptive response to tumor-infiltrating T-cells, and less likely a direct result of tumor genetic alterations such as *PTEN* deletion. PD-L1 expression in a large cohort of untreated PCa is currently under investigation to check its association with tumor aggressiveness.

874 Identifying Oncogenic Pathways in Renal Cell Carcinoma with Unclassified Histology (uRCC): A Validation Study of 59 Patients

Ying-Bei Chen, Mazyar Ghanaat, Ari Hakimi, Hikmat Al-Ahmadie, Samson W Fine, Anuradha Gopalan, Sahussapont J Sirintrapun, Gowtham Jayakumaran, Maria E Arcila, Chung-Han Lee, Martin H Voss, Darren Feldman, Robert J Motzer, James J Hsieh, Satish K Tickoo, Victor E Reuter. Memorial Sloan Kettering Cancer Center, New York, NY.

Background: uRCC constitutes a significant portion of aggressive non-clear cell RCC that has no standard therapy. The oncogenic drivers in these tumors are unclear. We recently conducted a molecular analysis of 62 high-grade primary uRCC, and identified recurrent somatic mutations in 29 genes, including *NF2* (18%), *SETD2* (18%), *BAP1* (13%), *KMT2C* (10%), and *MTOR* (8%). Our analysis revealed distinct molecular subsets with NF2-loss and dysregulated Hippo-YAP pathway (26%), hyperactive mTORC1 signaling (21%), FH-deficiency (6%), chromatin/DNA damage regulator mutations (21%) and ALK-translocation (2%) [Nat. Commun. in press]. Here we aimed to validate the molecular features of uRCC in an independent clinical cohort.

Design: FFPE tissue samples of the primaries (n=39) or metastases (n=20) from 59 patients with uRCC were analyzed by a CLIA-approved targeted NGS platform for somatic alterations. Diagnosis of uRCC in all cases was rendered at our institution by experienced GU pathologists based on the current WHO and ISUP consensus criteria.

Results: Patients were predominantly men (73%) with a median age of 52 yrs (20-76). At presentation, 25 (42%) had metastatic disease; 24 of the remaining 34 (71%) developed metastases with a median time of 10.5 mos. Systemic therapy was given to 42 patients. Median follow up was 19.9 mos, and 17 died of disease. Frequently mutated genes included *NF2* (27%), *SETD2* (12%), *FH* (12%), *TP53* (10%), *TERT* (8%), and *PIK3CA* (8%). *NF2* and *SETD2* were the two most frequently mutated genes as in the discovery cohort. Consistent with the molecular subsets identified previously, 27% of this uRCC cohort had inactivating mutations of *NF2* or other member of Hippo pathway; 10% harbored mutually exclusive *TSC1*, *TSC2* or *MTOR* mutations, suggesting hyperactive mTORC1 signaling; 24% (14) showed either *FH* somatic mutations/deletions or were subsequently found to carry *FH* germline mutations (9/14, 64%) by genetic testing; and 17% had mutations in DNA damage response/chromatin modifying genes. NF2-loss subset accounted for 41% of cancer-specific death, representing the largest molecular subset of uRCC that has poor outcome with current systemic therapy strategies. Further analysis to identify molecular and clinicopathologic associations is ongoing.

Conclusions: Molecular analysis of a uRCC validation cohort with more advanced disease reveals similar molecular subsets as in the discovery cohort of primary RCC. NF2-loss, FH-deficiency, DNA damage response/chromatin modulator defect, and mTOR hyperactivity are likely key oncogenic drivers in a large majority of uRCC.

875 Expression of Stearoyl-CoA Desaturase (SCD) Is a New Predictor of Prostate Cancer Progression After Radical Prostatectomy

Jinrong Cheng, Bo Xu, Chen Gao, Yingdong Feng, James Mohler, James Marshall. State University of New York at Buffalo, Buffalo, NY; Roswell Park Cancer Institute, Buffalo, NY.

Background: Previous studies from our group and others have shown that *de novo* lipogenic enzymes, including fatty acid synthase, are overexpressed in prostate cancer (PCA). However, no definitive association of expression of lipogenic enzymes and risk for PCA progression has been established. This study evaluates the expression of stearoyl-CoA desaturase (SCD), a key rate-limiting enzyme for monounsaturated fatty acid biosynthesis, and its predictive role in post-radical prostatectomy (RP) outcomes.

Design: Paraffin-embedded tissues from 707 patients who had RP at our institute, between 1993 and 2005, were used for tissue microarray construction. The protein expression level of SCD was assessed by IHC staining. The patients were followed for a median of 9.4 years. Treatment endpoints included biochemical recurrence, treatment failure and metastatic PCA. Cox proportional hazards analyses were used to evaluate the association of SCD expression with each endpoint. Bivariate associations with outcomes were considered; the associations were also controlled for established outcome predictors, including age at surgery,BMI, PSA, clinical and pathologic stage and grade, and margin status.

Results: About 17% patients in the cohort received neo-adjuvant androgen deprivation therapy (ADT); SCD stain in benign prostate epithelium and PCA tissue was mildly increased in ADT-patients as compared to non-ADT patients (1.93 vs. 1.52, p< .001 in benign and 1.10 vs. 0.97, p= .043 in PCA, respectively). Among non-ADT patients, the staining intensity of SCD in PCA tissue was positively correlated with that in benign tissue (r=0.49, p< .001). The SCD stain in PCA tissue was not associated with Gleason scores (0.96 vs. 1.09 in Gleason score of ≤ 6 vs. ≥ 7, p= .152). The increased expression of SCD in PCA tissue was significantly associated with reduced risks of biochemical recurrence (adjusted HR=0.456, p=.059), treatment failure (adjusted HR=0.509, p=.091) and metastatic PCA (adjusted HR=0.066, p=.007), respectively.

Conclusions: This study suggests SCD expression in PCA tissue represents a new independent predictor of post RP outcome.

876 Impact of Cribriform Architecture in Low Volume Gleason Score (GS) 3+4=7 or Grade Group (GG) 2 Prostate Cancers in Radical Prostatectomies (RP)

Bonnie Choy, Shane M Pearce, Blake B Anderson, Gladell P Paner. University of Chicago, Chicago, IL.

Background: It is now recognized that among the main Gleason pattern 4 architectures, cribriform confers a higher risk for PSA biochemical recurrence (BCR) in GS 7 prostate cancers. The aim of this study was to analyze the impact of the presence of cribriform architecture in the behavior of low volume (using 5% and 10% cut-offs) GS 3+4=7 prostate cancers treated with RP.

Design: 418 RPs with <10% tumor volume prostate cancer with GS 6 (GG 1) and GS 3+4=7 (GG 2) from a single institution's surgical pathology file from 2003 to 2007 were reviewed. Grading, including identification of cribriform architecture, was determined by 2 of the authors according to the 2014 ISUP consensus Gleason grading criteria. BCR was used as an end point. Median follow-up was 59.8 months.
Results: The cohort included 279 (67%) GS 6 and 139 (33%) GS 3+4=7 prostate cancers. Tumors with <5% volume were GS 6 (214, 82%), GS 3+4=7 without cribriform (37, 14%) and GS 3+4=7 with cribriform (11, 4%). BCR for tumors with <5% volume were GS 6 (1.4%), GS 3+4=7 without cribriform (5.4%) and GS 3+4=7 with cribriform (18.2%) (p=0.002). Tumors with <10% volume were GS 6 (279, 67%), GS 3+4=7 without cribriform (101, 24%) and GS 3+4=7 with cribriform (38, 9%). BCR for tumors with <10% volume were GS 6 (1.4%), GS 3+4=7 without cribriform (14.8%) and GS 3+4=7 with cribriform (18.4%) (p=0.00). Regardless of the volume cut-offs (5% or 10%), BCR-free survival was worse for GS 3+4=7 (with or without cribriform) compared to GS 6. However, although trends were seen, there was no statistically significant difference in BCR-free survival between GS 3+4=7 without cribriform and GS 3+4=7 with cribriform (p=0.3 for 5% and p=0.9 for 10% cut-offs), possibly due to the low number of GS 7 prostate cancers in the cohort.
Conclusions: This study showed a trend for increase in BCR-free survival with presence of cribriform architecture in low volume GS 3+4=7 prostate cancers. This study further supports the importance in identifying the cribriform architecture and reporting its presence in the surgical pathology reports of GS 7 prostate cancers.

877 Impact of the 2014 International Society of Urological Pathology (ISUP) Modified Gleason Grading on Previously Diagnosed Gleason Score 6 Prostate Cancers in Radical Prostatectomies

Bonnie Choy, Shane M Pearce, Blake B Anderson, Gladell P Paner. University of Chicago, Chicago, IL.
Background: The Gleason grading system for prostate cancer (PCa) underwent major revisions in 2005 and more recently in 2014, based on consensus conferences conducted by ISUP. The aim of this study was to analyze the impact of the 2014 ISUP Gleason grading criteria on PCas in radical prostatectomy (RP) specimens originally graded as GS 6 using pre-2014 ISUP modified Gleason grading.
Design: 506 RPs with diagnosis of GS 6 PCa from a single institution's surgical pathology file from 2003 to 2007 were reviewed. Grading, % Gleason pattern 4 (GP4), GP4 architectures and presence of intraductal carcinoma (IDC-P) were determined according to the 2014 ISUP modified Gleason grading criteria. PSA biochemical recurrence (BCR) was used as an end point. Median follow-up was 59 months.
Results: Using the 2014 ISUP criteria, out of the 506 original GS 6 PCas, 322 (63.6) were retained as new GS 6 (Grade group [GG] 1), and 180 (35.6%) were upgraded to GS 3+4=7 (GG 2) and 4 (0.8%) were upgraded to GS 4+3=7 (GG 3). No cases were upgraded to GS 8 or higher (GG 4 or 5). Breakdown of the PCas is shown in table 1.

% GP4	Cases (%)	BCR (%)	IDC-P	Glomeruloid	Cribriform
0	322 (63.6)	1 (0.3)	19 (5.9)	0 (0)	0 (0)
1-5	70 (13.8)	7 (10)	2 (2.9)	28 (40)	10 (14.3)
6-10	64 (12.6)	11 (17)	2 (3.1)	22 (34.4)	30 (46.9)
11-20	24 (4.7)	6 (25)	1 (4.2)	10 (41.7)	14 (58.3)
21-30	15 (3)	5 (33.3)	1 (6.7)	5 (33.3)	8 (53.3)
>30	11 (2.2)	4 (36.4)	0 (0)	3 (27.3)	6 (54.5)
Total	506 (100)	34 (6.7)	25 (4.9)	68 (13.4)	68 (13.4)

Conclusions: This study using the 2014 ISUP modified Gleason grading criteria on pre-2014 ISUP GS 6 PCas showed: 1) a significant decline in BCR rates in the new GS 6 PCas (from 6.7% to 0.3%); 2) an incremental increase in BCR with increasing % GP4 in the upgraded GS 7 PCas; 3) that most of the upgraded GS 7 PCas only had small amount (10% or less) of GP4; 4) that IDC-P can be identified in a subset (5.9%) of new GS6 PCas; and 5) glomeruloid is more common than cribriform in GS 7 with 5% or less GP4 whereas cribriform is more common in GS with 5% or more GP4, supporting that glomeruloid is an early lesion than cribriform. Overall, the findings of this study support the use of the 2014 ISUP modified Gleason grading and the ISUP recommendation of reporting the % GP4 in GS 7 PCa in RP.

878 Pathologic and Clinical Characteristics of Early Onset Renal Cell Carcinoma

Tyler Clemmensen, Win Shun Lai, Soroush Rais-Bahrami, Jennifer Gordetsky. University of Alabama at Birmingham, Birmingham, AL.
Background: Based on studies from the SEER database, renal cell carcinoma (RCC) is considered early onset in adults ≤46 years of age. Limited data exists regarding patients with early onset RCC. Our objective was to investigate the clinical and pathologic characteristics within this unique subset of patients with RCC.
Design: We retrospectively reviewed our surgical pathology database from 2011-2016 for patients with RCC. The clinical and pathologic characteristics of patients ≤46 years were compared to the overall population.
Results: We identified 98/604 (16%) cases of RCC in patients ≤46 years. The median age of patients with early onset RCC compared to our control group was 38.6 (range 19-46) vs. 64.4 (range 47-89) years, respectively. Early onset RCC patients included Caucasians (55%), African Americans (40%), Latino (4%), and Asian (1%). Histologic subtypes, included clear cell (54%), papillary (29%), unclassified (7%), chromophobe (5%), clear cell papillary (3%), multilocular cystic neoplasm (1%), and carcinoid (1%). 20/28 (71%) of early onset papillary RCCs occurred in African Americans. Risk factors for RCC included hypertension (47%), smoking (22%), obesity (12%), diabetes mellitus (9%), and chronic kidney disease (CKD) or end-stage renal disease (ESRD) (16.3%). Known genetic syndromes prior to diagnosis were identified in 6/98 (6%) patients (1 Von Hippel Lindau, 2 Familial Adenomatous Polyposis, 1 Marfan, 1 Tuberous Sclerosis, 1 Birt-Hogg-Dube). Five of 98 (5%) patients had disease recurrence. There was no significant difference between the two groups in terms of tumor size, focality, margin status, presence of necrosis, or sarcomatoid features. Non-Caucasians were more likely to develop early onset RCC (OR 1.98; p=0.001). Patients with early onset RCC were more likely to receive a radical nephrectomy (OR 1.98; p=0.001), have lower grade tumors (OR 0.69; p=0.033) and present with organ confined disease (p=0.008).
Conclusions: Despite having more indolent tumor characteristics and organ confined disease, early onset RCC patients were more likely to undergo a radical nephrectomy. In addition, a high percentage of these patients had either concurrent, or risk factors for developing CKD/ESRD. These findings suggest that the early onset RCC population is potentially being treated more agressivley than necessary. Nephron sparing surgery is recommended in this population if surgically feasible.

879 Myoid Gonadal Stromal Tumor of the Testis. An Immunohistochemical and Ultrastructural Study of Three Cases

Maurizio Colecchia, Giuseppe Renne, Roberta Rossi, Antonella Tosoni, Alessia Bertolotti, Salvatore Renne. Fondazione IRCCS Istituto Nazionale dei Tumori, Milano, Italy; European Institute of Oncology, Milano, Italy; DSC L.Sacco, Milano, Italy.
Background: Myoid gonadal stromal tumor is a distinct "emerging" entity reported in WHO Classification of the genitourinary tumours. Less than 10 cases are described in the literature and its rarity, the overlapping of morphological features with other gonadal stromal tumors and the debated histogenesis are opened questions.
Design: We reviewed H&E slides of the stromal testicular tumors retrieved from the archives of the IRCCS Istituto Nazionale dei Tumori , Milan between 1998 and 2016. The cases were stained with antibodies directed against S100, smooth muscle actin (SMA), desmin, caldesmon, inhibin, FOXL 2, Sox 9, steroidogenic factor-1 (SF1), ki-67, beta-catenin and WT1. Three cases were selected among a dozen of cases with the morphology of spindle-shaped stromal tumors. Microscopic features were evaluated reporting size, mitoses, presence of infiltrative margins, pleomorphism, capsule and relationship to the rete testis. Ultrastructural study was performed in two of the cases with available material
Results: The patients (53, 31 and 41 years-old) showed asymptomatic nodules with serum tumour markers within normal values. Clinical follow-up was negative for recurrence or metastatic disease after 74, 38 and 16 months. Greatest dimension range was cm.1-3.5. One tumor showed extension in the rete testis. At the ultrastructural level tumoral nuclei showed occasional grooves, granular chromatin, the cytoplasm showing rare lipid droplets and small cytoskeletal thin filaments with interspersed dense bodies. Mitotic rated varied from 0 to 2/10 HPF. No differentiated gonadal stromal cells have been identified. The spindle tumor cells were strongly positive for SMA, S100 protein, SF-1, focally for desmin and inhibin , while caldesmon, and Sox 9 were entirely negative. In two cases beta catenin showed a membranous staining, while WT1 was entirely negative. In one case a molecular analysis performed with Ion Torrent System Life technology showed no molecular alterations in the hot spot cancer panel.
Conclusions: The ultrastructural features support the origin from undifferentiated intertubular mesenchymal cells as previously suggested. Our observations highlight the importance of accurate morphological and immunohistochemical study for the characterization of this true entity occurring as a small lesion that carries a negligible risk after a conservative surgical approach .

880 Renal Cell Carcinoma (RCC) with Extensive Cystic Necrosis

Jennifer A Collins, Jonathan I Epstein. The Johns Hopkins University School of Medicine, Baltimore, MD.
Background: Extensive (>90%) cystic necrosis in RCC is uncommon and has been studied only in a few series predating current RCC classification. Necrosis is an adverse prognostic feature in RCC. Is extensive necrosis associated with a poor prognosis and high grade RCC, or if only limited viable tumor is present does it correlate with a better prognosis?
Design: From 2000-2015, potential cases were reviewed and only resections with >90% necrosis were included.
Results: We identified 21 cases with the central cyst composed of grummous necrotic debris, calcification, fibrin, cholesterol clefts and in a few cases with ghosts of tumor. 16 (76%) were male, mean age 59 yrs. (43-77). 11 (52%) were subclassified as papillary RCC (4 solid variant), 4 (19%) clear cell papillary RCC, 4 (19%) clear cell RCC, 1 (5%) sarcomatoid RCC and 1 (5%) RCC, unclassified. ISUP nucleolar grade was low (1-2) in 18 (86%) and stage was low (pT1-2) in 20 (95%) with the sarcomatoid RCC stage pT3a. Mean tumor size was 6.3 cm (2–17). In 52% (11) of cases, it was difficult to identify viable tumor requiring multiple sections; 4 cases were diagnosed in part due to the presence of necrotic tumor "ghost" architecture (3 papillary RCC, 1 unclassified RCC with tubules). Follow-up was available in 16 (76%) cases with a mean follow-up of 53 months (12-132 mos.). 12 (57%) patients are alive w/o disease. 3 (14%) died: 1 from cancer (sarcomatoid RCC); 2 unrelated to cancer. 1 patient (5%) with low grade clear cell RCC developed metastases, yet had a subsequent contralateral RCC. 5 (24%) were lost to follow-up.
Conclusions: Despite extensive necrosis, only 1/16 (6%) cases (sarcomatoid RCC) showed definitive recurrence. Of note, 100% with cystically necrotic papillary RCC or clear cell papillary RCC showed no disease recurrence. That clear cell papillary RCC, a tumor with virtually no malignant potential (19% of cases in this series), could have such extensive cystic necrosis would suggest that this finding is not indicative of rapid tumor growth outstripping its blood supply. If associated with low grade RCC, extensive cystic necrosis is a favorable prognostic feature, with the only cancer-related death from high grade sarcomatoid RCC. In about 50% of cases, it was difficult to identify tumor with the need to: 1) recognize the unique histology of necrosis associated with

cystically necrotic RCC; 2) extensively sample the fibrous capsule for viable tumor; 3) note architecture of necrotic "ghost" tumor and 4) recognize that tumor was often low grade, mimicking normal renal tubules sometimes requiring IHC to aid in the diagnosis.

881 Large Nested Variant of Urothelial Carcinoma (UC): A Clinicopathologic Study of 36 Cases

Eva Comperat, Jesse K McKenney, Arndt Hartmann, Simone Bertz, Ondrej Hes, Fadi Brimo. Hopital Tenon, UPMC, Paris, France; Cleveland Clinic, Cleveland, OH; Pathologisches Institut, University Erlangen-Nürnberg, Erlangen, Germany; Charles University, Plzen, Czech Republic; McGill University Health Center, Montreal, Canada.

Background: The large nested variant of urothelial carcinoma (LNUC) has been added to the WHO 2016 classification under the "nested variant" chapter. Few data exist about this entity and little is known about its clinical behaviour.

Design: Cases fulfilling the morphological criteria of LNUC were collected from 5 institutions. Both pure forms and mixed cases were studied with a minimum of 5% large nested carcinoma required for inclusion. Immunohistochemistry (CK7, p63, GATA-3, CK20, CDX-2, p53 and Ki-67) was performed in cases with available blocks. Positivity was defined as immunoreactivity ≥10% of the neoplastic cells.

Results: We retrieved 36 cases (32 males and 4 females). Average age was 66.7 years (38-84 years). Specimens were transuretheral resections (n=10) or cystectomies (n=26). Fourteen (39%) were pure LNUCs, and 16 (44%) cases were a mixture of LNUC and conventional UC, where the LNUC could be the minor component. In all except one of those cases, the LNUC comprised at least 40% of the tumor, while in one case it occupied only 5%. Four cases (11%) of the entire cohort were a mixture of LNUC and other variants of UC (3 squamous, 1 nested, 2 microcystic). Those variants never occupied > 50% of the tumour volume.

Lymphovascular invasion was present In 13 (36%) cases, and 8 patients (22%) had positive lymph nodes. Stage distribution was as follows: 3 (8%) pT1, 18 (50%) pT2, 10 (28%) pT3, 5 (14%) pT4, 17 (47%) pN0, 2 (6%) pN1, 5 (14%) pN2, 1 (3%) pN3 and 11 (30%) pNx. The percentage of cases showing positive staining was: CK7=87.5%, CK20=72%, GATA-3=91%, P63=100% and p53=59%. CDX2 staining was seen in 6% of cases.

6 (17%) patients died of disease (1 pure LNUC, 5 mixed UC). The mean overall survival was 29.2 months (3-150 m.). Overall survival was 44.5 and 17.9 months in pure and mixed LNUC, respectively.

Conclusions: LNUC is frequently seen admixed with either conventional UC or other variants of UC. It has an immunophenotype that is similar to conventional UC. Despite the bland cytologic appearance and deceptive pattern of invasion, our study validates the fully malignant potential of LNUC with metastatic spread and tumor related deaths. The data also suggest that pure LNUC patients may have a more favourable outcome than those with mixed forms.

882 Integrative Genomics of Prostate Cancer Progression

Joanna Cyrta, Juan Miguel Mosquera, Brian Robinson, Andrea Sboner, Himisha Beltran, Daniel Hovelson, Scott A Tomlins, Ronglai Shen, Mark A Rubin. Weill Cornell Medicine, New York, NY; Univ. Michigan, Ann Arbor, MA; Memorial Sloan Kettering Cancer Center, New York, NY.

Background: Primary prostate cancer (PPCa) often presents as multi-clonal, heterogeneous disease. To date, there is no large, systematic genomic study comparing distinct areas of PPCa to metastases. We report next generation sequencing (NGS) results on 10 PPCa and matched metastatic castration-resistant prostate cancer (mCRPC).

Design: Whole exome sequencing (WES) data from frozen mCRPC were available through the SU2C trial and/or Precision Cancer Care. All slides from corresponding radical prostatectomies were reviewed and distinct areas were selected based on histology, Gleason score (GS), topography and ERG/PTEN IHC, and processed separately for WES, PCR-based DNA-sequencing (DNAseq) and PCR-based RNA-sequencing (RNAseq). WES-based clonality score for each PPCa area *versus* metastasis was calculated.

Results: WES was performed on 36 PPCa areas (2-6/case) and 13 mCRPC samples (1-2/case). DNAseq and RNAseq were performed on 49 PPCa areas (2-7/case). Neuroendocrine differentiation (NED) was noted in two PPCa and three mCRPC. Gene alterations shared by PPCa and matched mCRPC included: *TP53*, *SPOP, PIK3CA, BRAF, FGFR3* and *MYC* point mutations or indels; and *PTEN, RB1* and *FANCA* deletions. The most frequent alteration found in mCRPC, but not in matched PPCa was *AR* amplification. Two patients had *BRCA2* germline mutation, both with mCRPC with NED. Clonality score, WES and DNAseq linked specific PPCa area(s) to corresponding metastases in most cases. WES also showed that some PPCa harbor relevant mutations at a very low allelic frequency (≤5%), suggesting the role of early subclonal events in PPCa progression. Transcriptome analysis further supported relationship between genomically similar PPCa areas.

Conclusions: Comparative NGS analysis can provide useful information to identify primary clone(s) that give rise to mCRPC. The study on an extended cohort (SU2C and Precision Cancer Care patients) is underway, with the potential to identify novel molecular drivers of metastatic progression and redefine histopathology criteria used to assess PPCa prognosis.

883 Molecular Characterization of Luminal and Basal Subtypes of Bladder Cancer

Vipulkumar Dadhania, Miao Zhang, Li Zhang, Jolanta Bondaruk, Tadeusz Majewski, Arlene Siefker-Radtke, Charles Guo, Colin Dinney, David E Cogdell, Shizhen Zhang, Sangkyou Lee, June G Lee, John N Weinstein, Keith Baggerly, David McConkey, Bogdan Czerniak. The University of Texas MD Anderson Cancer Center, Houston, TX.

Background: We have proposed that bladder cancer can be divided into two molecular subtypes referred to as luminal and basal with distinct pathogenesis, clinical behavior, and sensitivities to chemotherapy. In this project, we aim to validate these subtypes in several clinical cohorts and identify an immunohistochemical classifier that will permit a simple classification of the disease in primary care centers.

Design: We analyzed genomic expression profiles of bladder cancer in three cohorts of fresh frozen tumor samples: MD Anderson (n=132), Lund (n=308), and The Cancer Genome Atlas (TCGA) (n=408) to validate the expression signatures of luminal and basal bladder cancers and relate them to clinical outcomes. The TCGA cohort provided an opportunity to analyze the mutational profile of molecular subtypes based on the whole-exome DNA sequencing. The TCGA cohort also enabled the analysis of the protein expression profile using the reverse phase protein assay. In addition, we used an MD Anderson cohort of archival bladder samples (n=89) and tissue microarray to identify immunohistochemical markers that could identify molecular subtypes of bladder cancer.

Results: We have shown that bladder cancer can be divided into two intrinsic molecular subtypes referred to as luminal and basal in all of the datasets analyzed. Luminal cancers were characterized by the expression of markers similar to the intermediate/superficial layers of normal urothelium. These tumors showed the upregulation of of PPARγ target genes and they were enriched for FGFR3, ELF3, CDKN1A, and TSC1 mutations. They were also characterized by the overexpression of E-Cadherin, HER2/3, Rab-25, and Src. Basal tumors showed an expression signature similar to the basal layer of normal urothelium. They were characterized by the upregulation of p63 target genes, the enrichment of TP53 and RB1 mutations as well as the overexpression of CD49, Cyclin B1, and EGFR. Survival analysis showed that invasive basal bladder cancers were more aggressive when compared to luminal subtypes. The immunohistochemical expressions of two markers, luminal (GATA3) and basal (keratin 5/6) were sufficient to identify the molecular subtypes of bladder cancer with over 90% accuracy.

Conclusions: Our study has shown that bladder cancer can be consistently classified into two molecular subtypes referred to as luminal and basal, which have distinct clinical behaviors. A simple two marker classifier can be used for prognostic and therapeutic stratification.

884 Validation of ISUP/WHO Grading of Clear Cell Renal Cell Carcinoma

Julien Dagher, Brett Delahunt, Nathalie Rioux-Leclercq, Lars Egevad, Geoff Coughlin, Nigel Dunglison, Troy Gianduzzo, Boon Kua, Greg Malone, Ben Martin, John Preston, Morgan Pokorny, Simon Wood, Hemamali Samaratunga. Aquesta Specialized Uropathology, Brisbane, Australia; Rennes University Hospital, Rennes, France; University of Rennes, Rennes, France; Wellington School of Medicine and Health Sciences, Wellington, New Zealand; University of Queensland, Brisbane, Australia; Karolinska Institute, Stockholm, Sweden; Wesley Hospital, Brisbane, Australia; Greenslopes Hospital, Brisbane, Australia; Holy Spirit Northside Hospital, Brisbane, Australia.

Background: Since 1982, grading of renal cell neoplasia has been predominantly based on the recommendations of Fuhrman *et al*. This system requires the simultaneous assessment of nuclear size, nuclear shape and nucleolar prominence. Despite its widespread use, it is recognized that there are inherent problems relating to both prognostic utility and reproducibility. In 2012, the International Society of Urological Pathology (ISUP) introduced a new grading system for renal cell carcinoma using increasing nucleolar prominence to define grades 1 to 3, with extreme nuclear pleomorphism, sarcomatoid and/or rhabdoid differentiation defining grade 4. This system is incorporated into the latest World Health Organization (WHO) renal tumor classification, although few validation studies have been undertaken. This study was performed to ascertain the prognostic value of the ISUP/WHO grading system in clear cell renal cell carcinoma (ccRCC), compared to the Fuhrman grading.

Design: Between 2008 and 2015 inclusive, 681 cases of ccRCC were accessioned. In all cases patients were treated by partial or radical nephrectomy, with a curative intent. Histological material from these cases was reviewed and tumors graded according to Fuhrman nucleolar size, nuclear irregularity, and nuclear size and WHO/ISUP grading. The utility of each grading system in predicting metastasis free survival was compared.

Results: Patients were predominantly males (67.8%), with a mean age of 62 years. The distribution of the WHO/ISUP grades were: G1 8.7%; G2 48%; G3 22.9% and G4 20.4%, this compared with a Fuhrman grade distribution of G1 0.1%; G2 41%; G3 38.9% and G4 20%. Analysis of the individual components of Fuhrman grading resulted in widespread variation in the distribution of cases in each grading category. When compared with Fuhrman grading, ISUP/WHO grading resulted in an overall downgrading of tumors and provided superior prognostic information in terms of metastasis free survival ($p=3.6x10^{-5}$).

Conclusions: This study shows that the WHO/ISUP grading system outperforms Fuhrman grading in determining prognosis of ccRCC. We show that Fuhrman grading is confounded by the conflicting results obtained from assessment of three separate grading criteria.

885 The Significance of the Percentage of High-Grade Carcinoma in Predicting Outcome in Clear Cell Renal Cell Carcinoma

Julien Dagher, Brett Delahunt, Nathalie Rioux-Leclercq, Lars Egevad, Geoff Coughlin, Nigel Dunglison, Troy Gianduzzo, Boon Kua, Greg Malone, Ben Martin, John Preston, Morgan Pokorny, Simon Wood, Hemamali Samaratunga. Aquesta Specialized Uropathology, Brisbane, Australia; Rennes University Hospital, Rennes, France; University of Rennes, Rennes, France; Wellington School of Medicine and Health Sciences, Wellington, New Zealand; University of Queensland, Brisbane, Australia; Karolinska Institute, Stockholm, Sweden; Wesley Hospital, Brisbane, Australia; Greenslopes Hospital, Brisbane, Australia; Holy Spirit Northside Hospital, Brisbane, Australia.

Background: Heterogeneity of tumor grading is common in clear cell renal cell carcinoma (ccRCC). WHO/ISUP grading specifies that RCC should be graded based on the highest grade present in at least 1 high-power field. This does not take into account the proportion of high grade tumor present in a cancer, which may itself influence outcome.

Design: The database contained 681 cases of ccRCC accessioned between 2008 and 2015 and treated by nephrectomy. All cases were reviewed and grading assigned according to ISUP/WHO criteria. In addition, for tumors classified as grade 3 (G3) and 4 (G4), the percentage of tumor showing grade 3 and grade 4 morphology was assessed for each case. Survival analysis was performed for 6 grading subclasses (G3 <10%, G3 10-50%, G3 >50%, G4 < 10%, G4 10-50%, G4 >50%).

Results: There were 155 G3 and G4 cases in the series, with 91 G3 and 64 G4 tumours. 19 (20.9%) patients with G3 and 30 (46.9%) patients with G4 cancers developed metastatic disease. The 3 subgroups of <10%, 10-50% and >50% G3 cases were not significant in predicting outcome (p =0.47). Separating G3 into 2 groups of <50% vs. >50% was also not significantly associated with outcome (p = 0.22). In contrast, for the 3 subgroups of G4 ccRCC (<10%, 10-50% and >50% G4) a higher percentage of grade 4 predicted a worse outcome (p = 0.01). On multivariate analysis, that included tumour size and stage, there was a significant difference in survival between G4<10% and G4>50% tumors (p=0.018). The rate of metastasis of G3 >50% tumors was 27.8%, compared to 30.8% for G4 <10% tumors. Even though grade 4 tumours as a whole had a significantly worse outcome than grade 3 tumours (p=0.0004), the difference between G4 <10% and G3 tumours was not significant (p=0.27).

Conclusions: This study demonstrates that, utilizing WHO/ISUP grading, assessment of percentage of the high-grade component in G4 ccRCC provides prognostic information additional to grading alone.

886 Necrosis and Tumor Grading in Clear Cell Renal Cell Carcinoma

Julien Dagher, Brett Delahunt, Nathalie Rioux-Leclercq, Lars Egevad, Geoff Coughlin, Nigel Dunglison, Troy Gianduzzo, Boon Kua, Greg Malone, Ben Martin, John Preston, Morgan Pokorny, Simon Wood, Hemamali Samaratunga. Aquesta Specialized Uropathology, Brisbane, Australia; Rennes University Hospital, Rennes, France; University of Rennes, Rennes, France; Wellington School of Medicine and Health Sciences, Wellington, New Zealand; University of Queensland, Brisbane, Australia; Karolinska Institute, Stockholm, Sweden; Wesley Hospital, Brisbane, Australia; Greenslopes Hospital, Brisbane, Australia; Holy Spirit Northside Hospital, Brisbane, Australia.

Background: WHO/ISUP grading of clear cell renal cell carcinoma (ccRCC) is an important prognostic feature. The presence of microscopic tumor necrosis has also been shown to have prognostic importance. It has been suggested that microscopic necrosis should be included as a specific criterion in grading of these tumors. The aim of this study was to evaluate the combined impact of the newly established WHO/ISUP grading system and necrosis on metastasis-free survival for ccRCC.

Design: Between 2008 and 2015, 379 cases of ccRCC treated by radical nephrectomy and for which follow-up was available, were analysed. Clinical details and histological sections were retrieved and all cases were reviewed. World Health Organization/ International Society of Urological Pathology (WHO/ISUP) grade was assigned. Sections were assessed for the presence of microscopic necrosis. AJCC pT staging category and tumor size were also recorded. The development of metastatic disease was taken as the clinical end point and survival analysis utilizing univariate and multivariate models was undertaken.

Results: Patients were predominantly male (67%) with a mean age of 61 years and a mean tumor size of 4.9 cm. WHO/ISUP grades (G) were: G1, 36 cases (10%); G2, 188 (49%); G3, 91 (24%) and G4, 64 (17%). Staging categories were pT1-pT2, 235 tumors (62%) and pT3-pT4, 144 (38%). Microscopic tumor necrosis was seen in 128 cases (34%). Tumor necrosis was not seen in grade 1 tumors. For grades 2 and 4 tumors, those with necrosis had a significantly worse prognosis than those without necrosis (p=0.017 and p=0.006 respectively). The survival difference between grade 3 tumors with or without necrosis was not significant (p=0.054). Multivariate analysis, which included WHO/ISUP grade, pT staging category and necrosis showed all 3 variables to be independently associated with outcome (p=0.009, 0.005 and 0.001 respectively). For all tumor grades and pT staging categories it was found that the presence of necrosis was associated with a 2.91 fold greater risk of metastatic disease.

Conclusions: Tumor necrosis is an important prognostic factor for ccRCC and is independent of WHO/ISUP grade. This supports the suggestion that necrosis should be incorporated into tumor grading criteria.

887 The Impact of Routine Frozen Section Analysis During Penectomy on Surgical Margin Status and Long-Term Oncologic Outcomes

Alexandra Danakas, Caroline Bsirini, Hiroshi Miyamoto. University of Rochester, Rochester, NY.

Background: Intraoperative frozen section assessment (FSA) of biopsy or resection specimens often provides critical information for appropriate surgical management. However, to the best of our knowledge, there are no recent studies focusing on assessing the role of FSA in the status of surgical margins (SMs) relating to the outcomes of penectomy cases. Instead, a few review articles discourage its use in the assessment of SMs during penectomy, mainly because lesions often show well differentiated squamous proliferation that can mimic non-neoplastic conditions. The objective of the current study is to investigate the utility of routine FSA of the SMs in men undergoing penectomy for squamous cell carcinoma.

Design: A retrospective review identified consecutive patients (n=38) who underwent partial (n=26) or total (n=12) penectomy for squamous cell carcinoma at our institution from 2004 to 2015. FSA was correlated with the diagnosis of the frozen section control, the status of final SM, and patient outcomes.

Results: FSA of the SMs was performed in 20 (77%) partial penectomies and 9 (75%) total penectomies, while no FSA was done for SMs in other cases. FSAs were reported as positive (n=3, 10%), negative (n=24, 83%), and atypical (n=2, 7%). All of the positive or negative FSA diagnoses, including those in 7 cases of well differentiated carcinoma, were confirmed accurate on the frozen section controls, whereas the 2 cases with atypical FSA had non-malignant and carcinoma cells, respectively, on the controls. Final SMs were positive in 5 (13%) penectomies (2 partial and 3 total), including 3 (10%) FSA cases versus 2 (22%) non-FSA cases (P=0.574). Furthermore, 2 initially FSA-positive/ atypical cases achieved negative conversion by excision of additional tissue sent for FSA. In contrast, 2 FSA-negative cases showed carcinoma at the final SM where FSA was not submitted. During follow-up (mean: 41.2; median: 42; range: 2-136 months), 3 patients (non-FSA/final SM-negative, non-FSA/final SM-positive, FSA-negative/final SM-negative) developed tumor recurrence, and one of them (non-FSA/SM-positive) died of cancer. Kaplan-Meier analysis revealed that the number or diagnosis of FSA was not significantly associated with disease progression.

Conclusions: Overall, performing FSA during penectomy does not appear to have any significant impact on final SM status nor long-term oncologic outcomes. However, as seen in at least 2 cases, select patients may benefit from the routine FSA. Meanwhile, diagnostic accuracy of FSA of the SMs was found to be quite high.

888 Clinicopathologic Study of Sarcomatoid Urinary Bladder Carcinoma: A Matched Cohort Analysis of 30 Cases

Nooshin K Dashti, Frank Igor, Robert F Tarrel, Stephen A Boorjian, John C Cheville. Mayo Clinic, Rochester, MN.

Background: Sarcomatoid carcinoma of the urinary bladder (sarcomatoid UCa) is a rare variant of bladder cancer exhibiting epithelial and mesenchymal differentiation. It is believed that these tumors are of urothelial origin with divergent differentiation via the epithelial to mesenchymal transition (EMT). The objective of this study was to characterize the clinicopathologic features of sarcomatoid UCa.

Design: Thirty patients with sarcomatoid UCa treated by radical cystectomy were identified in the Mayo Clinic Cystectomy Registry. These cases were identified by pathologic review of all patients undergoing cystectomy between 1980 and 2016. Histologic pattern of the sarcomatoid component and presence of heterologous elements were assessed. A comprehensive panel of immunostains was performed. Patients were matched 1:2 by age, gender, pathological tumor stage and node status to patients with pure urothelial carcinoma. Survival analysis was done with the Kaplan-Meier method and log rank test. The results were compared to an unmatched cohort of pure urothelial bladder carcinoma.

Results: The 30 sarcomatoid UCa cases occurred in patients aged 50-89, median 72, with male sex predilection (63.3%). The morphologic pattern of sarcoma included spindled not otherwise specified (37%), undifferentiated pleomorphic sarcoma like (37%), myxoid (myxofibrosarcoma like, 13%), osteosarcoma (6.5%) and chondrosarcoma (6.5 %). Heterologous elements were identified in 4 cases, 2 osteosarcoma and 2 chondrosarcoma. Markers of mesenchymal differentiation were positive (Vimentin positive in 100% and E-cadherin lost in 100%). The median post-operative follow up period was 9.4 years. Sarcomatoid cancer was associated with a high rate of adverse pathological features: 21 patients (70%) had pT3–T4 disease, 8 (26.7%) had nodal invasion and 9 (30%) had distant metastasis. When matched to a cohort with pure urothelial carcinoma, no significant difference was noted in 10-year overall survival (42% vs 25 %, p: 0.534) or 10-year cancer specific survival (56% vs 51%, p: 0.891).

Conclusions: There is a significant morphologic overlap between sarcoma and sarcomatoid UCa. Loss of e-cadherin supports the hypothesis of EMT in sarcomatoid carcinomas. The sarcomatoid urothelial carcinoma is associated with high rate of locally advanced disease at radical cystectomy. However, when stage-matched to cases with pure urothelial carcinoma, patients with the sarcomatid variant did not have an increased rate of recurrence or adverse survival.

889 PD-L1 in Tumor Cells and the Immunologic Milieu of Bladder Carcinomas: A Pathologic Review of 177 Cases

Jonathan J Davick, Henry F Frierson, Alejandro Gru. University of Virginia, Charlottesville, VA.

Background: Programmed death ligand 1 (PD-L1) is a transmembrane protein that plays a major role in immune suppression. Its interaction with the receptor PD-1 results in downregulation of antitumoral immunity. Many cancers, including those from the bladder, have been shown to evade antitumoral immunity by utilizing this pathway. A

humanized monoclonal antibody that binds to PD-L1 has been shown to have therapeutic efficacy in patients with advanced urothelial cancer. However, the protein expression of PD-L1 in bladder tumors and its relationship to tumor histologic type, grade, and stage, have been incompletely analyzed. Hence, we examined PD-L1 in 177 bladder carcinomas using immunohistochemistry and the currently validated FDA method.
Design: Slides from 177 cystectomy specimens were reviewed for tumor type, grade of urothelial carcinoma, and pathologic stage. A tissue microarray (TMA) using four 0.6mm cores from each case was constructed. Immunohistochemistry using the FDA-approved antibody to PD-L1 (SP142, Ventana) was performed. For each case, the percent of tumor cells positive for PD-L1 and the percent of positive immune cells were scored. PD-L1 was considered positive if greater than 10% of the tumor cells or 5% of immune cells, respectively, demonstrated membranous staining.
Results: 140 neoplasms were urothelial carcinomas (UCs), 25 were squamous cell carcinomas (SCCs), 9 were adenocarcinomas, and 3 were small cell carcinomas. 33% of UCs, 40% of SCCs, 11% of adenocarcinomas, and 33% of small cell carcinomas were positive for PD-L1. A significant correlation between grade and PD-L1 positivity in tumor cells (40% of higher grade UC vs 7% of lower grade UC, $p = 0.003$) and in immune cells (47% of higher grade UC vs 30% of lower grade UC, $p=0.045$) was noted. 84 tumors had lymph node staging data. Lymph node metastasis was associated with lower PD-L1 in the primary tumors (18% in node positive vs 37% in node negative, $p = 0.04$). PD-L1 in immune or tumor cells was not associated with tumor (T) stage.
Conclusions: UCs and SCCs showed PD-L1 positivity more frequently than bladder adenocarcinomas. Tumor grade of UC and lymph node status, but not T stage, correlated with PD-L1 protein expression levels. Future studies should consider examining these specific pathologic parameters for bladder carcinomas in patients who are selected to receive PD-1/PD-L1 inhibitors in order to determine their potential association with therapeutic response.

890 SERPINE1 Is Associated with Prostate Cancer Bone Metastases

Inés de Torres, Jordi Temprana, Douglas Sanchez, Juan Morote, Santiago Ramon y Cajal, Mireia Olivan, Marta Garcia. Hospital Universitari Vall d'Hebron and Universitat Autònoma de Barcelona (UAB), Barcelona, Spain; Group of Biomedical Research in Urology, Vall d'Hebron Research Institute (VHIR) and Universitat Autònoma de Barcelona (UAB), Barcelona, Spain.
Background: The serine protease inhibitor SERPINE1 is a poor prognosis biomarker in various cancers, promoting tumor progression likely by titrating the extent and local of plasmin-initiated matrix. Prostate cancer (PCa) is the most common neoplasia in men and the second leading cause of death in males along Europe and USA. Bone is the most common site of this metastatic spread in CaP and half of the patients die within 30 months after the bone metastasis diagnosis because of a lack of an effective therapy.The aim of thi study was to generate an animal model of bone metastasis in order to select a cell population PCa with high metastatic potential to allow to identify the molecules responsible for the formation of bone metastasis by comparing genomic profiles of distinct PCa cell Populations.
Design: Human PCa cell line (PC-3) stably transfected with luciferase/green fluorescent protein was injected intracardially in nude mice. The IVIS System was used for monitoring tumor growth and detection of metastases in the living animal. Cells from bone metastasis were isolated and re-injected again. After three rounds of *in vivo* selection a PC-3 cell population with an increased bone metastatic potential was obtained. A gene expression analysis between selected cells with high and a low metastatic capacity was performed in order to identify those relevant molecules associated with metastatic disease. The candidate genes were validated in a tissue microarray (TMA) with metastatic and non-metastatic PCa by immunohistochemistry.
Results: The highly bone metastatic PCa cell population obtained by *in vivo* selection showed an increased bone metastasis pattern compared to parental cells. Differentially expressed genes found in the microarray were validated in the TMA, among them we found SERPINE1 significantly overexpressed in metastatic PCa patients compared to non-metastatic ones. ROC curves showed that SERPINE1 had an AUC of 0.75 in the same cohort of patients.
Conclusions: SERPINE1 is a protein involved in the metastatic process and is differentially expressed in metastatic CaP primary samples. A better understanding of the pathogenesis of CaP bone metastasis may lead to development of new therapeutic targets in order to choose an individualized treatment in patients with an increased risk of metastatic disease.

891 MiRNA as Diagnostic Biomarkers for Renal Cell Carcinoma Subtypes by Chromogenic In Situ Hybridization

Ashley Di Meo, Rola Saleeb, Samantha Wala, Adriana Krizova, Manal Gibril, Haiyan Zhai, Mereet Hanna, Maria Pasic, Andrew J Evans, Fadi Brimo, George M Yousef. St. Michael's Hospital, Toronto, ON, Canada; University of Toronto, Toronto, ON, Canada; London Health Sciences Center and Western University, London, ON, Canada; BioGenex Laboratories, Fremont, CA; McGill University Health Centre, Montreal, QC, Canada.
Background: Renal cell carcinoma (RCC) constitutes an array of morphologically and genetically distinct tumors including clear cell, papillary and chromophobe RCC. Accurate classification is critical since subtypes have different survival outcomes. This is usually done by morphology and IHC which are not always accurate
Design: We extracted RNA from ninety-three formalin-fixed paraffin-embedded (FFPE) tissues including 30 clear cell RCC, 28 papillary RCC, 30 chromophobe RCC, 4 unclassified RCC tumors and 11 oncocytomas. We measured the absolute expression of 6 miRNAs by qRT-PCR. Receiver operator characteristic curves were constructed and the areas under the curve were calculated to assess diagnostic performance. We also tested miRNA expression *in situ* hybridization (ISH) in an independent set of ninety-eight FFPE renal tumors
Results: We developed a two-step miRNA classifier. In the first step, expressions of selected miRNAs were found to discriminate clear cell and papillary RCC from chromophobe RCC and renal oncocytoma. Two miRNAs were able to discriminate clear cell and papillary RCC from chromophobe RCC and oncocytoma (AUC: 0.91, $p<0.0001$). In the second step, the absolute expression of miR-126 was used to distinguish clear cell from papillary RCC (AUC: 0.98, $p <0.0001$) and two miRNAs were used to differentiate most chromophobe from renal oncocytoma (AUC: 0.83, $p =0.003$).*In situ* hybridization revealed that miRNAs display a nuclear staining pattern that was able to distinguish clear cell RCC, papillary RCC, chromophobe RCC and renal oncocytoma.
Conclusions: miRNA expressions were able to distinguish between RCC subtypes and renal oncocytoma. miRNA assessment by *in situ* hybridization is a clinically useful diagnostic tool that can complement current methods for renal tumor classification.

1622 Correlation Between Programmed Death-1 Expression in Tumor Infiltrating Lymphocytes of Matched Primary and Metastatic Clear Cell Renal Cell Carcinoma (CCRCC) and Primary Non-Metastatic CCRCC: An Analysis of 85 Cases with Emphasis on Potential Pitfalls

Michelle DiMarco, Datta Patil, Rishi R Sekar, Viraj A Master, Adeboye O Osunkoya. Emory University School of Medicine, Atlanta, GA; University of Washington Medical Center, Seattle, WA.
Background: Programmed Death-1 (PD-1) is known to play a pivotal role in regulating host immune responses in a variety of malignances. Clear cell renal cell carcinoma (CCRCC) is the most common subtype of RCC and is frequently associated with metastasis. However, the correlation between PD-1 expression in tumor infiltrating lymphocytes of primary non-metastatic CCRCC and matched primary and metastatic CCRCC has not been well characterized, especially regarding PD-1 expression at the tumor-parenchymal interface and potential diagnostic pitfalls.
Design: A search was made through our Urologic Pathology database for nephrectomy cases of matched primary CCRCC and corresponding lung metastasis. In addition, cases of primary CCRCC without clinical or pathologic evidence of metastasis were also obtained. The slides were re-reviewed and sections of blocks with tumor and adjacent benign renal parenchyma were obtained for PD-1 immunohistochemical stains on all cases. Tumors were considered negative for PD-1 when less than 1% of the tumor had positive expression.
Results: Nineteen nephrectomy cases of matched primary CCRCC and metastatic CCRCC to the lung were obtained. Of these, 13/19 (68%) primary tumors exhibited PD-1 positivity and 11/19 (57%) of the corresponding metastatic nodules were PD-1 positive. Only 9/19 (47%) matched pairs were positive for PD-1 in both the primary and metastatic tumor. Sixty six cases of primary CCRCC without clinical or pathologic evidence of metastasis were also analyzed. Of these, 34/66 (51.5%) were positive for PD-1. A pattern of positivity concentrated at the interface between tumor and benign renal parenchyma was observed in 23/85 (27.05%) of all primary tumors.
Conclusions: Higher PD-1 expression was present in the primary tumors of patients with metastatic CCRCC compared to those without metastatic CCRCC. It is important to note that PD-1 expression in the primary tumor does not always match the corresponding metastatic tumor. Finally, the potential intratumoral heterogeneity of PD-1 expression in CCRCC implies that its utility as a predictive biomarker should be carried out with caution, especially in needle core biopsies of kidney tumors.

892 Polyoma Virus-Associated Urologic Malignancies in the Immunocompromised Setting: Report of 8 Cases

Michelle Don, Deepika Sirohi, Steven C Smith, Mahesha Vankalakunti, Jamie Koo, Shikha Bose, Mariza de Peralta-Venturina, Mahul B Amin, Daniel J Luthringer. Cedars-Sinai Medical Center, Los Angeles, CA; Virginia Commonwealth University Health System, Richmond, VA.
Background: Polyoma virus (PV) persists in a latent state and is shed in the urine of immunocompromised (IC) patients. It promotes oncogenic transformation of various cell types in vitro with putative roles in certain human malignancies. Herein, we describe the clinicopathologic features of 8 cases of PV-associated (PVA) urologic malignancies in the IC setting.
Design: Database search for urologic neoplasms in IC individuals identified 19 cases that were studied by immunohistochemical (IHC) techniques for PV (SV-40) to yield 8 PVA cases. Detailed evaluation of clinical parameters and pathologic features was undertaken.
Results: PVA tumors presented in patients at a mean age of 60.1 years (range 37-80), a M:F ratio of 1.7 and mean duration of immunosupression of 7.1 years (range 1-11). 7 occurred in the post-transplant (TX) setting (heart 1; kidney 3; combined heart/kidney 3) and 1 non-TX (steroid therapy for bullous pemphigoid). BK viremia antedated the tumors in 3 cases. Tumors were found in the bladder (n=5), ureter (n=1) and renal pelvis (n=2) and were classified as urothelial carcinoma (UC) (n=6) and collecting duct carcinoma (CDC) (n=2). All UCs showed variant morphology (including glandular/villoglandular, plasmacytoid, micropapillary, signet ring) with more than one pattern present in 4 of 6 cases. Sarcomatoid differentiation was identified in 4 of 6 UC cases and tumor necrosis in 3. All 8 cases showed strong SV-40 IHC reactivity; p53 IHC positivity colocalized with SV-40 in 6 of 6 cases studied. Background non-neoplastic epithelium was positive for SV-40 in 2 cases. 6 of 8 cases presented as high stage (p3 or greater), one was detected on autopsy (pT1), one (non-TX case) presented with in situ disease (pTiS). 1 patient died of metastatic disease after 7 months, with limited follow up in others. The non-TX case with in situ disease had recurrent localized disease over 21months.
Conclusions: A subset of UC and CDCs occurring in the IC setting are associated with PV. They are characterized by aggressive mixed variant histologic patterns, sarcomatoid differentiation and present with high stage disease. SV-40 is diffusely

positive in neoplastic cells that also show colocalization with p53, supporting a potential oncogenic role of T-antigen encoded by BK virus mediated through upregulation of the TP53 pathway.

893 GATA3 Expression in Benign Prostate Glands with Radiation Atypia: A Diagnostic Pitfall

David Dorn, Wei Tian, Rajah Shah, Ronald D Sanders, Shi Wei, Jennifer Gordetsky. Miraca Life Sciences, Irving, TX; The University of Alabama at Birmingham, Birmingham, AL.

Background: Radiation is a common therapy for the treatment of prostatic adenocarcinoma (PC). Patients who have undergone prostate radiation are at an increased risk for developing urothelial carcinoma (UC). Radiation changes can cause significant cytologic atypia in benign prostate glands that may be confused for UC. This potential diagnostic pitfall is especially relevant in cystoprostatectomy specimens, where involvement of the prostatic stroma by UC is pT4, and could alter post-operative management. GATA3 is a common marker to differentiate PC from UC. We investigate the expression of GATA3 in benign prostate glands with radiation atypia (RA).

Design: Our surgical pathology database was retrospectively reviewed for cases containing benign prostate tissue with RA. Immunohistochemical stain for GATA3 was performed on cases of benign prostate tissue with and without RA. PIN4 immunohistochemical stain was performed on prostate tissue with RA to confirm the presence of both basal and luminal cells.

Results: We identified 31 patients (28 biopsies, 2 cystoprostatectomies, 1 prostatectomy) that had benign prostate tissue with RA. Patients with RA had an average age of 70.3 years (range 48-80) and an average preoperative PSA of 5.9 (range 0.1-18.8). The average time between treatment with radiation therapy and the surgical procedure was 10 years (range 5-20). Benign prostate glands with RA showed significant nuclear pleomorphism with large nuclei, irregular nuclear contours, and prominent nucleoli (A). PIN4 immunohistochemical stain confirmed the presence of both basal and luminal cells in benign prostate glands with RA (B). 31/31 (100%) cases with benign prostate glands with RA showed staining for GATA3 in both basal and luminal cells (C). 8/8 (100%) cases with benign prostate glands without RA showed GATA3 positivity limited to basal cells (D).

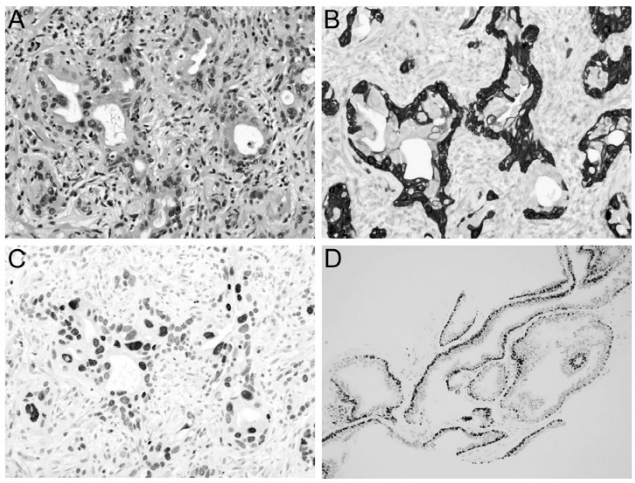

Conclusions: Benign prostate glands with RA show diffuse positivity for GATA3. This staining pattern along with the cytologic atypia from radiation can mimic UC and be a potential diagnostic pitfall.

894 High Suspicion (HS) versus Low to Intermediate Suspicion (LIS) Comparison Using 3D Magnetic Resonance Imaging/Transrectal Ultrasound Fusion Biopsies with Histopathologic Correlates

Zachary Dureau, Rachel Geller, Adeboye O Osunkoya. Emory University School of Medicine, Atlanta, GA.

Background: Transrectal ultrasound-guided biopsies (TRUS-GB) have traditionally been used to screen for prostate cancer (PCa). Few recent studies have also demonstrated the potential advantage of targeted magnetic resonance imaging-guided biopsies (TMRI-GB). More recently, a 3D method fusing these two modalities, known as a magnetic resonance imaging/transrectal ultrasound fusion biopsy (3D TMRI/TRUS-FB), has been utilized. This approach crafts three dimensional images while combining the systematic (but non-targeted) sampling approach of TRUS-GB with the high quality targeted approach of TMRI-GB. There are very limited studies in the literature correlating lesions targeted by suspicion and final histopathologic findings when using TMRI/TRUS-FB.

Design: A search was made through our Urologic Pathology files for prostate needle core biopsies that were obtained via 3D TMRI/TRUS-FB at our institution.

Results: Twenty-eight cases were identified. Mean patient (PT) age was 64 yrs (range: 45-78 yrs). Two hundred forty-nine total cores were sampled, with an average of 9 cores per procedure (range: 3-20 cores). One hundred and forty-four cores (58%) were considered high suspicion (HS) and 105 cores (42%) were considered low or intermediate suspicion (LIS). Following pathologic interpretation, 15/28 (54%) cores were negative for malignancy. One hundred twenty-four were from these cases. Fifty-two cores were considered HS and 72 cores were considered LIS. Thirteen of 28 (46%) cores were found to have PCa. One hundred forty-five cores were from PCa cases. Ninety-two of 125 (74%) cores were sampled as HS, with 49 (53%) of these being positive for PCa. Thirty-three of 92 (26%) cores were samples as LIS, with 5 (15%) of these being positive for PCa. The Gleason score (GS)/Grade Groups (GG) in this PTs were as follows: 3/13 (23%) PTs had a GS of 3+3=6 (GG1), 5/13 (39%) PTs had a GS of 3+4=7 (GG2), 3/13 (23%) PTs had a GS of 4+3=7 (GG3), and 2/13 (15%) had a GS of 4+5=9 (GG5).

Conclusions: In our cohort, 3D TMRI/TRUS-FB has 90% sensitivity and 40% specificity for detecting PCa. Biopsies from foci considered HS were positive in over 50% of cases compared to 15% from LIS foci. Given the superior image quality and relatively high sensitivity, 3D TMRI-TRUS-GB appears to be an effective method for the detection of PCa. In addition, it is highly conceivable that 3D TMRI-TRUS-GB may also play a critical role in active surveillance and tumor mapping of PTs with known PCa.

895 Genetic Profile of Ductal Adenocarcinoma of the Prostate

Lars Egevad, Amanda H Seipel, Thomas Whitington, Brett Delahunt, Hemamali Samaratunga, Peter Wiklund, Henrik Grönberg, Johan Lindberg. Karolinska Institutet, Stockholm, Sweden; Wellington School of Medicine and Health Sciences, University of Otago, Wellington, New Zealand; Aquesta Pathology, Brisbane, Australia.

Background: Despite being discovered almost 50 years ago little is known about the genetic profile of ductal adenocarcinoma of the prostate (DAC). In recent years, progress has been made in the understanding of the genetics of acinar adenocarcinomas and at least seven genetically different subtypes have been identified. DAC is known to present at an advanced stage with a high rate of extraprostatic extension and seminal vesicle invasion and short time to biochemical recurrence and metastatic disease. Our aim was to investigate the genetic profile of DAC to determine whether there is a genomic rationale for its aggressive behavior.

Design: Frozen tissue of 11 DAC cases with paired benign tissue was analyzed. After DNA extraction, copy number alteration analysis was performed as well as identification of mutations and indels. We compared the CNV fraction of the DAC genome with previous results from 74 primary acinar adenocarcinomas of the prostate.

Results: The CNV fraction of DAC was comparable to that of acinar adenocarcinoma of high Gleason scores. DAC harbored genetic changes similar to those seen in advanced and/or metastatic castration-resistant prostate cancer. The affected genes varied between cases with some tumors showing several genetic alterations while in others only single genes were affected. The alterations included amplifications of members of the ETS transcription factor family and the PIK3C pathway, deletions in MAP3K7 and CHD1 and mutations in TP53, SPOP and BRCA2.

Conclusions: The genetic alternations of DAC are comparable to those of advanced prostate cancer and this may account for the aggressive biological behavior of this cancer subtype.

896 Prognostic Significance of Prostate Cancer with Seminal Vesicle Invasion on Radical Prostatectomy: A National Registry Study

Lars Egevad, Anna Kristiansen, Linda Drevin, Brett Delahunt, Hemamali Samaratunga, Pär Stattin. Karolinska Institutet, Stockholm, Sweden; Uppsala University Hospital, Uppsala, Sweden; Wellington School of Medicine and Health Sciences, University of Otago, Wellington, New Zealand; Aquesta Pathology, Brisbane, Australia.

Background: Prostate cancer with seminal vesicle invasion (SVI) is known to have poor prognosis. We aimed to evaluate the prognostic significance of SVI after radical prostatectomy by comparing against cases with extraprostatic extension (EPE) alone and to correlate preoperative biopsy pathology with SVI and EPE.

Design: The National Prostate Cancer Register includes all prostate cancers diagnosed in Sweden. We analysed 31,415 cases diagnosed between 2000 and 2012 and treated with radical prostatectomy. Associations between pT3a and pT3b and progression were evaluated and adjusted for year, age, biopsy grade and serum PSA. Needle biopsy findings in these stages were compared.

Results: Patients with pT3b (n= 1274) had a higher risk of death from any cause [HR 1.5 (95% CI 1.2-2.0), P = 0.001] and death from prostate cancer [HR 2.3 (95% CI 1.5-3.3), p<0.001] than those with pT3a (n = 4097) and were more likely to be treated with postoperative radiotherapy [HR 1.6 (95% CI 1.4-1.8), P<0.001] or androgen deprivation therapy [HR 2.9 (95% CI 2.5-3.5), P<0.001], indicating clinical progression. Median cancer extent in preoperative biopsies of pT3a and pT3b was 14 and 24 mm (p<0.001), number of positive cores was 4 and 5, (p<0.001) and biopsy Gleason score was 8-10 in 11.6% and 27.3%, respectively (p<0.001).

Conclusions: SVI of prostate cancer is associated with worse outcome after radical prostatectomy than EPE alone. Needle biopsy findings may help to predict SVI, which has major implications in treatment planning.

897 Molecular Characterization of Prostatic Adenocarcinoma Gleason 4, Cribriform Pattern

Habiba Elfandy, Filippo Pederzoli, Eli Pullman, Svitlana Tyekucheva, Nicholas Schultz, Massimo Loda. Dana-Farber Cancer Institute, Harvard Medical School, Boston, MA; National Cancer Institute, Cairo University, Cairo, Egypt; Vita-Salute San Raffaele University, Milan, Italy; George Washington University, Washington, DC; Harvard School of Public Health, Boston, MA; Memorial Sloan Kettering Cancer Center, New York, NY; BWH, Harvard Medical School, Boston, MA; DFCI, Boston, MA.

Background: The Gleason grading system is widely accepted for assessment of prostate cancer architectural pattern. Among the five different grades, Gleason grade 4 is undoubtedly a heterogeneous group, encompassing different architectural variants. Recently, cribriform pattern has gained more attention as an independent adverse risk factor. Cribriform growth has been associated with earlier PSA relapse, higher stage, short overall survival and higher cancer-specific mortality. Thus far however, its genetic peculiarities remain undefined. We aimed to uncover the distinct molecular features of cribriform pattern.

Design: We built upon the prior publication on prostate Tumor Cancer Genome Atlas (TCGA) to specifically analyze cribriform pattern 4 tumors and their molecular phenotype to assess potential differences from tumors with non-cribriform Gleason 4 pattern. Publicly available data from TCGA portal were analyzed and the scanned H&E images of the paraffin blocks selected for molecular tests were re-review and graded.
Results: Out of 333 cases, Gleason grade 4 was present in 266 cases; at the histological review, cribriform pattern was identified in 164 cases (62%), and was found to be more associated with higher-grade groups (Groups 2 & 3 vs. 4 & 5, c-square 19.339, p<0.001). Mutations in SPOP and FOXA1 are more commonly found in prostate cancer showing a cribriform pattern (c-square 8.654, p=0.003) when compared to non-cribriform 4, while there appears to be no significant difference in ERG, ETV1/4 and FLI1 fusions (c-square 0.13, p=0.9). Methylation clusters were differently distributed in cribriform and non-cribriform cases (c-square 16.675, p=0.001). Furthermore, a positive significant correlation between the percentage of cribriform pattern and CNA was found (Pearson coefficient 0,370, p<0.001).
Conclusions: Cribriform pattern has a distinct molecular characterization among Gleason 4 prostate cancer, which may explain its negative influence on patient prognosis. Better understanding of its genetic profile may positively impact treatment of prostate cancer patients.

898 Study of Role of Tumor Associated Macrophages and Tumor Infiltrating Dendritic Cells as Predictors of Response to BCG Immunotherapy in Non Muscle Invasive Papillary Urothelial Carcinoma

Saba El-Gendi, Amal Rahmy, Mohamed Adel Atta, Heba Farid. Faculty of Medicine, Alexandria, Egypt.
Background: Although, Bacillus Calmette-Guérin (BCG) immunotherapy is mandatory for high-risk non-muscle invasive urothelial carcinoma (NMIUC), yet, around one third of patients experience BCG treatment failure.Tumor biology, including tumor progression and therapy response are influenced by the tumor microenviroment with its stromal cells, blood vessels and infiltrating leukocytes. Tumor-associated macrophages (TAMs) and tumor infiltrating dendritic cells (TIDCs) represent major components of the tumor stroma.
Design: Based on previous reports stating that the level of bladder tumor infiltration by immune cells prior to BCG treatment might have an impact on the response to therapy, the current study was undertaken. Our aim was to semiquantitatively assess, using immunohistochemistry, the level of tumor infiltration by CD68+ TAMs and CD1a+ dendritic cells (DCs) in the TUR samples of papillary NMIUC prior to BCG immunotherapy, and to study their potential prognostic significance.
Results: High TAM and high TIDC infiltration were observed in 93.7% and 49.2% of cases respectively. The infiltration of both CD68+TAMs and CD1a+TIDCs in the tumor stroma correlated significantly with their infiltration into the tumor epithelium. 60.3% of the studied cases experienced tumor recurrence , with significantly higher recurrence rates noted among patients with high TAM and high TIDC infiltration scores compared to patients with low infiltration scores,($X^2_{(Yate's)}$=4.080, $p_{(Yate's)}$ =0.043) and ($X^2_{(Yate's)}$=10.536, $p_{(Yate's)}$ = 0.001), respectively. Kaplan-Meier analysis revealed that patients with high infiltration of either immune cells experienced significantly lower median relapse free survival.Univariate Cox regression analysis revealed that high overall and high stromal CD68+TAM infiltration scores, and high stromal CD1a+TIDC score increased the risk of recurrence . High overall CD68+TAM and high stromal CD1a+TIDC infiltration were independent predictors of increased risk for recurrence on multivariate analysis.
Conclusions: The infiltration scores and location of TAMs and TIDCs in pretreatment biopsy of NMIUC influence the BCG treatment outcome. Patients with low infiltration experienced significantly lower rates of BCG treatment failure. These observations present new predictor biomarkers of the response to BCG immunotherapy that could affect the choice of treatment after validation in larger cohorts.

899 Are Men with Gleason Score 3+4=7 Cancer on Biopsy Candidates for Active Surveillance?

Jonathan I Epstein, Jeff Tosoian. Johns Hopkins Hospital, Baltimore, MD.
Background: Using the current Gleason grading system, Gleason score 6 cancer at RP has an excellent prognosis with no risk of metastatic behaviour and almost all men cured by definitive therapy. Consequently, active surveillance is often recommended for men with Gleason score 6 cancer on biopsy with close follow-up and repeat biopsies to account for possibile undersampling of higher grade cancer. With contemporary grading, almost 90% of men with Gleason score 3+4=7 at radical prostatectomy (RP) are cured by defintive therapy. It is now controversial if some men with limited Gleason score 3+4=7 on biopsy are also candidates for active surveillance. We studied how often men with Gleason 3+4=7 on biopsy had adverse pathology at RP.
Design: 608 men with limited Gleason 3+4=7 adenocarcinoma of the prostate on biposy were studied from 2005-2016. All cases had extended core sampling (>10 cores). Cases were restricted to men with limited cancer to 1 or 2 cores and a maximum percentage of 50% core involvement with a serum PSA of <10 ng/ml. PSA Density (PSAD) is defined as PSA/Gland volume. Adverse pathology at RP was defined by 1) Gleason >4+3=7; or 2) seminal vesicle invasion; or 3) pelvic lymph node metastases.
Results: Overall, 150/608 (25%) had adverse pathology at RP, with 94% of cases having Gleason score >4+3=7. There was no difference in the risk of adverse RP pathology based on age, maximum percentage positive core, or 1 vs. 2 positive cores. For example, even with only 1 positive core with <10% involvement, 22/78 (28%) had adverse pathology. The only differences were serum higher PSA and PSAD with adverse pathology; in multivariable analysis, PSAD remained significant. However, even with a PSAD of <0.08 (27.5% of all men with Gleason 3+4=7 on biopsy) there were still 28/167 (17%) with adverse pathology at RP. In contrast of 5,087 men with Gleason 6 on biopsy and serum PSA of <10 ng/ml (low risk disease), only 4.9% had adverse pathology at RP. With 1-2 cores of Gleason 6 on biopsy with PSAD<0.15 and no core with >50% cancer (very low risk disease), only 4.5% had adverse pathology at RP.
Conclusions: Even with very limited Gleason score 3+4=7 on biopsy or low PSAD, 28% and 17%, respectively, had unacceptably adverse findings at RP. In contrast, with Gleason score 6 cancer on biopsy, the risk of adverse pathology was <5%. These findings argue against routine active surveillance in men with Gleason score 3+4=7 on biopsy. Whether newer imaging techniques or molecular testing can identify a subset of men with Gleason 3+4=7 on biopsy with lower risk of unsampled adverse tumor at RP remains to be studied.

900 Composite Pheochromocytoma/Paraganglioma-Ganglioneuroma: A Clinicopathologic Study of 8 Cases with Analysis of Succinate Dehydrogenase

Lori Erickson, Sounak Gupta, Manli Jiang, Jorge Torres-Mora, Michael Rivera, Jun Zhang. Mayo Clinic, Rochester, MN.
Background: Ganglioneuromas represent the most well differentiated spectrum of neoplasia arising from the sympathetic nervous system. Small series of cases have documented the co-occurrence of Ganglioneuromas with a Pheochromocytoma (Pheo)/ Paraganglioma (PGL) component. We report the clinicopathologic features of 8 such cases, which were graded based on the Grading system for Adrenal Phaeochromocytomas and Paragangliomas (GAPP criteria), and evaluated for syndrome associations and clinical outcome. Mutations of the succinate dehydrogenase (SDH) complex subunits, which in certain contexts have been implicated in predicting metastatic behavior and in identifying possible paraganglioma syndromes, were screened for by absence of SDHB expression.
Design: The cases were diagnosed between 2003 and 2015, and clinical follow-up was available for all cases with a mean follow up of 22 months (1-47). These were reviewed and graded based on GAPP criteria which included: histological pattern, cellularity, comedo-necrosis, capsular/vascular invasion, Ki67 labeling and catecholamine type. IHC was performed on representative tissue blocks for SDHB and Ki67. Proliferative index was calculated by manual quantification of Ki-67 positive cells at selected hot-spots using ImageJ (NIH).
Results: In our series, composite Pheo/PGL-Ganglioneuromas predominantly involved the adrenal (Pheo: 7, PGL: 1). These cases had an equal gender distribution (males: 4, females: 4), with a mean age at diagnosis of 67yrs (range: 53 to 86yrs), an average size of 5.2cm (range: 2 to 8.2cm), an average weight of 49.3g (7.8 to 144.7g), and the majority were functionally active (7 of 8, 88%). The ganglioneuromatous component comprised ≤10% of the tumor in the majority of cases (6/8, 75%). The cases had an average GAPP score of 3.9 (range 2 to 6; well to moderately differentiated), with a mean Ki67 proliferation rate of 1.9% (range 0.3 to 3%), and all cases showed retained SDHB expression (8/8, 100%). None of the patients (0/8, 0%) developed metastatic disease on follow up. A single patient had a retroperitoneal composite PGL-Ganglioneuroma arising in the setting of Neurofibromatosis Type 1. No recurrent disease or associations were identified. One patient had a composite Pheo-Ganglioneuroma and concurrent adrenal cortical adenoma.
Conclusions: In our study, composite Pheo/PGL-Ganglioneuromas predominantly affected the adrenal gland in older patients, and no disease recurrences were identified. We report the spectrum of clinicopathologic features identified in a series of uniformly treated patients with clinical follow up.

901 Testis Specific Y-Like Gene-5(Tspyl-5) a Potential Biomarker to Stratify Tumor Phenotype in Prostate Cancer Patients

Magda Esebua, Senthil R Kumar, Lester Layfield. University of Missouri, Columbia, MO.
Background: TSPYL-5, a putative tumor suppressor gene, belongs to the nucleosome assembly protein family. The TSPYL-5 gene is located on 8Q22.1, a region reported to be amplified in prostate cancer. However, the exact role of TSPYL-5 in prostate cancer remains unclear. We investigated TGPYL-5 gene and protein expression in low-grade (GS 2-6) Intermediate grade (GS7) and advanced prostate carcinoma (GS 8-10).
Design: Archival formalin fixed paraffin embedded (FFPE) 21 prostate carcinoma cases ((4 - GS6; 13 - GS7; 3 - GS 8, 1-GS9) were obtained from the Pathology department after institutional IRB approval.
TSPYL-5 gene expression was analyzed by qRT–PCR and RT-PCR. Methylation analysis was performed by methylation specific PCR and pyrosequencing.
TSPYL-5 protein expression was performed by immunohistochemistry (IHC). Immunoreactivity was scored using a semi-quantitative system, combining intensity of staining on a 0 to 3+ scale (0 = no staining, 1+= week staining, 2+= moderate staining, and 3+ = strong staining). The percentage of cells staining positive was scored on 1 to 4 scale (1= 0–25% positive PC cells, 2 = 26–50% positive cells, 3 = 51–75% positive cells, and 4 = 76–100% positive cells). Composite score (CS) (0-12) was obtained by multiplying the staining intensity and percent of immunoreactive cells.
Results: 1. Prostatic carcinoma with GS6 expressed TSPYL-5 protein (CS-12). Cancer with GS ≥8 showed no expression(CS-0). Variable intermediate expression was observed with GS7(CS-8): GS 7(3+4) IHC expression was similar to GS6. GS7(4+3) was similar to GS8 and higher.
2. IHC analysis of TSPYL-5 identified expression patterns that mirrored the mRNA expression data. Low TSPYL-5 mRNA expression was observed in tumor samples with GS6, while tumor tissues with GS of 8 or above exhibited almost no TSPYL-5 mRNA expression, variable intermediate expression was observed with tumors with a GS7. However, in a few tumor samples with GS7 (4+3), very low or no TSPYL-5 expression was observed.
3. DNA Methylation in the 5' region of TSPY-5 was inversely correlated with TSPY-5 mRNA and protein expression.

Conclusions: We observed both by mRNA expression and IHC that TSPYL-5 expression diminishes in high grade tumors, possibly due to DNA methylation. Such a difference in TSPYL-5 expression could be exploited to identify the clinical behavior of intermediate grade prostate tumors (GS-7) to distinguish them from more aggressive phenotype.

902 Pathologic Factors Predicting Higher Clinical Stage in Testicular Non-Seminomatous Germ Cell Tumors (NSGCT): A Proposal for Upstaging Based on Rete Testis or Hilar Soft Tissue Invasion

Alaleh Esmaeili Shandiz, Karen Trevino, Thomas M Ulbright, Muhammad Idrees. Indiana University School of Medicine, Indianapolis, IN.

Background: Careful examination of orchiectomies and assessment of pathologic risk factors associated with recurrence and metastasis of NSGCTs are important in determining therapy and prognosis. Although some features (size, rete testis invasion) have been identified as predictors for relapse in seminomas, there are limited data on the prognostic significance of hilar soft tissue and rete testis invasion in NSGCTs.

Design: We reviewed 105 cases of NSGCTs, including slides from all orchiectomies. Clinical information was collected from physician notes. The following parameters were recorded: patient age, tumor size, dominant tumor histology, lymphovascular invasion (LVI), and tumor invasion into rete testis, tunica albuginea, tunica vaginalis, hilar soft tissue, epididymis, and spermatic cord. Univariate and multivariate analyses were performed comparing clinical stage I patients to clinical stage II/III patients in reference to these factors.

Results: Mean patient age was 28.6 years (range16-52). 56 patients (53%) were clinical stage I and 49 (47%) were clinical stages II/III. Mean tumor size was 3 cm in stage I and 5 cm in stages II/III patients. Statistical analysis revealed a significant correlation between stages II/III at presentation and LVI ($p= 0.0007$) and invasion of hilar soft tissue ($p< 0.0001$), rete testis ($p= 0.0023$), epididymis ($p= 0.0142$), spermatic cord ($p= 0.0055$) and tunica albuginea ($p= 0.0259$). Data showed no significant association between the clinical stage at presentation and age, pagetoid spread to rete testis, and invasion of tunica vaginalis. There was no statistical difference in clinical stage between patients with rete testis stromal invasion or hilar soft tissue invasion (currently pT1) compared to those with lymphovascular invasion (pT2) ($p=0.79$ and 0.12, respectively) or with each other ($p=0.07$).

Conclusions: Direct rete testis stromal and epididymal invasion but not pagetoid spread into the rete predict advanced disease at diagnosis. Our data support that rete testis stromal invasion and hilar soft tissue invasion relate to higher clinical stage similar to LVI. We therefore propose upstaging to pT2 when invasive tumor growth into these structures is identified and such assessment should become a part of routine testicular cancer synoptic reporting.

903 Prostatic Adenocarcinoma (PCA) with Poorly Formed Gland (PFG) and Cribriform Morphology: Grade Group (GG), Canary Histologic Analysis, and 17-Gene Expression Assay Comparison in 218 Patients

Sara M Falzarano, Eric A Klein, Cristina Magi-Galluzzi, Jesse K McKenney. Cleveland Clinic, Cleveland, OH.

Background: Grading PCA is complicated by biologic heterogeneity in GG2. Novel methods evaluating prognosis include a 17-gene expression assay and the Canary method of pattern evaluation based on individual architectures and regression tree modeling (Canary Nodes 1-7). We compared these 3 methods in a cohort of active surveillance candidates emphasizing PFG and cribriform patterns relevant to GG2.

Design: PCA biopsies from a single institution that were tested for the commercial 17-gene expression assay from 2011 to 2015 were identified. GG, Canary architectural pattern, Canary node group, and 17-gene expression assay data [Genomic Prostate Score (GPS) and NCCN risk concordance/discordance] were recorded and correlated.

Results: 218 cases had available slides for review; 194 were informative [24 (11%) failed genomic testing (insufficient tumor)]. Comparisons were based on histologic patterns: borderline GG1 vs GG2 due to varying thresholds for designating PFG (vs tangential sectioning); PFG without intervening well-formed glands; borderline cribriform due to simple epithelial bridges across gland lumens; glomerulations; small cribriform glands (< 12 luminal spaces); and large cribriform glands (≥ 12 luminal spaces).

Pattern (n)	GG	Canary Pattern	Canary Node	17 Gene Classifier Mean GPS (Range)	17 Gene Classifier NCCN Concordance
Borderline PFG (66)	48 GG1 18 GG2	Az	5	23 (0-53)	16 Discordant (24%) 13 more favorable 3 less favorable
PFG (3)	3 GG2	Bz	1	19 (17-36)	0 Discordant
Borderline Cribriform (16)	9 GG1 7 GG2	Bx	4	28 (14-58)	3 Discordant (19%) 3 more favorable
Glomerulations (6)	6 GG2	Cx	4	30 (5-32)	1 Discordant (17%) 1 more favorable
Small Cribriform (20)	20 GG2	Dx	3	28 (5-52)	1 Discordant (5%) 1 more favorable
Large Cribriform (2)	2 GG2	Ex	1	27 (22-33)	0 Discordant

For the borderline grading patterns, discordant NCCN risk prediction was more common in cases classified as GG1 [18 GG1 (15 more favorable, 3 less favorable) compared to only 1 GG2 (more favorable) from the borderline cribriform group.

Conclusions: For heterogeneous histologic patterns of GG2 PCA, there is variability in prognostic assessment between these 3 methods; however, definitive cribriform patterns had stronger agreement. Additional studies are needed to determine the optimal method of assessing clinical risk.

904 Down-Regulation of Fructose-1, 6-Bisphosphatase-1 (FBP1) in High Grade Urothelial Carcinoma (UC); as a New Diagnostic Marker to Differentiate Nested Variants of Urothelial Carcinoma from Benign Entities

Taliya Farooq, Anas Mashlah, Faisal Saeed, Islam Humayun, Jonathan I Epstein, Minghao Zhong. New York Medical College at Westchester Medical Center, Valhalla, NY; Johns Hopkins University, Baltimore, MD.

Background: Nested variants of urothelial carcinoma are characterized by deceptively bland histomorphology and aggressive clinical behavior. Previously, TERT promoter mutation has been described as specific molecular finding for Nested Variants of Urothelial Carcinoma (NVUC). But to date, no good reliable IHC markers have been discovered to differentiate benign mimickers of NVUC including Von Brunn's Nests (VBN) from NVUC. Recently, loss of FBP1 has been found to be associated with several high grade tumors and may be responsible for Warburg effect at molecular level (Nature, 513:251-5). Fructose-1, 6-bisphosphate is intermediate in glycolysis and its level is mainly controlled by upregulation of fructose-6-phosphate kinase and downregulation of FBP-1. Here, we would like to evaluate the potential role of FBP1 IHC stain to differentiate NVUC from benign entities.

Design: Tissue microarray slides (TMA) were constructed from 141 cases of UC, including 97 high-grade (HG) and 44 low-grade (LG) cases. We also retrieved Nested (21) and Large Nested (5) variants of urothelial carcinoma from two institutes. The TMA slides and full section slides were subjected to IHC stain for FBP1 (Sigma, 1:100 dilutions). The morphology and FBP-1 staining intensity of urothelial component were carefully examined.

Results: 1). Normal urothelium are strongly positive for FBP1. 2). Among 141 case of UC from TMA, 79% HG UC and 56% LG UC had decrease or loss of FBP1. 3) Decrease expression or loss of FBP-1 was noticed in 19/21 (90%) NVUC and 4/5 (80%) of LNVUC (non-neoplastic urothelium severs as internal control.

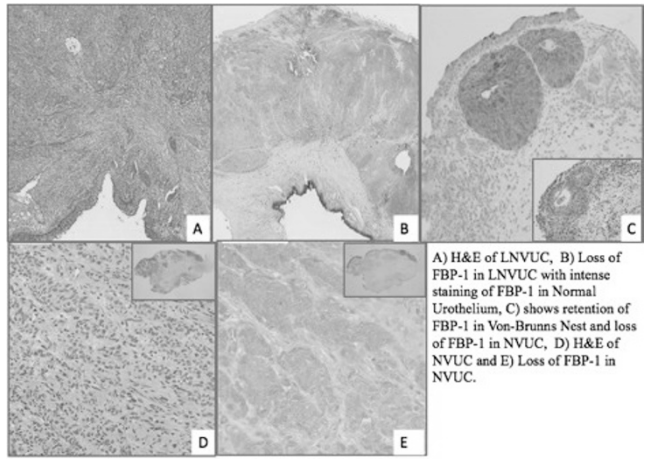

A) H&E of LNVUC, B) Loss of FBP-1 in LNVUC with intense staining of FBP-1 in Normal Urothelium, C) shows retention of FBP-1 in Von-Brunns Nest and loss of FBP-1 in NVUC, D) H&E of NVUC and E) Loss of FBP-1 in NVUC.

Conclusions: 1) Loss of FBP1is associated with UC and especially high grage UC. 2) Loss of FBP-1 can be used as a diagnostic marker to differentiate NVUC from other benign entities including VBN. 3) Down-regulation of FBP1 may be one of the molecular mechanisms of urothelial carcinoma to gain cancer cell proliferation and tumourigenicity. It may be potential target for novel therapy.

905 Metastatic Tumors to the Bladder: Avoiding the Diagnostic Pitfall

Alexander Feldman, Jennifer Gordetsky. University of Alabama at Birmingham, Birmingham, AL.

Background: Although rare, metastatic tumors to the bladder can present a diagnostic dilemma to pathologists considering a differential diagnosis of primary bladder cancer. We investigated the clinical and pathologic characteristics of metastatic tumors to the bladder.

Design: We retrospectively reviewed our surgical pathology database from 2013 to 2016, identifying patients with metastatic tumors to the bladder. Clinical, pathologic, and imaging findings were reviewed.

Results: We identified 46 cases of metastatic tumors to the bladder (table 1). Mean age was 61 years (range: 25-87). Females (34/46, 73.9%) were more likely to have metastatic tumors compared to males (12/46, 26.1%;), $p=0.001$. Overall, colorectal origin was most common (21.7%), followed by cervical and ovarian primaries (19.6%, 19.6%). Cervical and ovarian cancers predominated in the female cohort (26.5%, 26.5%), followed by endometrial origin (13.0%). Colorectal and prostate tumors were the most common amongst males (50.0% and 33.3%, respectively). In total, 39/46 (84.8%) patients had a clinical history of premalignancy or malignancy in another organ and 40/46 (87.0%) patients had imaging supporting a metastatic tumor. Only 2/46 (4.3%)

patients had a history of urothelial carcinoma. One case of metastatic cervical squamous cell carcinoma was originally misdiagnosed as urothelial carcinoma and corrected after clinical/radiological correlation.

Conclusions: At our institution women are more likely to have metastatic tumors to the bladder. Gynecologic, colorectal, and prostatic malignancies are the most common secondary tumors of the bladder. In the absence of an in situ urothelial lesion, pathologists should have a high index of suspicion. Clinical history, imaging, and immunohistochemical studies can be useful in avoiding the diagnostic pitfall (table 2).

Table 1. Primary Sites of Metastatic Carcinoma to the Bladder

Tumor Origin	Total (%)	Females (%)	Males (%)
Colorectal	10 (21.7%)	4 (11.8%)	6 (50.0%)
Cervix	9 (19.6%)	9 (26.5%)	N/A
Ovary	9 (19.6%)	9 (26.5%)	N/A
Endometrium	6 (13.0%)	6 (17.6%)	N/A
Prostate	4 (8.7%)	N/A	4 (33.3%)
Lymphoma	3 (6.5%)	2 (5.9%)	1 (8.3%)
Breast	1 (2.2%)	1 (2.9%)	N/A
GYN NOS	1 (2.2%)	1 (2.9%)	N/A
Neuroendocrine (small bowel)	1 (2.2%)	1 (2.9%)	0
Peritoneum	1 (2.2%)	1 (2.9%)	0
Stomach	1 (2.2%)	0	1 (8.3%)
Total	46	34	12

Table 2. Immunohistochemical Stains for Differentiating Urothelial Carcinoma From Metastatic Tumors

Metastatic Tumor	Primary Malignancy of Bladder	Positive in Metastatic Tumor	Positive in Primary Malignancy of Bladder
Colorectal Adenocarcinoma	UC with glandular differentiation	CDX2, Villin	GATA3, p63
Prostatic Adenocarcinoma	UC	NKX3.1, PSA	GATA3, p63, 34βE12
Endometrial Carcinoma	UC	PAX8, CA-125	GATA3, p63
Cervical SCC	UC with squamous differentiation	HPV	N/A
Ovarian Surface Epithelial Tumors	UC	PAX8, WT1, CA-125	GATA3, 34βE12

UC=urothelial carcinoma, SCC=squamous cell carcinoma

906 Correlation of Retrograde Nephroureteroscopy Biopsies with Resections for Presence of Urothelial Carcinoma and Carcinoma Upgrading

Shiraz Fidai, Tatjana Antic. The University of Chicago Medical Center, Chicago, IL.

Background: Biopsies of the upper urinary tract are frequently obtained to aid in the diagnosis of urothelial carcinoma (UC). Tumors can be small papillary lesions or large masses with variable histocytologic features depending on the area of sampling. Additionally, tumors can be multifocal. The retrograde nephroureteroscopy usually provides a very limited specimen. Therefore, this study was designed to compare presence of tumor and grade on biopsy vs. presence of tumor and grade in the resection specimen.

Design: The University of Chicago Department of Pathology archive was searched for all nephroureterectomies performed between 2005 to 2015. There were a total of 126 patients. The biopsy diagnoses were divided into seven categories: non-diagnostic, no tumor, atypical/reactive, atypical/suspicious for UC, low-grade papillary UC (LGPUC), high-grade papillary UC (HGPUC), and UC, and then compared with the final resection.

Results: The mean age was 69 years (range 41-93). Of the 126 patients, 47% (n=59) had biopsies with diagnoses as follows: non-diagnostic (n=3), no tumor (n=4), atypical/reactive (n= 3), atypical and suspicious for UC (n=1), LGPUC (n=12), HGPUC (n=25) and UC (n=11).

Of these 59 biopsies, 32% (n=19) were eventually upgraded. LGPUC comprised 42% (n=8) of them. Remaining 11 cases were further broken down into non-diagnostic (n=3), no tumor (n=4), atypical/reactive (n= 3) and atypical/suspicious for UC (n=1).

Total Nephroureterectomies	126	
Total biopsies performed	59	
Biopsy diagnosis category	% Upgraded	Upgraded diagnosis in final resection
Non-Diagnostic (n=3)	16%	High grade UC
		High grade papillary UC
		High grade UC
No Tumor (n=4)	21%	Low-grade papillary UC
		High grade papillary UC
		High grade UC
		High grade UC
	16%	High grade UC
		High grade UC
		High grade UC
Atypical and Suspicious for UC (n=1)	5%	High grade UC
Low-grade papillary UC (n=8)	42%	High grade papillary UC

Conclusions: Size and multifocality of the UC of the upper urinary tract plays significant role in obtaining an adequate specimen for either diagnosis or grading of UC. The non-diagnostic and negative biopsy samples do not exclude carcinoma (17%), and if there is a high clinical suspicion for UC, multiple biopsies should be obtained. Additionally, there should be a clinical understanding that some of the low grade tumors will be upgraded into the high grade category (32%).

907 Prediction of Tumor Focality in the Upper Urinary Tract Based on Concurrent or History of Cystectomy or Biopsy Proven Bladder Cancer

Shiraz Fidai, Tatjana Antic. The University of Chicago, Chicago, IL.

Background: Urothelial carcinoma (UC) is well known for being multifocal in its incidence, involving the upper tract (kidney and ureter) and bladder, in synchronous or metachronous fashion in the same patient over time. Although urinary bladder UC is more common, many patients develop upper tract UC, subsequent to the cystectomy. In some cases, bladder tumors are treated by resection and medication. However, upper tract UC almost always requires resection, although some studies suggest that partial resections are possible. In this study, the relationship between cystectomy or biopsy status was used to predict if the tumors in the upper tract are more likely to be multifocal and feasibility of partial resection as a treatment option.

Design: The University of Chicago Department of Pathology archive was searched for all nephroureterectomies performed between 2005 to 2015. There were a total of 123 patients. The resection specimens were evaluated for the focality of the tumor in kidney and ureter. Additionally, clinical history of whether the patient had a concurrent cystectomy with the nephroureterectomy, previous history of cystectomy, or prior biopsy proven diagnosis of UC was studied.

Results: The mean age was 69 years (range 41-93). The focality was divided as follows: unifocal (either renal pelvis or ureter or continuous tumor involving both), multifocal (either renal pelvis or ureter or combination of renal pelvis and ureter).

	Renal Pelvis	Ureter		
Unifocal	44	14	14	Unifocal cases with bladder UC (%)
Previous/ Concurrent Cystectomy/ Biopsy Confirmed UC	4	5	9	25%
Multifocal	6	7	38	Multifocal cases with bladder UC (%)
Previous/ Concurrent Cystectomy/ Biopsy Confirmed UC	4	4	21	56%

Conclusions: Unifocal UC is slightly more common than multifocal UC (59% vs 41%) in nephroureterectomies. This study showed that having history of cystectomy/ concurrent cystectomy or biopsy proven UC in the bladder doubles the probability of having multifocal tumors in nephroureterectomies. Therefore, partial resection would not be the best treatment option for these patients.

908 Clinicopathologic Features and Outcome in Primary T2 Prostatic Urethral Urothelial Carcinomas at a Single Academic Institution: Is There a Role for Substaging?

Joel Friedman, Aaron M Udager, Rohit Mehra, Scott A Tomlins, Lakshmi P Kunju, Angela Wu. University of Michigan Health System, Ann Arbor, MI.

Background: It is now accepted that primary prostatic urethral urothelial carcinomas (PUCas) should be staged per urethral staging guidelines, yet there are not many studies about the prognosis of patients with high stage urethral cancers or whether type or extent of invasion affects prognosis. Thus, we reviewed our experience with T2 PUCas.

Design: All patients from 1/2001-4/2016 with T2 PUCas and in which the PUCa was the highest stage disease at presentation were included. All pathology, including prior TURs, were reviewed to ensure that patients did not have any documented T2 or higher stage disease at other urinary tract sites. Medical records and slides were reviewed. Focal invasion was defined as all microscopic foci of invasion into the stroma <0.1 cm.

Results: Twenty-five patients were included (18 cystoprostatectomies including 2 with nephrectomies; 6 TURPs/excisions; 1 prostatectomy). Twenty (80%) had concurrent bladder involvement (T1 and flat urothelial carcinoma in situ (CIS) (8); CIS only (12)) and 4 (16%) had upper tract CIS. All patients had flat CIS involving the prostatic urethra, and most (19; 76%) had invasion into the prostatic stroma via CIS extending into prostatic glands. The remainder had either direct invasion from the overlying urethra into the stroma (5) or a combination of both (1). One case showed divergent differentiation (extensive glandular). Most had focal, microinvasive disease in the prostatic stroma (17, 68% focal invasion; 8, 32% nonfocal invasion). Seven (28%) had regional node metastasis at presentation. Followup was available in 21 patients (2-132 months; median 24 months). Seven (33%) had local recurrence (4 urethral CIS; 2 upper tract urothelial carcinoma; 1 with both) and ten (48%) developed distant metastases (most commonly bone, liver, distant nodes). Ten (48%) died of disease, 3 (14%) died of other causes, 8 (38%) are alive with no evidence of disease (NED). Of those with NED, 5 had >43 months of followup; all had focal, microinvasive disease in their prostate.

Conclusions: All T2 PUCa patients had extensive CIS, usually involving multiple sites; the most common pattern of invasion was microinvasion via CIS involved prostatic glands. Divergent differentiation was rare. Distant metastases and death from disease were relatively common. There was a small subset of patients with microinvasive disease and long term followup who had a good prognosis. Additional cases will be reviewed to determine if substaging may be beneficial in predicting prognosis.

909 Clinicopathologic Characteristics of Patients Undergoing Prostate Core Biopsy with High-Risk (PI-RADS 5) Lesions by Multiparametric Prostate Magnetic Resonance Imaging

Joel Friedman, Aaron M Udager, Nicole Curci, Chandy Ellimoottil, Rohit Mehra, Scott A Tomlins, Jeffrey S Montgomery, John Wei, Matthew Davenport, Angela Wu, Lakshmi P Kunju. University of Michigan Health System, Ann Arbor, MI.

Background: Multiparametric Prostate Magnetic Resonance Imaging (mpMRI) utilizes a PI-RADS classification system to identify clinically significant (Gleason score (GS) 7 or higher) prostate adenocarcinoma (PCa) with PI-RADS 5 lesions typically corresponding to a high-risk of clinically significant PCa.

Design: All patients who underwent mpMRI between 1/1/2015 and 6/30/2016 at a large academic institution were identified. Patients with one or more PI-RADS 5 lesions who underwent an ultrasound-MRI fusion PBx were retrospectively reviewed to assess for presence or absence of PCa, location (targeted vs. 12-core/non-targeted cores), GS, and percentage pattern 4 in GS 7 tumors.

Results: 138 patients with PI-RADS 5 lesions {1 lesion (107), 2 lesions (27), 3 lesions (4)} were identified, of which 76 (55%) underwent an in-house MRI fusion PBx. In the targeted cores, 7 (9%) patients had no PCa and 69 (91%) patients showed PCa. In 7 patients without PCa (total 12 PI-RADS 5 lesions), the targeted cores showed extensive simple atrophy (2), florid adenosis (1), central zone histology (2), atypical small acinar proliferation (1), focal high-grade prostatic intraepithelial neoplasia (1), granulomatous inflammation (1), carcinoid (1), focal simple atrophy (2) and focal adenosis (1). Clinically significant PCa was noted in 79% (60/76) cases, {GS 3+4 (35), GS 4+3 (16) and GS 8-10 (9)}. In 7 (9%) patients with GS 7 or higher PCa, the highest GS was found in the non-targeted cores. The median % Gleason pattern 4 in GS 7 tumors was 30 (inter-quartile range = 10-60). Of the remaining 62 (45%) patients who did not receive an MRI fusion PBx, 3 had saturation PBx and 27 had a radical prostatectomy (all show GS 7 or higher PCa); 9 received radiation and/or hormone therapy.

Conclusions: The vast majority of patients (79%) with PI-RADS 5 lesions showed GS 7 or higher PCa on targeted cores; however, a small subset (9%) showed no evidence of malignancy. The benign mimickers of PI-RADS 5 lesions include florid adenosis (1), granulomatous inflammation (1), carcinoid (1), central zone acini (2) and simple atrophy (2). PI-RADS 5 lesions can be biopsied for confirmation of clinically significant disease in the vast majority of cases or used to guide the patient's treatment towards more definitive therapies.

910 Comparison Between Pathologic Findings in Targeted MRI Guided Prostate Needle Core Biopsies and Transrectal Ultrasound Guided Prostate Needle Core Biopsies in Patients with Normal, Enlarged and Markedly Enlarged Prostates

Rachel Geller, Sherif G Nour, Kareem Elfatairy, Adeboye O Osunkoya. Emory University Hospital, Atlanta, GA.

Background: Prostate volume under 30 cc is considered normal. As the volume of the prostate increases, the rate of cancer detection by transrectal ultrasound guided prostate needle core biopsies (TRUS-GB) decreases. Despite the advances in targeted MRI guided needle core biopsies (TMRI-GB) techniques, systematic (but non-targeted) TRUS-GB remains the standard diagnostic tool for prostate cancer (PCa). In this study, we sought to compare the pathologic findings in TMRI-GB and TRUS-GB in patients with variably sized prostates.

Design: A search was made through our Urologic Pathology files for patients who had TMRI-GB and previous TRUS-GB. We categorized the prostate volumes as normal (<30 cc), enlarged (30-59 cc), or markedly enlarged (≥60 cc). In each volume category, we reviewed pathologic findings and compared overall cancer detection rate and clinically significant cancer detection rate. Clinically significant carcinomas (CSCs) are defined as tumors with Gleason score ≥7 (Grade group 2).

Results: Forty-nine patients were identified. Mean prostate volume was 47 cc (range: 25-123 cc). Overall cancer detection rate by TRUS-GB versus TMRI-GB was 63% (31/49) versus 78% (38/49). Clinically significant PCa (Gleason score ≥ 3+4=7/Grade group 2) was identified in 27 cases, and only 3 CSCs arose in normal volume prostates. Of these, TRUS-GB identified 67% (2/3) and TMRI-GB identified 100% (3/3). In prostates ≥ 30 cc, TRUS-GB identified 46% (11/24) CSCs and TMRI-GB identified 96% (23/24) CSCs. When larger prostates were further stratified, in patients with enlarged prostates (30-59 cc), TRUS-GB identified 53% (10/19) CSCs and TMRI-GB identified 100% (19/19) CSCs. In addition, in markedly enlarged prostates (≥60 cc) TRUS-GB identified 20% (1/5) CSCs and TMRI-GB identified 80% (4/5) CSCs.

Conclusions: Compared to TRUS-GB, the rate of detection of CSCs is much improved by TMRI-GB in patients with enlarged prostates (≥30 cc), including a significant number of patients with markedly enlarged prostates (>60 cc). TMRI-GB should be considered as the primary modality of initial prostate sampling in patients with both enlarged and markedly enlarged prostates. It is also conceivable that patients on active surveillance with both enlarged and markedly enlarged prostates would benefit more from TMRI-GB.

911 Detection of Clinically Significant Prostatic Adenocarcinoma in Patients with Targeted MRI Guided Prostate Needle Core Biopsies: Critical Role in Patients on Active Surveillance

Rachel Geller, Brianna L Vey, Sherif G Nour, Kareem Elfatairy, Adeboye O Osunkoya. Emory University School of Medicine, Atlanta, GA.

Background: Despite the advances in targeted MRI guided needle core biopsies (TMRI-GB) techniques, systematic, but non-targeted, transrectal ultrasound guided needle core biopsies (TRUS-GB) remains the standard diagnostic tool for prostatic adenocarcinoma (PCa). We examined the detection rate of clinically significant (CS) PCa in all men who underwent TMRI-GB at our institution with a focus on the detection of CSPCa in men on active surveillance for previously diagnosed small volume Gleason score (GS) 3+3=6 Grade group (GG) 1 PCa.

Design: A search was made through our Urologic Pathology files for patients (PTs) who had TMRI-GB (2013-2016). CSPCa was defined as GS ≥ 3+4=7 (GG2).

Results: Eighty-four PTs were identified. Twenty-nine percent of PTs (24/84) had previous benign TRUS-GB, 30% of PTs (26/84) had no prior biopsy, and 41% of PTs (34/84) had previous malignant TRUS-GB. Thirty-five percent of PTs (29/84) had benign findings on TMRI-GB, and 20% of PTs (17/84) were found to have PCa GS 3+3=6 (GG1). The remaining 45% (38/84) PTs had CSPCa detected by TMRI-GB. Fifty-eight percent of PTs (22/38) had PCa GS 3+4=7 (GG2), 29% of PTs (11/38) had PCa GS 4+3=7 (GG3), 5% of PTs (2/38) had PCa GS 4+4=8 (GG4), and the remaining 8% had PCa 4+5=9/5+4=9 (GG5). Of malignant diagnoses rendered by TMRI-GB, 69% (38/55) were CSPCa. Of the men on active surveillance, with both a malignant TRUS-GB and TMRI-GB, 65% (15/23) were upgraded to CSPCa.

Conclusions: TMRI-GB appears to be an effective option for detection of CSPCa which may otherwise have been unsampled in patients on active surveillance. These patients would subsequently benefit from definitive therapy. It is also conceivable that TMRI-GB may also play an important role in the management of patients considering focal therapy for PCa. Finally, TMRI-GB should also be utilized in PTs who have opted for prognostic molecular testing of PCa, especially in those with multifocal tumors.

912 Nuclear Grade Is an Independent Predictor of Recurrence in Prostate Carcinoma

William R Gesztes, Allen P Burke, Daniel J Kim, Inger L Rosner, Jennifer Cullen, Huai-Ching Kuo, Yongmei Chen, Shiv K Srivastava, Isabell Sesterhenn. Center for Prostate Disease Research (CPDR), Rockville, MD; Joint Pathology Center (JPC), Silver Spring, MD; Walter Reed National Military Medical Center (WRNMNC), Bethesda, MD.

Background: The significance of nuclear grade in prostate carcinoma has been long debated. The aim of the current study is to analyze histologic features that predict prostate cancer recurrence after radical prostatectomy.

Design: 1,651 prostatectomies (whole mounts, entirely embedded) were retrospectively studied from an ongoing cohort of military patients. The tumors were re-classified using the 2016 WHO grade group system. Histologic findings were recorded independent of knowledge of outcome. The following variables were considered in multivariate analysis: age, grade group, nuclear grade (three-point scale), stage, race and ductal features. The outcome variable was biochemical recurrence, defined as PSA level ≥ 0.2 ng/mL after 8 weeks post- surgery and before the development of metastasis or last follow-up, followed by a successive confirmatory PSA level ≥ 0.2. Mean follow-up was 8.4 years.

Results: Of all variables tested, three were significant independent of the others. Pathologic stage pT3-T4 was more likely to recur than T2a-T2c ($p<0.0001$, HR 4.8), and pT2R1 more likely to recur than pT2a-T2c ($p<0.0001$, HR 5.3). Tumors with GG5 were more likely to recur than GG1 ($p<0.0001$, HR 2.9). Nuclear grade III was more likely to recur than Nuclear grade I ($p=0.0008$, HR 3.2), and nuclear grade II more likely than Nuclear grade I ($p=0.01$, HR 2.1).

Conclusions: Independent of stage, nuclear grade was equally as predictive of BCR as tumor growth pattern (GG). Consideration should be given to its incorporation into grading system.

913 Role of SATB2 in Distinguishing the Site of Origin in Glandular Lesions of the Bladder/Urethra: An Immunohistochemical Study

Giovanna Giannico, Allen M Gown, Jonathan I Epstein, Justin A Bishop. Vanderbilt University Medical Center, Nashville, TN; PhenoPath Laboratories, Seattle, WA; Johns Hopkins Medical Institutions, Baltimore, MD.

Background: The differential diagnosis of glandular lesions of the bladder/urethra can be challenging due to significant morphologic and immunohistochemical overlap between primary lesions and metastasis/direct extension from adjacent organs. Special AT-rich sequence-binding protein 2 (SATB2), encoded on chromosome 2q32-33, is a recently described DNA-binding protein involved in osteoblast lineage commitment and expressed in colorectal and appendiceal neoplasms.

Design: In this study, we hypothesized that immunohistochemistry for SATB2 may be of value in distinguishing primary adenocarcinoma of the bladder/urethra and urothelial carcinoma with glandular differentiation from gastrointestinal and endocervical primaries. SABT2 nuclear labeling was semiquantitatively scored as 0 (no tumor cells staining), 1+ (≤25% tumor cells), 2+ (26% to 50%), 3+(>50%).

Results: The study included 45 primary adenocarcinomas of the bladder/urethra, 18 urothelial carcinomas with glandular differentiation, 26 adenocarcinomas of the uterine cervix, and 21 colorectal adenocarcinomas extending to the bladder. Positive SATB2 immunostaining (2-3+) was observed in 21/45 (47%) primary bladder/urethral adenocarcinomas, 16/21 (76%) colorectal adenocarcinomas, and in the glandular component of 4/18 (22%) urothelial carcinomas with glandular differentiation. SABT2 was negative in 25/26 of endocervical adenocarcinomas and showed focal weak staining (1+) in 1/26 (4%).

DIAGNOSIS	SCORE, N (%)2-3+	SCORE, N (%)0-1+
Bladder/urethral adenocarcinoma	21/45 (47)	24/45 (53)
Colorectal adenocarcinoma	16/21 (76)	5/21 (24)
Urothelial carcinoma with glandular differentiation	4/18 (22)	14/18 (78)
Endocervical adenocarcinoma	0/26 (0)	1/26 (4)

Conclusions: We conclude that SABT2 immunohistochemistry is not useful in supporting urothelial versus gastrointestinal origin in the differential diagnosis of glandular lesions of the bladder/urethra.

914 CD34+ Tubular Basement Membrane in Germ Cell Tumors: Staging Pitfall

Amanda Gohlke, Cora Uram-Tuculescu, Susan Pitt, Mahul B Amin, Steven C Smith. Virginia Commonewealth University Health System, Richmond, VA; Cedars-Sinai Medical Center, Los Angeles, CA.

Background: Staging is an important factor for treatment planning and prognosis in germ cell tumors, including seminoma. Vascular invasion is a key parameter, establishing pT2, for which an immunohistochemical (IHC) marker, such as CD34, may be performed exceptionally to confirm suspicion of vascular invasion. We recently reviewed two consultation cases of seminoma that had been incorrectly upstaged due to 'aberrant' CD34 positivity in the tubular basement membrane of entrapped seminiferous tubules with germ cell neoplasia in situ (GCNIS). Herein, we endeavored to further characterize the prevalence of this potential pitfall, as follows.

Design: Cases of pure seminoma were identified retrospectively and reviewed to identify examples of seminomas with at least focal "interstitial" pattern of entrapped seminiferous tubules (whether involved by GCNIS or incidental). Representative blocks were recut and stained to assess the prevalence of CD34 positivity by our routine CLIA-compliant protocol. ERG immunostain was used as a specific marker of endothelium to exclude true vascular invasion in selected cases.

Results: Of 28 consecutive seminoma cases, 14 examples with interstitial pattern were identified and studied. In all cases studied, CD34 IHC highlighted the basement membrane of entrapped seminiferous tubules at similar intensity to its reaction in adjacent positive internal control vascular endothelium. ERG did not stain the tubular basement membrane, highlighting only nuclei of endothelial cells.

Conclusions: Entrapped seminiferous tubules stained positively for CD34 with high prevalence, presenting a diagnostic pitfall for staging. We recommend use of deeper sections, more specific vascular markers (such as ERG), and careful sampling to establish appropriate stage.

915 Programmed Death-1 Expression in Micropapillary Urothelial Carcinoma of the Bladder: Role for Immune Checkpoint Inhibitors

Abigail L Goodman, Adeboye O Osunkoya. Emory University Hospital, Atlanta, GA.

Background: There is now increasing evidence supporting the role of immune checkpoint inhibitors in the management of patients with malignant melanoma and other malignancies. Programmed Death-1 (PD-1) plays a pivotal role in regulating host immune responses. However, PD-1 expression in micropapillary urothelial carcinoma (UCA) has not been well characterized. In this study, we sought to analyze the expression of PD-1 in a large cohort of patients with micropapillary UCA of the bladder.

Design: A search was performed through our Urologic Pathology files and expert consult files of the senior author for cases of micropapillary UCA of the bladder. Only cases with available tissue blocks were selected. Immunohistochemical stains for PD-1 was performed on all cases. Cases were considered negative for PD-1 when less than 5% of cells had positive expression.

Results: Twenty-seven cases were identified. The mean patient age was 68 years (range: 39–87 years). There was a male predominance. The pathologic stages were as follows: 1 case of pTa, 4 cases of pT1, 5 cases of pT2, 12 cases of pT3a, 4 cases of pT3b, and 1 case of pT4a. Other pathologic parameters were as follows: 16/27 (60%) had angiolymphatic invasion, 12/27 (44%) had lymph node metastasis and 7/12 (58%) of those had extra-nodal extension. Nineteen of 27 (70%) cases had positive PD-1 expression in the adjacent lymphocytes. Although 8/27 (30%) cases had negative PD-1 expression in the adjacent lymphocytes, positive expression was present in all stage categories (early and advanced cases). Positive PD-1 expression was also noted in a subset of patients who failed platinum based neoadjuvant chemotherapy.

Conclusions: This is one of the largest studies to date on the expression of PD-1 in micropapillary UCA of the bladder. There is clearly a role for immune checkpoint inhibitors such as recently FDA approved anti-PD-1 agents Atezolizumab and Nivolumab in the management of patients with micropapillary UCA of the bladder. In addition, a subset of patients who have failed platinum based neoadjuvant chemotherapy for micropapillary UCA may also benefit from these agents.

916 Microsatellite Unstable (MSI-H) Prostate Cancer (PCA): Correlation of Morphology, Mismatch Repair Immunohistochemistry (MMR-IHC) and Next Generation Sequencing (NGS)

Anuradha Gopalan, Wassim Abida, Sumit Middha, Joshua Armenia, Joseph S Sirintrapun, Ying-Bei Chen, Hikmat Al-Ahmadie, Samson W Fine, Satish K Tickoo, David Solit, Michael F Berger, Nikolaus Schultz, Howard I Scher, Jinru Shia, Victor E Reuter. MSKCC, NY, NY.

Background: Recent reports of hypermutated (HYP-M) subtype in advanced metastatic (MET) and rarely primary (PRIM) PCA show association with DNA mismatch repair (MMR) gene defects and microsatellite instability (MSI). Morphology and utility of MMR IHC in these tumors have not been reported in detail. We studied morphology of HYP-M tumors, correlated MMR IHC with somatic MMR gene mutations (MUT) detected by NGS and compared with tumors with isolated MMR gene defects but not HYP-M.

Design: PRIM from 103 and MET from 348 patients underwent targeted NGS and screening for HYP-M (>20 MUT)/isolated MMR gene abnormalities. Morphology of these tumors was studied. IHC for MSH2/MSH6/MLH1/PMS2 was correlated with NGS results. MSIsensor, software that derives MSI status from paired sequence data, was used to confirm MSI-H (MSI-High) status. Data was correlated with clinical history.

Results: By MSIsensor, MSI-H was present in 3/103 (2.9%) PRIM and 5/348 (1.4%) MET. Two PRIM had matched MET and 2/5 MET cases had >1 MET; all had concordant MSI status. MET included lymph node (5), lung (1), adrenal (1), soft tissue (1) and bone (2). All 8 MSI-H tumors were HYP-M (range 23-45 MUT). None of the 6 cases with isolated MMR gene abnormalities were MSI-H (range 1-10 MUT).

IHC showed loss of MSH2/MSH6 in 7/8 MSI-H tumors (sensitivity 87.5%). One tumor, with retained MMR IHC, had a germline MUT in PMS2 - c.137G>T, which likely led to a non-functional but antigenically active PMS2 protein. IHC profile was 100% concordant between PRIM/MET, sequential PRIM samples pre/post radiation and hormonal therapy(n=1) and across all MET sites (n=1).

11 tumors had ≥ 1 somatic MMR gene MUT. These included 3/8 (37.5%) MSI-H (all 3 had MUT in MSH2/MSH6 ± MUT in MLH1) and 7/443 (1.6%) non-MSI-H/ non-HYP-M cases. One patient had two different MSH6 somatic MUT across 3 MET sites, suggesting sporadic MSI-H.

Gleason score of two PRIM was 9; one was small cell CA. Morphology was acinar/cribriform/solid adenocarcinoma in 7 and small cell in 1 case. Only one tumor had pronounced inflammatory infiltrate. Overall, morphologic patterns of MSI-H PCA were not distinct relative to their non-MSI-H counterparts.

Conclusions: 2.9% of PRIM and 1.4% of MET PCA are MSI-H, primarily deficient in MSH2/MSH6. NGS, currently used to guide management in advanced cancers, reliably detects MSI. Somatic mutations in MMR genes are associated with MSI-H, but not exclusively. MSI-H prostate carcinoma may show intense lymphocytic infiltrate, but overall morphologic patterns are not as distinctive as in colorectal/endometrial tumors.

917 Anaplastic Features Do Not Influence Expression of PD-1 and PDL-1 in Testicular Seminomas

Zakaria Grada, Siraj M El Jamal, Yiang Hui, Nour Almardini, Kara A Lombardo, Ali Amin. Rhode Island Hospital and Alpert Medical School of Brown University, Providence, RI; University of Mississippi Medical Center, Jackson, MS.

Background: Programmed cell Death 1 (PD1) immunotherapy for aggressive solid tumors has shown promising data in achieving complete remission. Also inhibition of the interaction between PD1 and Programmed Death receptor Ligand 1 (PDL1) enhances T-cell responses and mediates robust anti-tumor activity. Approximately 10–15% of pure seminomas fail to respond to chemotherapy with first-line treatment. Some studies have found correlation between "anaplastic" histomorphologic features and the outcome in seminoma. We aimed to analyze correlations between anaplastic features and expression of PD1/PDL1 in testicular seminomas.

Design: Forty-five cases of pure seminoma were retrieved from the archives of Rhode Island Hospital from 2008-2016. The slides were reviewed for anaplastic features (mitotic count, nuclear anaplasia, necrosis and lymphocytic infiltration rate). The cases were divided into three groups based on lymphocyte-to-tumor ratio: <30%=1, 30-50%=2 and >50%=3. Immunohistochemistry for PD1/PDL1 was performed. The expression was graded based on intensity (weak=1, intermediate=2 and strong=3) and extent of expression (0-5%=0, 5-25%=1, 25-50%=2, >50%=3). Statistical analysis was performed using Spearman rho test.

Results: Age range was 19-62 (median: 37) years. Eleven cases (36%) presented with advanced stage (2 and 3, AJCC 2010). PDL1 was expressed in both tumor cells and lymphocytic population, and PD1 expression was limited to the lymphocytes. There was no statistical significant correlation between mitotic rate, nuclear anaplasia or necrosis with PD1/PDL1 expression. However, the tumor-infiltrating lymphocyte density positively correlated with PDL1 expression on the tumor cells (R value = 0.71; p<0.0001). In 86% of cases, weak to strong PD1 expression was noted in the lymphocytes. Five cases with advance pathological stage and lymphovascular invasion showed direct correlation between lymphocyte density and PD1 and PDL1 expressions.

Conclusions: Seminomas with anaplastic features show similar PD1/PDL1 expression compared to those without anaplastic features. However, our data suggest that seminomas with higher lymphocyte density overexpress these markers independent of tumor stage. Therefore, anti-PD1/PDL1 immunotherapy works best if utilized in classic seminomas without anaplastic features.

918 Characteristics of Small Renal Cell Carcinomas (≤4 cm) Upstaged to pT3 on Final Pathology

Tiffany Graham, Win Shun Lai, Jessica Zarzour, Soroush Rais-Bahrami, Jennifer Gordetsky. University of Alabama at Birmingham, Birmingham, AL.

Background: Many renal cell carcinomas (RCCs) are incidentally found on radiologic imaging, increasing the detection of small renal masses (≤4cm). While these tumors are considered clinical stage T1a, a subset is found to have extra-renal extension on final pathology (pT3). Pre-operative prediction of upstaging is important in choosing the appropriate surgical management approach. Herein, we analyze the clinical, pathologic, and imaging characteristics of RCCs classified as clinical T1a that were upstaged to T3 on final pathology.

Design: We retrospectively reviewed our surgical pathology database from 2010-2016 for patients with RCCs ≤4 cm based on final pathology. Clinical, pathologic, and imaging characteristics were reviewed. Cases with extra-renal extension were identified and given a R.E.N.A.L. nephrometry score (R=radius, E=exophytic/endophytic, N=nearness to sinus/collecting system, A=anterior to coronal plane, L=location to polar line).

Results: Thirty of 255 (11.8%) RCCs ≤4 cm were upstaged to pT3 on final pathology, which included 19 (63.3%) Caucasians, 10 (33.3%) African Americans and 1 (3.3%) Other. Average patient age was 61±8.5 years. Average pre-operative creatinine was 2.01±2.7 mg/dL. Average overall R.E.N.A.L. nephrometry score was 7.24±1.61. 16/30 (53.3%) patients underwent radical nephrectomy and 14/30 (46.6%) underwent partial nephrectomy. Average tumor size was 2.9±0.71 cm. RCC subtypes included 24/30 (80%) clear cell RCCs, 3/30 (10%) Papillary RCCs, 2/30 (6.7%) unclassified RCCs, and 1/30 (3.3%) mucinous tubular and spindle cell carcinoma. Average grade was 2.6±0.72. Extrarenal extension was most common in the perinephric fat (80%), followed by renal vein (10%), and renal sinus (10%). Renal vein involvement, lymph node metastasis, and sarcomatoid features were seen in 13.3%, 10%, and 3.3% cases, respectively. Compared to the pT1a control group, pT3 tumors ≤4 cm were more likely to have larger tumor sizes (2.9±0.71 cm vs. 2.5±1.0 cm;p=0.046), tumor necrosis (30% vs. 0.1%; p=.002) and a higher Grade (2.6±0.71 vs. 2.3±0.6;p=.023).

Conclusions: The prediction of which clinical T1a renal masses will be upstaged to pathologic T3 stage affects clinical management. Tumors close to 4 cm, areas of necrosis, and elevated R.E.N.A.L. nephrometry score may be helpful in pre-operative planning for patients with small renal masses. If a renal biopsy is preformed, tumor grade should also be considered.

919 Association of Genomic Prostate Scores (GPS) with Prostatectomy Rates and Pathology at the Time of Prostatectomy

Nancy Greenland, Bradley Stohr, Jeffry Simko. University of California, San Francisco, San Francisco, CA.

Background: The Oncotype Dx Prostate Cancer Assay is a clinical gene expression-based predictor of prostate cancer aggressiveness, with increasing Genomic Prostate Scores (GPS) correlating with higher probabilities of adverse pathology. These scores have the potential to influence clinical decision-making regarding prostatectomy. We hypothesized that patients with increased GPS would be more likely to undergo prostatectomy, and, at prostatectomy, have extraprostatic extension and higher percentages of Gleason pattern 4.

Design: GPS is calculated based on relative expression for 17 genes, with 12 cancer-related genes associated with stromal response, androgen signaling, proliferation, and cellular organization, and 5 housekeeping genes used as reference. Gene expression is assessed on the prostate needle biopsy sample of largest amount of the highest grade. Between May 2013 and August 2015, GPS was determined for 319 prostate cancer biopsies from 296 patients at the University of California, San Francisco (UCSF). Associations between pathology findings and GPS were performed using either unpaired Student's t-test or multivariable regression.

Results: As of April 2016, 75 of the 296 patients (25.3%) had undergone prostatectomy. GPS was strongly associated with increased likelihood of prostatectomy after controlling for percentage Gleason pattern 4 at biopsy, with a prostatectomy odds ratio of 1.75 (95% confidence interval of 1.30-2.36, $P < 0.001$) per 10 point increase in GPS. In patients who underwent prostatectomy, GPS were higher in patients found to have extraprostatic extension (mean 37.4 -$\pm$ 2.3 versus 31.0 $\pm$ 1.7, $P = 0.03$). However, extraprostatic extension was not associated with either GPS ($P = 0.09$) or biopsy percentage of Gleason pattern 4 ($P = 0.80$) in multivariable analysis. Gleason pattern 4 percentages at prostatectomy were associated with biopsy percentage of Gleason pattern 4 ($P = 0.003$) but not GPS ($P = 0.58$).

Conclusions: GPS may be influencing clinical decision-making, as patients with higher GPS were more likely to undergo prostatectomy after controlling for biopsy findings. However, GPS was only weakly associated with worse pathology at the time of prostatectomy. More research is needed to fully understand the clinical significance of this test and to ensure it does not result in unnecessary procedures.

920 NKX3.1 and PSMA Are Reliable Markers for Prostatic Carcinoma in Bone Metastasis After Decalcification

Sergei R Guma, Jonathan Melamed, Ming Zhou, Fang-Ming Deng. New York University Medical Center, New York, NY.

Background: Prostate specific antigen (PSA), prostate specific membrane antigen (PSMA) and NKX3.1 are sensitive and prostate-specific markers frequently used for the diagnosis of metastatic prostate cancer (mPCa). International Society of Urological Pathology recommends use of PSAas the first IHC marker to identify PCa. If the tumor is equivocal/weak/negative for PSA, then P501S and NKX3.1 are suggested. However, no specific studies have attempted to compare the staining sensitivity of these markers post specimen decalcification of bone specimens. In this study we analyze the staining sensitivity of PSA, PSMA and NKX3.1 in bone specimens with mPCa after decalcification.

Design: We studied 18 cases of mPCa to the bone. All cases were decalcified for 1 to 4 hours prior to H&E staining and IHC workup. Four cases were biopsies from vertebral bodies, 5 from the femur, 3 from the iliac bone, 2 from ribs, 2 from the pubic ramus, 1 from the sacrum and 1 from the skull. Immunohistochemical staining pattern of PSA, PSMA and NKX3.1 was defined as follows: negative(no staining), focally positivity (= < 10%) and diffusely positive (= > 10%). Focal and diffuse positivity is considered positive.

Results: PSA was positive in 59% (9/15) cases, while PSMA and NKX3.1 were positive in all cases. This difference was statistically different ($p = 0.006357$). The frequency of positive NKX3.1 staining in decalcified samples of prostatic carcinoma metastatic to the bone is also statistically higher than that of PSA staining, when analyzed by the Chi-square test (Chi-square statistic: 9.2647; $p = 0.002336$). When comparing PSMA and NKX3.1 positive staining, NKX3.1 tended to be diffusely positive at a higher frequency. However this difference was not statistically significant.

Conclusions: This study demonstrates that PSMA and NKX3.1 are more sensitive markers than PSA for mPCa to the bone following decalcification. We recommend use of PSMA and NKX3.1, rather than PSA, as the IHC markers to confirm mPCa to the bone.

921 Argininosuccinate Synthetase Loss in High Grade Neuroendocrine Carcinomas of the Urinary Bladder: Implications for Targeted Therapy with ADI-PEG 20

Sounak Gupta, Divya Sahu, Prabin Thapa, John C Cheville, Donna Hansel. UCSD, La Jolla, CA; Mayo Clinic, Rochester, MN.

Background: High grade neuroendocrine carcinomas (HGNEC) of the urinary bladder encompass small cell (SCNEC) and large cell neuroendocrine carcinomas (LCNEC) and are currently managed with neoadjuvant chemotherapy and radical cystectomy for localized disease. We evaluated the potential to incorporate arginine metabolism targeting as a targeted therapy approach. Arginine is a semi-essential amino acid, with argininosuccinate synthetase (ASS1) serving as the rate-limiting step in its biosynthesis. Neoplasms that show low-absent ASS1 expression require extracellular arginine, and can be targeted using arginine-degrading enzymes such as pegylated arginine deiminase (ADI-PEG 20), which are currently in clinical trials. Initial studies have shown that a high percentage of SCNEC (14 of 19, 74%) lack ASS1 expression. Herein, we have sought to validate these findings in a large cohort of HGNEC.

Design: The cohort consisted of 74 patients with HGNEC (SCNEC: 63; LCNEC: 5; mixed features: 6) treated by radical cystectomy. The majority had advanced local disease (≥pT2: 71 of 74, 96%), and 47 (of 74, 64%) died of disease. Tissue microarrays were constructed using four representative 1.0 mm cores from each patient and were immunostained for ASS1 (Polaris Pharmaceuticals, San Diego, CA). Semi-quantitative analysis of IHC intensity was performed using a range of 0 (absent), 1+ (weak), 2+ (moderate) and 3+ (intense) staining. Normal urothelium and hepatic parenchyma showed 2 to 3+ staining and were used as positive controls. ASS1 expression status was dichotomized into cases with absent to weak staining, and those with moderate to high expression.

Results: 58 (74%) patients with HGNEC showed complete absence of ASS1 expression, while the number of patients with absent to low (0 to 1+) expression included 63 (of 74, 85%) cases. 5-year survival from disease-specific death was not statistically significant between these groups. This data suggests that loss occurs in the majority of patients, which is an indicator of response to ADI-PEG 20. Interestingly, all patients with LCNEC (5 of 5, 100%) and mixed morphologic features (6 of 6, 100%) showed absent ASS1 expression.

Conclusions: Our findings show that a large proportion of HGNEC including SCNEC, LCNEC and tumors with mixed morphology show low (85%) to absent (74%) expression of ASS1. These tumors are potential candidates for arginine deprivation therapy using drugs such as ADI-PEG20. Further studies are needed to validate these findings and to determine the therapeutic efficiency of such agents.

922 6p21 Amplified Renal Cell Carcinoma: A Distinct Entity with Potential Implications for Clinical Management.

Sounak Gupta, Sarah H Johnson, George Vasmatzis, Priya Rao, Brian A Costello, Bradley C Leibovich, R H Thompson, John C Cheville, William R Sukov. Mayo Clinic, Rochester, MN; MD Anderson Cancer Center, Houston, TX.

Background: A subset of RCCs show TFEB overexpression secondary to *MALAT1-TFEB* gene fusion. We hypothesized that alternate mechanisms of TFEB overexpression such as gene amplification, were also likely to have the same effect. We sought to determine the frequency of amplification of *TFEB* and the adjacent *VEGFA* gene at 6p21. As patients with metastatic RCCs are managed with anti-VEGF therapies, we retrospectively assessed potential therapeutic response in patients with amplified tumors.

Design: 876 RCCs [Papillary (P): 395, Clear Cell (CC): 310, Chromophobe (Ch): 130, Unclassifiable: 41] were screened for amplification by FISH for *TFEB* and *VEGFA*. Cases were classified as having low level (LAmp: 5-10 copies) and high level amplification (HAmp: >10 copies). A subset was analyzed for copy number status (n=6; 3 SNP genomic microarray, 3 TCGA), and by mate pair sequencing (MPS, n=1) for structural changes. Each case was reviewed for histopathology, and response to VEGF-targeted therapy. The cBioPortal platform was used to analyze TCGA data for 6p21 amplification (794 cases-P: 280; CC: 448; Ch: 66).

Results: 10/875 (1.1%) internal cases, 1 external case and 3/794 (0.4%) TCGA cases showed TFEB HAmp, while 14/875 (1.6%) internal cases showed TFEB LAmp. All but one case had concurrent *VEGFA* amplification (HAmp: 12/13; LAmp: 14/14). This was confirmed with SNP genomic microarray (n=6) and MPS. MPS showed 6p rearrangement resulting in *DEK-ARMC12* fusion, with implications for Wnt signaling. These tumors occurred in adults (mean age: 64) with the majority being initially classified as P RCC (17/28, 61%). The average size was 8.8cm, with over half being ≥pT3 (15/28, 54%). Most showed high ISUP nucleolar grade (≥Gr3: 21/23, 91%) and oncocytic and tubulo-papillary features. While 3 (of 28, 11%) cases showed biphasic features, none exhibited smaller cells clustered around basement-membrane material. Metastases were seen in 12 (of 26, 46%) cases and death from disease in 11 (of 26, 42%). Of the latter group, 4 (of 24, 17%; HAmp: 3, LAmp: 1) patients received targeted therapy including Sunitinib, and Pazopanib and had a mean survival of 31 months (range: 17-50) post nephrectomy. No significant differences were identified between the HAmp and LAmp groups.

Conclusions: Our results suggest that a subset of RCC show genomic amplification of the 6p21 region including *TFEB* and *VEGFA*. These are aggressive tumors primarily occuring in older individuals that have a specific histologic appearance. Clinical data suggests that these tumors may respond to anti-VEGF therapy.

923 Molecular Characterization of High Grade Neuroendocrine Carcinoma of the Urinary Bladder

Sounak Gupta, Loren P Herrera Hernandez, Donna Hansel, Sarah H Johnson, Rafael E Jimenez, Farhad Kosari, John C Cheville. Mayo Clinic, Rochester, MN; UCSD, La Jolla, CA.

Background: High grade neuroendocrine carcinomas (HGNEC) of the urinary bladder include a morphologic spectrum of NEC with small cell (SCNEC), large cell (LCNEC), and combined features (mixedNEC). A limited number of studies have shown that these HGNEC show similar behavior including responsiveness to neoadjuvant chemotherapy for localized disease. As a diagnosis of HGNEC has a significant impact on patient management, we sought to characterize the molecular signature of these tumors to better define them, including determining whether there is a molecular basis of morphologic divergence of LCNEC from conventional SCNEC.

Design: Flash frozen specimens for 10 well-characterized cases of HGNEC were retrieved. These cases (9 pure SCNEC and 1 pure LCNEC) were analyzed by RNA-seq as well as Mate Pair Sequencing (MPS). MPS was performed for whole genome DNA. Paired reads were mapped to the human GRCh38 reference genome, and discordant

mate pair reads, mapping >15 kb apart or in different chromosomes, were selected for further analysis. RNA-seq data on 20 typical urothelial carcinomas (UC), obtained from the publicly available The Cancer Genome Atlas (TCGA) database, served as controls.
Results: As expected, RNA-seq analysis revealed a unique expression profile for UC and HGNEC. UC were characterized by the expression of Uroplakins (*UPK1A*, *UPK2, UPK3B*), Claudins (*CLDN3, CLDN4*) and Cytokeratin 7 (*KRT7*). HGNEC showed characteristic neuroendocrine differentiation [*SYP* (Synaptophysin), *CHGA* (ChromograninA), *CHGB* (ChromograninB), *NCAM1* (CD56), *INSM1* (Insulinoma-associated 1), *PCSK1* (Proprotein Convertase Subtilisin/Kexin Type 1), *SCG2* (Secretogranin 2) and *ASCL1*]. Overall, HGNEC showed higher levels of expression of transcription factors and markers of epithelial to mesenchymal transformation. Surprisingly, the LCNEC showed a distinct pattern of neuroendocrine differentiation compared to SCNEC, characterized by low-absent *SYP, CHGA*, *CHGB, INSM1* and *ASCL1* expression, moderate *NCAM1* and *PCSK1* and high *SCG2*. MPS showed numerous copy number variations (CNV), including large deletions and amplifications, and there was significant heterogeneity between cases.
Conclusions: HGNEC show complex molecular alterations with numerous CNV, including large deletions and amplifications, and significant heterogeneity between cases. LCNEC show a distinct pattern of neuroendocrine differentiation from SCNEC. Additional studies will be required to validate these changes as contributing to morphologic divergence. Our study helps to define the molecular signature of HGNEC of the urinary bladder.

924 Clear Cell Papillary Renal Cell Carcinoma: A Whole Exome Sequencing Study

Sabina Hajiyeva, Weihua Huang, Changhong Yin, Ximing J Yang, John T Fallon, Minghao Zhong. New York Medical College, Valhalla, NY; Northwestern University, Chicago, IL.
Background: Clear cell papillary renal cell carcinoma (CPRCC), a recently recognized, distinct renal neoplasm, composes of cells with clear cytoplasm lining cystic, tubular, and papillary structures. These tumors have immunohistochemical and genetic profiles distinct from clear cell renal cell carcinoma and papillary renal cell carcinoma. Molecular-genetic changes are distinct as well: Alterations of chromosome 3p and the *VHL* gene are lacking. Although low copy number gains of chromosomes 7 or 17 have been identified in a few tumors, most of these carcinomas do not possess these abnormalities. The comprehensive, characteristic genetic alterations, however, have not yet been identified
Design: Three tumors with an original diagnosis of clear cell renal papillary renal cell carcinoma were retrieved from the surgical pathology archives and reviewed. All cases had typical morphology and IHC pattern (CA9+ and CK7+). Microdissection was used in some cases to ensure that at least 20% of the cells were neoplastic. Genomic DNA was extracted from formalin-fixed paraffin-embedded (FFPE) tissues by Qiagen AllPrep DNA/RNA Kit. The isolated genomic DNA was subject to targeted sequencing by using Illumina Exome Enrichment & Sequencing Kits. We used Illumina NextSeq 500 system for paired-end (151 bp × 2) sequencing and Illumina on-instrument NextSeq Reporter to generate the variant call format (VCF) files through BWA alignment/mapping and somatic variant caller. By using Illumina VariantStudio, we performed variant filtering, annotation and interpretation with various sources of variant databases. And finally, we focused on variants in most frequently mutated genes associated with RCC from TCGA
Results: The WES generated data with mean coverage > 50× and 20,000-30,000 single nucleotide variants (SNV) for each specimen. No recurrent mutation was identified in these tumors. No *VHL* mutations was identified neither. Interestingly, CCRCC associated gene mutations: *SETD2, MAGEC1, BTNL3, NBPF14, TXNIP* and PRCC associated gene mutations: *SETD2, FAT1* were identified in clear cell papillary renal cell carcinoma
Conclusions: This is the first comprehensive, molecular evaluation of clear cell papillary renal cell carcinoma. It seems like that CPRCC is heterogeneous at molecular level. Negative of *VHL* gene mutation may indicate non-responsive for Anti-VEGF therapy for this tumor. Both CCRCC and PRCC associated gene mutations were also found in clear papillary RCC. This may explain that CPRCC has overlapping features of CCRCC and PRCC at morphological and IHC levels

925 Non-Invasive Spread of Urothelial Carcinoma (UCa) within Urachal Remnants: An Underecognized Phenomenon with Potential for Overstaging as Muscularis Propria (MP)-Invasive Disease

Lisa Han, Gladell P Paner. University of Chicago, Chicago, IL.
Background: It is well recognized that urothelial CIS may spread into von Brunn's nests and cystitis cystica/glandularis in the lamina propria (LP) with potential for overstaging as LP-invasion (pT1), particularly in fragmented TURBT samples. However, a much deeper extension by UCa within pre-existing urachal remnants in the bladder MP is unrecognized and has never been previously characterized.
Design: Herein, we describe 6 examples of non-invasive spread by UCa within pre-existing urachal remnants identified in the dome of cystectomy specimens.
Results: The patient's age ranged from 53 to 87 yo (mean 70.5) and all were males. Highest tumor stage were pTis (1), pT1 (2) and ≥pT2 (3). In 6/6, the main bladder tumor involved (at least) the dome where all (6/6) urachal remnant extensions were also identified. The urachal remnants contained flat or urothelial CIS (5/6) and non-invasive papillary UCa (PUC) (2/6) (1 had mixed). The UCa extensions had regular outer contour that followed the remnant outline and with no stromal reaction. The 2 PUCs exhibited papillae within the urachal lumina and inverted growth. In 4/6, admixed benign remnant epithelium was identified that consisted of glandular (3) and/or urothelial (3) cells. In 6/6, urachal remnant involvement by the non-invasive UCa extended into the MP, including into the deeper half of MP in 2 cases. In 5/6, urachal UCa extension was deeper than the overlying bladder mucosa urothelial CIS (4/6) and LP-invasive UCa (1/6). In 3/6, the depths of MP layer extensions by the non-invasive UCa within the urachal remnants were deeper than the stage of the main tumor (pTis/pT1) in the entire bladder.
Conclusions: We report a heretofore-described phenomenon of non-invasive extension by UCa from the bladder surface into urachal remnants within the MP. Recognition of this unique process, although rare, is important to avoid potential overstaging of superficial UCa as MP-invasive disease that may impact the patient's tumor management.

926 Comparison of PELP1 and GATA3 Protein Expression in Urothelial Carcinoma in Cystoprostatectomy Specimens

Lakshmi Harinath, Shweta Patel, Edward Lynch, William Thompson, Jan F Silverman. Allegheny General Hospital, Pittsburgh, PA.
Background: Urothelial carcinomas can have a variety of histologic appearances and therefore, immunohistochemistry (IHC) is occasionally needed to make a definitive diagnosis. PELP1 is a novel nuclear hormone coregulator that has recently been associated with the development of breast carcinoma. In one study, PELP1 was found to have a higher frequency of expression and stronger staining intensity as compared to GATA3 in metastatic breast carcinomas in surgical pathology specimens. Since GATA 3 is also used as a marker for urothelial carcinoma, we evaluated the IHC staining pattern PELP1 and GATA3 in urothelial carcinoma in cystoprostatectomy specimens.
Design: We examined twenty four cases of previously diagnosed invasive urothelial carcinoma in cystoprostatectomy specimens. We stained all of the slides with GATA3 and PELP 1 antibody. The intensity of staining and the percentage of tumor cells expressing both the proteins were graded. The staining intensity was graded from weak (1+) to strong (3+). The percentage of cells that expressed the proteins was rated as less than 25%, 25-75% and above 75%.
Results: We found that in 87.5 % (21/24) of cases, GATA 3 and PELP1 protein expression were concordant. The PELP1 antibody had a punctate intranuclear staining pattern, whereas the GATA3 displayed a homogenous nuclear staining pattern. In 12.5% (3/24) of cases, PELP1 stained the tumor cells more diffusely as compared to GATA3, although the staining intensity appeared to be less than GATA3 due to the characteristic delicate nuclear staining pattern.
Conclusions: 1) We believe that this is the first study demonstrating PELP1 staining in urothelial carcinoma.
2) PELP1 and GATA3 have equivalent staining in urothelial carcinoma.
3) However, a potential advantage of PELP1 antibody is the more diffuse staining as compared to GATA3 in a small percentage of the cases.
4) The heterogeneity of GATA3 staining could be source for a false negative staining. Therefore, we believe that adding PELP1 antibody in the work up of metastatic urothelial carcinoma can be of value.

927 Prognostic Biomarkers of Systemic Inflammation in Patients with Metastatic Renal Cell Carcinoma

Wayne B Harris, Omer Kucuk, Bradley C Carthon, Theresa W Gillespie, Viraj A Master, Adeboye O Osunkoya. Emory University School of Medicine, Atlanta, GA.
Background: Patients with metastatic renal cell carcinoma (mRCC) are typically assigned to a specific risk group at baseline.Once assigned to a favorable-, intermediate- or poor-risk category, the discussion of risk is seldom revisited. The assumption is that the risk classification does not change. There is no established mechanism for reassigning the risk status of individual patients in a manner that reflects the impact of therapy on clinical outcome. The goal of the current study was to devise a dynamic prediction model for mRCC based on fluctuations in the intensity of systemic inflammation (ISI).
Design: A search was made at our institution for patients diagnosed with mRCC. Inclusion criteria were as follows: age ≥18, treatment with targeted therapy for clear cell or non-clear cell mRCC and the concomitant assessment of C-reactive protein (CRP) and albumin levels on three or more occasions that were at least 10 days apart. Discovery, expansion and external validation cohorts were identified. Established prognostic variables were evaluated by univariate and multivariate analyses. Algorithms for the modified Glasgow Prognostic Score (mGPS) were used to quantify intensity of systemic inflammation (ISI) at all time points with CRP and albumin as prognostic covariates for overall survival (OS) in an extended Cox regression model.
Results: A total of 181 patients were identified, and ISI was assessed on 3186 occasions. Changes in risk status were observed in 131/181 (72%) patients. The hazard ratio for OS was 21.41 (95% CI 8.26-55.50) with a type3 p-value of <0.001 for the reference cohort and 9.68 (2.07-45.31) with a type3 p-value of 0.006 for the external validation cohort when time points associated with severe inflammation were compared to all other time points. The bias-corrected c-statistic was 0.839 (0.773-0.905) and 0.818 (0.691-0.946), respectively. Of the remaining 28% in whom changes in risk factors were not observed, those for whom severe systemic inflammation (SSI) was never detected were among the longest survivors, whereas those with persistent SSI were among the shortest.
Conclusions: Time-dependent effects of prognostic biomarkers are of sufficient magnitude that they can no longer be disregarded in prediction models for mRCC. ISI is a biomarker for mRCC that reflects changes in the risk status of individual patients over time.

928 Should Gleason Score 6 Prostate Cancer Be Renamed as "Not Cancer"? Incidence of Extra-Prostatic Extension at Radical Prostatectomy (RP) with Pure Gleason Score 3+3=6 Cancer

Oudai Hassan, Jonathan I Epstein. Johns Hopkins University, Baltimore, MD.
Background: In part because pure Gleason Score 6 (GS6) prostate cancer at RP has no ability to metastasize to lymph nodes and because even without definitive therapy it is a relatively indolent disease, some experts have questioned whether GS6 cancer should

be renamed with a term that does not contain the word "cancer". The word "cancer" creates fear and contributes to the overtreatment of GS6 cancer. The risk of locally aggressive behavior in pure GS6 prostate cancer, defined by extra-prostatic extension (EPE) or seminal vesicle invasion (SV), using contemporary grading criteria has not been studied in large cohorts.

Design: All cases with GS6 and Gleason Score 3+4=7 (GS347) on RP between 2005-2016 at our institution were included. Focal EPE was defined subjectively as a few neoplastic glands outside the prostate on 1-2 sections, while non-focal EPE was defined as anything more than focal EPE. Despite the subjective nature of this definition, it has correlated with recurrence following RP in many studies.

Results: 3,291 men with GS6 and 4,478 men with GS347 were studied. 167/3291 (5.1%) GS6 cases showed focal EPE compared with 657/4478 (14.7%) GS347 cases and the subset of 120/1031 (11.7%) GS347 cases with less than 5% Gleason pattern 4. 93/3291 (2.8%) GS6 cases showed non-focal EPE compared with 705/4478 (15.8%) GS347 cases and the subset of 78/1031 (7.6%) GS347 cases with less than 5% Gleason pattern 4.

StudyGroups/Subsets	total	focal EPE	nonfocal EPE
Gleason Score 6	3,291	167 (5.1%)	93 (2.8%)
Gleason Score 3+4=7 with <5% pattern 4	1,031	120 (11.7%)	78 (7.6%)
All Gleason Score 3+4=7	4,478	657 (14.7%)	705 (15.8%)

We found SV invasion in one patient with GS6, and there is another case coded as SV invasion where slides are being retrieved and reviewed.

Conclusions: EPE was present in a small, but significant percentage (5.1% focal EPE and 2.8% nonfocal EPE) of our cohort of pure GS6 prostate adenocarcioma. Furthermore, we also had at least one patient with pure GS6 prostate cancer with SV invasion. The incidence of EPE with GS6 was lower than with GS347, and there was an increase in incidence of EPE with higher percentage of Gleason pattern 4. Overall, these findings support the concept that although pure GS6 prostate cancer is relatively indolent, it still can be locally aggressive and argues against removing the label "cancer" from these lesions.

929 High Expression of MAP1B in Urothelial Carcinoma: with Special Attention to Prognostic Impact and Biological Aggressiveness

Hong-Lin He, Yow-Ling Shiue, Chien-Feng Li. Institute of Biomedical Science, National Sun Yat-sen University, Kaohsiung, Taiwan; E-DA Hospital, I-Shou University, Kaohsiung, Taiwan; Chi Mei Medical Center, Tainan, Taiwan.

Background: Urothelial carcinoma (UC) is one of the common epithelial malignancies in Taiwan and worldwide. The underlying pathogenetic mechanism remains obscure. Analysis of the publicly available transcriptome of urothelial carcinoma (GSE31684) revealed that *Microtubule Associated Protein 1B (MAP1B)* is the most significant, upregulated microtubule bundle formation-associated gene in relation to advanced disease status and worse patients' survival. This study aimed to investigate the functional role, clinicopathological significance and prognostic impact of MAP1B in urothelial carcinomas of upper urinary tract (UTUC) and urinary bladder (UBUC).

Design: Immunohistochemical study was performed to evaluate the protein expression of MAP1B in 340 UTUCs and 295 UBUCs. The associations between MAP1B expression and various clinicopathological parameters and survival were statistically analyzed. Endogenous expression levels of MAP1B in various UC cell lines and their effects on cell behavior were determined by reverse transcription polymerase chain reaction and functional assays.

Results: High expression of MAP1B was significantly associated with advanced tumor status (UTUC, P=0.005; UBUC, P<0.001), advanced nodal status (UTUC, P=0.002; UBUC, P=0.012), increased vascular invasion (UTUC, P<0.001; UBUC, P=0.045), high histological grade (UBUC, P=0.016) and high mitotic activity (UTUC, P=0.001; UBUC, P=0.006). Moreover, at univariate level, MAP1B overexpression was significantly associated with worse disease-specific survival and metastasis-free survival in both UTUC and UBUC (all P<0.0001). MAP1B expression remained an independent adverse prognostic factor for disease-specific and metastasis-free survival in both groups (all P≤0.001) in multivariate comparison. The endogenous mRNA levels of MAP1B were higher in RTCC1 and J82 UC cells. Further *in vitro* study suggested that silencing of MAP1B via shRNA significantly impairs cell proliferation, migration and invasion abilities, as well as increases apoptosis in UC cell lines RTCC1 and J82.

Conclusions: High expression of MAP1B was associated with an aggressive phenotype. It acted as not only a key adverse prognostic factor but also a potential therapeutic target in urothelial carcinoma.

930 Validation of Gene Expression Signatures for Genomic Identification of Neuroendocrine Prostate Cancer

Samar Hegazy, Alexander W Wyatt, Jonathan Lehrer, Hatem Abou Ouf, Mohammed Alshalalfa, Ewan A Gibb, Beatrix Palmer-Arontsen, Nicholas G Erho, Elai Davicioni, Tamara L Lotan, Harrison Tsai, Tarek A Bismar. University of Calgary, Calgary, AB, Canada; University of British Columbia, Vancouver, BC, Canada; GenomeDx Biosciences Inc, Vancouver, BC, Canada; Johns Hopkins School of Medicine, Baltimore, MD.

Background: Neuroendocrine prostate cancer (NEPC) is a rare, aggressive variant of PC with rapid progressive clinical course and resistance to androgen deprivation therapy (ADT). The early identification of patients harboring tumors with NEPC-like genomic profiles is of significant interest and could be useful to guide optimal therapy for these men.

Design: The Decipher GRID was queried for two signatures that have been previously reported to predict NE-status (Kumar et al. and Alshalafa et al., 2016) as well as expression levels of four genes known to be associated with NE disease (RB1, CCND1, CHGA, AURKA). The signatures were evaluated in a retrospective cohort of 16 men diagnosed with *de novo* NEPC (NBX, RP, TURP and penile Mets) and radical prostatectomy specimens from a prospective cohort of 2,829 men with localized adenocarcinoma. To assess biological changes associated with treatment-induced NEPC, TURP samples from 7 patients with post-treatment NEPC were compared to biopsy samples from 25 patients prior to ADT. All cohorts were profiled with the Decipher assay (GenomeDx Biosciences Laboratory, San Diego, CA). The molecular signatures and genes associated with de novo NE disease were compared using the area under the receiver operating curve (AUC) metric. Treatment-induced NEPC changes were assessed with whole-transcriptome differential expression analysis using a p-value adjusted Wilcoxon test followed by pathway enrichment analysis using EnrichR.

Results: Consistent with known NEPC gene expression patterns, expression of RB was lower and expressions of CHGA and AURKA were higher in the neuroendocrine as compared to the adenocarcinoma cohort (AUC=0.77, 0.80, 0.80 respectively, $p < 0.001$). Expression of CCND1 trended lower in the neuroendocrine cohort (as expected), but failed to attain significance (AUC=0.64, p=0.056). NEPC signature scores were consistently higher in the neuroendocrine compared to the adenocarcinoma cohort with AUCs of 0.91 and 0.92 for Alshalafa and Kumar signatures, respectively ($p < 0.001$).

Conclusions: The previously reported NEPC signatures demonstrated promise as tools to discriminate between PC and NEPC. With validation in larger cohorts, these signatures may aid clinicians with improved identification of NEPC. Future studies are required to determine the clinical significance for tumors that harbor high NEPC signature scores.

931 Adult Genitourinary Rhabdomyosarcomas: An Analysis of Neuroendocrine Differentiation

Loren P Herrera Hernandez, Sounak Gupta, Rafael E Jimenez, Sarah H Johnson, Farhad Kosari, Andrew L Folpe, John C Cheville. Mayo Clinic, Rochester, MN.

Background: Prior studies on rhabdomyosarcomas (RMS) have shown that they can be difficult to distinguish from small cell carcinomas (SmCC), as many express markers of neuroendocrine differentiation (NED), which can be a diagnostic pitfall. We sought to identify genitourinary RMS in adults with significant morphologic overlap with SmCC, and analyzed markers of NED.

Design: 11 RMS (kidney: 3, bladder: 6, prostate: 2) occurring in adults (mean: 56yrs, range, 37 to 74), and predominantly in males (males: 8, females: 3) were included. The diagnosis was confirmed with IHC for a combination of desmin, myogenin and MyoD1, and absence of Pax3/7 gene rearrangements. Significant morphologic overlap with SmCC was not seen in renal (0/3) or prostate (0/2) RMS, as opposed to bladder RMS (4 of 6, 67%). 5 of 6 cases tested (83%) showed evidence of NED by IHC (synaptophysin, chromogranin, CD56). Of these, 5 cases were pure RMS, and 1 likely arose from urothelial carcinoma (UC) based on the presence of a conventional UC component. 3 cases of bladder RMS with NED were evaluated by RNA-seq, with 9 SmCC of the bladder and TCGA data on 20 typical UC serving as controls.

Results: RMS showed robust expression of *Myogenin* and *Myod1*, which drive skeletal muscle differentiation. No such expression was seen in SmCC and UC. RMS showed equivalent expression of *SYP* (synaptophysin, 82%), *CHGB* (chromograninB, 66%) and *NCAM1* (CD56, 39%) compared to SmCC. However, *CHGA* (chromograninA, 5%) expression was markedly lower. Less common markers of NED: *INSM1* (Insulinoma-associated 1, 50%) and *PCSK1* (Proprotein Convertase Subtilisin/Kexin Type 1, 22%), showed similar expression in RMS relative to SmCC. However, RMS lacked expression of *SCG2* (Secretogranin 2, 14%). The NED marker *ASCL1* was exclusive to SmCC. Transcription factors which promote EMT: *SNAI1* (SNAIL1), *TWIST1* and *ZEB2,* showed high relative expression in RMS compared to both SmCC and UC. Transcription factor *GATA3* showed similar expression in UC, SmCC and RMS.

Conclusions: RMS, SmCC and UC may share a similar lineage due to common *GATA3* expression. Shared NED in SmCC and RMS is highlighted by expression of markers such as *SYP, CHGB*, *NCAM1, INSM1* and *PCSK1*. Divergent NED between SmCC and RMS is highlighted by *ASCL1* expression only in SmCC. This divergent differentiation can be partially attributed to genetic programming by myogenic and EMT-related transcription factors, which have higher expression in RMS. We conclude that RMS with NED is distinct from SmCC. We cannot exclude their arising as part of a sarcomatoid UC but hypothesize that they are a true sarcomatous entity.

932 Evaluation of RNA ISH Assay for TFE3 Expression in Comparison to IHC and FISH: Do We Have a Third Approach?

Kareem Hosny Mohammed, Momin T Siddiqui, Tong Yang, Diane Lawson, Cynthia Cohen. Emory University Hospital, Atlanta, GA.

Background: The role of Transcription Factor E3 (TFE3) gene has been established in 20-40% of pediatric renal cell carcinoma (RCC) cases in which malignant transformation has been reported with the disturbance of TFE3 expression. Immunohistochemistry (IHC) is usually used as the first line for diagnosis. However, its use for nuclear TFE3 detection needs validation to confirm its presence or absence, and many pathologists do not rely on IHC. Traditionally, Fluorescence In Situ Hybridization (FISH) is used to confirm IHC results of TFE3 expression. This use of FISH is associated with expensive cost and delay in obtaining results. Given these problems, there is an essential need to develop a third approach for evaluation of TFE3 in RCC cases. RNA In Situ Hybridization (RISH) assay for TFE3 is under evaluation for its ability to detect the translocation of TFE3. We investigated whether detection of "TFE3 RISH" using the RNAscope (Leica Biosystems, Buffalo Grove, IL), the Bond III autostainer (Leica), and a probe TR95 from Advanced Cell Diagnostics (ACD, Newark, CA) can be used as a novel approach to assess validity of TFE3 expression obtained by IHC.

Design: 29 RCC suspected of translocation of TFE3 because of young patient age and/or histopathology were evaluated, 18 by IHC expression and 11 by FISH. All cases were reevaluated for TFE3 RISH expression. RISH expression was identified using an integrated scoring system by multiplying the percentage of stained area (0-100%)

and the staining intensity (0-3) for each slide. A cut-off of more than 240 was used to define a positive result of TFE3 expression. A two-sample *t*-test was used to detect the correlation between RISH results and both IHC and FISH.
Results: In comparison to IHC, RISH showed an excellent detection profile with the same specificity, and positive predictive value (PPV) (100%). The sensitivity of RISH was 62.5%, and the negative predictive value (NPV) was 72.7%. The difference between the mean of RISH positive (268.75) and the mean of RISH negative (168.75) was statistically significant (*p*-value = 0.0115*)*. In comparison to FISH, RISH detection profile showed 0% sensitivity, 0% PPV, 88% specificity and 80% NPV. The difference between RISH positive mean and RISH negative mean was insignificant (*p*-value = 0.9873*)*.
Conclusions: TFE3 RISH has a relatively good diagnostic profile in detection of TFE3 in RCC cases. Validation of IHC cases of RCC by RISH could be a novel approach to confirm RCC cases instead of the gold standard approach of performing FISH that is both money and time consuming.

933 Paraganglioma of the Urinary Bladder: A Pathologic and Clinical Study of 26 Cases

Chad J Hruska, Bogdan Czerniak, Charles Guo. UT MD Anderson Cancer Center, Houston, TX.
Background: Paraganglioma is a rare neuroendocrine neoplasm in the urinary bladder. To understand its clinicopathologic features, we studied a large series of patients with bladder paraganglioma from a single institution.
Design: We identified 26 patients with paraganglioma of the urinary bladder from our pathology database. The specimens included transurethral resection or biopsy (n=21), partial cystectomy (n=3), and radical cystectomy (n=2) specimens. Histologic slides were reviewed for pathologic analysis, and clinical data were collected from the medical records.
Results: The patients included 16 women and 10 men, with a mean age of 48 years (range, 16–77 years). Common symptoms included hematuria, hypertension, and micturition. Two patients also had Carney syndrome. The tumors presented as a submucosal nodular lesion in the bladder wall, with a mean size of 2.8 cm (range, 0.7–5.8 cm). Tumor cells were arranged in distinctive nests separated by delicate plexiform vascular fibrous septae. Immunohistochemical studies showed that the tumor cells were positive for synaptophysin (12/12), chromogranin (19/19), S-100 (9/12), CD56 (2/2), GATA-3 (1/2), and SDHB (1/1) and were negative for cytokeratin (0/13). Electron microscopy showed numerous secretory granules in the tumor cells. At the time of initial diagnosis, 6 patients had metastasis to lymph nodes (n=4) and/or distant organs (n=4). Clinical follow-up was available for 15 patients. Six patients, including 4 patients who initially presented with metastasis, died in a mean of 119 months (range, 17–336 months). Ninepatients were alive at a mean of 67 months (range, 3–231 months), but 3 of them developed tumor recurrence.
Conclusions: Bladder paraganglioma demonstrates distinct morphologic and immunohistochemical features. Most paragangliomas are indolent, but a small subset shows aggressive behavior with early metastasis. The presence of metastasis is associated with a high mortality rate. It is important to differentiate paraganglioma from other neoplasms in the bladder, particularly invasive urothelial carcinoma. Immunohistochemistry is highly effective in the differential diagnosis.

934 Histologic Spetrum of Metastatic Castration-Resistant Prostate Cancer

Jiaoti Huang, Yu Yin, George Thomas, Lawrence True, Tomasz M Beer, Martin Gleeve, Owen Witte, Josh Stuart, Chris Evans, Adam Foye, Jack Youngren, Eric Small. Duke University, Durham, NC; Anhui Medical University, Hefei, Anhui Province, China; Oregon Health Sciences University, Portland, OR; University of Washington, Seattle, WA; University of British Columbia, Vancouver, BC, Canada; UCLA, Los Angeles, CA; UC Davies, Sacramento, CA; UCSF, San Francisco, CA.
Background: Nearly all prostate cancer (PCa) research involving human tissue has used primary PCa tissue as biopsy of metastatic PCa is rarely done. This is a major issue since it is metastatic PCa that kills patients but our knowledge of metastatic PCa is extremely limited. This study is done to collect biopsy tissue from metastatic PCa to study histology, signaling molecules and genomics.
Design: 300 men with heavily treated, metastatic castration-resistant PCa (mCRPC) are enrolled after IRB approval and patient consent. Biopsy is done under radiology guidance. Multiple cores are taken, with half snap-frozen and half fixed in formalin. Frozen tissue undergoes laser-capture microdissection to obtain pure tumor cells for genomic studies. Formalin fixed tissue is used for H&E staining and IHC studies.
Results: The biopsy sites include bone (54%), lymph nodes (27%), liver (11%), soft tissue (2%), and rarely, lung, brain and bladder (8%). By morphology, ~30% tumors are adenocarcinoma (adenoCa), ~13% are small cell neuroendocrine carcinoma (SCNC), and 29% show a previously unrecognized histology which we have termed intermediate atypical carcinoma (IAC) (The rest has mixed morphology). IAC differs from adenoCa in that it has homogeneous, darkly-stained, round and regular nuclei without prominent nucloli or glandular structure. It differs from SCNC in that it has abundant cytoplasm, round and regular nuclei, no nuclear molding, mitotic figures or crush artifact. Vast majority of the tumors (~80%), irrespective of histology, express androgen receptor (AR) although AR pathway activity is significantly reduced in SCNC. A 50-gene signature reliably distinguishes the 3 histologic types. Patients with AdenoCa has a median survival of ~25 months. SCNC has a much worse prognosis (12 months). IAC has an intermediate prognosis (19 months).
Conclusions: 1. This large study reveals 3 distinct histologic patterns for mCRPC, and mixed histology in a minority of cases; 2. IAC is only seen in mCRPC but not primary PCa with unique histology, biologic behavior and genomics. 3. In contrast to primary SCNC, mCRPC with SCNC histology expresses AR; 4. AR signaling is significantly reduced in SCNC, explaning their independence from androgen and non-responsiveness to AR-targeted therapies.

935 Evaluation of Histological Changes in Radical Prostatectomy (RP) After Neoadjuvant Androgen Deprivation Therapy (NeoADT): Comparison Between Conventional and Newer Therapy Regimens

Kuo-Cheng Huang, Leili Mirsadraei, Ying-Bei Chen, Joseph S Sirintrapun, Hikmat Al-Ahmadie, Samson W Fine, Karim A Touijer, James Eastham, Karen A Autio, Dana E Rathkopf, Satish K Tickoo, Howard I Scher, Victor E Reuter, Anuradha Gopalan. Memorial Sloan Kettering Cancer Center, New York, NY.
Background: Conventional NeoADT with Lupron ± Bicalutamide (Lup/Bic) for advanced prostatic adenocarcinoma (PCA) neither eradicates disease nor effects complete androgen suppression. Newly approved therapies targeting androgen receptor signaling and biologic therapies are increasingly used in combination with Lup/Bic in clinical trials of castration sensitive localized high risk/ oligometastatic PCA. While a low rate of pathologic complete response has been reported with some newer regimens, there is paucity of literature describing differences in pathologic features. We aimed to compare histological changes in PCA between newer and conventional NeoADT.
Design: 36 RP post NeoADT were divided into groups (Gp) based on therapy as: **Gp 1** – Lup + Bic (n=10); **Gp 2** – Degarelix alone (n=16); **Gp 3** – Degarelix + Ipilimumab (n=5) and **Gp 4** – GnRH analog + Enzalutamide or Abiraterone (n=5). Qualitative parameters assessed: classic morphologic effects of ADT in tumor cells (0 - none/ minimal; 1 – partial; 2 – profound), stroma (fibrosis, myofibroblastic reaction) and presence of variant histologies: intraductal, neuroendocrine (NE). Quantitative parameters assessed: **Cellularity of Dominant Tumor (CDT)**, **Cellular Fraction of Dominant Tumor (CFDT)** showing grade 1 or 2 morphologic changes, **Total Residual Cancer Burden corrected for cellularity (TRCB -C)**, **Minimal residual Disease (MRD)** and pathologic **Complete Response Rate (CRR)**, last 3 per published methods (J Clin Oncol 32:3705). Gp 1-4 were compared using Statplus.
Results: Summarized in table

	Gp1	Gp2	Gp3	Gp4	p-value
CDT (% tumor cells/dominant tumor volume)	16	69	31	17	<0.001
CFDT (% tumor cells)*	90	31	64	99	<0.001
TRCB-C (cm3)*	1.3	3.9	2.2	2.0	0.21
MRD (N/total cases)	4/10	1/16	1/5	0/5	-
CRR (N/total cases)	0/10	0/16	0/5	0/5	-

*-mean value
Intraductal carcinoma was seen in 9, 6, 3, 4 cases in Gp1-4, respectively. Focal NE features were present in 1 case. Stromal response parameters were not significantly different between groups.
Conclusions: •Pathologic complete response was not observed with any NeoADT regimen.
•While cases treated with conventional NeoADT (Lup + Bic) showed the most effect on cellularity of residual dominant tumor (CDT), among newer regimens, addition of Abiraterone or Enzalutamide resulted in maximum proportion of tumor cells showing partial to profound morphologic effects (CFDT).
•Further investigations are underway to determine the biological significance of our findings.

936 How Useful Is MRI Guidance in Detecting Prostate Cancer versus Systematic Biopsy - A Single Institution Experience Based on Evaluation of >1,000 Biopsies

Ian Hughes, Vamsi Parimi, Joseph Yacoub, Gopal Gupta, Stefan Pambuccian, Maria M Picken. Loyola University Medical Center, Maywood, IL.
Background: Prostatic adenocarcinoma (PCa) is one of the most common cancers among men. Use of systematic [sextant] biopsies (SBx) of the prostate guided by PSA values has often led to negative results and extensive, unnecessary, and costly followups. Conversely, rare patients may present with metastases, despite repeated SBx being negative. Increasingly this standard procedure is being coupled with multiparametric MRI (mpMRI) interpreted through the Prostate Imaging Reporting and Data System (PIRADS) (a simple 5-point scale rating the radiographic lesions from benign [1] to most likely malignant [5]). The result is a new approach allowing targeted biopsy (TBx) of suspicious lesions. The objective of our study was to compare the rates of PCa detection per biopsy in SBx vs TBx.
Design: This single-institution retrospective study included 138 patients who underwent concomitant SBx and mpMRI-guided prostate (TBx) needle core biopsies from 7-2015 to 9-2016. The rate of cancer detection of carcinoma among SBx and TBx was analyzed.
Results: There were 1067 region-specific needle core biopsies including 807 SBx and 260 TBx. Out of 807 SBx, in 104 PCa was diagnosed histologically for a SBx rate per biopsy of 12.9%. Out of 260 TBx, in 81 PCa was diagnosed histologically for a TBx rate of cancer per biopsy 31.2%. (Z-score -6.7662; p <0.0005).

	Number of Cores with PCa	Total Cores	Cores with PCa (%)
Systematic Biopsies	104	807	12.9%
Targeted Biopsies	81	260	31.2%

Conclusions: Our study demonstrated that mpMRI-guided TBx has an increased rate of cancer detection (31.2%) over the traditional SBx (12.9%) and this difference was statistically significant (p value <0.0005). By employing this additional technique the rate of cancer per biopsy taken was approximately doubled showing that mpMRI is a worthwhile addition to the biopsy process. The remaining negative cases may in part be attributed to a number of factors such as difficulty biopsying small lesions, sampling errors, benign radiologic mimickers of PCa, and radiologist learning curves. As this technique becomes more widespread and radiologists/technicians become more familiar with it, the cancer yield may yet increase further. Increasing the yield of cancer detection may improve early diagnosis of clinically aggresive cancer and increase the safety of "watchful waiting" strategy in patients under surveillance.

937 Missing Cancer by Targeted Prostate Biopsy - How Often Does It Matter? - A Single Institution Experience

Ian Hughes, Vamsi Parimi, Joseph Yacoub, Gopal Gupta, Maria Picken. Loyola University Medical Center, Maywood, IL.

Background: Use of systematic biopsy (SBx) of the prostate guided by PSA values has often led to underdiagnosis of carcinoma and extensive, unnecessary, and costly followups. Multiparametric MRI, based on Prostate Imaging Reporting and Data System (PIRADS), allows a single 5-point scale rating the radiographic lesions from benign [1] to most likely malignant [5]. This system allows targeted biopsy (TBx) of suspicious lesions. Recent application of mpMRI to targeting prostate cancer has been shown to increase the yield of cancer detection. However, there is paucity of data as to how often TBx may miss its target. The objective of this study was to determine how often negative TBx may be associated with detection of cancer in SBx and whether this is clinically significant.

Design: This single-institution retrospective study included 138 patients who underwent mpMRI-guided prostate needle core biopsies between 7-2015 and 9-2016. Three cases were eliminated because they contained no SBx for comparison to their TBx. The total of 135 patients with 1062 region-specific needle core biopsies comprised of cases with both SBx (807) and TBx (255). Data was analyzed regarding frequency of negative TBx in the presence of positive SBx and their clinical significance was determined based on Gleason score (GS).

Results: In this group the rate of PCa detection by SBx versus TBx was 12.9% and 31.2% respectively ($p<0.0005$). Overall, out of 135 patients, 57 patients had TBx positive for PCa while 78 (57.7%) had negative biopsies (Table 1). Among the latter, in 17 cases (21.8%) SBx were positive for PCa. However, in 15/17(89%) patients GS was ≤6 and only in 2/17 cases (11%) GS was >6, in both cases GS 7 (3+4).

SBx	TBx	# of Patients (n=135)
-	-	61
+	-	17
-	+	22
+	+	35

Conclusions: While the rate of PCa detection in TBx was higher than in SBx, a relatively high percentage of patients (57.7%) had TBx negative for PCa. Among the latter, 21.8%, had SBx positive for PCa. However, only 2/17 patients (11%) had clinically significant PCa (GS >6) missed by TBx. These results suggest that TBx are uncommonly negative if there is clinically significant PCa present in the prostate. Negative cases may in part be attributed to a number of factors including difficulty biopsying small lesions, sampling errors, and benign radiologic mimickers of PCa.

938 Atypical Adrenal Adenomas: A Radiological and Pathological Study of 159 Cases

Ling Hui, Mohamed G Elbanan, Khaled M Elsayes, Miao Zhang. MD Anderson Cancer Center, Houston, TX.

Background: Most non-functional adrenal cortical adenomas are discovered incidentally on imaging studies and treatment options include active surveillance and surgical excision. Some adrenal lesions are defined as "atypical adrenal adenomas" by the radiologists, where the behavior of these lesions is thought to be unpredictable clinically and most of them are treated surgically. Herein, we studied the pathological features of these radiologically atypical adrenal adenomas.

Design: We identified 159 cases of radiologically atypical adrenal adenomas in our institutional databases. All patients underwent surgical excision. Radiologically atypical adrenal adenomas are defined as large in size (>4 cm), with heterogeneous enhancement, calcification, necrosis, hemorrhage or the presence of distinctive components known as "collision tumor". We reviewed all cases for pathological features including Weiss score. Tumors with Weiss scores 1-2 were defined as adrenal cortical neoplasm with uncertain malignant potential. Follow-up information was obtained from medical records and/or provided by referring physicians.

Results: There were 80 male and 79 female patients with a mean age of 54.7 yrs (Range: 12 to 78 yrs). Among the 159 cases, there were 6 cases of adrenal cortical neoplasm with uncertain malignant potential (Weiss score 1, n=5; Weiss score 2, n=1), 153 cases of adrenal cortical adenomas (Weiss score 0). Among these 153 cases, 13 cases were large tumors (=or> 4.0 cm); 4 cases showed a myelolipoma component; 5 cases showed hemorrhage within the tumor; 3 cases showed cytological atypia and pleomorphism; 1 case had multinodular architecture. Follow-up information showed no recurrence or metastatic disease in all 159 patients (Mean follow up=39.4 months).

Conclusions: Our studies showed that the vast majority (96%) of radiologically "atypical adrenal adenomas" are pathologically benign adrenal adenomas. Less than 5% of patients had a Weiss score of 1-2 with benign clinical behavior on follow-up. Therefore, these lesions can be followed clinically and do not warrant immediate surgical intervention.

939 Cell Polarity Reversal Distinguishes True Micropapillary Growth from Retraction Artifacts in Invasive Urothelial Carcinoma

Yiang Hui, Kara A Lombardo, M Ruhul Quddus, Andres Matoso. Warren Alpert Medical School of Brown University, Providence, RI.

Background: Focal micropapillary features are a common finding in invasive urothelial carcinoma and are often difficult to distinguish from retraction artifact morphologically. Cell polarity reversal has been demonstrated in micropapillary tumors by EMA immunostaining. We have previously described the use of E-cadherin as a cell polarity marker in micropapillary serous borderline tumors. This study aimed to evaluate the utility of EMA and E-cadherin in distinguishing between true micropapillary growth and retraction artifact.

Design: We identified 29 invasive urothelial carcinomas with micropapillary features and 30 muscle-invasive urothelial carcinomas without reported micropapillary features but with areas of retraction artifact. Immunohistochemical staining for EMA and E-cadherin was performed. Cell polarity reversal was considered present if E-cadherin showed membranous apical cup-like staining or if EMA demonstrated a well-defined basal staining towards the stroma.

Results: Twenty-seven of 29 cases (93%) of urothelial carcinoma with micropapillary features demonstrated EMA (Figure 1A) or E-cadherin (Figure 1B) staining patterns consistent with cell polarity reversal. The pattern of staining consistent with micropapillary architecture was identified with both markers in 20 of these 27 cases (74%). Six cases showed reversal of polarity by E-cadherin alone while one showed polarity reversal by EMA alone. In contrast, three of 30 cases (10%) of invasive urothelial carcinoma without reported micropapillary features showed reversal of cell polarity by both EMA and E-cadherin. Retraction artifacts showed circumferential staining by E-cadherin (Figure 1C) and lacked well-defined basal staining by EMA (Figure 1D).

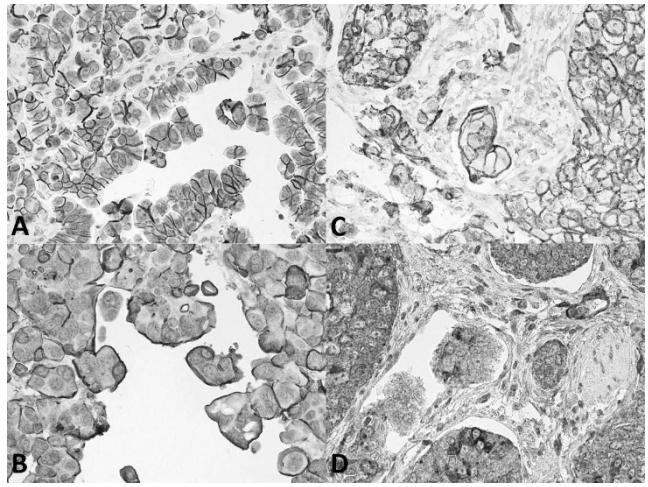

Conclusions: Morphologic identification of micropapillary features correlates well with immunohistochemical patterns of staining for cell polarity reversal by EMA and E-cadherin. Our data suggest that cell-polarity reversal is easier to identify with E-cadherin staining. Both markers may aid in distinguishing retraction artifact from true micropapillary features where morphology alone is equivocal.

940 Correlation of Prostate Cancer PI-RADS v2 Assessment Categories with Gleason Pattern and Tumor Quantity in Whole Mount Radical Prostatectomy Specimens

Michael J Hwang, Jeffrey Weinreb, Peter Humphrey, Jamil Syed, Preston Sprenkle, Angelique Levi. Yale School of Medicine, New Haven, CT.

Background: Multiparametric magnetic resonance imaging (mpMRI) is having a growing impact on prostate cancer management with PI-RADS v2 (Prostate Imaging–Reporting and Data System version 2) as a standardized interpretation and reporting system. It uses a 5-point scale (PI-RADS Assessment Category of 1 to 5) based on specific imaging criteria to predict the likelihood of clinically significant cancer for a given lesion. The relationship between PI-RADS assessment category and the percentage of Gleason pattern (GP) 4 or 5 in whole mount radical prostatectomy (WMRP) has not been fully studied. We investigated the correlation of PI-RADS assessment category with the quantity of high-grade GP in the corresponding WMRP nodules using image analysis software for quantitation.

Design: A total of 22 completely embedded prostate glands with preoperative mpMRI data were included in this study. The surface area of low-grade (GP 3) and high-grade (GP 4 or 5) components were measured by software on digitized images (ImageJ; NIH v1.50i) and volume of each nodule was calculated in milliliters. Each suspicious nodule on mpMRI was matched to the corresponding nodule in the WMRP specimen. The Mann-Whitney U test and Fisher's exact test were used for statistic analysis.

Results: A total of 76 cancer nodules were detected in WMRPs and 24 of these nodules were identified by mpMRI. Statistically, PI-RADS 5 nodules were larger in size and volume than PI-RADS 4 nodules ($p<0.05$) and had a higher percentage of a high-grade component ($p=0.058$). PI-RADS 3 and PI-RADS 4 nodules were similar in size, volume and percentage of high-grade component. mpMRI-identified nodules were larger in size (2.09 vs. 0.49 cm; $p<0.001$), volume (2.8 vs. 0.07 ml; $p<0.001$), and more likely to harbor a high-grade GP (82.7% vs. 29.2%; $p<0.001$) compared to nodules not identified by mpMRI.

PI-RADS Assessment Category	Mean Tumor Diameter (cm)	Mean Tumor Volume (ml)	Mean High-Grade GP (%)
PI-RADS 3 (n=5)	1.9	2.1	14.2
PI-RADS 4 (n=10)	1.7	0.8	12.9
PI-RADS 5 (n=9)	2.7	5.3	42.1

Conclusions: This data highlights the evolving role of mpMRI in the detection of prostate cancer, illustrates the importance of standardization of PI-RADS assessment categories, and may have implications in targeting PI-RADS 5 lesions and the number of cores taken at the time of biopsy.

941 Nuclear Factor (NF)-κB Immunohistochemistry in Bladder Cancer as a Predictor of Tumor Progression as Well as Chemosensitivity

Satoshi Inoue, Eiji Kashiwagi, Hiroki Ide, Alexander Baras, George J Netto, Hiroshi Miyamoto. University of Rochester, Rochester, NY; Johns Hopkins University, Baltimore, MD.

Background: NF-κB is a protein complex of transcriptional factor, and its phosphorylation is required for optimal induction of target genes. Recent evidence suggests the involvement of NF-κB signals in the growth of urothelial cancer as well as resistance to chemotherapy. The current study aims to determine the expression status of NF-κB and phospho-NF-κB (p-NF-κB) in bladder cancer and its prognostic significance.

Design: We immunohistochemically stained for NF-κB and p-NF-κB in 149 bladder tumor and paired non-neoplastic bladder tissue specimens as well as in separate tissue microarrays consisting of muscle-invasive bladder cancer specimens from patients who received at least 3 cycles of cisplatin + gemcitabine neoadjuvant chemotherapy.

Results: NF-κB/p-NF-κB was positive in 100% (9% 1+, 40% 2+, 51% 3+)/69% (44% 1+, 24% 2+, 1% 3+) of tumors, which was significantly higher than in non-neoplastic urothelial tissues [100% (25% 1+, 40% 2+, 35% 3+)/46% (36% 1+, 10% 2+)]. Twenty-nine (56%) of 52 lower grade tumors *vs.* 74 (76%) of 97 high-grade carcinomas (P=0.015) and 52 (62%) of 84 non-muscle-invasive tumors *vs.* 51 (78%) of 65 muscle-invasive carcinomas (P=0.033) were immunoreactive for p-NF-κB. However, there were no statistically significant associations between NF-κB levels and tumor grade or pT stage and between expression pattern of NF-κB/p-NF-κB and pN status. Kaplan-Meier and log-rank tests revealed that patients with p-NF-κB-positive muscle-invasive tumor had significantly higher risks of disease progression (P=0.001) and cancer-specific mortality (P=0.002). No significant associations between p-NF-κB positivity in non-muscle-invasive tumors and recurrence/progression and between NF-κB levels and patient outcomes were found. Multivariate analysis further identified p-NF-κB positivity in muscle-invasive tumors as an independent predictor of disease progression [hazard ratio (HR)=6.424, P=0.003] or cancer-specific mortality (HR=4.718, P=0.012). In a separate set of tissue specimens, p-NF-κB was positive in 38 (69%) of 55 cases with chemotherapy, including 13 (54%) of 24 responders versus 25 (81%) of 31 non-responders (P=0.044). There was no statistically significant difference in NF-κB levels between responders and non-responders.

Conclusions: NF-κB is likely to be activated in most of bladder cancers. The current results also suggest that p-NF-κB positivity precisely predicts disease progression and, more interestingly, chemoresistance, in patients with muscle-invasive tumor.

942 The Discovery of Methylation and RNA Biomarkers of Prostate Cancer Upgrading After Surgery in Patients with Gleason Score 6 Biopsies

Nafiseh Janaki, Prasuna Muppa, Simone Terra, Aqsa Nasir, Hamed Rahi, George Vasmatzis, John C Cheville, Farhad Kosari. University Hospitals Cleveland Medical Center, Cleveland, OH; Mayo Clinic, Rochester, MN; University of Minnesota, Minneapolis, MN.

Background: Men with Gleason score (GS) 6 prostate cancer on needle biopsy specimen are candidates for active surveillance. However, nearly a third of these men have significant prostate cancer (GS7 and higher) that is missed by needle biopsy sampling error, and approximately half of men on active surveillance will need treatment at some point in their surveillance. The objective of this study was to identify biomarkers in GS6 cancer in needle biopsy that predicted GS7 and higher cancer at prostatectomy. We focused in tumors with intact *PTEN* loci to identify biomarkers that can complement assays based on *PTEN*.

Design: Forty nine cases of fresh frozen prostate cancer from radical prostatectomy specimens were collected by laser capture microdissection, including 19 cases of insignificant (very low risk) and 30 cases of GS7 and higher (intermediate and high risk) prostate cancer. In cases of GS7, the Gleason pattern 3 and 4 were collected and analyzed separately. DNA and RNA were isolated and used to generate a total of 108 RNA and methylation sequencing files.

Results: 1- Gene expression analysis identified over 50 potential candidates. More than half of the candidates with representation on the U133 chipset were validated in an independent microarray dataset.

2- Most of the validated transcripts, such as members of the receptor protein tyrosine kinase family also had supporting methylation data.

3- The list of 30 most highly differentially methylated regions included a number of genes involved in ion transport.

Conclusions: The methylation and RNA markers identified in this study can be combined with a panel of molecular biomarkers that include *PTEN* to predict the presence of Gleason score 7 and higher prostate cancer in men with Gleason score 6 cancer on needle biopsy.

943 Pseudosarcomatous Myofibroblastic Proliferations of the Urinary Bladder Lack the *USP6* Gene Rearrangement Common in Nodular Fasciitis

Judith AS Jebastin, Nilesh S Gupta, Shannon Carskadon, Nallasivam Palanisamy, Sean R Williamson. Henry Ford Health System, Detroit, MI.

Background: Rearrangement of the ubiquitin-specific protease 6 (*USP6*) gene has been recently recognized as a recurrent alteration in soft tissue nodular fasciitis. Pseudosarcomatous myofibroblastic proliferation of the urinary bladder, also variably known as postoperative spindle cell nodule, fibromyxoid pseudotumor, among other terms, is generally histologically and immunohistochemically similar to nodular fasciitis. We studied whether the *USP6* gene rearrangement also occur in these bladder lesions.

Design: We searched for pseudosarcomatous myofibroblastic proliferations of the urinary bladder (and synonyms) in our pathology database. *USP6* fluorescence in-situ hybridization (FISH) analysis was performed using bacterial artificial chromosome (BAC) derived break-apart probes. FISH was validated to be positive in four well-characterized cases of nodular fasciitis (figure 1 A-B), one aneurysmal bone cyst, and negative in eight histologic mimics of nodular fasciitis

Results: None of the bladder pseudosarcomatous myofibroblastic proliferations (0/10) was detected to harbor *USP6* rearrangement (figure 1 C-D), including 8 large tumors (making up multiple tissue cassettes of lesional tissue) and 2 small lesions (entirely examined in 1 or 2 tissue cassettes). Two of 10 patients had known history of previous instrumentation in the bladder, and 1 had prior uterine surgery.

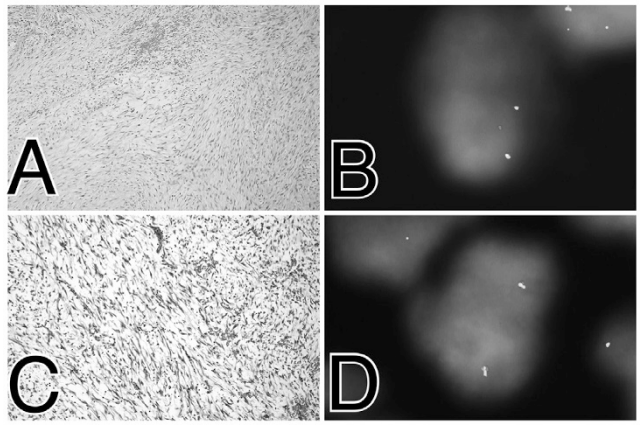

Conclusions: *USP6* gene rearrangement is lacking in pseudosarcomatous myofibroblastic proliferations of the urinary bladder, despite morphologic and immunophenotypic similarity to nodular fasciitis. In contrast to nodular fasciitis, *USP6* FISH is unlikely to be a robust confirmatory tool for the diagnosis of pseudosarcomatous myofibroblastic proliferations of the urinary bladder. Distinct molecular alterations/pathways, yet to be discovered, may be responsible for these tumors.

944 Mcl-1 Protein Overexpression and *MCL1* Gene Amplification in Urothelial Carcinoma of the Urinary Bladder

Bhaskar VS Kallakury, Sungeun Kim, Christine E Sheehan, Tipu Nazeer, Jeffrey Ross. Georgetown University Hospital, Washington, DC; Albany Medical College, Albany, NY.

Background: Myeloid cell leukemia 1 (Mcl-1) has been known to play roles of anti-apoptosis, development of lymphocytes and homeostasis of hematopoietic progenitors. Mcl-1 delays cell-cycle progression through interactions with cyclin dependent kinase 1 (CDK-1), proliferating cell nuclear antigen (PCNA) and checkpoint 1 protein (CHK-1). Overexpression of Mcl-1appears to be relevant to chemoresistance of different cancer cell lines including urothelial carcinoma of the bladder (UCB), but has not been previously studied as a predictor of prognosis for the disease.

Design: Formalin-fixed paraffin-embedded tissue sections from 52 UCB were immunostained by an automated method (Ventana/Roche, Tucson, AZ) using rabbit polyclonal Mcl-1 (clone S-19, Santa Cruz). Cytoplasmic (cMcl-1) immunoreactivity was scored based on staining intensity (weak, moderate, intense) and percentage of positive cells (focal <= 10%, regional 11-50%, diffuse >50%). *MCL1* amp was determined by hybrid capture based comprehensive genomic profiling (CGP) on a separate cohort of 806 UCB clinical samples. Results were correlated with clinicopathologic variables.

Results: cMcl-1 immunoreactivity was noted in all (100%) tumors, with intense diffuse overexpression observed in 25/52 (48%) tumors; and correlated with high tumor grade [13/17 (77%) grade 3 vs 9/16 (56%) grade 2 vs 3/19 (16%) grade 1, p=0.001], advanced tumor stage [14/19 (74%) advanced (pT2 and pT3) versus 11/33 (33%) low (pTa and pT1) stage, p=0.005], and with overall survival on Cox univariate analysis (p=0.003). On multivariate analysis, cMcl-1 overexpression (p=0.018) and advanced tumor stage (p=0.043) independently predicted shortened survival. On CGP, 64 (8%) of 806 UCB featured *MCL1* gene amplification.

Conclusions: Cytoplasmic Mcl-1 protein overexpression appears to occur independently from MCL1 gene amplification and is an independent predictor of UCB clinical outcome. Further study of Mcl-1 as a prognostic factor and potential therapy target in UCB appears warranted.

945 The Utility of AMACR as a Diagnostic Marker for Urothelial Carcinoma In Situ, a Study Supported by Morphometric Image Analysis and Triple Immunohistochemical Panel [CK 20, CD44 and p53]

Nora N Kamel, Zahraa S Elalfy, Shady E Anis, AbdelRazik H Farrag, Wafaa E Abdel-Aal, Samira AM Salem, Elia A Ishak. National Research Centre, Giza, Egypt; cairo university, cairo, Egypt.

Background: UCIS is considered one of the challenging diagnoses due to its morphological similarity with reactive conditions. The triple immunohistochemical panel of stains (TIP) CK20, CD44 and p53 have been used to differentiate questionable cases leaving a group of indeterminate cases that does not follow the expected staining pattern.Recent studies proved the morphometric image analysis to be a reliable tool used in controversial cases of UCIS. We studied the utility of AMACR in diagnosing UCIS and differentiating it from reactive atypia (RA).We evaluated the role of AMACR in the indeterminate group (by TIP) in relation to the results of the morphometric numerical values of the image analysis.

Design: A retrospective study of 72 cases of different urinary tract biopsies and cystectomies were diagnosed and categorized into two groups as UCIS and RA. The

TIP was performed for all cases accordingly three new groups emerged according to the pattern of staining,Group 1 confirmed RA,group 2 confirmed UCIS and group 3 indeterminate.All specimens were stained for AMACR.All H&E slides were examined for the area of interest with a high resolution Leica digital camera for further software analysis using Leica Qwin program.

Results: According to histology 32 cases were RA and 40 UCIS. After the TIP 30 cases proved to be RA and 18 cases UCIS while 24 cases were indeterminate.The cases with confirmed diagnoses (48) showed a highly significant correlation with AMACR. Non of RA were positive (100 % negativity) while UCIS showed positive stain in 14 (77.8%) cases (p value 0.001) with sensitivity (77%) and specificity(100%),100% positive predictive value and 88.2% negative predictive value.

AMACR	RA by TIP	UCIS by TIP
Positive	30(100%)	4(22.2%)
negative	0(0%)	14(77.8%)
Total	30(100%)	18(100%)

In the indeterminate group 14 cases were negative for AMACR while 10 were positive. Assessment of the morphometric parameters in the indeterminate cases revealed a detectable difference between the AMACR positive and AMACR negative groups, with notable increase in the measurements of nuclear area, perimeter, pleomorphism and nuclear/cytoplasmic ratio in the AMACR positive group supporting the diagnosis of UCIS.

Conclusions: Our results indicate that AMACR can be used to differentiate between UCIS and RA. AMACR positivity is highly supportive of the diagnosis of UCIS especially in the indeterminate group in which the TIP results are controversial.

946 Correlation of MET Complete Status and Outcome in Patients with Metastatic Clear Cell Renal Cell Carcinoma Treated by Sunitinib

Solene-Florence Kammerer-Jacquet, Sarah Medane, Karim Benasalah, Jean-Christophe Bernhard, Frantz Dupuis, Mokrane Yacoub, Alain Ravaud, Gregory Verhoest, Romain Mathieu, Benoit Peyronnet, Angelique Brunot, Brigitte Laguerre, Alexandra Lespagnol, Jean Mosser, Frédéric Dugay, Marc-Antoine Belaud-Rotureau, Nathalie Rioux-Leclercq. Hospital University, Rennes, France; Hospital University, Bordeaux, France; Centre Eugène Marquis, Rennes, France.

Background: Clear cell renal cell carcinoma (ccRCC) are highlymetastatic tumors with a 50% risk of metastases. Anti-vascular growth epithelial factor (VEGF) therapies are currently used in first line of metastatic ccRCC but most of patients develop resistance. Cabozantinib, an inhibitor of tyrosine kinases including VEGFR, MET and AXL recently shows interesting results in second line treatment. Moreover, the HGF/MET signaling pathway implicated in angiogenesis may be responsible for resistance to anti-VEGF therapy. To better understand MET role in metastatic ccRCC and potential resistance, we assessed MET complete status in a well-characterized population of 90 patients with metastatic ccRCC treated by first line sunitinib therapy.

Design: For this purpose, we studied MET expression by immunohistochemistry (IHC), MET amplification by fluorescence in situ hybridization on FFPE sample and MET mutation by next generation sequencing on 90 primary tumors. MET status was then correlated to pathological criteria using Chi-squared test and clinical outcome using Kaplan Meier curves compared by log rank test.

Results: One third (31.1%) of ccRCC had low expression of MET (absent to weak intensity in IHC) versus 68.9% with high expression (moderate to strong intensity). Expression of MET was associated with a gain in FISH analyses ($p = 0.0284$) without amplification. No mutation was detected. High expression of MET was also associated with lymph node metastases, and sarcomatoid component. No statistical difference was observed between the two groups of patients in terms of progression-free survival and overall survival after sunitinib introduction ($p = 0.72$ and $p = 0.93$, respectively).

Conclusions: This study is the first to analyze complete MET status in a well characterized metastatic ccRCC treated by first line sunitinib therapy. High expression of MET, although not associated with sunitinib resistance, may suggest a benefit from MET inhibitors.

947 Hilar Fat Infiltration: An Independent Prognostic Factor in Metastatic Clear Cell Renal Cell Carcinoma with Sunitinib First-Line Treatment

Solene-Florence Kammerer-Jacquet, Angelique Brunot, Karim Benasalah, Boris Campillo-Gimenez, Mathilde Lefort, Sahar Bayat, Alain Ravaud, Frantz Dupuis, Mokrane Yacoub, Gregory Verhoest, Romain Mathieu, Benoit Peyronnet, Alexandra Lespagnol, Jean Mosser, Julien Edeline, Brigitte Laguerre, Jean-Christophe Bernhard, Nathalie Rioux-Leclercq. Hospital University, Rennes, France; Centre Eugene Marquis, Rennes, France; EHESP, Rennes, France; Hospital Universty, Bordeaux, France.

Background: Selecting patients with metastatic clear-cell renal cell carcinoma (ccRCC) who might benefit from treatment with targeted tyrosine kinase inhibitors (TKI) is still a challenge and a crucial issue even more with the advent of new therapies. Hilar fat infiltration is a validated prognostic factor in non-metastatic ccRCC (TNM 2009 staging system) but never studied in metastatic patients. We aimed to assess its phenotype and prognostic impact in metastatic patients with ccRCC treated by first-line sunitinib.

Design: In a retrospective and multicentric study, we compared 90 ccRCC according to hilar fat infiltration, at pathological, immunohistochemical and molecular levels and also at clinical outcome. Patients and tumor characteristics were studied using univariate and multivariate Cox regression models.

Results: Hilar fat infiltration was found in42 patients (46.7%), who had a worse prognosis (Heng criteria) ($p=0.003$), more liver metastasis ($p=0.036$) and progressive diseases at first radiological evaluation ($p=0.024$). Corresponding ccRCC were associated with poor pathological prognostic factors well known in non-metastatic ccRCC. For these patients, median progression-free survival (PFS) was 4 months versus 13 months ($p=0.02$), and median overall survival (OS) was 14 months versus 29 months ($p=0.006$). In multivariate Cox regression model integrating all the variables, only poor prognosis according to Heng criteria and hilar fat infiltration remained independently associated with both PFS and OS.

Conclusions: Hilar fat infiltration was first demonstrated to be a potential predictive marker of resistance and an independent prognostic factor**,** which could be used to better select patients who could benefit from anti-angiogenic therapy.

948 Nomogram Predicting Prognosis in Metastatic Patients with Clear Cell Renal Cell Carcinoma Treated by First-Line Sunitinib

Solene-Florence Kammerer-Jacquet, Frédéric Dugay, Karim Bensalah, Angelique Brunot, Benoit Peyronnet, Romain Mathieu, Gregory Verhoest, Mathilde Lefort, Sahar Bayat, Alexandra Lespagnol, Jean Mosser, Julien Edeline, Brigitte Laguerre, Frantz Dupuis, Mokrane Yacoub, Alain Ravaud, Jean-Christophe Bernhard, Marc-Antoine Belaud-Rotureau, Nathalie Rioux-Leclercq. Hospital University, Rennes, France; Centre Eugene Marquis, Rennes, France; EHESP, Rennes, France; Hospital Universty, Bordeaux, France.

Background: The selection of patients with metastatic clear cell renal cell carcinoma (ccRCC) who might benefit from treatment with targeted tyrosine kinase inhibitors (TKI) is still a challenge and a crucial issue regarding the advent of new therapies. Our aim was to identify a nomogram predicting prognosis in m-ccRCC patients treated with sunitinib.

Design: We performed global genomic analysis by array-comparative genomic hybridization on 73 primary ccRCC from metastatic patients treated with first-line sunitinib. We also determined expression of CAIX, VEGF, PD-L1 and PD-1 by immunohistochemistry, *VHL* mutation by Next-Generation Sequencing and promoter methylation by Methylation-Specific Multiplex Ligation-dependant Probe Amplification. These data were analyzed in relation with response to sunitinib, progression-free survival (PFS) and overall survival (OS).

Results: Primary ccRCC of primary-refractory patients and long-term responders had a distinct phenotype with poor Heng score ($p=0.002$), liver metastases ($p=0.012$), hilar fat infiltration ($p=0.001$), microvascular invasion ($p=0.045$) and PD-L1 overexpression ($p=0.022$). Moreover, they had more chromosomal imbalances ($p=0.004$) both gains ($p=0.012$) and losses ($p=0.029$) with identified recurrent alterations. Poor Heng score, liver metastasis, hilar fat infiltration and loss of 8q were independently associated with both shorter PFS and OS. These variables integrated in a nomogram predicted prognosis with a 0.74 and 0.77 c-index in PFS and OS respectively.

Conclusions: This nomogram could be used for personalized metastatic ccRCC treatment to better select patients who could benefit from anti-angiogenic therapy.

949 PD-L1 Expression in High Grade Locally-Advanced Renal Cell Carcinoma

Shivani Kandukuri, Toni K Choueiri, Michelle S Hirsch. Brigham And Women's Hospital, Boston, MA; Dana Farber Cancer Institute, Boston, MA.

Background: Recent studies have shown PD-L1 expression in up to 30% of renal cell carcinomas (RCCs) depending on tumor subtype, with expression being associated with increased grade, increased stage, and poor outcome. However, aggressive RCC has not been specifically addressed. We evaluated a cohort of high-grade and locally-advanced tumors for PD-L1 expression and correlated the findings with clinical outcome.

Design: 48 RCCs, including 11 clear cell (CC) RCCs, 7 papillary (P) RCCs, 2 high grade chromophobe (Ch) RCCs, 7 Xp11.2 RCCs, 4 fumarate hydratase-deficient (FHD) RCCs, 8 collecting duct carcinomas (CDCAs), and 9 unclassified (UC) RCCs, were evaluated. All cases were high grade ($\geq$ FNG 3) and/or high pT-stage ($\geq$ pT3a N0 M0, or any pT N1 +/- M1 disease). Presence of sarcomatoid differentiation was documented. PD-L1 immunostaining was performed on whole mount sections from the primary tumor, and scored positive if present in $\geq$5% of tumor cells. Clinical follow-up in PD-L1 positive cases was obtained.

Results: 19 cases (40%; 3 CCRCC, 2 PRCC, 1 ChRCC, 1 Xp11.2, 3 FHD, 4 CDCA, 4 UCRCC) were PD-L1+, 9 (47%) of which had sarcomatoid differentiation, and 29 cases (60%; 8 CCRCC, 5 PRCC, 1 ChRCC, 6 Xp11.2, 1 FHD, 4 CDCA, 4 UNRCC) were PD-L1 negative, 5 of which had sarcomatoid differentiation (17%). PD-L1 expression ranged from 10-100% (median 20%; 5 cases >50%: 1 ChRCC, 1 FHD, 3 UCRCC). For PD-L1 positive cases only: median age 58 (range: 18-77), 11M:8F, 80% (15 case) were FNG 4 tumors, 8 (42%) patients had metastatic carcinoma in lymph nodes at the time of nephrectomy. Follow-up information was available in 14 patients: median follow-up 9 months (range: 0-72), 6 (43%) developed additional metastases, 4 (29%) patients (3 with UNRCC) died of disease (2 with 10% PD-L1 staining and 2 with 90-100% PD-L1 staining).

Conclusions: High-grade locally advanced RCCs express PD-L1 in their primary tumors, with the highest expression occurring in non-CC, non-papillary RCC. PDL1 expression in UCRCC and FHDRCC, when present, was more likely to show a diffuse staining pattern, and was associated with poor outcome, and suggest a rationale for PD-1/PD-L1 inhibitors.

950 Morphologic and Clinical Features of So-Called 'Oncocytic Papillary Renal Cell Carcinoma'

Shivani Kandukuri, Thing Rinda Soong, Paola Dal Cin, Michelle S Hirsch. Brigham And Women's Hospital, Boston, MA.

Background: A distinct low-grade oncocytic variant of papillary renal cell carcinoma (OncPRCC) has been described. However, there is controversy as to whether such tumors are a discrete entity. As few cases are reported in the literature, the goal of this study was to evaluate the morphologic, immunohistochemical (IHC), and genetic features of OncPRCC, and to compare the findings to other oncocytic renal epithelial neoplasms (RENs).

Design: A retrospective review of RENs was performed to identify tumors with eosinophilic cytology and distinct papillary or tubulopapillary architecture. Tumors that met morphologic criteria for OncPRCC were immunostained for CK7, CK20, AMACR, CD10, cKIT, HNF1b, S100a1, HMB45, RCC, and CAIX. IHC findings were compared to other RENs, including renal oncocytoma (RO), Chromophobe RCC (ChRCC), clear cell RCC (CCRCC), and papillary renal cell carcinoma (PRCC). Associated pathologic, genetic, and clinical information for the OncPRCCs was recorded.
Results: 10 OncPRCC were identified. Median patient age was 65 years (range 48-90) with a male predilection (M:F 4:1). 3 cases were diagnosed by core biopsy, the remaining were pT1 (n=5) or pT3 (n=2). Fibrovascular cores and tubules were lined by a single oncocytic cell layer in all cases; 1 case also showed focal solid growth of clear cells. Karyotypes were available for 2 cases: both contained +7; one case also had +17. FNG was 2 in 8 cases and 3 in 2 cases. IHC findings in OncPRCC were as follows: 7/10 CK7+, 1/10 CK20+, 8/10 AMACR+, 7/10 CD10+, 4/10 RCC+, 9/10 HNF1b+, 10/10 S100a1+, 1/10 CA1X+; all cases were negative for cKIT and HMB45. Overall, IHC results were not entirely specific but mimic that seen in PRCC, with diffuse expression of CK7, AMACR and CD10 being the most sensitive and specific findings to support the diagnosis. With respect to other oncocytic RENs, CK7+/CAIX- argues against (granular) CCRCC; CK7+/AMACR+/RCC+/cKIT- argues against RO; and S100a1+/HNF1b+ argues against ChRCC. Only one 1 case recurred in a LN 4 years after nephrectomy; all remaining patients were diseae free (median follow-up 48 months, range 24-84).
Conclusions: OncPRCC is an oncocytic REN that has overlapping morphologic features with PRCCs (type I and type II), RO, and ChRCC. Although most OncPRCC appear to be indolent, unusual associated morphologic features, such as solid growth, may suggest more aggressive behavior. When suspicious about a diagnosis of OncPRCC or when limited material is available for review, a directed IHC panel, including CK7, AMACR, CD10, CAIX, may be helpful in excluding other oncocytic RENs, especially RO.

951 Immunohistochemistry of Sex Hormone Receptors and Related Signals in Bladder Cancer as Predictors of Chemosensitivity

Eiji Kashiwagi, Hiroki Ide, Satoshi Inoue, Takashi Kawahara, George J Netto, Alexander Baras, Hiroshi Miyamoto. Johns Hopkins University, Baltimore, MD; University of Rochester, Rochester, NY.

Background: Recent preclinical evidence suggests that androgen receptor (AR) and estrogen receptor (ER) signals play an important role in urothelial tumorigenesis and cancer progression. We have also demonstrated that androgens activate several transcription factors and other molecules that are known to involve tumor outgrowth, including ELK1, FOXO1, and prostaglandin receptors (*e.g.* EP2, EP4), via the AR pathway in bladder cancer cells. Meanwhile, cisplatin-based systemic chemotherapy remains the mainstay of the treatment of muscle-invasive bladder cancer in both neoadjuvant and adjuvant settings, but some patients do not respond to it. The current study aims to determine the expression status of AR, ERβ, EP2, EP4, and phosphorylated forms of ELK1 and FOXO1 in bladder cancers from patients undergoing chemotherapy.
Design: We immunohistochemically stained for AR/ERβ/p-ELK1/p-FOXO1/EP2/EP4 in transurethral resection specimens of muscle-invasive bladder tumor from patients who subsequently received at least 3 cycles of cisplatin + gemcitabine neoadjuvant chemotherapy prior to radical cystectomy. Responders and non-responders to the neoadjuvant therapy were pathologically defined as the absence and presence of muscle-invasive, extravesical, or metastatic disease at the time of cystectomy, respectively.
Results: AR was positive in 14 (45%) of 31 non-responders, which tended to be higher than in responders [5 (21%) of 24; *P*=0.060]. AR-positive cases included 12 (46%) of 26 male non-responders versus 4 (21%) of 19 male responders (*P*=0.082) as well as 2 (40%) of 5 female non-responders versus 1 (20%) of 5 female responders (*P*=0.490). Similarly, ERβ was positive in 22 (71%) of 31 non-responders, which was significantly higher than in responders [9 (38%) of 24; *P*=0.013]. ERβ-positive cases included 17 (65%) of 26 male non-responders versus 8 (41%) of 19 male responders (*P*=0.121) as well as 5 (100%) of 5 female non-responders versus 1 (20%) of 5 female responders (*P*=0.010). Additionally, 38% *vs.* 71% (p-ELK1; *P*=0.039), 41% *vs.* 69% (p-FOXO1; *P*=0.068), 69% *vs.* 95% (EP2; *P*=0.030), and 69% *vs.* 90% (EP4; *P*=0.095) were positive in responders *vs.* non-responders, respectively.
Conclusions: Positivity of p-ELK1, p-FOXO1, EP2, and EP4 in bladder tumors is likely to associate with chemoresistance. Moreover, although the case number in the current study may be relatively small, our results suggest that AR expression particularly in male tumors and ERβ expression particularly in female tumors serve as predictors of response to chemotherapy.

952 Immunohistochemical Phenotype Analysis of a Large Series of Sarcomatoid Renal Cell Carcinoma

Fumi Kawakami, Kanishka Sircar, Pheroze Tamboli, Jaime Rodriguez-Canales, Christopher G Wood, Jose A Karam. University of Texas MD Anderson Cancer Center, Houston, TX.

Background: Sarcomatoid renal cell carcinoma (sRCC) represents a clinically important subset of RCC with biphasic epithelioid (E-) and sarcomatous (S-) components. Accurate biopsy diagnosis of sRCC requires differentiating it from sarcomatoid urothelial carcinoma and retroperitoneal sarcoma involving the kidney as well as subtyping the sRCC according to underlying parent histology. Hence, we evaluated the immunohistochemical features of a large cohort of sRCC.
Design: Immunohistochemistry was performed on tissue microarray sections from nephrectomy specimens in 118 patients with sRCC (94 patients with clear cell sRCC [cc-sRCC]) and 24 patients with non-clear cell sRCC [non-cc-sRCC]) and 87 patients with clear cell RCC lacking sarcomatoid features (ccRCC). Immunostains with antibodies to CK AE1+AE3, CD10, CAIX, PAX2, PAX8, GATA3, and CD105 were evaluated by digital image analysis. CK AE1+AE3, CD10, CAIX, PAX2, PAX8, and GATA3 were evaluated by the semiquantitative method (percentage of positive cells [0-100] x intensity of the staining [0-3]). CD105 was evaluated by percentage of positive stained area.
Results: sRCC expressed CK AE1+AE3 or PAX8 in 97/104 cases (93.3%). CK AE1+AE3, CD10, PAX2, and PAX8 were positive in 92/106 (86.8%), 63/107 (58.9%), 51/105 (48.6%), and 81/106 (76.4%) cases of the S- component of sRCC, respectively. Labeling of these individual markers was significantly higher in ccRCC: CK AE1+AE3, 87/87 (100%, P<0.0001); CD10, 81/87 (93.1%, P<0.0001); PAX2, 66/87 (75.9%, P<0.0001); and PAX8, 82/87 (94.3%, P<0.0001). CAIX positivity was not significantly different between cc-sRCC (54/85 [63.5%]) and ccRCC (61/86 [70.9%], P=0.4263). Notably, only 1 non-cc-sRCC case (1/21 [4.8%]) was CAIX positive. Among sRCC, all 42 CAIX and PAX8 double positive cases were cc-sRCC (sensitivity 50.60% [42/83]) while none of the non-cc-sRCC showed CAIX and PAX8 double positivity (specificity 100% [21/21]). No ccRCC case was positive for GATA3 (0/87); however 5/106 (4.7%) cases of the S-component of sRCC expressed GATA3. CD105 labeled the S-component of cc-sRCC (63.9% [mean] ± 19.1% [SD]) to a greater extent than ccRCC (54.1 [mean] ± 11.2 % [SD], P<0.001).
Conclusions: CK AE1+AE3 and PAX8 immunostains can detect most sarcomatoid RCC though a few sRCC may aberrantly express GATA3. CAIX expression was maintained in cc-sRCC and it is useful to differentiate sarcomatoid RCC of clear cell and non-clear cell parent subtypes. CD105 showed significantly higher expression in cc-sRCC (S-) compared to ccRCC lacking sarcomatoid features, indicating potential utility as a biomarker of sarcomatoid change.

953 GATA3 Positivity in Benign Radiated Prostate Glands: A Potential Diagnostic Pitfall

Armen H Kharardjian, Jonathan I Epstein, Sara E Wobker. The Johns Hopkins Hospital, Baltimore, MD; University of North Carolina, Chapel Hill, NC.

Background: Histologic changes following radiation therapy to the prostate include multilayering of glands, urothelial metaplasia, and marked random nuclear atypia, that mimic invasive urothelial carcinoma. We have noted several consult cases that were stained for GATA3, where positive labeling contributed to a misdiagnosis of urothelial carcinoma. To more formally investigate this potential pitfall, we describe the immunohistochemical findings of GATA3 and other prostate and urothelial markers in 30 cases of benign radiated prostates.
Design: Cases of benign prostate tissue with radiation atypia from 1990-2015 were obtained from our institution. Cases were evaluated immunohistochemically (IHC) for PSA, P501S (Prostein), NKX3.1, GATA3, and uroplakin 2.
Results: 19 core needle biopsies, 8 TURP, and 3 cystoprostatectomies were evaluated. GATA3 was positive in 100% of cases, with 70% showing strong to moderate-strong staining in a mostly patchy manner within a gland. Uroplakin was negative in 100% of cases. PSA was positive in 93.3% of cases, with 89.2% showing strong to moderate-strong staining in a mostly diffuse manner. P501S was positive in 96.7% of cases, with 93.1% showing strong to moderate-strong staining in a mostly patchy manner. NKX3.1 was positive in 82.8% of cases, with 33.3% showing strong to moderate-strong staining in a mostly patchy manner. Figure 1 shows H&E of a benign radiated prostate gland with atypia and multilayering (A) with strong GATA3 positivity (B), positive staining for PSA (C), and P501S (D).

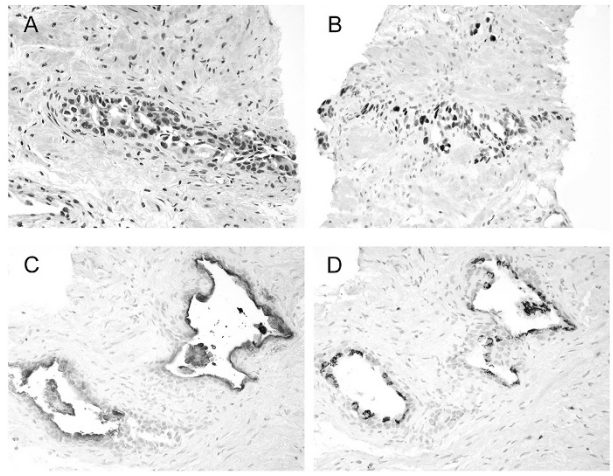

Conclusions: Our findings highlight that GATA3 is often positive in benign prostate glands with radiation atypia, which along with the morphological features, present a pitfall for the misdiagnosis of urothelial carcinoma. It is also recognized that benign prostate glands with radiation atypia are often positive for high molecular weight cytokeratin and p63, further resembling urothelial carcinoma. PSA and P501S are the best prostate specific markers for use in radiated prostate, with the caveat that they are often patchy and do not stain all radiated glands.

954 Peyronie Disease – A Contemporary Interinstitutional Cohort Emphasizing Histopathology

Caleb King, Kathryn G Lindsey, Laura Spruill, Steven C Smith. Virginia Commonwealth University School of Medicine, Richmond, VA; Medical University of South Carolina, Charleston, SC.

Background: Of the few contemporary series studying Peyronie disease, a superficial fibromatosis involving the tunica albuginea of the penis, none have focused on the expected range of histomorphologic findings for surgical specimens. Our study aims to outline the spectrum of expected changes for the pathologist encountering this relatively uncommon condition.

Design: We performed a retrospective review of surgical specimens of Peyronie disease based on diagnostic terms "fibromatosis" and "Peyronie" in penile excisions from two referral centers, tabulating clinicopathologic features and evaluating histologic characteristics.

Results: Of 35 cases reviewed, 32 lesions were deemed to represent Peyronie disease (3 reclassified as balanitis or fibrocalcific atherosis). Patients ranged from 34 to 88y (median 55y), 89% of Caucasian and 11% of African ancestry, with lesions described as 1-10 years in duration, a subset with prior GU trauma or surgery (18%). Clinical exams documented lesions with maximal curvature ranging from 30-360 degrees (median 90) upon tumescence, 90% reporting comorbid erectile dysfunction. Specimens ranged from 1-5cm (median 2.6), described generally as dense, tan, and fibrotic, with variable osseous component. The dense fibrosis involving the tunica albuginea was predominantly nodular in 27%, hyalinized and lamellar in 53%, and mixed in 20%. Inflammation, mild-moderate perivascular only, was present in 34%. Ossification was present in 38%, representing the entire specimen in 6%. Overall three patterns were seen – fibrosis only (63%), fibrosis with foci of ossification (28%), or predominantly metaplastic bone (9%).

Conclusions: Peyronie disease is a distinctive penile fibrosing disease associated with significant morbidity in the sexual function of middle-aged to older, mostly Caucasian men. The three general patterns observed here provide prospective guidance on the morphologic range expected for specimens encountered in this setting.

955 Racial Disparity in Expression of GDF-15 and NF-kB in Prostate Cancer and Benign Prostate

Oleksandr Kravtsov, Malvika Solanki, James R Lambert, Kathleen Torkko, M Scott Lucia, Kenneth Iczkowski. Medical College of Wisconsin, Milwaukee, WI; University of Colorado, Aurora, CO.

Background: African-American (AA) men typically have worse prostate cancer (PC) outcome than Caucasian (C) men. Growth differentiation factor 15 (GDF-15, PDF, NAG-1) is a stress-induced TGF-β superfamily anti-inflammatory cytokine with immunomodulatory functions. High expression of GDF-15 is associated with prostate cancer progression [PMID:12894347]. NF-kB is a transcription factor of the Rel family which is involved in cell proliferation, apoptosis, and angiogenesis, and is a pro-inflammatory mediator. GDF-15 was previously shown to suppress NF-kB activity [PMID:25327758].

Design: Tissue microarrays with 91 cases from AA and 88 from C men had 3-4 evaluable punched cores/case of prostate cancer (PC) and matched benign prostatic tissue. Cases were matched for Gleason score (mean 6.47 for both AA and C), stage, and margin status. TMAs were stained with validated goat polyclonal antibody to GDF-15 and rabbit monoclonal antibody to NF-kB. Reactivity was evaluated by 2 observers as 0-3+ and averaged for evaluable cores in a case. Wilcoxon Rank-Sum test was used to evaluate racial differences in median values.

Results: Both markers had higher expression in PC than benign tissue. GDF-15 reactivity in PC was higher in AA than C. NF-kB expression in PC was higher in C than AA. GDF-15 in PC was inversely correlated with NF-kB (r= - 0.34, p=0.001 for AA and r= - 0.24, p=0.025 for C).

Median values:	GDF-15 in benign	GDF-15 in PC	NF-kB in benign	NF-kB in PC
African American	1.0	2.0	0.5	1.0
Caucasian	0.5	1.5	0.5	1.5
p-value	0.14	<0.0001	0.29	0.0001

Conclusions: GDF-15 and NF-kB are racially differentially expressed proteins and are inversely related. Those findings may aid in explanation of worse cancer outcome in AA patients and investigation of the role of inflammation in prostate cancer. Stronger expression of GDF-15 and weaker expression of NF-kB in PC in AA patients, suggests a lessened ability to mount an inflammatory response to cancer, despite AA men's tendency toward more frequent prostatic inflammation [PMID:9605645]. This work is supported by the Department of Defense PCBN, Award No. W81XWH-10-2-0056 and W81XWH-10-2-0046.

956 Historic Gleason Score (GS) 3+5=8 (Grade Group (GG) 4) Prostate Cancer (PC) Has Low Reproducibility with 2014 ISUP Grading

Oleksandr N Kryvenko, Nouf Hijazi, Robert Poppiti, Paul J Taylor Smith, Merce Jorda, Jonathan I Epstein. University of Miami and Others, Miami, FL.

Background: GG4 includes 4+4, 3+5, and 5+3 combinations. Two recent studies using retrospective cohorts suggested that pattern 5 in GG4 PC imparts worse prognosis.

Design: Biopsies (Bx), radical prostatectomies (RP), and transurethral resections of the prostate (TURP) from 5 hospitals from 2005 to 2016 retrospectively reported as GS 3+5=8 (GG4) as the highest grade in a case were re-reviewed and graded according to the guidelines of the 2014 ISUP consensus conference.

Results: Table summarizes grading after re-review. Additionally, 2 (4%) Bx and 1(2%) RP were reclassified as GS 5+3 (GG4), 1 (2%) RP was reclassified as GS 4+4 (GG4). Two (4%) Bx and 1 (2) RP had treatment effect and no grade was assigned. In 6/12 (50%) Bx and 4/17 (24%) RP that retained GS 3+5 (GG4) after re-review, foci of patterns 3 and 5 were juxtaposed to one another without intermixture. In downgraded biopsies, pattern 5 was originally incorrectly assigned to poorly formed glands (n=23), foamy gland PC (n=4), dense secretion (n=1), & no clear reason (n=1). Upgrades in biopsies were because of assigning common grade to separate cores with different grades (n=10), grading of glomeruloid and fused glands as pattern 3 (n=2), inclusion of <5% pattern 3 in grading (n=2), & no clear reason (n=1). In 5/12 (42%) of downgraded RP, pattern 5 was a tertiary grade. Other reasons for RP downgrade were assigning pattern 5 to dense cribriform (n=3) and poorly formed glands (n=1), & dense secretion (n=1). The upgrades in RP were because of assigning common grade to separate tumor nodules with different grades (n=8), grading of glomeruloid and fused glands as pattern 3 (n=3), & inclusion of <5% pattern 3 in grading (n=3). Overall, cases signed out by urologic pathologists were more likely to retain the grade (14/20, 70% vs. 16/79, 20%, p<0.0001).

	3+5=8 (%)	Downgrade (%)				Upgrade (%)
		Total	GG1	GG2	GG3	
Bx (n=53)	12 (23)	25 (47)	1	15	9	12 (23)
RP (n=44)	17 (39)	12 (27)	-	11	1	12 (27)
TURP (n=2)	1 (50)	-	-	-	-	1 (50)

Conclusions: Only 23% of Bx and 39% of RP reported as GS 3+5=8 (GG4) in retrospective cohorts after 2005 retain this grade with contemporary grading. Assignment of common grade to separate biopsy cores or separate tumor nodules with different grades, and microscopic interpretation of patterns 4 prone to less interobserver reproducibility (i.e. poorly formed and fused glands) or a more recently described glomeruloid pattern 4 appear as the most common reasons of incorrect grading in the historical cohort.

957 The Impact of Consistent Reporting of the Presence or Absence of Muscularis Propria in Bladder Biopsies at an Academic Center

Razvan Lapadat, Eva M Wojcik, Guliz Barkan, Maria Picken, Stefan Pambuccian. Medical College of Wisconsin, Milwaukee, WI; Loyola University Medical Cente, Maywood, IL.

Background: The quality of surgical pathology reports is crucial to the management of patients with bladder tumors. Since the determination of invasion of muscularis propria (detrusor muscle) is the most important prognostic information that guides further management of patients with bladder tumors, one of the most important elements of the surgical pathology reports of bladder biopsies is a statement of adequacy regarding the presence or absence of muscularis propria in the biopsy. The aim of this study was to assess the impact of consistent reporting of the presence or absence of muscularis propria in all bladder biopsies on the quality of bladder biopsies at an academic healthcare institution.

Design: Pathology electronic medical records were searched for bladder biopsy diagnoses and were divided in two periods with respect to the implementation of an adequacy statement requirement: 2000-2008 (P1, before implementation) and 2009-2015 (P2, after implementation). All bladder biopsies reports issued in these periods were reviewed for the presence of an adequacy statement regarding the presence or absence of muscularis propria. The pathologic diagnoses, presence or absence of malignancy, and in cases of urothelial carcinoma, the level of invasion were also recorded. Comparison between the adequacy, diagnoses and levels of invasion in biopsies diagnosed during the two periods (P1 and P2) were performed using the two-tailed Fisher test with p<0.05 considered significant.

Results: 1816 bladder biopsies were reported in P1 and 1652 were reported in P2. All P2 biopsies contained an adequacy statement. The rate of "positive" biopsies containing urothelial carcinoma (in situ, papillary or invasive) increased in P2 (774/1816, 42.6% vs. 893/1652, 54%, p=<0.0001). The reported rate of presence of muscularis propria was higher in the second period (688/1816, 37.88% vs. 913/1652, 55.26%, p<0.0001). No significant differences between the reported rates of lamina propria invasion (275/774, 35.53% vs. 316/893, 35.38%, p=0.99) or muscularis propria invasion (90/774, 11.62% vs. 97/893, 10.86%, p=0.69) were found.

Conclusions: Our results suggest that the consistent reporting of adequacy of bladder biopsies, even in the absence of tumor, gives urologists feedback that can lead to improvement of the quality of biopsies. The adequacy of reporting rates can be used as a target of quality assurance efforts by monitoring the rates and providing confidential fedback to pathologists.

958 Interobserver Reproducibility of the Paris System for Reporting Urinary Cytology

Lester Layfield, Theresa Long, Robert L Schmidt, Magda Esebua, Shellaine R Frazier, Tamar Giorgadze. University of Missouri, Columbia, MO; University of Utah and ARUP Laboratories, Salt Lake City, UT; Weill Cornell Medicine, New York, NY.

Background: The Paris System for Reporting Urinary Cytology represents an improvement in classification of urinary specimens. The system uses six categories: unsatisfactory, negative for high grade urothelial carcinoma (NHGUC), atypical urothelial cells (AUC), suspicious for high-grade urothelial carcinoma (SUS), high-grade urothelial carcinoma (HGUC), and other malignancies. Currently, little data exists as to the interobserver reproducibility of this system. We report our findings for the interobserver reproducibility of the Paris System for Reporting Urinary Cytology in a large series of urine cytologies.

Design: Three-hundred and fifty-seven urine specimens were independently reviewed by four cytopathologists unaware of the previous diagnoses. The specimens were all Papanicolaou stained ThinPrep® preparations of voided and instrumented urines obtained from the bladder. Each cytopathologist rendered a diagnosis according to the Paris System categories. Three of the reviewers were board certified in cytopathology

and the fourth had over a decade of experience in examining urinary tract specimens. Agreement was assessed using absolute agreement and weighted chance-corrected agreement (kappa). Disagreements were classified as low risk and high risk based on the potential impact of a misclassification on clinical management.
Results: The average absolute agreement was 65% with an average expected agreement of 44%. The average chance corrected agreement (kappa) was 0.32. Nine hundred and ninety-nine of 1902 comparisons between rater pairs were in agreement, but 12% of comparisons differed by two or more categories for the category NHGUC. 24% differed by a single category for the category NHGUC. Raters had the highest agreement (63%) for the NHGUC category, but showed poor agreement for the other categories. The SUS category had an agreement of only 13%. The categories AUC and HGUC had agreement between raters of about 21%.
Conclusions: Interobserver agreement for the diagnostic categories proposed by the Paris System was good for the category "negative for high grade urothelial carcinoma" (NHGUC) but was poor for the other categories. Our findings indicated that the classification scheme recommended by the Paris System show adequate precision for the category NHGUC, but the other categories demonstrated unacceptable interobserver variability.

959 GLUT1 Expression Is Related to Tumor Recurrence and Survival in Renal Cell Carcinoma Clear Cell Type

Katia RM Leite, Paulo A Carvalho, Celine M Pinheiro, Sabrina T Reis, Miguel Srougi, William C Nahas. University of Sao Paulo Medical School, Sao Paulo, Brazil; Sao Paulo State Cancer Institute - ICESP, Sao Paulo, Brazil; Cancer Hospital of Barretos, Barretos, Sao Paulo, Brazil.
Background: Renal cell cancer, clear cell type (RCCcc) has as main carcinogenesis pathway the mutation of von Hippel-Lindau gene(VHL) that controls Hypoxia Induced Factor 1 (HIF-1α) that is consequently overexpressed. *SLC2A1* (*GLUT1*) is an important gene downstream from HIF-1α , responsible for the glucose uptake across the plasma membrane, important for tumor cell survival and cancer growth.
Our aim is to search for GLUT1 expression in RCCcc using a tissue microarray (TMA) and immunohistochemistry (IHC) correlating with the main prognostic factors, tumor recurrence and overall survival.
Design: Specimens from radical or partial nephrectomy of 148 patients treated surgically between 1988 and 2006 were used to construct the TMA. Two or three 6 mm fragments from the most representative area of the tumor were arranged side by side with an interval of 3 mm. GLUT1 expression was detected by IHC using the monoclonal antibody EPR3915 (ABCAM) in a 1:100 dilution. The results were classified in 4 categories regarding the intensity of the staining, 0 (negative), 1 (mild), 2 (moderate) and 3 (strong). Statistical analysis used the chi-square and ANOVA tests to correlate GLUT1 expression and prognostic factors. A Kaplan-Myer curve was designed for survival analysis.
Results: The evaluation was possible in 128 cases. GLUT1 was negative, mild, moderate and strong in 11(8.6%), 34 (26.6%), 53 (41.4%) and 30(23.4%) respectively. Sixteen (12.5%) patients reccured. GLUT1 was moderate or strongly positive in 87.6% of the cases (p=0.008). The Kaplan-Meir curve showed relation between GLUT1 expression and survival. Survival was 100% for GLUT1 negative cases and 70% for those strongly positive. There was no statistical difference for GLUT1 expression and Fuhrman grade (p=0.253), WHO/ISUP grade (0.082), presence of necrosis (p=0.124), intravascular tumor embolization (p=0.110) or tumor stage (p=0.225). There was a marginal difference regarding tumor size. The mean tumor size was 3.6 cm in GLUT1 negative cases and 5.9 cm for those GLUT1 strongly positive (p=0.063).
Conclusions: GLUT1 immune-expression is related to tumor recurrence and survival in RCCcc.

960 Comparative Analysis of Histopathology Assessment Criteria to Predict Progression in PT1 Bladder Cancer

Mariah Z Leivo, Debashis Sahoo, Leili Mirsadraei, Donna Hansel. University of California at San Diego, La Jolla, CA.
Background: Diagnosis of pT1 bladder cancer disease occurs in the context of progression of a high-grade in situ carcinoma or in the de novo setting. Several prior studies have attempted to propose metrics using histopathological parameters that could predict disease recurrence and/or progression. However, given the limitations, different methodologies, and unique terminologies applied in each of these studies, the methodology to best define pT1 substage remains undefined. We performed a head-to-head comparison of published and novel methods to measure pT1 disease as a predictor of progression.
Design: we re-reviewed all pT1 bladder cancer specimens seen at our institution from 2001 through 2015. Patients were excluded if they had a prior diagnosis of invasive disease and if the diagnosis of invasion changed on re-review. In total, 151 patients were included for study. Specimen analysis included qualitative measures such as "focal" or "extensive" invasion, as well as quantitative metrics including optimal micrometer measurements of invasive depth and total tumor diameter, relative percentage of invasive disease to tumor volume, volume of invasive disease measured in mm3, and relationship to the muscularis mucosae, among others. Concurrent feature that include stromal response, inflammation, CIS, angiolymphatic invasion and extent of muscle were factored into analysis. Patient follow-up, including repeat TUR pathology, subsequent therapy, and time to recurrence or death were used to identify patients with recurrence and/or progression. Significance is considered $P<0.05$.
Results: Histopathological parameters that were significant in pT1 measurement as a predictor of progression include above or below MM, focal versus extensive invasive disease, optical micrometer depth, % invasive cancer in specimen, aggregate cancer length, and calculated invasive tumor volume. The best performance was seen with aggregate cancer length and above vs below MM. Factors that independently associated with outcome in addition to pT1 measurement included angiolymphatic invasion, inflammation and desmoplasia. Not significant were necrosis, G3 histology, divergent differentiation including micropapillary and CIS.
Conclusions: The results from this comprehensive histopathological study suggest that key parameters may be of value in standardized reporting of pT1 disease and may be optimized with above vs below MM or aggregate cancer length.

961 Re-Evaluation of 31 "Unclassified" Eosinophilic Renal Cell Carcinomas in Young Patients

Yunjie Li, Victor E Reuter, George J Netto, Jonathan I Epstein, Pedram Argani. Johns Hopkins University School of Medicine, Baltimore, MD; Memorial Sloan Kettering Cancer Center, New York, NY.
Background: Many renal cell carcinomas (RCCs) in children and young adults are unclassified and are characterized by eosinophilic cytoplasm. We hypothesized that some of these RCC may be related to the recently described succinate dehydrogenase (SDH)-deficient RCC, fumarate hydratase (FH)-deficient RCC, and eosinophilic solid and cystic (ESC) RCC which demonstrates solid and cystic architecture, coarse cytoplasmic precipitates, and patchy expression of cytokeratin (CK) 20.
Design: We reviewed 31 unclassified RCCs with eosinophilic cytoplasm in patients aged 35 years or younger. On all cases, immunohistochemistry (IHC) for SDHB, FH, and CK20 was performed. IHC for 2-succinocysteine (2SC) was performed on RCC with loss of FH labeling.
Results: Three RCC (10%) (median age 19 years) demonstrated loss of FH labeling as well as aberrant 2SC labeling and were reclassified as FH-deficient RCCs. Importantly, none of these cases demonstrated the characteristic macronucleoli typical of FH-deficient RCC; instead, all demonstrated a nested tubular appearance that suggested oncocytoma. Two of 3 FH-deficient tumors were partially cystic while one was multifocal. Seven RCC (23%) (median age 20 years) demonstrated loss of SDHB and were reclassified as SDH-deficient RCCs. Importantly, these cases demonstrated fewer cytoplasmic vacuoles and inclusions than typical SDH-deficient RCC. Three of 7 SDH-deficient RCC were submitted with the differential diagnosis of oncocytoma, while 2 of 7 SDH-deficient RCCs mimicked the biphasic morphology of the t(6;11) RCC. Ten RCC (32%) (median age 27 years) were reclassified as ESC RCCs. Four of 10 ESC RCC were multifocal (1 bilateral), while 2 of 10 ESC RCC patients had a history of a prior malignancy (bladder and CNS). One patient presented with hematogenous metastases not previously described in ESC. Eleven RCC (35%) remained unclassified. No patient demonstrated evidence of or family history supporting a known syndrome.
Conclusions: The majority of previously unclassified eosinophilic RCC in young patients can now be classified. FH and SDH deficient RCC in young patients may not show typical morphologic features found in adult cases and instead may present as oncocytoma-like lesions, so FH and SDHB IHC should routinely be performed on such cases. Whether these SDH and FH-deficient RCC harbor somatic or germline alterations remains unclear. The association of ESC RCC in young patients with multifocality and history of prior neoplasia suggests the possibility of a genetic predisposition.

962 Urothelial Carcinoma with Loss of MSH2 and/or MSH6 Expression: A Clinicopathologic Study of 11 Cases

Li Liang, Priya Rao. The University of Texas MD Anderson Cancer Center, Houston, TX.
Background: Patients with Lynch syndrome have been known to have an increased risk of developing carcinoma of the upper urothelial tract; however, the clinicopathologic features of these tumors have not been well characterized.
Design: We retrospectively identified 11 cases in our institutional database from 2007-2016 that were shown to have loss of MSH6 (n=3) or MSH2/MSH6 (n=8) expression by immunohistochemistry.
Results: Patients' age at the diagnosis of urothelial carcinoma ranged from 43-84 years old (mean:62; median:61). Five out of 11 patients had previous history of colorectal adenocarcinoma (n=2), endometrial adenocarcinoma (n=2) or both (n=1), whereas the other 6 patients developed urothelial carcinoma as the presenting malignancy. Eight of 11 patients (73%) developed multifocal urothelial carcinoma. In addition to tumors of upper urinary tract, which occurred in all patients, 5 patients also developed bladder tumors. Two patients had low-grade urothelial carcinoma, three patients had high-grade urothelial carcinoma, and 6 patients had both. Tumor stage: Ta (n=3), T1 (n=2), T2 (n=2), T3 (n=3), and unknown (n=1). Nine patients underwent surgical resection and 2 of them received neoadjuvant therapy. The other 2 patients were treated with Mitomycin-C and/or endoscopic laser ablation. Lung metastasis was found in 2 patients. Followup data showed 9 patients to be NED (15-120 months; mean: 53 months) and 2 patients to be AWD (16 months and 13 years). Tumor-infiltrating lymphocytes (TIL), defined for the purpose of this study as intratumoral lymphocytes readily recognizable at 4X, were present in 4/10 cases (40%). We also noted the presence of an associated myxoid stroma in 4/10 cases (40%).
Conclusions: Patients with loss of one or more MSI markers tend to have multifocal tumors synchronously or sequentially, involving either upper urinary tract alone, or both upper urinary tract and bladder.

Case	Age	UUT/bladder	Stage	MSH6/MSH2	MSI	Followup
1	67	+/-	Ta	-/+	Stable	NED,9y
2	52	+/+	T2	-/-	High	NED,10y
3	51	+/-	T3	-/-	High	NED,15m
4	62	+/+	T3	-/+	NA	NED,41m
5	73	+/-	T1	-/+	Low	NED,28m
6	75	+/+	Ta	-/-	NA	NED,18.5m
7	84	+/-	Ta	-/-	NA	NED,29m
8	55	+/-	T3	-/-	NA	NED,18m
9	56	+/-	T2	-/-	NA	AWD,16m
10	61	+/+	NA	-/-	NA	NED,8y
11	43	+/+	T1	-/-	High	AWD,13y

963 Linking Histological Phenotype to Molecular Changes in Sunitinib Resistant Clear Cell Renal Cell Carcinoma

Zsuzsanna Lichner, Rola Saleeb, Henriett Butz, Roy Nofech-Mozes, Sara Riad, Kapus Andras, George M Yousef. St Michael's Hospital, Toronto, ON, Canada; University of Toronto, Toronto, ON, Canada.

Background: The receptor tyrosine kinase (RTK) inhibitor sunitinib is the first line treatment for advanced kidney cancer. Sunitinib inhibits angiogenesis via blocking signaling through VEGFR. About 80% of patients develop resistance after a drug-sensitive period. Molecular changes early in treatment may impact drug resistance, but are poorly understood

Design: Clear cell renal cell carcinoma model cell lines (ACHN, 786-O and Renca) were used to model sunitinib resistance in *in vitro* assays and *in vivo* in xenografted NSG mice. Sunitinib dose *in vivo* was 40 mg/kg/day and *in vitro* was 1 µM. mRNA expression was screened with Illumina HT-12 bead chip array and miRNA expression was assessed with Nanostring nCounter assay. R statistical packages were used for data processing and Reactome and miRPath softwares were used for downstream analysis.

Results: Sunitinib treatment led to several early changes in tumor histology. *In vivo* tumors in xenograft mice showed the emergence of live tumor areas within the necrotic spaces. These areas showed membranous staining for E-cadherin, while the rest of the tumor and vehicle-treated tumors were negative. *In vitro* model cell lines developed cancer spheroids when treated with sunitinib. These cancer spheres had significantly higher proliferative ability under treatment than the adherent cells. Cancer spheroids were highly tumorigenic and metastatic, and expressed established cancer stem cell markers, such as NCAM1, LGR5 and DNAJB9. The most significant molecular categories upregulated in spheroids included cell-cell adhesion related molecules, such as integrins, G-protein coupled receptors and cadherins. Cancer spheres showed membranous staining for E-cadherin, similar to the *in vivo* tumors. Additionally, histological similarities were observed between cancer spheroids and E-cadherin positive tumor areas within the necrotic patches. Further, their molecular similarity was verified by comparing their mRNA expression profile.

Conclusions: Sunitinib treatment causes early morphological changes in the tumor *in vivo* and *in vitro*. The formation of highly metastatic and tumorigenic cancer spheres in model cell lines is the most prominent effect in vitro. We provide preliminary evidence that sunitinib induced cancer spheres in model cell lines and E-cadherin positive tumor areas within the necrotic patches, in xenografted animals, are related.

964 Immunohistochemical Evaluation of NKX3.1 Expression in Prostatic Ductal Adenocarcinomas

Haiyan Liu, Myra L Wilkerson, Fan Lin. Geisinger Medical Center, Danville, PA.

Background: NKX3.1 is a prostate-specific homeobox gene located on chromosome 8p21. Our study of 1864 tissue microarray sections from various organs demonstrated that NKX3.1 expression was observed in 100% prostatic acinar adenocarcinomas (n=157), 32% of breast ductal carcinomas (n=90), and 11% of breast lobular carcinomas (n=40). However, to our knowledge, the expression of NKX3.1 was not well documented in prostatic ductal adenocarcinomas (PDACs).

Design: Immunohistochemical analysis of NKX3.1 (CP422A.B, Biocare) expression was conducted on 20 cases (from 19 patients) of PDAC on surgical biopsy specimens. A panel of potentially useful immunomarkers for identification of prostatic origin, including PSA, PAP, P504S, ERG, and CK7, was also performed. Nuclear staining for NKX3.1 and ERG and cytoplasmic staining for PSA, PAP, P504S and CK7 were interpreted as negative (<5% of tumor cells stained), 1+ (5-25%), 2+ (26-50%), 3+ (51-75%), and 4+ (>75%).

Results: One hundred percent (20/20) of PDACs expressed NKX3.1, with strong and diffuse (4+) staining in 19 of 20 cases. In contrast, PSA was positive in 17 of 20 cases, with strong and diffuse positivity in 7 of 20 cases. PAP and P504S were observed in 100% of cases, with strong and diffuse staining in 10 of 20 and 11 of 20 cases, respectively. Only 2 cases showed focal (1+) positivity for CK7, and 3 cases showed 4+ nuclear positivity for ERG.

Table 1. Summary of the immunostaining results

Case	NKX3.1	PSA	PAP	P504S
1	4+, S	1+, I	4+, S	4+, S
2	2+, W	neg	3+, I	4+, I
3	4+, S	4+, I	4+, I	4+, I
4	4+, S	1+, W	3+, S	3+, I
5	4+, S	2+, W	3+, W	4+, S
6	4+, S	2+, I	4+, S	3+, S
7	4+, S	2+, W	3+, W	4+, S
8	4+, S	4+, S	4+, S	3+, I
9	4+, S	4+, S	4+, S	4+, S
10	4+, S	neg	3+, I	2+, W
11	4+, S	4+, S	4+, S	3+, I
12	4+, S	neg	3+, I	3+, I
13	4+, S	4+, S	4+, S	4+, S
14	4+, S	4+, S	4+, S	4+, S
15	4+, S	2+, S	2+, S	3+, S
16	4+, S	3+, S	4+, S	3+, S
17	4+, S	2+, W	3+, W	4+, S
18	4+, S	4+, S	4+, S	4+, S
19	4+, S	4+, S	4+, S	4+, S
20	4+, S	3+, I	3+, I	4+, S

Note: S-Strong; I-Intermediate; W-Weak; Neg-Negative

Conclusions: These data demonstrate that NKX3.1 is the most sensitive immunomarker for PDAC. NKX3.1 should be included in a panel of immunomarkers for the identification of prostatic origin (including acinar and ductal adenocarcinomas) when working on metastatic tumors of unknown primary. In addition, based on this small number of cases, CK7 appears to be negative in the majority of PDACs.

965 NKX3.1 Is the Most Sensitive Immunohistochemical Marker in Identifying Metastatic Prostatic Carcinomas

Haiyan Liu, Myra L Wilkerson, Fan Lin. Geisinger Medical Center, Danville, PA.

Background: NKX3.1 is a prostate-specific homeobox gene located on chromosome 8p21. Our recent study of 1864 tissue microarray sections from various organs demonstrated that NKX3.1 expression was observed in 100% of prostatic acinar adenocarcinomas (n=157), 32% of breast ductal carcinomas (n=90), and 11% of breast lobular carcinomas (n=40). However, to our knowledge, the expression of NKX3.1 was not well documented in metastatic prostatic carcinomas (MPCAs), especially in decalcified specimens.

Design: Immunohistochemical analysis of NKX3.1 (CP422A.B, Biocare) expression was conducted on 36 MPCAs on small tissue or needle core biopsy specimens, including bone (n=14), lymph node (n=9), bladder (n=7), lung (n=3), brain (n=2), and liver (n=1). A panel of potentially useful immunomarkers for identification of prostatic origin, including PSA, PAP, and ERG, was also performed. Nuclear staining for NKX3.1 and ERG and cytoplasmic staining for PSA and PAP were interpreted as negative (<5% of tumor cells stained) and positive (>5% of tumor cells stained).

Results: The results are summarized in Table 1. Thirty-six of 36 cases of MPCAs expressed NKX3.1, with strong and diffuse (>50% tumor cells stained) nuclear staining in all cases. In contrast, PSA was positive in 24 of 36 cases (67%). PAP and ERG were observed in 97% and 14% of cases, respectively.

Liver (1)	1/100%	1/100%	1/100%	0/0%
Pos-Positive				

Table 1. Summary of the immunostaining results

Site (n)	NKX3.1 (Pos/%)	PSA (Pos/%)	PAP (Pos/%)	ERG (Pos/%)
Bone (14)	14/100%	10/67%	13/87%	4/27%
Lymph Node (9)	9/100%	7/78%	9/100%	1/11%
Urinary Bladder (7)	7/100%	3/43%	7/100%	1/14%
Lung (3)	3/100%	2/67%	3/100%	0/0%
Brain (2)	2/100%	1/50%	2/100%	0/0%

Conclusions: These data demonstrate that NKX3.1 is the most sensitive immunomarker for MPCAs, including on decalcified specimens. NKX3.1 should be included in a panel of immunomarkers for the identification of prostatic origin when working on metastatic tumors of unknown primary.

966 Concordance Study of 4 Anti-PD-L1 Antibodies in Primary and Metastatic Bladder Cancer

Thomas Long, Regan Fulton, Masha Kocherginsky, Tatjana Antic, Cigdem Ussakli, Allen M Gown, Maria Tretiakova. University of Washington, Seattle, WA; University of Chicago, Chicago, IL; PhenoPath, Seattle, IL.

Background: Therapy with anti-PD-L1 immune checkpoint inhibitors has been approved for several cancers, and recently also for urothelial carcinoma (UC). Diagnostic immunostaining (IHC) for PD-L1 is the standard companion test for selecting patients for anti-PD-L1 therapy, but various therapeutic agents have been developed with unique IHC assays, each using different antibody, staining platform and scoring protocol. This poses a logistical problem for the diagnostic laboratories in offering PD-L1 testing. We

performed a comparative study of PD-L1 expression in primary and metastatic UC using platform independent clone E1L3N and 3 FDA-approved clones: 22C3 (KEYTRUDA), 28.8 (OPDIVO), SP142 (TECENRIQ).
Design: Tissue microarrays with 145 primary UC, 84 regional LN metastases, and 12 distant UC metastases were stained according to manufacturer protocols with 22C3 (DAKO), 28.8 (DAKO), E1L3N (CELL SIGNALING), and SP142 (VENTANA) at PhenoPath laboratories. Each core was analyzed by 2 pathologists for % positive cells multiplied by intensity, with combined score calculated as 0=negative, 1-49=low positive, 50-200=high positive.
Results: Of all UC cases 43 stained positive with at least 2 of 4 antibodies: 30 (20.7%) primary UC, 11 (14.3%) LN metastases, and 2 (16.7%) distant metastases. High expression was present in 28-48% primary UC and 25-33% metastases. Complete concordance for PD-L1 expression by all 4 antibodies was achieved in 85.3% cases: 80.6% in primary UC and 92% in metastases. Only 1 case (0.4%) showed a major discrepancy. TMA core heterogeneity within cases was 6.4% (E1L3N), 8.9% (22C3), 9.8% (28.8) and 10.2% (SP142). 119 of 649 (18.3%) of total TMA cores were positive for some level of PD-L1 expression with mean combined scores of 59.6 (28.8), 47.5 (22C3), 40.7 (E1L3N) and 36.9 (SP142). Pairwise antibody comparison for each core also showed high concordance (range 0.65-0.99).

Pairwise		CONCORDANCE CORRELATION COEFFICIENTS (CI 95%)		
Marker 1	Marker 2	UC primary (N=374)	UC met regional (n=203)	UC met distant (N=72)
22C3	28.8	**0.76** (0.69-0.82)	**0.96** (0.95-0.96)	**0.98** (0.97-0.99)
22C3	E1L3N	**0.80** (0.73-0.85)	**0.91** (0.89-0.92)	**0.88** (0.82-0.92)
22C3	SP142	**0.65** (0.55-0.74)	**0.76** (0.73-0.79)	**0.99** (0.99-1.00)
28.8	E1L3N	**0.93** (0.92-0.95)	**0.88** (0.85-0.90)	**0.90** (0.86-0.94)
28.8	SP142	**0.88** (0.84-0.91)	**0.67** (0.64-0.71)	**0.98** (0.97-0.99)
E1L3N	SP142	**0.91** (0.88-0.93)	**0.81** (0.78-0.83)	**0.88** (0.83-0.92)

Conclusions: A significant subset (18.3%) of UC stained positive for PD-L1 with 85.3% concordance between all 4 antibodies and only 1 major discrepancy. The results show strong evidence that various PD-L1 IHC assays may be diagnostically equivalent in bladder tumors despite some tumor heterogeneity and variability in assay sensitivity.

967 Frequency of Succinate Dehydrogenase and Fumarate Hydratase-Deficient Renal Cell Carcinoma Based on Immunohistochemical Screening with SDHA/SDHB and FH/2SC

Tilcia Lopez, Sounak Gupta, Yingbei Chen, Loren P Herrera Hernandez, John C Cheville, Rafael E Jimenez. Hospital Calderón Guardia, San José, Costa Rica; Mayo Clinic, Rochester, MN; Memorial Sloan Kettering Cancer Center, New York, NY.
Background: Mutations of the succinate dehydrogenase (SDH) enzyme subunits commonly leads to a loss of function of the holoenzyme complex. This complex, comprised of the SDH subunits (A, B, C, D, SDHAF1 and SDHF2), is a component of the mitochondrial complex II and plays a key role in the Krebs cycle. The presence of germline *SDH* mutations leads to a genetic predisposition to SDH-deficient neoplasms, including RCCs and paragangliomas. Similarly, loss of function of fumarate hydratase (FH), another enzyme that plays a key role in the Krebs cycle, leads to a genetic predisposition to hereditary leiomyomatosis associated RCC (HLRCC). SDHA/SDHB IHC was performed to screen for SDH loss. Loss of FH leads to an accumulation of its substrate, S-(2-succino)-cysteine (2SC), and this can be screened for using IHC for FH/2SC. Herein, this immunostaining strategy was used to determine the incidence of SDH-deficient RCCs and HLRCCs.
Design: Apart from having carried a diagnosis of RCC and tissue available for analysis, cases were not otherwise selected based on histopathologic or clinical features for the study. Tissue Microarrays (TMA) were constructed from these cases using four 1.0mm cores of representative tissue from each tumor. Representative TMA sections were immunostained for SDHA, SDHB, FH and 2SC. SDHA/SDHB antibodies (Abcam; clones 2E3GC12FB2AEZ and 21A11AE7) were used at a dilution of 1:200. A granular pattern of immunostaining for SDHA/SDHB in adjacent renal tubules and vascular endothelium was considered a positive internal control. FH/2SC IHC was performed as previously described (Pathol. 2011; 225:4–11).
Results: 992 RCCs [papillary (P): 411, clear cell (CC): 203, chromophobe (Ch): 87, oncocytoma: 291] were subjected to IHC for SDHA/SDHB. Loss of SDHA/SDHB was seen in 1 of 411 P RCCs (0.24%), 1 of 203 CC RCCs (0.49%), 0 of 87 Ch RCCs (0%) and 3 of 291 Oncocytomas (1.03%). The overall frequency was 5 of 992 cases (0.5%). Diffuse nuclear and cytoplasmic 2SC staining but retained FH expression, suggestive of dysfunctional FH protein, was seen in 1 of 411 P RCCs (0.25%).
Conclusions: While the spectrum of SDH-deficient RCCs primarily involves oncocytic neoplasms, there are reports of rare non-oncocytic SDH-deficient RCCs. While the overall frequency of SDH-deficient RCCs (0.5%) and HLRCC (within the P RCC cohort, 0.25%) was low, SDH-deficient RCCs had the highest incidence in oncocytic neoplasms (1.03%).

968 Metastatic Lymph Node Involvement in Anterior Prostatic Fat and Implications for the Pathologist

Nicolas Lopez-Hisijos, Iskender Sinan Genco, Alex Gorbonos, Stefan Pambuccian, Guliz Barkan. Loyola University Medical Center, Maywood, IL.
Background: Since 2009, in our institution, the anterior prostatic fat (APF) has been submitted as part of the pelvic lymph node dissection (PLND) in radical prostatectomies (RP). Recent studies have suggested that the histologic assessment of the APF may be unnecessary, especially in low grade tumors. Our aim in this study was to determine the rate of LNI in the APF and the best way of processing this tissue.
Design: We searched our database for RP specimens from 1/1/2009 to 7/30/2016. We excluded cysto-prostatectomies, cases with no APF, and malignancies other than prostatic adenocarcinoma. We recorded the Gleason score (GS), grade group of the RP and core biopsy (CB), the number and location of lymph nodes (LN), the percentage of tissue involved by tumor in the RP, and the number of CBs involved by tumor. The cases with lymph node involvement (LNI) were reviewed to determine their size and palpability in correlation with the gross description.
Results: We found 611 RP specimens, of which 273 were reviewed. Of these, 14 (5%) had LNI and 3 (1.1%) had LNI present in the APF. The histologic grade and T stage of the cases with LNI was generally high. The LNs involved by metastatic tumor in sites other than the APF ranged from 0.4-5.0cm in diameter with a mean diameter of 1.7 cm. In the cases with LNI in the APF only, the LNs were much smaller, 0.2cm and 0.3cm. Also the grade and stage of these two cases was lower. The third case with LNI in the APF had high grade and stage and also had metastatic disease in other sites. The LNs involved in this case were 1.2cm and 2.0cm in diameter, similar to the group with LNI in other sites.

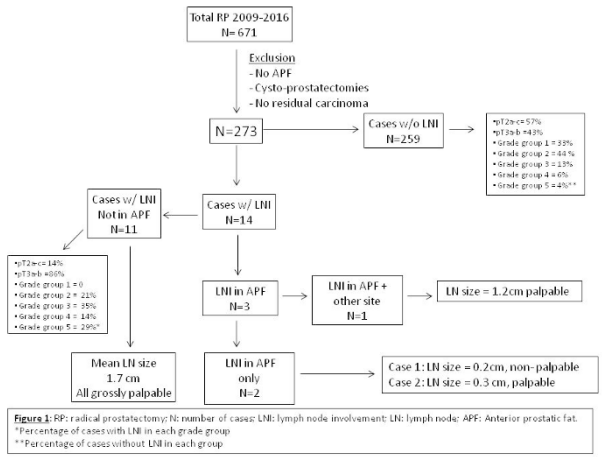

Conclusions: Based on our results we believe that a low tumor burden and grade does not preclude the necessity of processing the APF for histologic assessment. Furthermore, since very small non-palpable lymph nodes can be involved, we recommend submitting the entire specimen even if no grossly identifiable lymph nodes are present. Since the clinical follow-up interval in patients with LNI in the APF is short, the implications of involvement by low grade tumors in small LNs in the APF are not clear and should be the focus of future studies.

969 Clinical Significance of Urothelial Papillary Proliferation of Unknown Malignant Potential (UPUMP): A Retrospective Study of 79 Patients

Brett M Lowenthal, Mahul B Amin, Donna Hansel. University of California San Diego, San Diego, CA; University of Tennessee Health Sciences Center, Memphis, TN.
Background: UPUMP is a new category of urothelial lesions described in the 2016 WHO Classification of Tumours of the Urinary System & Male Genital Organs which encompasses lesions previously termed flat & papillary urothelial hyperplasia. It is defined as marked urothelial thickening with minimal or no cytologic atypia & no true papillary formation. The biologic potential & clinical outcomes of this entity have yet to be understood. This study reviews UPUMP comparing lesions categorized previously as urothelial hyperplasia of flat & papillary types.
Design: All bladder cases seen at our institution from 2001-2014 were reviewed for age, gender, symptomatology, current diagnosis, prior bladder diagnoses, follow-up bladder diagnoses & length of clinical follow-up. Only cases diagnosed as urothelial hyperplasia without associated overlying carcinomatous changes (low or high grade) were included in the study. Each case was categorized as a flat or papillary lesion.
Results: Of the 79 UPUMP cases identified, flat architecture comprised 35 cases (44%), while papillary architecture comprised 44 cases (56%). Mean clinical follow-up for flat vs. papillary hyperplasia was 64.9 & 62.5 months, respectively. Among lesions with flat architecture, 63% were on surveillance for urothelial carcinoma, while 37% were de novo. Among lesions with papillary architecture, 61% were on surveillance for urothelial carcinoma, while 39% were de novo. Of the de novo cases, 23% of flat & 24% of papillary hyperplasia subsequently developed bladder neoplasia; 2 de novo patients were lost to follow up. Subsequent neoplasia was non-high grade in 8% for flat lesions vs. 24% for papillary lesions, & high grade in 15% for flat lesions vs. 6% for papillary lesions. The non-neoplastic associations in UPUMP lesions (flat vs. papillary) included hematuria (62% vs. 65%), urinary retention (23% vs. 12%), fistula (15% vs. 0%), infection (15% vs. 12%), incontinence (0% vs. 12%), & cystocele (8% vs. 0%).

Conclusions: Our data on UPUMP indicate that just over one third of UPUMP cases are de novo lesions. Both architectural patterns of de novo UPUMP are associated with subsequent neoplasia in less than 25% cases. The overall similar associations with de novo disease & its progression in both categories of hyperplasia provide scientific justification for the WHO 2016 use of the descriptor "unknown malignant potential" for these lesions & for grouping them together into one category.

970 The Association of Cribriform Lesions with Prostatic Adenocarcinoma Outcomes: A Meta Analysis

Xunda Luo, Nirag Jhala, Jasvir S Khurana. Temple University Hospital, Philadelphia, PA.

Background: The International Society of Urological Pathology (ISUP) recently proposed that all cribriform lesions in prostate adenocarcinoma (PA) should be assigned a Gleason score of 4. This was based on several recent studies suggesting a correlation between presence of cribriform lesions and poor outcomes. However, a systematic review on this correlation is currently lacking, which inspired the present study.

Design: Using the key words 'prostate adenocarcinoma', 'cribriform pattern', and 'prognosis', the Pubmed database was searched for all English-language articles published up to September 2016. All PA cases with radical prostatectomy performed at TUH from January 2015 to January 2016 were also reviewed for the prevalence of cribriform lesions, extra prostatic extension (EPE), and seminal vesicle invasion (SVI). Immunohistochemistry for basal cells were performed when a differentiation between cribriform lesions and intraductal carcinoma was necessary. Odds ratios (OR) and their 95% confidence intervals (95% CI) were calculated using meta-analysis.

Results: Fourteen publications which matched the criteria were reviewed. Four of thesewere case control studies (sample size: 133-233). They reported the prevalence of cribriform lesions in patients with and without adverse outcomes including positive surgical margin(s), EPE, biochemical prostate-specific antigen recurrence, distant metastasis, and disease-specific death. These studies were included for meta-analysis. Of the 109 TUH cases reviewed, EPE was observed in 40% of the cases with cribriform lesions and 10.2% of the cases without, whereas SVI was observed in 36% of the cases with cribriform lesions and 1.7% of the cases without. The meta-analysis using the fixed effects model revealed a significant increase in the incidence of adverse outcomes in patients who had cribriform lesions relative to those who did not (OR=11.37, 95% CI: 6.00-21.54, I^2=0%; Figure 1).

Figure 1

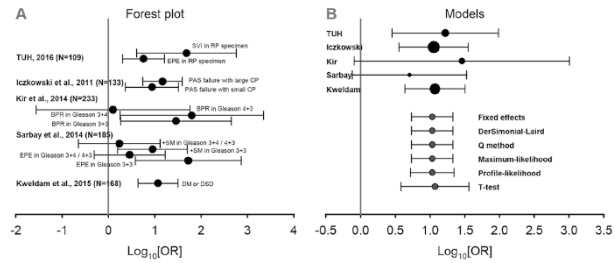

Conclusions: The meta-analysis results suggest that presence of cribriform lesions does associate with aforementioned adverse clinical outcomes. The evidence strongly backs the vote of the 2014 ISUP consensus meeting on categorizing all cribriform lesions as Gleason 4 lesions.

971 The Use of the Composit Biopsy Grade Score in the Outcome Prediction for Radical Prostatectomy

Xunda Luo, Nirag Jhala, Huaqing Zhao, Jasvir S Khurana. Temple University Hospital, Philadelphia, PA; Lewis Katz School of Medicine, Temple University, Philadelphia, PA.

Background: Recently the International Society of Urological Pathology (ISUP) proposed a 5-tier prognostic grade group for prostatic adenocarcinoma. The present study aimed to further investigate the predictive value of a composite biopsy grade score based on this grade group on the extraprostatic extension (EPE) and seminal vesicle invasion (SVI) of the tumor in radical prostatectomy (RP).

Design: All cases in the present institution from January 2015 to January 2016 with both biopsy and RP material available were reviewed. The composite biopsy grade score (CBGS) was calculated by averaging the products of the tumor grade and the percentage of tissue involved for all biopsy sites in biopsies. The same two parameters in RP specimens were multiplied to obtain the RP grade score. Statistical analyses on the correlation between the two measures and the predictive power of the CBGS on EPE and SVI were performed using SPSS Statistics Version 20 (IBM Corporation, Somers, NY, USA).

Results: A total of 109 cases were included. The CBGS correlated well with the RP grade score (r^2=0.68, p<0.001, s=0.87). Compared to the perineural invasion (PNI) status at biopsy, the CBGS provided a more sensitive and specific means to predict EPE and SVI status in RP (Table 1, Figure 1).

Predictor	EPE			SVI		
	Cutoff	Sensitivity	Specificity	Cutoff	Sensitivity	Specificity
CBGS	34.75	0.77	0.82	34.75	0.84	0.78
PNI		0.73	0.70		0.68	0.66

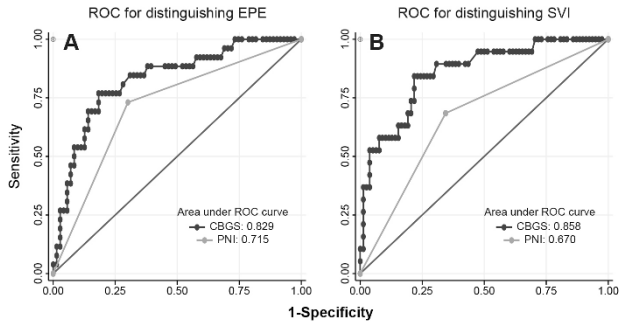

Although PNI status at biopsy was an independent predictor for EPE and SVI in following RP in univariate statistical analyses (for EPE: OR=2.43, 95% CI=[1.62, 3.63]; for SVI: OR=1.99, 95% CI=[1.31, 3.02]), it was no longer a significant factor after the effect of the CBGS had been adjusted in multivariate logistic regressions (EPE: OR=0.57, 95% CI=[0.17, 1.90]; SVI: OR=1.52, 95% CI=[0.35, 6.55]). The CBGS, however, remained an independent predictor in these multivariate analyses (EPE: OR=10.54, 95% CI=[2.71, 41.07]; SVI: OR=33.48, 95% CI=[5.50, 203.79]).

Conclusions: The CBGS is useful for biopsy – RP correlation and is better than PNI for EPE/SVI prediction.

972 Ethnicity Background and the Predictive Power of the Composite Biopsy Grade Score on the Outcomes of Prostatic Adenocarcinoma

Xunda Luo, Priti Lal, Nirag Jhala, Jasvir S Khurana. Temple University Hospital, Philadelphia, PA; Hospital of the University of Pennsylvania, Philadelphia, PA.

Background: Preliminary data shows that a composite biopsy grade score (CBGS) combining the 2014 International Society of Urological Pathology grade group and percentage of biopsy tissue involved by cancer may be a useful predictive tool for extraprostatic extension (EPE) and seminal vesicle invasion (SVI) in prostatic adenocarcinoma (PA). In the present study, the predictive value of the CBGS on patients of different ethnicity backgrounds was evaluated in two academic university hospitals.

Design: All African-American and Caucasian patients with PA from hospital A (2015-2016) and a group of African-American and Caucasian patients with PA (2004-2008) from hospital B were enrolled. Biopsy and radical prostatectomy (RP) material were reviewed. The CBGS was calculated by averaging the products of the tumor grade group and the percentage of tissue involved for all biopsy sites. The predictive power of the CBGS on EPE and SVI in RP were analyzed with SPSS Statistics Version 20 (IBM Corporation, Somers, NY, USA).

Results: A total of 86 cases from hospital A (41 African Americans and 45 Caucasians) and 57 cases from hospital B (17 African Americans and 40 Caucasians) were included. The patients from both A and B were comparable in age. Although the difference in CBGS was not statistically significant between the ethnical groups (F=0.32, p=0.57) at diagnosis, African Americans were more likely to present with EPE and SVI at RP, although the trends were not statistically significant (*odds ratio*: 1.20-2.31, *95% CI*: 0.10-14.05). The predictive powers of CBGS (area under ROC curve: 0.68-0.92; sensitivity: 0.68-1.00; specificity: 0.64-0.97) were on par with more complex nomograms. CBGS cutoffs for best sensitivity and specificity were lower for African Americans as per data from both hospitals (Table 1).

Table 1. Patient and ROC characteristics

	Hospital A		Hospital B	
	AA (N=41)	C (N=45)	AA (N=17)	C (N=40)
Age (mean±SD)	61.7 ± 6.7	62.7 ± 7.3	61.2 ± 5.9	59.8 ± 6.6
2-way ANOVA	Ethnicity: F=0.030, p=0.863; Institution: F=2.034, p=0.156			
Log CBGS (mean±SD)	1.4 ± 0.5	1.2 ± 0.8	0.6 ± 0.8	1.0 ± 0.7
2-way ANOVA	Ethnicity: F=0.317, p=0.574; Institution: F=15.729, p<0.001			
EPE (N)	15	9	5	8
AA/C	*OR*=2.308, *95% CI*=[0.876, 6.077]		*OR*=1.667, *95% CI*=[0.454, 6.112]	
Area under ROC curve	0.77	0.92	0.84	0.68
Cutoff	34.50	43.75	7.25	14.48
Sensitivity	0.75	0.88	0.79	0.70
Specificity	0.76	0.87	0.77	0.64
SVI (N)	10	8	1	2
AA/C	*OR*=1.492, *95% CI*=[0.525, 4.242]		*OR*=1.188, *95% CI*=[0.100, 14.047]	
Area under ROC curve	0.86	0.84	0.91	0.80
Cutoff	34.50	47.29	9.00	61.25
Sensitivity	0.90	0.75	1.00	0.80
Specificity	0.71	0.87	0.74	0.97

Note. AA: African American, C: Caucasian, N: sample size, ANOVA: analysis of variance, CBGS: composite biopsy grade score, OR: odds ratio, CI: confidence interval, ROC: receiver operating characteristic

Conclusions: African Americans with PA are more likely to present with EPE and/or SVI comparing to the Caucasian patients with the same CBGS. This ethnicity background-related variability needs to be considered in predicting pathological stage and selecting patients for active surveillance.

973 The Role of SATB2 Immunohistochemistry in the Differential Diagnosis of Malignant Glandular Lesions of the Urinary Bladder

Nicholas Mackrides, Merce Jorda, Andre Pinto. University of Miami, Miami, FL.

Background: Primary adenocarcinomas of the urinary bladder (which include urachal neoplasms) are uncommon, and before rendering the diagnosis, careful consideration must be taken in order to exclude the involvement by a tumor from a separate anatomic site. Other lesions frequently encountered, although not adenocarcinomas *per se*, are

urothelial carcinomas with glandular differentiation. Secondary adenocarcinomas can involve the bladder by direct extension or metastasis, frequently originating from the gastrointestinal tract (commonly from a colorectal primary). The distinction between these entities is essential because of differences in staging, treatment, and prognosis. Special AT-rich sequence-binding protein 2 (SATB2) is a marker that has been demonstrated to be predominantly expressed in lower gastrointestinal tract epithelium and colorectal adenocarcinoma. The goal of this study was to evaluate if immunohistochemistry (IHC) for SATB2 can be of value in the differential diagnosis of malignant glandular neoplasms of the bladder.

Design: IHC for SATB2 was performed on formalin fixed, paraffin embedded tissue from a total of 21 cases, including 13 primary bladder malignancies and 8 metastatic colorectal carcinomas to the bladder. The primary tumors consisted of 6 urothelial carcinomas with glandular differentiation, 4 (non-urachal) adenocarcinomas and 3 urachal adenocarcinomas. The metastatic tumors consisted of 2 appendiceal and 6 colorectal adenocarcinomas (confirmed by clinical history and follow up studies). Interpretation of SATB2 was based on presence or absence of nuclear positivity, reviewed by two pathologists.

Results: A total of 22 cases were retrieved. One case was discarded due to ambiguity in regards to site of origin (primary vs. metastatic). Among the metastatic tumors (2 appendiceal and 6 colorectal adenocarcinomas), 8/8 (100%) were positive for SATB2, compared to 2/13 (15.4%) primary bladder carcinomas. The latter group consisted of 1/3 (33.3%) urachal adenocarcinomas, 1/4 (25%) non-urachal primary bladder adenocarcinomas, and 0/6 (0%) urothelial carcinomas with glandular differentiation (absent in both glandular and conventional urothelial components).

Conclusions: SATB2 is an extremely sensitive (100%) and relatively specific marker (84.6%) for metastatic lower gastrointestinal neoplasms to the urinary bladder when compared to primary bladder carcinomas. In this small cohort, we have demonstrated that SATB2 has utility in determining the site of origin, and integrating this marker into a panel of IHC stains could be a valuable diagnostic tool.

974 Testicular Hemangioma: A Single Institutional Experience

Steven A Mann, Thomas M Ulbright, Muhammad Idrees. Indiana University School of Medicine, Indianapolis, IN.

Background: Testicular hemangioma (THA) is a rare neoplasm limited mostly to case reports with scant clinicopathological information. Its rarity may lead to misdiagnosis and overtreatment. A review of institutional cases was conducted to further characterize the morphologic and clinical features.

Design: A search was performed for hemangiomas arising in the testis. Clinical information was collected from institutional records and consultation notes. Diagnoses were confirmed and tumors subtyped in cases with available H&E slides. An immunohistochemistry (IHC) panel including CD31, factor VIII, GLUT1, ERG, D2-40, SF-1, inhibin, and S100 was performed.

Results: Sixteen cases were identified from 1998-2015, 8 in-house and 8 consults. H&E slides were available for 13 and IHC was performed in 12. Average age was 31 years (range 10-75). Among in-house cases, 4 presented as palpable masses, 3 with pain, and 1 was found incidentally by ultrasound. Orchiectomy was performed in 11 cases, 4 had tumor excision and 1 was observed clinically after biopsy confirmation. Frozen section in 3 cases led to conservative management. Average size was 8 mm (range 3-16). Tumors varied from gray-tan to red-pink and soft to firm with well-circumscribed or irregular borders. There were 7 capillary HAs (capHA) with bland nuclei and well-defined lumens, and 6 epithelioid HAs (eHA), with plump nuclei, prominent nucleoli, and more cytoplasm. Three cases were reported as hemangioma not otherwise specified. Two capHAs were highly cellular and infiltrative while the remaining 5 were lobular with a sclerotic stroma and a fibrotic capsule. One eHA had a fibrotic capsule and the remaining 5 were infiltrative with tunica albuginea and/or rete involvement. All endothelial tumor cells were diffusely and strongly positive for ERG1 and FVIII. CD31 positivity ranged from strongly to weakly positive (1 capHA stained negative). All other markers were negative. No recurrences were reported (follow-up ranged 1-99 months).

Conclusions: THA occurs over a wide age range. Most present as a mass and a few with pain. Compared to prior reports, eHAs were overrepresented and the commonly reported cavernous subtype was not identified. This difference may be partially attributed to consultation bias. The eHAs tend to be infiltrative and capHAs circumscribed. ERG1 and FVIII were the most useful immunostains. Outcomes were the same for orchiectomies and conservatively managed cases, warranting the latter.

975 GATA-3 Is a Specific Marker for Clear Cell Papillary Renal Cell Carcinoma

Jose G Mantilla, Tatjana Antic, Maria Tretiakova. University of Washington, Seattle, WA; University of Chicago, Chicago, IL.

Background: Clear cell papillary renal cell carcinoma (CCPRCC) shows an invariably indolent behavior, with no reported cases of death from disease or metastasis. Histologically, they have tubulo-papillary architecture with clear cell cytology and low grade nuclei in linear arrangement. Given their indolent behavior, it is of utmost importance to reliably distinguish them from their malignant morphologic mimics, such as clear cell (CCRCC) and papillary renal cell carcinoma (PRCC), among others. GATA3 is a transcription factor that is typically expressed in the distal convoluted tubules and collecting system, as well as urothelium, but consistently shown to be absent in the proximal nephron and in RCCs.

Design: We retrospectively reviewed 33 cases with features of CCPRCC at the two institutions. All cases were stained with antibodies against GATA3, CK7 and CAIX. Cases with morphology, immunophenotype or cytogenetics inconsistent with CCPRCC were reclassified accordingly. Additionally, we stained tissue microarrays with 103 typical CCRCC and 62 PRCC, each case represented in triplicate.

Results: 20 cases were consistent with CCPRCC; all of them showed diffuse positivity for CK7 and cup-like reactivity with CAIX. Of these lesions, 15 (75%) showed strong nuclear reactivity for GATA3, 13 diffuse and 2 focal. Although some of non-CCPRCC neoplasms showed at least partial CK7/CAIX co-expression, none of them were immunopositive for GATA3.

Diagnosis	n	GATA-3(+)	GATA-3(-)
CCPRCC	20	15	5
CCRCC w/ prominent fibromuscular stroma or CCPRCC-like	7	0	7
Monosomy 8 RCC (confirmed)	2	0	2
PRCC with cytoplasmic clearing	2	0	2
PRCC (typical)	65	0	65
CCRCC (typical)	106	0	106
Acquired Cystic Disease RCC	1	0	1
Chromophobe RCC	1	0	1

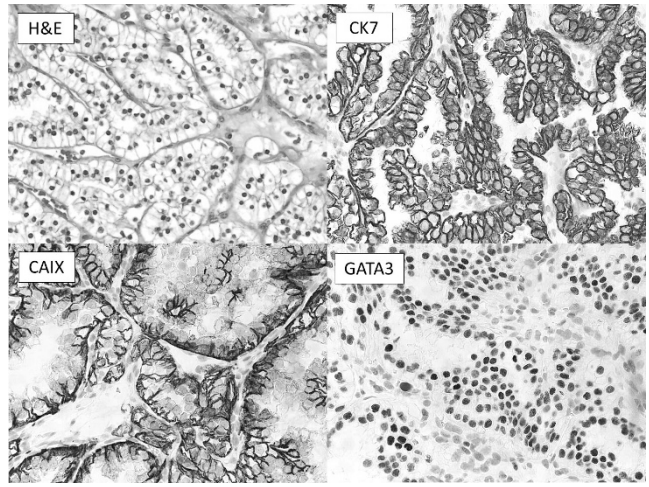

Conclusions: GATA3 is consistently expressed in 75% of CCPRCC in our series. These findings, when present, are highly specific and useful for distinguishing this indolent lesion from its malignant counterparts, to avoid unnecessary treatment; it also provides insight into the possible histogenesis of these neoplasms, suggesting CCPRCC origin from the distal portion of the nephron, as opposed to other variants of RCC.

976 Utility of Clinical Risk Stratification in the Selection of Muscle-Invasive Bladder Cancer (MIBC) Patients for Neoadjuvant Chemotherapy (NAC) Prior to Radical Cystectomy (RC): A Retrospective Cohort Study

Douglas A Mata, Friedrich-Carl von Rundstedt, Oleksandr N Kryvenko, Anup Shah, Iny Jhun, Seth P Lerner. Brigham and Women's Hospital, Boston, MA; Baylor College of Medicine, Houston, TX; University of Miami Miller School of Medicine, Miami, FL; University of Pittsburgh Medical Center, Pittsburgh, PA.

Background: Level I evidence supports the use of cisplatin NAC for MIBC prior to RC. On average, 30-40% of patients achieve pT0 stage after receiving NAC. Recently, a risk-stratification model developed at MDACC specified criteria for patient selection for NAC. We applied this model to our RC cohort and evaluated the effect of NAC on survival in high vs. low risk patients.

Design: Chart review of RC patients at two institutions between 2004-2014. Clinical stage was determined by the EUA, TURBT, and preop imaging. Patients with cT2-T4a node-negative disease were included. Those with sarcomatoid features were excluded. Per the MDACC model, patients were classified as high risk if they had hydronephrosis, ≥cT3b-T4a disease, variant histology (*i.e.*, micropapillary or small cell), or LVI. Variables were examined for associations with CSS, OS, and risk-category reclassification.

Results: We identified 166 patients (median follow-up 22.2 months). In all, 117 (70.5%) did not receive NAC, 68 (58.1%) of whom we classified as high risk. CSS and OS were significantly decreased in these high-risk patients ($p = 0.01$). The estimated hazard ratios of high-risk classification for cancer-specific and overall death were 3.2 (95% CI: 1.2 to 8.6) and 2.2 (95% CI: 1.1 to 4.4), respectively. On post-RC final pathology, 23 (46.9%) low-risk patients were up-classified and 17 (25.0%) high-risk patients were down-classified. Complete responses (pT0) were achieved in 7 (6.0%) and partial responses (pT1, pTa, pTis) were achieved in 28 (23.9%) patients. Of 49 patients who did receive NAC, 41 (83.7%) were categorized as high risk prior to treatment. On final pathology, 3 (37.5%) low-risk patients were up-classified and 17 (41.5%) high-risk patients were down-classified. Complete responses were seen in 13 (26.5%) and partial responses were seen in 10 (20.4%) patients. Although NAC use was not significantly associated with CSS or OS ($p > 0.05$), it was associated with a 1.2 times ↑ odds (95% CI: 0.4 to 2.1) of post-RC reclassification from high to low risk.

Conclusions: We validated the clinical risk-stratification model and showed that high-risk patients had lower CSS and OS. NAC was associated with a higher probability of risk reclassification from high to low risk.

977 Histopathologic and Immunohistochemical Findings in Orchiectomy Specimens of Patients Undergoing Gender Reassignment Surgery

Andres Matoso, Li J Wang, Shamlal Mangray, Kara A Lombardo, Murray B Resnick, Evgeny Yakirevich. Brown University, Providence, RI.

Background: Hormonal therapy followed by gender reassignment surgery (GRS) is becoming increasingly common in patients with gender dysphoria seeking a male to female physical adaptation. The histopathologic changes seen in gonads of these patients have not been described.

Design: The study included 7 orchiectomies from 4 patients. Immunohistochemistry (IHC) for MAGE-A4, INSL3, steroid factor-1 (SF1), OCT4, PLAP, CD117, WT1, inhibin and estrogen receptor (ER) was performed in all cases. Controls included non-tumoral sections with normal spermatogensis of orchiectomy specimens for germ cell tumors.

Results: All patients received estradiol, 2 espiranolactone, 2 finasteride and 1 progesterone. All patients had undergone hormonal therapy for at least 6 months, and up to 6 years prior to surgery. The average age was 28 (range: 21-37). The average testicular size was normal in 6/7 (85%) specimens with an average size of 4.05 cm (range: 3.2-4.4). One testis was hypotrophic and measured 2.0 cm in greatest dimension. All specimens (7/7; 100%) showed aspermatogenesis and diffuse atrophy of seminiferous tubules with prominent Sertoli cells as highlighted by strong and diffuse staining for WT1, SF1 and inhibin. IHC for MAGE-A4 was strongly positive in spermatogonia basally located within seminiferous tubules, consistent with maturation arrest at that level in 5 testes from 3 patients. All specimens with maturation arrest at the levels of spermatogonia also had complete abscence of Leydig cells as demonstrated by IHC for INSL3 and SF1. In 1 patient both testes showed maturation arrest at the level of primary spermatocyte and a number and distribution of Leydig cells that was similar to controls (mean 33/HPF). IHC for CD117 was weakly positive in spermatogonia in control cases and showed a peculiar linear stain between Sertoli cells in study cases. There was hyperplasia of the epithelium of the proximal epididymis with stratification and formation of micropapillae in all study cases but not in controls. ER was strongly and diffusely positive in the head of the epididymis and focally positive in the rete testis. None of the cases showed germ cell neoplasia in-situ confirmed by negative IHC for OCT4, PLAP or CD117. There was no sex cord stromal tumors or germ cell tumor.

Conclusions: This is the first study to describe the histopathologic findings in orchiectomies from patients undergoing GRS. Hypospermatogenesis with maturation arrest at the level of spermatogonia, absence of Leydig cells and hyperplasia of the epididymal epithelium are likely secondary to pre-surgical hormonal therapy.

978 Gynecologic Organ Involvement by Malignancy in Radical Cystectomies (RC) for Urothelial Carcinoma (UC)

Cathleen E Matrai, Abimbola Ayangbesan, David M Golombos, Brian Robinson, Douglas S Scherr, Francesca Khani. Weill Cornell Medicine, NYC, NY.

Background: In women, treatment of UC with RC includes TAHBSO. While concurrent prostate cancer is high in men undergoing RC, a similarly high incidence of GYN organ involvement by either direct extension of UC or occult primary malignancy has not been shown. Some urologists are considering reproductive organ-sparing RC (ROSRC) in women for better preservation of sexual/urinary function, but there is a paucity of data to support altering the current standard of care. Our study reports the frequency of GYN involvement by malignancy in female RC in order to evaluate the potential for ROSRC in select women.

Design: We identified 111 consecutive RC cases for UC in women in our surgical pathology files from 1997-2016. Pathologic, pre-op radiologic, and clinical outcome data were obtained. Cases were grouped into those which had GYN involvement by UC (GYN-UC), GYN involvement by primary malignancy (GYN-P), and benign or no GYN pathology (GYN-NEG). Clinicopathologic and radiologic features in these groups were compared.

Results: GYN-UC was seen in 17% of cases (19/111), GYN-P in 2% (2/111), and GYN-NEG in 81% (90/111). Of GYN-UC cases, 32% (6/19) showed isolated vaginal wall involvement and 68% (13/19) had uterine and/or ovarian involvement. Cases with GYN-P consisted of an endocervical adenocarcinoma and a minimal serous carcinoma of the endometrium, both of which were unknown prior to RC. LVI was significantly more frequent in GYN–UC vs GYN-NEG (74% vs 23%; 14/19 vs 21/90 cases; p=0.0001) as was LN positivity (42% vs 19%; 8/19 vs 17/90; p<0.05). Perineural invasion (PNI) was also more frequent in cases with GYN-UC vs GYN-NEG (21% vs 4%; 4/19 vs 4/90; p<0.05). In GYN-UC, GYN-P, and GYN-NEG cases, 26% (5/19), 50% (1/2), and 24% (22/90) received neoadjuvant chemotherapy, respectively. The rate of recurrence/metastasis did not significantly differ among the groups. Of the 16 GYN-UC cases with pre-op imaging, only 1 showed radiologic evidence of GYN-UC (6%, 1/16). One of 2 GYN-P cases showed a corresponding radiologic abnormality.

Conclusions: Although ROSRC may improve urinary/sexual function in women, patient selection for this procedure is critical in order to avoid compromising oncologic outcome. Our study showed that LVI, PNI, and LN positivity were more frequent in cases with GYN-UC than in GYN-NEG. Worth noting is that these pathologic features are often unknown prior to complete resection, and pre-operative imaging did not detect GYN-UC in the vast majority of patients in our study. ROSRC, if considered at all, must be approached with great caution since appropriate patient selection presents a challenge.

979 The Incidence and Outcome of Xp11.2 Translocation Renal Cell Carcinomas (RCC): A Single Institutional Experience

Daniel Matson, Holly L Harper, Les J Henderson, Jennifer J Laffin, E Jason Abel, Wei Huang. University of Wisconsin-Madison, Madison, WI; Case Western Reserve University, Cleveland, OH.

Background: Xp11.2 translocation RCCs (tRCC) are a group of neoplasms characterized by chromosomal translocations with breakpoints involving the TFE3 transcription factor gene, which maps to the Xp11.2 locus. The result fuses the TFE3 transcription factor gene with one of multiple reported genes including ASPL, PRCC, NonO (p54nrb), PSF, or CLTC. The reported incidence of tRCCs is 1-4% and limited outcome data are available.

Design: 160 cases of clear cell RCC (ccRCC) from 1993 to 2005 were randomly selected from the UW Pathology archive. A tissue microarray (TMA) was constructed with duplicate cores (0.6 mm) from each tumor. A TFE3 break-apart fluorescence in situ hybridization (FISH) assay was used to detect Xp11.2 translocations (RP11-1137J13 labeled Orange (5-TAMRA dUTP)) and (RP11-57A11 labeled Green (5-Fluorescein dUTP)) (BAC clones, Empire Genomics). Pathological parameters and clinical outcome data were evaluated.

Results: 3 cases with TFE3 rearrangements were identified among the 155 ccRCC cases with adequate FISH signal (3/155, 2%). The pathological and clinical data are summarized in Table 1 and 2.

Case	Age at Surgery (y)	Gender	Race	Tumor Size (cm)	Grade	pTNM at Surgery	Mets Site
1	60.1	F	W	16	2	pT4N0M0	-
2	59.9	M	W	10	2	pT3aN1M0	-
3	57.9	M	O	10	4	pT3aN1M1	Liver, Lung
F: female, M: male, mets: metastasis, y: years, O: other, W: white							

Case	Recurrence after Surgery (m)	Recurrence Site	Survival Status	Length of Survival (m)
1	8	Lung, Colon	DOD	55.4
2	3	Lung	DOD	51
3	-	-	DOD	1.3
DOD: dead of disease, m: month				

Conclusions: Xp11.2 tRCCs have a low incidence (2%) at our institution but they tend to occur in patients of older age (mean 59.3 y) who present with advanced disease. Mean survival after surgery is 35.9 months and all patients ultimately died of their disease. Xp11.2 tRCCs represent a small but understudied subset of RCC.

980 The Incidence and Outcome of t(6;11) Renal Cell Carcinomas (RCC): A Single Institutional Experience

Daniel Matson, Holly L Harper, Les J Henderson, Jennifer J Laffin, E Jason Abel, Wei Huang. University of Wisconsin-Madison, Madison, WI; Case Western Reserve University, Cleveland, OH.

Background: t(6;11) RCCs are known as primarily pediatric renal neoplasms and are characterized by t(6;11)(p21;q12) translocations which results in an Alpha-TFEB gene fusion. The result is native TFEB overexpression. The reported cases of genetically confirmed t(6;11) RCCs is around 30 (2013 data). Limited outcome data are available.

Design: 156 cases of relatively young patients (≤ 50 years) with clear cell RCC (ccRCC) or papillary RCC (pRCC) from 1994 to 2013 were selected from the UW Pathology archive. A tissue microarray (TMA) was constructed with duplicate cores (0.6 mm) from each tumor. A TFEB break-apart fluorescence in situ hybridization (FISH) assay was used to detect t(6; 11) translocations (BAC clones, Empire Genomics). Pathological parameters and clinical outcome data were evaluated.

Results: Three cases with TFEB rearrangement were identified among the 153 RCC cases with adequate FISH signal (3/153, 2%). The pathological and clinical data are summarized in Table 1 and 2.

Case	Age at Surgery (y)	Gender	Race	Tumor Size (cm)	Grade	pTNM at Surgery	Mets Site
1	49	M	AA	5.3	3	pT1bNxMx	-
2	44	M	W	2.5	2	pT3NxMx	-
3	16	F	W	3.6	3	pT1N0Mx	-
AA: African American, F: female, M: male, Mets: metastasis, W: white							

Case	Recrrence after Surgery (m)	Recurrence Site	Survival Status	Length of Survival (m)
1	27	Retroperitoneum	DOD	60
2	-	-	Alive	60
3	-	-	Alive	37
DOD: dead of disease, m: month				

Conclusions: t(6;11) RCCs can occur in adults. The incidence of t(6;11) RCCs is low, at 2% among relatively young patients with ccRCC or pRCC. One of three patients (49 years) had a recurrence 27 months after surgery and ultimately died of his disease. Our data indicate that t(6:11) RCC represent a small but understudied subset of RCCs which can recur as aggressive disease despite adequate surgical resection.

981 Anti-TFE3 and Anti-TFEB Antibodies for the Detection of Translocation Renal Cell Carcinomas (tRCC) by IHC: A Single Institutional Experience

Daniel Matson, Holly L Harper, Les J Henderson, Jennifer J Laffin, E Jason Abel, Wei Huang. University of Wisconsin-Madison, Madison, WI; Case Western Reserve University, Cleveland, OH.

Background: Strong nuclear staining for the proteins TFE3 and TFEB by immunohistochemistry (IHC) is reported to be sensitive and specific for Xp11.2 and t(6;11) tRCCs. However, limited data are available regarding the diagnostic utility of commercially available antibodies for this application.

Design: We tested three TFE3 and two TFEB commercial antibodies on two RCC tissue microarrays (TMA) (see Table 1). TMA1 comprised 384 duplicate cores representing 157 clear cell RCCs (ccRCC) and 3 TFE3 tRCCs. TMA2 comprised 400 duplicate cores representing a combined 153 ccRCCs and papillary RCCs, and 3 TFEB tRCCs.

Abs	Anti-TFE3			Anti-TFEB	
Vendor	Santa Cruz (P-16)	Bio SB	Cell Marque (MRQ-37)	AbCam	Santa Cruz (V-17)
Cat No	sc-5958	#BSB2275	354R	Ab2326	sc-11004
Clone	Goat Polyclonal	Rabbit Monoclonal	Rabbit Monoclonal	Goat Polyclonal	Goat Polyclonal
Dilution	1:400	1:25	NA	1:2000	NA
Detection	Multimer HRP	Multimer HRP	Multimer HRP	BioCare Medical Polymer	Multimer HRP
Instrument	Ventena Discovery XT	Ventena Discovery XT	Ventena Discovery XT	Lab Vision	Ventena Discovery XT
NA: not applicable					

Results: Three antibodies yielded detectable staining for their target. 155 cases from TMA1 and 153 cases from TMA2 were stained with anti-TFE3 and anti-TFEB antibodies respectively. Sensitivity and specificity for tRCC was evaluated for each antibody alongside matching FISH data confirming the presence or absence of translocations (see Table 2).

		Staining Results					
		Positive (n)	Negative (n)	IHC+/FISH+ (n/n)	Sn (%)	Sp (%)	PP (%)
Anti-TFE3	Santa Cruz (P-16)	54	101	3/3	100	66.5	5.6
	Bio SB	52	103	3/3	100	67.8	5.8
Anti-TFEB	AbCam	80	73	1/3	100	47.3	1.3
n: number, Sn: sensitivity, Sp: specificity, PP: positive predivtive value							

Conclusions: Tested commercial anti-TFE3 antibodies are sensitive but not specific for Xp11.2 tRCC. One anti-TFEB antibody yielded nuclear staining but had limited sensitivity and specificity for t(6;11) tRCC. There is an unmet need for anti-TFE3 and anti-TFEB antibodies to facilitate the rapid and accurate diagnosis of tRCCs.

982 What the Pathologist Needs to Know About the Role of Fumarate Hydratase in the Diagnosis of HLRCC Renal Cancer

Maria J Merino, Christopher Ricketts, Xu Naizhen, WMarston Linehan, Vanessa Moreno. NIH/NCI, Bethesda, MD.

Background: Renal cell carcinoma (RCC) is a disease composed of different types of kidney cancer with different morphologies, response to therapy, and genetic mutations. Hereditary leiomyomatosis and renal cell carcinoma (HLRCC) is associated with germline fumarate hydratase (*FH*) mutations and an aggressive form of RC. HLRCC tumors have biallelic loss of *FH* function which correlates with loss of FH immunohistochemical (IHC) staining. Occasionally, cases with negative staining are identified that are negative for FH mutation, and focal positivity can be seen in HLRCC tumors. We further studied the use of of FH staining in the primary tumor and metastases of HLRCC and correlated with anti-2S and NQO1 antibodies.

Design: Renal tumors from 205 patients were reviewed and classyfied into three groups. Group 1had 65 tumors (65 patients) morphologically consistent with HLRCC. Group 2 had 35 poorly differentiated RCCs not classified as HLRCC but with some features suggestive of HLRCC. Group 3 had 105 tumors with all other histological types. FH protein expression was evaluated in 205 cases by IHC using a mouse monoclonal antibody against human FH protein (Santa Cruz Biotechnology). Staining for 2SC and NQO1 was done in selected cases. Status of the *FH* gene, and clinical data, was available for 81.5% of the HLRCC patients

Results: IHC analysis of the 65 tumors consistent with HLRCC demonstrated that 60 (92.3%) tumors were entirely negative for anti-FH antibody staining in the tumor areas. Five HLRCC tumors showed equivocal results with very focal areas of weak immunoreactivity in small areas (<2%). These 5 cases did have germ line mutations in the FH gene. Six cases gave negative FH staining but were negative for the germ line mutation. In 47/65 the FH germ line mutation was confirmed. All other 140 cases show strong positivity for FH staining. There was good correlation with 2SC and NQO1 staining

Conclusions: Morphological suspicion or diagnosis of HLRCC is important for appropriate clinical management and genetic counseling. FH IHC should be preferentially used as an ancillary screening method in combination with histopathologic evaluation to aid in the clinical identification and gene screening of patients with potential HLRCC renal tumors. Pathologists should be aware that occasional cases with weak and focal staining can occur. The pattern of staining in metastases will be discussed.

983 Chromosomal Aberration Pattern in Oncocytic Papillary Renal Cell Carcinoma: Analysis of 28 Cases

Kvetoslava Michalova, Petr Steiner, Delia Perez Montiel, Maris Sperga, Saul Suster, Reza Alaghehbandan, Kristyna Pivovarcikova, Ondrej Daum, Ondrej Ondic, Pavla Rotterova, Milan Hora, Michal Michal, Ondrej Hes. Charles University, Medical Faculty and University Hospital, Plzen, Czech Republic; Institute Nacional de Cancerologia, Mexico City, Mexico; East University, Riga, Latvia; Medical College, Wisconsin, Milwaukee, WI; Faculty of Medicine, University of British Columbia, Vancouver, Canada.

Background: The oncocytic variant of papillary renal cell carcinoma (OPRCC) is currently considered as a possible new variant of papillary renal cell carcinoma (PRCC) in the 2016 WHO classification. OPRCC is a poorly understood entity, especially concerning its chromosomal numerical aberration pattern. Because there is a striking cytologic similarity between renal oncocytoma (RO) and OPRCC, the most frequently affected chromosomes in RO and PRCC were analyzed.

Design: 147 OPRCC in our registry were reviewed in order to select a group of morphologically uniform tumors. 28 of 147 cases with predominant papillary or tubulopapillary architectural patterns were selected. The diagnosis of OPRCC was confirmed by immunohistochemistry (vimentin, AMACR and CK7). Loci 1p36, BCL1 ba, and chromosomes 7, 14, 17, X, and Y were examined by FISH.

Results: The patients were 16 males, 11 females, and in 1 case the gender was unknown. Age ranged 55-85 years (mean 70 years). The tumor size ranged 0.8-10 cm (mean 4 cm). Immunohistochemically, all cases showed positivity for vimentin, 27/28 for AMACR and 21/28 for CK 7. 23/28 cases were analyzable. In 13/23 cases multiple chromosomal aberrations were found, in 4 of which they were consistent with the pattern expected in PRCC (i.e. polysomy of chromosomes 7, 17). 7/13 cases showed variable chromosomal numerical aberrations, particularly losses of chromosomes 17 and Y in combination with other chromosomal anomalies. In 10/23 tumors chromosomal abnormalities corresponded with an arrangement usually seen in renal oncocytoma (RO), including normal chromosomal status, translocation in 1p36, BCL1 ba and abnormalities in chromosome 14.

Conclusions: Chromosomal numerical aberration pattern in OPRCCs is variable despite their uniform morphology (oncocytic cells, papillary/tubulopapillary pattern) and consistent immunohistochemical profile (vimentin and AMACR positivity). Majority of OPRCC shared several chromosomal aberration to that seen in RO, while a subset of these tumors showed "classic" chromosomal aberration pattern similar to that observed in PRCC.

984 Primary Signet Ring Stromal Tumor of the Testis: A Study of 15 Cases Revealing Their Relationship to Pancreatic Analogue Solid Pseudopapillary Neoplasm Arising in Paratesticular Location

Kvetoslava Michalova, Michael Michal, Dmitry V Kazakov, Monika Sedivcova, Ondrej Hes, Ladislav Hadravsky, Abbas Agaimy, Maria Tretiakova, Carlos E Bacchi, Arndt Hartmann, Naoto Kuroda, Stela Bulimbasic, Marijana Coric, Tatjana Antic, Michal Michal. Faculty of Medicine in Plzen and Charles University Hospital, Plzen, Czech Republic; Biomedical Center, Faculty of Medicine in Plzen and Charles University Hospital, Plzen, Czech Republic; Biopticka Laborator s.r.o., Plzen, Czech Republic; 3rd Medical Faculty and Charles University Hospital Royal Vineyards, Prague, Czech Republic; University Hospital, Friedrich-Alexander University Erlangen-Nuremberg, Erlangen, Germany; University of Washington, Seattle, WA; Botucatu, SP, Brazil; Kochi Red Cross Hospital, Kochi, Japan; University Hospital Centre, Zagreb, Croatia; The University of Chicago, Chicago, IL.

Background: Primary signet ring stromal tumor of the testis (PSRSTT) is an extremely rare tumor which is morphologically and immunohistochemically very similar to the recently described pancreatic analogue solid pseudopapillary neoplasm arising in a paratesticular location (SPNPT). We collected a large series of PSRSTTs in an attempt to analyze their relationship to SPNPT.

Design: The authors studied 15 cases of PSRSTTs using histological, immunohistochemical and molecular genetic methods and compared the results with one case of SPNPT.

Results: The size of PSRSTTs ranged from 0.5 to 2 cm (mean 1.15), while SPNPT measured 4.8 cm in the largest dimension. Microscopically, PSRSTTs predominantly showed the proliferation of low-grade epithelioid cells containing characteristic cytoplasmic vacuoles dislodging the nucleus (signet ring cells) separated by fibrous septa into trabeculae and nests. SPNPT consisted of two distinct components: a signet ring cell component which histologically was identical to that in PSRSTT merging with a component indistinguishable from pancreatic solid pseudopapillary neoplasm (SPN), i.e. poorly cohesive low grade cells with eosinophilic cytoplasm growing in a solid fashion. The immunoprofile of PSRSTT and SPNPT was identical, characterized by immunoreactivity for β-catenin, cyclin D1 (nuclear positivity for both antibodies), CD10, vimentin, Galectin 3, Claudin7, α-1-antitrypsin, CD56, NSE and negativity with chromogranin, inhibin, calretinin, NANOG, OCT3/4 and SALL4. Molecular genetically, both SPNPT and most cases of PSRSTT shared the same mutation within exon 3 of the *CTNNB1* encoding β-catenin.

Conclusions: Based on histological similarities between PSRSTT and SPNPT and their identical IHC and molecular genetic features, we assume that they both are of the same origin and pathogenesis and thus they can be considered as a morphological spectrum of a single entity.

985 Morphologic, Clinical and Molecular Features of Large Cell Neuroendocrine Carcinoma (LCNEC) of the Bladder

Leili Mirsadraei, Xueli Hao, Min-Yuen Teo, Kuo-Cheng Huang, Ying-Bei Chen, Anuradha Gopalan, Joe Sirintrapun, Samson W Fine, Satish K Tickoo, Bernard H Bochner, Guido Dalbagni, Dean F Bajorin, Barry S Taylor, David Solit, Gopakumar V Iyer, Victor E Reuter, Hikmat Al-Ahmadie. Memorial Sloan Kettering Cancer Center, NY, NY.

Background: Primary LCNEC of the urinary tract is a rare and poorly characterized neoplasm. Distinctive histologic features observed in pulmonary LCNEC include organoid nests, rosette-like structures, trabecular growth, and peripheral palisading. Tumor cells are large with abundant cytoplasm, vesicular chromatin, prominent nucleoli, brisk mitotic activity and large areas of necrosis. Here, we report our clinical and pathologic experience with LCNEC from a large cohort of primary small cell/neuroendocrine carcinoma (SC/NEC) of the bladder.

Design: We searched for cases of LCNEC from a database of SC/NEC of bladder (n=194) based on histopathologic criteria seen in pulmonary LCNEC. Relevant IHC results and molecular data were reviewed and correlated with clinical outcome.

Results: We identified 21 cases of LCNEC (11%). All tumors contained large and polygonal cells with abundant basophilic cytoplasm, round to oval nuclei, vesicular chromatin and prominent nucleoli. Growth patterns included organoid nests (n=16), trabecular arrangement (n=12), sheets (n=8), peripheral palisading (n=5), rosette formation (n=2), and nuclear molding (n=2). High mitotic rate, necrosis, karyorrhexis and apoptosis were seen in all cases. Results of neuroendocrine markers were available in 18 tumors (16 positive for synaptophysin, 8 for chromogranin, 8 for CD56 and 4 for NSE). A component of small cell carcinoma was also identified in 8 cases and other histologies were seen in 11 cases, including urothelial carcinoma, NOS (n=6), glandular (n=5), nested (n=4), micropapillary (n=2), and sarcomatoid components (n=1). Pure LCNEC was seen in 2 cases. Pathologic stages were T1 (n=1), T2 (n=14), and T3 (n=6). Vascular invasion was identified in 6 cases. Regional lymph node metastasis was present in 4 cases and visceral metastases in 6 (liver, spine, brain, bone and adrenal). Clinical follow-up was available for 18 patients (2 to 95 mo.); 14 received chemotherapy, 6 are alive without disease, 4 are alive with residual or metastatic disease, 5 died of disease, and 3 were lost to follow-up.

Next generation sequencing was performed in 8 cases, all of which harbored mutations in *TP53* and *TERT* promoter. *RB1* mutations (n=4) and alterations in chromatin remodeling genes (n=5) were also seen.

Conclusions: LCNEC is rare, representing 11% of NEC of the bladder and most are diagnosed at an advanced stage. Pure LCNEC is rare (10%) and often contains other variant histologies. The molecular profile of LCNEC is similar to that of urothelial carcinoma and small cell carcinoma of the bladder.

986 Clinicopathologic and Molecular Characterization of a Cohort of Urobasal and Nonbasal Subtypes of High-Grade Urothelial Carcinomas (HGUCa)

Sambit K Mohanty, Shivani Sharma, Matthew Geller, Nitin Bhardwaj, Jasreman Dhillon. CORE Diagnostics, Gurgaon, India; Winthrop University Hospital, Mineola, NY; Moffitt Cancer Center, Tampa, FL.

Background: Advances in genomics have catalyzed changes in the landscape of UCa, as reflected in the classification of HGUCa. While advanced stage in general is associated with poor outcome, there is a considerable heterogeneity in the clinical behavior. Recent studies have attempted to elucidate the profile of HGUCa, however, there is a paucity of data to support clinical use of molecular analysis. Therefore, we sought to assess and correlate the molecular characteristics of HGUCa in a cohort of 187 HGUCa.

Design: FISH assay for FGFR3, EGFR, and ERBB2 amplification, ATM (6q) and TP53 deletion, and PCR-based analysis for KRAS mutations were performed. Statistical comparisons were made using Pearson's chi-square test and logistic regression analysis.

Results: 141 and 46 tumors were urobasal and nonbasal subtypes, respectively and the details were described.

Characteristics	Total	Basal (CK5/6 and CK14)	Luminal (GATA3 and FOXA1)	PS3-like	Non-basal	p-value	FGFR3 amplification (FISH)	ATM (6q deletion, FISH)	EGFR amplification (FISH)	ERBB2 amplification (FISH)	TP53 deletion (FISH)	KRAS (PCR)	p-value
Cohort size	187	141	24	22	46		73	15	17	19	85	9	
Mean age	66.25	65	71.4	65.7	62.9	0.391	68.9	69.1	70.8	78.2	68	67.2	0.345
Gender													
Female	53	32	10	11	21	<0.003	27	4	5	8	20	5	0.634
Male	134	109	13	12	25		66	11	12	11	45	4	
Positive lymph nodes	35	21	4	10	14		3	0	2	3	7	0	0.738
Positive metastasis	33	14	3	16	19	0.308	2	0	1	2	10	0	0.312
Cystectomy	133	95	15	20	25	0.0001	8	7	12	13	48	2	0.019
Neoadjuvant chemotherapy	64	20	5	17	22		5	9	4	6	17	7	0.071
pT0	8	2	6	0	6	<0.0001	7	5	0	0	0	0	<0.0001
pTa, pT1, pTis	19	6	8	1	10		18	3	3	3	11	6	
pT2	103	83	10	10	20		43	7	11	10	34	2	
pT3	22	14	0	8	8		3	0	2	3	8	0	
pT4	35	14	0	11	11		2	0	1	3	12	0	
Positive lymph node on histology	39	15	2	22	24	<0.0001	3	0	2	3	5	0	<0.0001
Sarcomatoid	15	9	0	6	6	<0.0001	0	1	5	7	5	1	<0.0001
Squamous	49	22	0	27	27		1	1	5	4	28	0	
Micropapillary	11	7	1	3	4		1	3	3	7	4	0	
Glandular	6	4	1	1	2		0	2	0	0	11	4	

Clinicopathologic, Immunohistochemical, and Molecular Profiles in High-grade Urothelial Carcinomas

Categories	FGFR3 amplification (FISH)	ATM (6q deletion, FISH)	EGFR amplification (FISH)	ERBB2 amplification (FISH)	TP53 deletion (FISH)	KRAS (PCR)	p-value
Urobasal (141)	11	3	10	13	16	3	<0.0001
Non-basal (46)	62	12	7	6	49	6	
PS3-like (22)	3	2	6	5	39	0	
Luminal (24)	59	10	1	1	10	6	

Comparison Between Immunohistochemical Profile and Molecular Markers in High-grade Urothelial Carcinomas

The urobasal tumors revealed TP53 and ATM deletion and were ERBB2 and EGFR amplified, and showed greater likelihood of metastasis and detrusor muscle invasion ($p<0.0001$), whereas the nonbasal luminal-like tumors exhibited FGFR3 amplification ($p<0.0001$). ERBB2 and EGFR amplification with TP53 loss were observed in metastatic tumors. While KRAS mutation was observed in glandular phenotype, sarcomatoid, micropapillary, and squamous differentiation were enriched in the basal category of HGUCa, with EGFR, ERBB2, and TP53 abnormalities (<0.0001). Survival and follow-up analyses is currently in progress.

Conclusions: HGUca is an aggressive neoplasm with molecular heterogeneity culminating in variable biologic outcome of the disease. Molecular characterization, particularly in locally aggressive or metastatic setting ramifies actionable genomic alterations that can significantly impact the disease outcome, even in patients with refractory tumors.

987 Effect of Neoadjuvant Intense Androgen Deprivation Therapy in Neuroendocrine Differentiation of Prostate Cancer

Laleh Montaser, Carla Calagua, Rachel Schaefer, Rosina Lis, Zhenwei Zhang, Massimo Loda, Mary-Ellen Taplin, Steven P Balk, Huihui Ye. East Tennessee State University, Johnson City, TN; Beth Israel Deaconess Medical Center, Boston, MA; Dana-Farber Cancer Institute, Boston, MA.

Background: In prostate cancer (PC), neuroendocrine differentiation (NED) is associated with castration resistance. Androgen deprivation therapy may induce NED in castration resistant PC. In a phase II neoadjuvant clinical trial, 58 men with intermediate to high risk PC received intense androgen deprivation therapy (IADT) combining leuprolide with abiraterone plus prednisone prior to surgery. We quantified NED of tumors in 50 trial cases, using computational image analysis of synaptophysin immunostains, to assess if NED is enriched after IADT treatment.

Design: Tumor sections from 50 trial cases and 50 grade- and stage- matched untreated control cases were subjected to synaptophysin immunostains. Tumors in 10 of 50 trial cases and 14 of 50 untreated control cases demonstrated ≥ 5% synaptophysin immunoreactivity, respectively. Image analysis was performed to evaluate the extent of positive cells (low-medium-high immunointensity) in those 10 treated and 14 untreated tumors. First, we annotated all areas of invasive tumors on the slide images with 600 µm circle markers in Pannoramic Viewer, excluding benign glands, PIN, and intraductal carcinoma. Next, we captured images corresponding to each annotation marker. For each image, we used Definiens image analysis software (version 4.2, Definiens Tissue Studio) to perform segmentation, cell identification, and quantifying tumor cells that are negative or positive for synaptophysin.

Results: Overall, we acquired 611 microscopic images of treated cases and 1,325 images of untreated cases. Results from image analysis revealed no significant difference in percentage of synaptophysin-positive tumor cells of all and medium-high levels between treated and untreated tumors, while total numbers of synaptophysin-positive and all tumor cells were both significantly reduced in treated tumors.

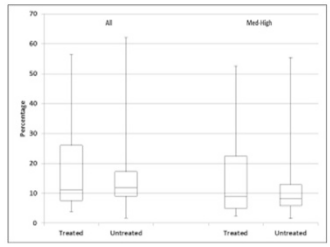

Figure 1A. Percentage of synaptophysin-positive tumor cells of all and medium-high levels in treated vs untreated tumors ($p = 0.81$ and 0.91, respectively).

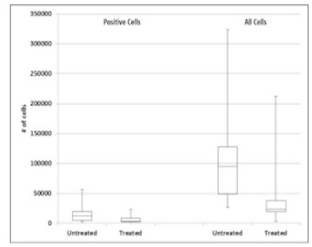

Figure 1B. Total numbers of synaptophysin-positive and all tumor cells in untreated vs treated tumors ($p = 0.047$ and 0.005, respectively).

Conclusions: Our study demonstrated that there is no significant increase in NED in PC after neoadjuvant IADT.

988 RNA Sequencing of Patient Matched Pre-Androgen Deprivation Therapy and Post-Androgen Deprivation Therapy Prostate Cancer Identifies Mechanisms of Progression to Castration-Resistant Prostate Cancer

Carlos S Moreno, Felipe O Giuste, Kathryn L Pellegrini, Nitya V Sharma, Veronique Ouellet, Dominique Trudel, Anne-Marie Mes-Masson, John A Petros, Fred Saad, Adeboye O Osunkoya. Emory University School of Medicine, Atlanta, GA; McGill University, Montreal, QC, Canada; University of Montreal, Montreal, QC, Canada.

Background: Patients with localized prostate cancer often undergo radiation therapy or radical prostatectomy. However, for a subset of patients who have recurrent/systemic disease (or advanced denovo prostate cancer), the standard of care is androgen deprivation therapy (ADT); nevertheless, the benefits from ADT are typically short-lived. Recurrent/systemic disease that follows ADT treatment is termed castration-resistant prostate cancer (CRPC), which is both aggressive and lethal. However, the mechanisms underlying CRPC remain unclear. The primary objective of this study was to analyze thegene expression profiles of prostate cancer in patient with matched pre-ADT and post-ADT tissue samples.

Design: RNA from 34 formalin-fixed paraffin-embedded patient-matched pre-ADT needle core biopsies and corresponding post-ADT radical prostatectomy prostate cancer samples were sequenced using Illumina's TruSeq RNA Access Library Prep kit. On average, we obtained 91M reads per sample, with 64x coverage of the transcriptome. Sequence alignment and gene level expression quantifications were obtained using the STAR read aligner. Multiple dimensional scaling plots were used to detect confounding factors and sample outliers. The final statistical model included corrections for sequencing batch effects, sequence coverage, and individual patient variation.

Results: Applying the quasi-likelihood F-test in the edgeR bioconductor package, we identified 132 significantly differentially expressed genes between pre-ADT needle core biopsies and corresponding radical prostatectomy samples, including several androgen-regulated genes including KLK3 and prostate specific antigen. Ingenuity Pathway Analysis determined that androgen receptor signaling and dihydrotestosterone targets were significantly downregulated. In addition, a number of secreted extracellular matrix proteins and proteases were altered by ADT. Most importantly, we also observed upregulation of genes downstream of mitogen-activated protein kinasesignaling, beta-estradiol, and cell cycle advancement.

Conclusions: ADT may increase cancer proliferation markers as well as induce a compensatory increase in estrogen signaling in response to the loss of androgen signaling. This study also suggests possible mechanisms of progression to more aggressive cancer phenotypes as a result of ADT and could have significant therapeutic implications in patients with CRPC.

989 The Unrecognized Morphologies of HLRCC Renal Cancer That Pathologists Need to Know. Molecular and IHC Findings

Vanessa Moreno, Xu Naizhen, Ramaprasad Srinivasan, Marston W Linehan, Maria J Merino. National Cancer Institute, Bethesda, MD.

Background: Hereditary leiomyomatosis and renal cell carcinoma (HLRCC) is an autosomal dominant familial syndrome characterized by germline mutations of fumarate hydratase (FH) gene. The most common patterns associated with these tumors are papillary, tubular and solid. Here, we describe unusual patterns (cystic and sarcomatoid) and their molecular features.

Design: We reviewed the tumors of 65 patients diagnosed as HLRCC-kidney cancer with or without metastasis. Diagnoses was confirmed by IHC staining with FH and 2SC antibodies. Mutational analysis was performed on 47 patients.

Results: Of the 65 patients, 24 had a sarcomatoid or cystic pattern. Eight (8/24) patients presented with a large cystic mass identified either by imaging or gross examination. Metastasis to lymph nodes (2/8), and mediastinum (1/8) showed the same cystic characteristics than the primary. Five (5/8) of these had intracystic papillary growth. The remaining 16 (16/24) patients demonstrated either focal or more extensive areas with a sarcomatoid component. The primary tumors showed lack of FH staining by IHC; however, several metastatic lesions located in the chest, liver and retroperitoneum showed a positive staining with a granular cytoplasmic pattern. All the cases were positive for 2SC. 16 patients (16/24) had a confirmed FH germline mutation, and from this group 6 had cystic morphology and 10 a sarcomatoid pattern. Half of the patients who had a sarcomatoid morphology and confirmed FH germline mutation (5/10) harbor a missense mutation at the R233H position, while the patients who had a cystic morphology with confirmed FH germline mutation did not show any difference regarding their mutational analysis.

Conclusions: Predominantly cystic and sarcomatoid morphologies have not been associated with HLRCC-associated tumors. These morphologies can present as a pure or mixed component either in primary or in metastatic lesions. The cysts can be outlined by very oncocytic cells and can be a pitfall for oncocytomas. Cystic lesions may have intracystic papillary growth and some may present as simple cysts and can be misinterpreted as benign lesions, clinically and by imaging. Meanwhile, the sarcomatoid patterns are misinterpreted as high grade clear cell tumor. Recognition of these patterns is important to establish correct diagnosis, therapy and genetic counseling.

990 Genomic Alterations of *PTEN*, *CHD1*, *ASAP1*, and Aneusomy Are Associated with Prognostic Grade Group Upgrade from Needle Biopsy to Prostatectomy

Prasuna Muppa, R Jeffrey Karnes, Stephen J Murphy, Farhad Kosari, Irina V Kovtun, Laureano J Rangel, William R Sukov, Rafael E Jimenez, George Vasmatzis, John C Cheville. Mayo Clinic, Rochester, MN.

Background: The International Society of Urological Pathology has published a 5-tiered prognostic grade grouping (PGG) for prostate cancer. We have recently identified alterations of *PTEN*, *RB1*, *CHD1*, *ASAP1*, and *HDAC9* that are associated with clinically significant prostate cancer and the presence of Gleason pattern 4. The objective of this study was to determine if alterations in these genes were associated with PGG upgrading from needle biopsy to radical prostatectomy.

Design: A total of 250 patients who had undergone needle biopsy and prostatectomy in 2014 at our institution were selected for this study. Of those, a total of 97 patients were PGG1 and 50 patients were PGG2 at the time of biopsy. We performed fluorescence in situ hybridization (FISH) analysis for alterations of *RB1*, *PTEN*, *CHD1*, *ASAP1*, and *HDAC9* in the biopsy specimens. Two independent reviewers scored the FISH results of each case and included a determination of aneusomy. For each PGG group, we compared the FISH results of patients who upgraded on prostatectomy with patients who remained in the same PGG.

Results: A total of 47 patients that were in PGG1 on biopsy were upgraded to PGG2 on prostatectomy. Similarly, a total of 17 PGG2 patients were upgraded to PGG3 on prostatectomy. PGG1 group with upgrade were more frequently had aneusomy for at least one of the 5 genes/chromosomes when compared to PGG1 with no upgrade (p=0.02). When compared to PGG1 patients with no upgrade, PGG1 patients with upgrade also showed a greater frequency of *PTEN* loss (p=0.02), *HDAC9* aneusomy (p=0.05), *CHD1* loss (p=0.02), and *ASAP1* gain or loss (p=0.01). Similarly, when compared to PGG2 patients with no upgrade, PGG2 patients with upgrade to PGG3 showed a more frequent loss of *PTEN* than patients that did not upgrade (p=0.005). However, there was not enough evidence to prove that alterations of *RB1*, *ASAP1*, *HDAC9* and aneusomy were associated with upgrading.

Conclusions: *PTEN* loss, *CHD1* loss, and at least one aneusomy of chromosomes containing *PTEN*, *RB1*, *CHD1*, *ASAP1*, and *HDAC9* on biopsy specimens were associated with upgrade from the PGG1 to PGG2 on prostatectomy. *PTEN* loss was the only alteration on PGG2 biopsies associated with PGG3 upgrade at prostatectomy.

991 Does MRI/Ultrasound Fusion Guided Biopsy Improve Prostate Cancer Detection? A Bi-Institutional Retrospective Study

Paari Murugan, Mariah Z Leivo, Dina El-Rayes, Ayman Soubra, Benjamin Spilseth, David Karow, Kellogg Parsons, Christopher Kane, Christopher Warlick, Badrinath Konety, Donna Hansel. University of Minnesota, Minneapolis, MN; University of California San Deigo, La Jolla, CA.

Background: The standard transrectal ultrasound (TRUS) guided prostate biopsy is associated with significant sampling error. Advances in technology such as multiparametric MRI have helped increased cancer detection rates. More recent modalities such as MRI/ultrasound fusion platforms that allow MRI suspicious regions to be biopsied under TRUS guidance (targeted biopsies) hold promise of further enhancing cancer detection. There are limited studies in literature that have investigated the efficacy of targeted biopsies.

Design: Patients with lesions identified on mpMRI underwent targeted biopsy utilizing fused MRI and real time TRUS images (UroNav). Following this, standard biopsies were obtained. Two genitourinary pathologists retrospectively reviewed prostate biopsies of 266 patients who underwent this procedure at our institutions between 2014 and 2016.

Results: Targeted biopsy revealed carcinoma in 126(47.4%) compared to 157(59%) standard biopsy cases. The fusion guided biopsy detected prostate cancer that was missed by standard biopsy in 8.6% cases (23/266), of which 52.2%(12/23) were clinically significant. However, a diagnosis of cancer was made on non-targeted cores in 20.3%(54/266) of cases that were negative on target cores, of which 35.2%(19/54) were clinically significant. The overall sensitivity of the target biopsies in detecting clinically significant cancer was 72.73% compared to 77.69% for standard biopsies. While the targeted procedure did upgrade 17.7%(26/147) cases that were clinically insignificant on standard biopsy, the converse was true for as many as 18.5%(33/178) cases. Both target and standard biopsies were negative in 86(32.3%) of cases. Gleason score >6 cancer was found at a 3% lesser rate among target cores compared to standard biopsies (80 vs 85 cases, p=0.64) while cancers that demonstrated >50% core involvement were found at a 2% higher rate in the targets (48 vs 46 cases, p=0.82). The cancer detection rate in patients with high risk imaging (PIRADS score of 4-5) was 64.6% vs 35.1% in those classified as low risk (PIRADS 1-3) (p<0.0001).Although chronic inflammation was present in 73/266(27.4%) of target biopsies, this was not significantly different compared to standard cores (p=0.13).

Conclusions: We could not demonstrate increased detection of cancer or of clinically significant cancer in our cohort of men undergoing targeted biopsy compared to standard biopsy. Additional studies across multiple institutions are necessary to address the ultimate clinical importance of targeted biopsies.

992 Infrequent PD-L1 Protein Expression and Gene Amplification in Prostatic Adenocarcinomas (PACs)

Saleh N Najjar, Bhaskar VS Kallakury, Christine E Sheehan, Tipu Nazeer, Jeffrey Ross. Albany Medical College, Albany, NY; Georgetown University Hospital, Washington, DC.

Background: Programmed death-1 (PD-1) and its main ligand (PD-L1) regulate T-cell function and tumor cell proliferation. Blockade of this immune check point has been a promising clinical therapeutic strategy in many cancers with FDA approval of anti PD-L1 therapy in melanoma and squamous carcinoma. Loss of the tumor suppressor gene PTEN is common in prostate cancer and is thought to upregulate PD-L1 expression. Given the lack of effectiveness of anti PD-L1 therapy in early phase data, we evaluated PD-L1 protein expression and association with PTEN in PACs.

Design: Formalin-fixed paraffin-embedded tissue sections from 129 PACs were immunostained by an automated method utilizing rabbit monoclonal PD-L1/CD274 (Spring Bioscience, clone SP142) and ultraView DAB detection (Roche/Ventana, Tucson AZ). Membranous PD-L1 immunoreactivity was scored as negative, low positive (1 – 24%) and high positive (= or > 25%) in both the tumor cells and tumor infiltrating lymphocytes (TILs).

PD-L1 gene amplification was assessed by hybrid capture-based comprehensive genomic profiling (CGP) on a separate set of 675 PACs. Results were correlated with clinicopathologic variables.

Results: PD-L1 immunoreactivity was noted as low positive in 7/129 (5%) tumors. No PD-L1 immunoreactivity was noted in the TIL component of any cases, despite the presence of TILs in the majority of cases. PTEN status was available in 88 (68%) tumors, with loss of PTEN protein expression in 47/88 (53%) tumors while only 3/47 (6%) of PTEN negative tumors were PD-L1 positive. While 6/7 (86%) PD-L1 positive tumors were low Gleason grade, this did not reach statistical significance. *PD-L1* (CD274) gene amplification was identified in only 1 (0.1%) of 675 PCA submitted for CGP.

Conclusions: The observed paucity of PD-L1 protein expression and *PD-L1* gene amplification in prostate cancer and absence of its upregulation in PTEN negative tumors may explain the lack of effectiveness of PD-L1 blockade strategy in the treatment of PACs.

993 Glucocorticoid Receptor Expression Is Highly Prevalent in Primary Untreated Prostate Carcinoma

Daniel Nava Rodrigues, Gunes Guner, Igor Vidal, Ines Benedetti, Ibrahim Kulac, Jessica Hicks, Qizhi Zheng, Johann De Bono, Angelo M De Marzo. Johns Hopkins University, Baltimore, MD; University of Cartagena, Cartagena, Colombia; The Institute of Cancer Research, London, United Kingdom.

Background: Metastatic prostatic carcinomas initially respond to anti-androgen therapy, but resistance is inevitable, even to newer second generation anti-androgens (e.g. enzalutamide or abiraterone). Recent work suggested that upregulation of the glucocorticoid receptor (GR) leads to a bypass of androgen receptor (AR) blockade as a mechanism of enzalutamide resistance (PMID 24315100). This model of upregulation is based on low or absent baseline expression of GR in untreated carcinomas. Also, baseline GR levels may correlate with therapeutic response and it is important to have a robust assay and a detailed understanding of levels of GR throughout the progression of prostate cancer.

Design: Validation of an IHC assay was performed with a monoclonal anti-GR antibody using two approaches. First, the antibody recognized a single band by western blotting of GR-positive cell lines and was negative in GR-negative cells. Second, a chromogenic in situ hybridization (CISH) assay was established using ACD RNAscope. CISH and IHC were performed on 31 cell lines showing a high concordance rate ($p<.0001$, chi-square).

Results: TMAs from 242 patients and from untreated lymph node metastases (n = 35) were used for IHC. In normal prostate, both basal and luminal cells stained for GR protein in the majority of cells (mean 95%). Prostatic adenocarcinoma had lower and more heterogeneous GR staining than normal prostatic epithelium (figure 1) using an H-score (P=0.0001).

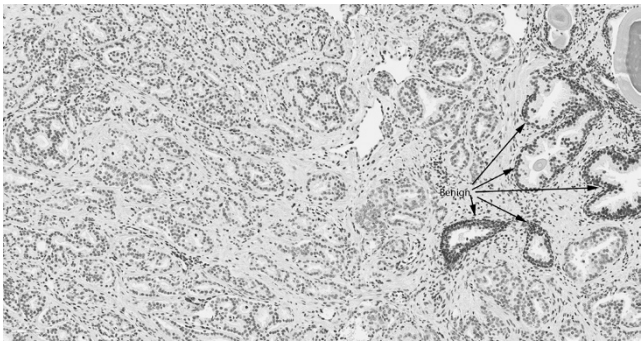

Lymph node metastases had lower GR staining compared to normal epithelium, but no significant difference was seen between these and primary carcinomas. GR expression levels in tumors did not correlate with stage, grade or biochemical recurrence in univariate or multivariate analyzes.

Conclusions: We established a validated GR IHC assay. While expression is downregulated compared to normal appearing prostate epithelium, virtually all primary prostate cancers and untreated lymph node metastases express variable levels of GR protein in a high fraction of cells. Assessements of castrate resistant tumors before and after enzalutamide/abiraterone resistance will be presented.

994 Protein Expression and Genomic Alterations of PMS2 in Urothelial Bladder Cancer

Sahar Nozad, Mohammed Shiekhmohammed, Bhaskar VS Kallakury, Christine E Sheehan, Julia A Elvin, Jo-Anne Vergilio, James Suh, Shakti H Ramkissoon, Siraj M Ali, Alexa Schrock, Sumanta Pal, Sumanta Pal, Hugh A Fisher, Badar Mian, Tipu Nazeer, David Fabrizio, Garrett Frampton, Caitlin Connelly, Vincent Miller, Philip Stephens, Laurie M Gay, Jeffrey Ross. Albany Med Col, Albany, NY; Georgetown University Hosp, Washington, DC; Foundation Med, Cambridge, MA.

Background: *PMS2* is a mismatch repair (MMR) gene playing a critical role in DNA repair. We studied the prognostic significance of PMS2 immunostaining and the potential predictive capacity of genomic alterations (GA) in the noncoding promoter region of *PSM2* for total mutation burden (TMB) and potential responsiveness to immune checkpoint inhibitors in urothelial bladder cancer (UCB).

Design: FFPE tissue sections from 54 UCB were immunostained by an automated method (Ventana) using rabbit monoclonal PMS2 (clone EPR3947; Ventana/Cell Marque). Nuclear immunoreactivity (nPMS2) was scored based on staining intensity (weak, moderate, intense) and percentage of positive cells (focal <= 10%, regional 11-50%, diffuse >50%). Results were correlated with clinicopathologic variables. Comprehensive genomic profiling (CGP) was performed on a separate cohort of 1,133 UBC using a hybrid-capture, adaptor ligation assay to a mean coverage depth of >672X. TMB was calculated from a minimum of 1.11 Mb of sequenced DNA as previously described and reported as mutations/Mb. The results were analyzed for all classes of GA including base substitutions (sub), insertions and deletions (short variants; SV), fusions, and copy number changes including amplifications (amp) and homozygous deletions.

Results: nPMS2 immunoreactivity was noted in 51 (94%) UCB, with diffuse overexpression (>50% tumor) noted in 32 (59%) UCB; and correlated with high grade [15/18 (83%) grade 3 vs 11/19 (58%) grade 2 vs 6/17 (35%) grade 1, p=0.015], advanced tumor stage [16/21 (76%) advanced (pT2 and pT3) versus 16/33 (49%) low (pTa and pT1) stage, p=0.043], and with overall survival [23/30 (77%) expired versus 7/19 (37%) alive (p=0.005) [follow up available in 49 cases]. On multivariate analysis, advanced tumor stage (p=0.032) and diffuse nPMS2 overexpression (p=0.049) independently predicted shortened survival. In a separate cohort, CGP showed that 433/1,133 (39%) UBC had $\geq$10 mut/Mb and 154 (14%) had $\geq$20 mut/Mb. GA in the coding region of *PMS2* were identified in only 4 (<1%) and PMS2 non-coding promoter GA occurred in only 1 (<1%) UBC. All (100%) of *PSM2* GA were associated with a high TMB.

Conclusions: Overexpression of nuclear PMS2 protein is associated with high tumor grade and advanced tumor stage and is an independent predictor of shortened survival for UCB. *PSM2* GA are extremely infrequent in UCB, but are uniformly associated with high TMB and potential for responsiveness to immunotherapy. Further study of the biologic and clinical significance of PMS2 in UCB appears warranted.

995 Genomic Mapping of Primary Unifocal and Multifocal Renal Cell Carcinoma

Rebecca C Obeng, Adam Lorentz, Usama Alqassab, Dean Laganosky, Christopher Keith, Fei Lian, Kenneth Ogan, Viraj A Master, John G Pattaras, Michael Rossi, Rebecca Arnold, Jeremy Goecks, John A Petros, Adeboye O Osunkoya. Emory University, Atlanta, GA; Beth Isreal Deaconess Medical Center, Boston, MA; George Washington University, Washington, DC.

Background: The efficacy of molecular-targeted therapy for renal cell carcinoma (RCC) can be hindered by genetic heterogeneity of the tumor. The aim of this study was to determine the degree of genomic heterogeneity in unifocal or multifocal primary RCC.

Design: DNA from all geographically and histologically distinct tumor foci was extracted from a cohort of patients with unifocal or multifocal clear cell RCC and corresponding blood samples. Sequencing libraries generated from multiplex bar-coded PCR amplification were prepared for the Illumina HiSeq platform. Galaxy workflow was used to identify somatic mutations in genes including VHL, PBRM1, SETD2, BAP1, KDM5C, KIT, NFE2L2, MET, TP53, CDKN2A, FGFR3, PIK3CA, BRAF, and MUC4 by comparing the tumor samples to buffy coat sequencing from the same patients. A mutation was confirmed if it was in at least 10% of reads, in all overlapping sequences, and if the overall count was at least 50. Additionally, less than 0.5% mutation in the buffy coat had to be present.

Results: Twenty-nine tumor foci (different tumor nodules and some within the same tumor nodule) from 5 patients with matched blood and tissue samples were analyzed. The tumors were representative of both early (3/5 patients [pT1aN0M0]) and late stage (1/5 patients [pT3aN0M0] and 1/5 patients [pT3aN1M1]) clear cell RCC. All patients had detectable nonsynonymous, frameshift, stop, gain, or splice site somatic mutations. Sixty-four mutations were identified and 22/29 foci had at least one mutation. The patient with the greatest number of mutations (34 mutations in 9 genes across 5 foci) had pT3aN0M0 disease. In two patients, the same mutation (in BAP1 or VHL) was seen in all foci, however heterogeneity within each tumor was the predominant finding. Even adjacent foci with identical histologic appearances within the same tumor nodule harbored distinct mutations.

Conclusions: Mutations were detected in early and late stage (unifocal or multifocal) clear cell RCC. Intertumoral and intratumoral genomic heterogeneity was detected even in early stage tumors and every geographically distinct tumor focus had a unique genomic profile (even within the same tumor nodule). Precise genotyping of RCC is possible (including retrospectively), but complete genomic information requires sampling of all tumor foci. As genetic biomarkers of RCC progression and drug susceptibility information become available, it will be important to incorporate genotyping of multiple tumor foci for effective therapy.

996 Pan-Cancer Analysis of the Mediator Complex Transcriptome Identifies CDK19 and CDK8 as Therapeutic Targets in Advanced Prostate Cancer

Anne Offermann, Johannes Braegelmann, Niklas Kluemper, Stefan Duensing, Maria Svensson, Zaki Shaikhibrahim, Jutta Kirfel, Sven Perner. Pathology, University Hospital of Luebeck and Research Center Borstel, Luebeck, Germany; Urology, University of Heidelberg, Heidelberg, Germany; Department of Research and Education, Örebro, Sweden.

Background: The Mediator is a multi-protein complex which serves as a hub for diverse signaling pathways to regulate gene expression. Since gene expression is frequently altered in cancer a systematic understanding of the Mediator complex in malignancies could improve the development of novel therapeutic approaches.

Design: We performed a systematic analysis of the Mediator subunit expression profiles across 23 cancer entities (n=8568) using data from The Cancer Genome Atlas (TCGA). Finding CDK19 specifically up-regulated in prostate cancer (PCa), expression of CDK19 and CDK8 was evaluated on a PCa progression cohort (n=622) by immunohistochemistry. Further, the functional role of CDK19 and CDK8 in PCa cell lines was evaluated by gene knockdown and inhibitor treatment followed by migration and invasion assays as well as RNA-sequencing.

Results: Cluster analysis of the TCGA expression data segregated tumor entities, while PCa was marked by high expression of CDK19. In primary PCa CDK19 was associated with increased aggressiveness and shorter disease free survival. Highest levels of CDK19 and CDK8 were present in metastases. In cell lines, inhibition of CDK19 and CDK8 by knockdown or treatment with the selective CDK8/CDK19 inhibitor Senexin A significantly decreased migration and invasion. Additionally, Senexin A affected significantly the gene expression profile in DU145 cells.

Conclusions: Our analysis revealed distinct transcriptional expression profiles of the Mediator complex across cancer entities indicating differential modes of transcriptional regulation. It identified CDK19 and its paralog CDK8 to be involved in PCa pathogenesis, which could be confirmed by in-vitro analysis. Based on these data, we suggest CDK19 and CDK8 as potential therapeutic targets in advanced PCa.

997 SOX4 Expression in Prostatic Adenocarcinoma with Matched Lymph Node Metastasis

Claudia Ormenisan Gherasim, Anand C Annan, Birdal Bilir, Carlos S Moreno, Adeboye O Osunkoya. Emory University School of Medicine, Atlanta, GA.

Background: Large-scale gene expression studies have identified increased expression levels of the Sex-determining region Y-related high-mobility group box 4 (SOX4) gene in a variety of human malignancies. SOX4 has a role in embryonic development, differentiation, and tumor development, and progression of malignant melanoma, leukemia and lung cancer. The role of SOX4 in prostatic adenocarcinoma has not been well characterized in humans, although it has been shown to be essential for progression of prostatic adenocarcinoma in transgenic mice. The aim of this study was to investigate the expression of SOX4 in prostatic adenocarcinoma, with an emphasis on cases with matched lymph node metastasis.

Design: A search was performed for radical prostatectomy specimens with prostatic adenocarcinoma and corresponding lymph nodes metastasis at our institution. Immunohistochemical stains for SOX4 were performed on both the primary tumor and matching lymph node metastasis. SOX4 expression in the nucleus and cytoplasm of the tumor cells, and adjacent prostatic stroma was documented.

Results: Twenty-four cases were selected. Mean patient age was 60.7 year (range: 38-71years). The Gleason scores (Grade groups) were as follows: Gleason score 3+4=7 (Grade group 2) 6/24 (25%) cases, Gleason score 4+3=7 (Grade group 3) 10/24 (42%) cases, Gleason score 4+4=8 and 5+3=8 (Grade group 4) 2/24 (8%) cases and Gleason score 4+5=9 (Grade group 5) 6/24 (25%) cases. Eighteen of 24 (75%) cases were positive for SOX4 and 22/24 (92%) of the metastatic lymph nodes were positive for SOX4. Interestingly, there was also positive SOX4 expression in the prostatic stroma adjacent to the tumor cells.

Conclusions: We have demonstrated positive SOX4 expression in a cohort of aggressive prostatic adenocarcinoma with lymph node metastasis. Increased number of cases with SOX4 expression in the lymph node metastasis compared to the primary tumors further suggests that SOX4 may play a role in systemic spread of prostatic adenocarcinoma. The positive SOX4 expression in the peritumoral prostatic stroma suggests that SOX4 may play a key role in tumor stromal interactions and is consistent with SOX4 regulation of the epithelial to mesenchymal transition in prostatic adenocarcinoma.

998 Does Injection of 2-Aminobicyclo-(2,2,1)-Heptane-2-Carboxylic Acid (BCH) Affect Amino Acid Transporter Density in Prostate Cancer Xenografts?

Claudia Ormenisan-Gherasim, Funmilayo Tade, Oladunni O Akin-Akintayo, Birdal Bilir, Walter G Wiles, Guolan Lu, Baowei Fei, Carlos S Moreno, Mark M Goodman, David M Schuster, Adeboye O Osunkoya. Emory University, Atlanta, GA; Emory University School of Medicine, Atlanta, GA.

Background: FACBC (^{18}F-fluciclovine) is a PET radiotracer recently approved by the FDA for recurrent prostate cancer imaging. It is believed to be transported via the amino acid transporters LAT1, ASCT2 and SNAT2 with a possible indirect relationship to PAT1. We have previously demonstrated 37% inhibition of fluciclovine uptake in PC3 xenografts injected with BCH, a LAT1 inhibitor. This study aims to explore if this inhibitory effect is also due to reduction of transporter density by BCH at the transcriptional level.

Design: After posthumous dissection of PC3 xenografts (BCH injected and contralateral control) from 6 SCID mice, immunohistochemical staining with antibodies for LAT1, PAT1, ASCT2 and SNAT2 were performed. . Transporter expression was determined using visual intensity (+1, +2, +3) and proportion scores. Differences in expression between BCH injected tumors and controls were analyzed using paired T-test.

Results: Injection of BCH led to significant ($p<0.05$) reduction in the LAT 1 transporter density compared to controls. Although not statistically significant (P=0.07), there was a trend of higher expression of ASCT2 transporters in BCH injected tumors compared to their controls. BCH injection had no significant effect on SNAT2 and PAT1 transporter expression compared to their controls. Figure 1 shows amino acid receptor expression in prostate cancer (PC3) xenografts injected with BCH compared to their controls.

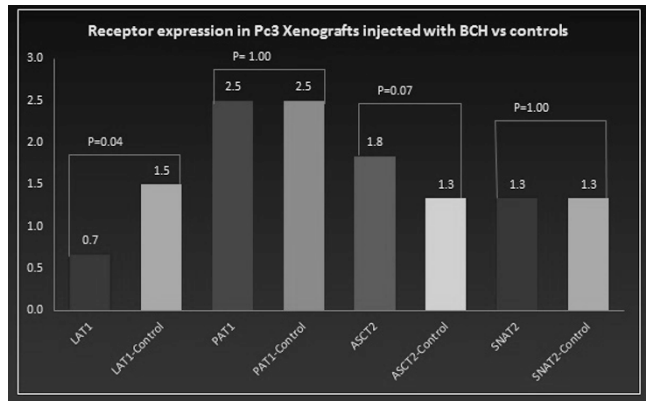

Conclusions: Reduction in fluciclovine uptake after BCH injection seen in our earlier study is due in part to direct inhibitory effect of BCH on LAT1 transporter density after downregulation from BCH exposure. The resultant decreased amino acid influx could then cause an upregulation of ASCT2 transporters, ameliorating the effect on fluciclovine uptake. These findings may have clinical implications for therapy and fluciclovine imaging of prostate cancer.

999 Accuracy of PIRADS on Targeted Prostate Needle Core Biopsies: A Single Institutional Radiopathologic Correlation

Vamsi Parimi, Ian Hughes, Maria M Picken. Loyola University Medical Center, Maywood, IL.

Background: The Prostate Imaging Reporting and Data System (PIRADS) was implemented at our institution as a standard for interpreting multiparametric MRI (mpMRI). PIRADS provides guidance regarding the acquisition and interpretation of prostate mpMRI and proposes a simplified 5-point scale with a score of 5 indicating the highest likelihood of a clinically significant prostatic adenocarcinoma (PCa). The objective of our study was to assess the accuracy of PIRADS for detecting PCa using mpMRI on prostate needle core biopsy (PNCB).

Design: This single-institution retrospective interpretation of prospectively acquired data comprised of 138 patients with mpMRI guided PNCB of which 17 patients subsequently underwent radical prostatectomy. Of 138 patients, 226 targeted needle core biopsy PIRADS score (1-5) were compared to histopathologic diagnosis and Gleason score(GS). Consensus of the PIRADS score was achieved by more than one radiologist. PIRADS scores ≤3 was considered negative for PCa for statistical calculations.

Results: Of 226 (PIRADS: Mean±STD=3.29±0.72) PNCB; 156 were diagnosed benign by histopathology evaluation (PIRADS: Mean±STD=3.29±0.7) and 70 as prostatic adenocarcinomas (PIRADS: Mean±STD=4.18±0.74; GS: Mean±STD=6.87±0.94) PIRADS scores among benign and malignant prostate PNCB are statistically different (t-value=4.74; p-value<0.0001). Observed associations of PIRADS scores among malignant PNCB to the percentage of PCa (Rho=0.32; p=0.053) in PNCB and length of cores (Rho=0.23; p=0.20) involved by PCa (mm) showed weak association and no significance. The point biserial correlation coefficient between GS and PIRADS is strong and positive (r_{pb}=0.85; p<0.0001). The relative observed malignancy to benign diagnosis agreement between histopathology and radiology PIRADS is 69.3% (Kappa statistic: 41.9%). Sensitivity for PIRADS =3, ≥ 4 and ≥ 5 is 50%, 50% and 100%. The PPV for PIRADS ≥ 4 and ≥ 5 are 50% and 81.25% respectively. The overall accuracy of MRI based PIRADS score in diagnosing PCa is 76.35%. Diagnostic Odds Ratio: 40.5%.

		PiRads				
		2	3	4	5	Total
Gleason Score	3+3	1	7	13	7	28
	3+4	0	3	12	10	25
	3+5	0	0	0	1	1
	4+3	0	1	3	2	6
	4+4	0	0	2	0	2
	4+5	0	0	2	4	6
	5+4	0	0	0	2	2
	B9	18	80	52	6	156
	Total	19	91	84	32	226

Conclusions: Our study demonstrates the accuracy, practical utility but also limitations of PIRADS in MRI guided prostatic needle core biopsy.

1000 Comparison of Standard and MRI Targeted Biopsy in Anterior-Predominant Prostate Cancer

Yu-Ching Peng, Ying Wang, Hongying Huang, Peng Lee, Jonathan Melamed, Ming Zhou, Fang-Ming Deng. NYU Langone Medical Center, New York, NY.

Background: Anterior-predominant prostate cancer (APC) represents a clinical challenge in terms of detection due to its deeper location. Here we compared standard v.s. MRI targeted biopsy in terms of detection of prostate cancer, Gleason score, tumor size and percentage.

Design: We analyzed 46 APC cases, which had both standard and MRI targeted biopsy from 2014 to 2016 in our institution. Detailed prostate maps from radical prostatectomy (RP) were reviewed. We compared the detection rate between standard and MRI targeted biopsy. Furthermore, we compared the detection rate of clinical significant disease. Insignificant detection was defined by biopsy showing Gleason score 3 + 3 = 6 disease, while the RP has more than Gleason score 6 disease. We further compared Gleason score between biopsy and RP. We compared tumor size and percentage between standard and MRI targeted biopsy.

Results: The total detection rate of adenocarcinoma was significantly higher in MRI biopsy (91.30% MRI vs 76.09% standard, p<0.05, Table 1). The detection of clinical significant disease was also higher in MRI biopsy (82.61% MRI vs 58.70% standard, p<0.05). Standard biopsy showed higher rate of same Gleason score compared to RP (54.76% MRI vs 60.00% standard, p<0.05, Table 2]). Higher percentage of standard biopsy cases showed upgrading (26.19% MRI vs 40.00% standard, p<0.05, Table 2). Interestingly, 19.05% of MRI biopsy cases showed downgrading, whereas none of standard biopsy did. However, the over grade in MRI biopsy would not affect the decision of clinical management. MRI biopsy detected larger tumor (6.46 mm MRI vs 3.80 mm standard, p<0.05) and higher percentage of tumor in the core (53.98% MRI vs 30.09% standard, p<0.05).

Method	Detected	Missed	Detection rate
Standard	35	11	76.09%
MRI	42	4	91.30%

Method	Same	Upgrade	Downgrade
Standard	21 (60%)	14 (40%)	0
MRI	23 (54.76%)	11 (26.19%)	8 (19.05%)

Conclusions: MRI targeted biopsy has a higher detection rate than standard biopsy in detecting APC. MRI targeted biopsy has a lower rate of upgrading and a higher rate of downgrading. MRI targeted biopsy detected higher tumor size and percentage. Particularly, MRI targeted biopsy has a higher value than standard biopsy on detection and clinical management of anterior-predominant prostate cancer.

1001 Fibromyxoid Stromal Response (FMR) Is Associated with Perineural Invasion (PNI) in Penile Squamous Cell Carcinoma

Will Penny, Steven Post, Charles Quick, Christina Stallworth, Roni Cox. UAMS, Little Rock, AR.

Background: Multiple factors have been shown to effect the prognosis of penile invasive squamous cell carcinomas (SqCC). The most important prognostic factors include the histologic grade, anatomic level of infiltration, and perineural invasion (PNI). The association of a fibromyxoid stromal response (FMR) with infiltrative growth pattern, PNI, and tumor recurrence has been shown in tumors at other anatomic sites, including vulvar squamous cell carcinoma. The objective of this study is to examine the importance of FMR in penile SqCC.

Design: A total of 59 cases of penile SqCC were retrieved from our pathology archives between 1998-2016. H&E stained slides were evaluated for stromal response (fibromyxoid or inflammatory). FMR was defined as a myxoid background with associated immature collagen and fibroblasts. Inflammatory stromal response (IR) was defined as a band-like, dense lymphoplasmacytic infiltrate. Additional parameters recorded included: PNI, lymphovascular invasion (LVI), histologic subtype, tumor grade and stage, tumor thickness, tumor size, and margin status. P16 immunostaining was used as a surrogate marker for HPV. Lymph node involvement (+/- extranodal extension), local recurrence, and metastatic disease were recorded.

Results: Mean patient age was 62 years (range 40-81). Mean tumor size was 3.35 cm (range: 0.3 – 13.5). Histologic grading was: G1 – 11, G2 – 25, and G3 – 23. Pathologic stage was: pT1 – 20, pT2 – 22, pT3- 16, and 1 case pT4. Mean tumor thickness was 12.3 mm. LVI was present in 33 cases and PNI was present in 26 cases. Of the 53 cases with paraffin embedded tissue available for p16 staining, 22 showed block positive staining. 31 cases had a mixed stromal response (FMR + IR), 7 cases had FMR only, 16 cases had IR only and 5 cases had no stromal response. Five cases had a positive surgical margin. Lymph node metastasis was present in 24 cases, with extranodal extension in 15 cases. 7 cases had local recurrence and distant metastasis was present in 8 cases. Average clinical follow-up was 25 months (range 1-122). By univariate analysis, an association between FMR and PNI was identified (P= 0.0008). No correlation with LVI, p16 status, tumor size, tumor thickness, local recurrence, or nodal metastases was found.

Conclusions: The presence of fibromyxoid tumor response (FMR) is associated with the presence of perineural invasion (PNI), which is one of the most important prognostic factors in penile squamous cell carcinomas. This association suggests that presence of FMR may provide an easily identifiable histologic indicator of PNI and adverse prognosis.

1002 Frequency of Subtypes in High Grade Urothelial Carcinoma of the Urinary Bladder

Delia Perez Montiel, Carolina Silva Morera, Anna Scavuzzo, Julia Mendoza Perez, Miguel Angel Jimenez, Lourdes Pena, Guadalupe Moncada, David Cantu de Leon. Instituto Nacional de Cancerologia, Mexico City, Mexico.

Background: Urothelial carcinoma is the most common neoplasm of the urinary bladder. The spectrum of cytologic and architectural patterns is wide. Specific subtypes such as micropapillary microcystic, giant cell, rhabdoid, among others have been described with quite variable frequency of presentation. The purpose is to describe the frequency of subtypes in a single institution.

Design: All cases of urothelial carcinoma treated either with transurethral resection or radical cystectomy at the Instituto Nacional de Cancerología of México, from 2005 to 2015 were reviewed. All slides were reviewed by two pathologist to account for the percentage of subtypes in each tumor. Immunohistochemical stains were performed in selected the cases to confirm the diagnosis.

Results: During 11-year study period, 244 cases of primary high grade urothelial carcinoma were suitable for review. Thirty six cases showed one or more subtypes (15%). Micropapillary variant was present in 14 cases (5%), microcystic 5 cases (2%), sarcomatoid, nested, lymphoepithelioma-like, small cell (neuroendocrine), trophoblastic differentiation and giant cell osteoclast-like 2 cases (1.2%) each one. Clear cells glycogen rich and signet ring cell 2 cases (0.8%) each one, signet cell areas were associated to extensive desmoplasic stroma. Rabdoid and lipid rich 1 case (0.4%) each one. Interestingly, two cases of giant cell variant were associated to sarcomatoid differentiation. The percent of these subtypes varies from 5 to 80% of the tumor. All subtypes, except clear cell glycogen rich, had muscularis propia invasion. Divergent differentiation to squamous was found in 54 cases (22%) and glandular in 5 cases (2%).

Conclusions: Urothelial carcinoma subtypes were identified in 15% of tumors, and have to be taken into account by the surgical pathologist to avoid misdiagnosis with other entities including prostatic adenocarcinoma, others carcinoma secondarily involving bladder or metastatic lesions.

1003 Plasmacytoid Urothelial Carcinoma: A Single Institution Immunohistochemical and Molecular Study of 26 Cases

Carmen Perrino, Liang Cheng, Mohammad Idrees, John N Eble, Chia-Sui Kao, David Grignon. Indiana University, Indianapolis, IN; Stanford University, Stanford, CA.

Background: Accurate diagnosis of plasmacytoid urothelial carcinoma (PUC) is important given its poor prognosis and frequent presentation at a high stage. We aim to assess the expression of immunohistochemical (IHC) stains pertinent to the differential diagnosis and to assess molecular aberrations in a series of cases of PUC from a single institution.

Design: Twenty-six cases were identified via a search of the pathology database at Indiana University (1996-2012) for urinary bladder specimens (2 biopsy, 3 transurethral resection, and 21 radical cystectomy) with a final diagnosis of urothelial carcinoma described as "signet ring" (n=5) or "plasmacytoid" (n=21). IHC stains were performed on a select block and scored for intensity (0: no staining; 1: weak; 2: moderate; 3: strong) and proportion of cells stained (0: 0%; 1: >0 to ≤25%; 2: >25 to ≤50%; 3: >50 to ≤75%; 4: >75 to 100%). Fluorescence in situ hybridization (FISH) using the UroVysion Bladder Cancer Kit and to detect FGFR3 mutations was performed on 15 cases.

Results: Among bladder origin markers, GATA3 was the most sensitive (96%), followed by p63 (62%), uroplakin (46%), and thrombomodulin (19%). Keratin 7 (85%) and keratin 20 (77%) were positive in most cases. Breast carcinoma markers were usually negative; PR stained 1 case (intensity 1, proportion 1), while mammaglobin and ER were negative in all cases. Neuroendocrine markers CD56 and TTF-1 were each positive in 1 case (intensity 1, proportions 1 and 2). Gastrointestinal adenocarcinoma marker CDX2 was positive in 4 cases, while nuclear beta-catenin was negative in all cases. CD138 was positive in 73% and e-cadherin expression was lost in 73% of cases. Nuclear p53 staining was present in 96% of cases. UroVysion FISH detected polysomy of chromosomes 3 (13%), 7 (20%), and 17 (20%) and deletion of chromosome 9p21 (60%). FGFR3 mutations were detected by FISH in 60% of cases.

Conclusions: Urinary bladder origin markers GATA3 and p63 are the most sensitive for detection of PUC. Occasional staining with markers pertinent to the differential diagnosis (PR in breast carcinoma, CDX2 in gastrointestinal signet ring carcinoma) may be detected, and in the appropriate context should not exclude urothelial origin. Finally, molecular aberrations commonly detected in conventional urothelial carcinoma are present in the plasmacytoid variant.

1004 Morphologic Analysis of Renal Cell Carcinoma, Unclassified

Carmen Perrino, David Grignon, Mohammad Idrees, John N Eble, Liang Cheng. Indiana University, Indianapolis, IN.

Background: Renal cell carcinoma, unclassified (RCCU) is a category that includes a morphologically and biologically heterogeneous group of tumors that are unable to be diagnosed as other well-defined entities. This diagnosis is, at times, misunderstood by clinicians due to the assumption that these tumors are uniformly associated with a poor prognosis. We aim to describe the morphologic findings of tumors within this category and to determine the most frequent morphologic features leading to classification difficulty.

Design: The pathology database was queried for in-house cases with a final diagnosis of "renal cell carcinoma, unclassified." Fifty two cases of RCCU were examined, of which 40 were from radical and 12 were from partial nephrectomy specimens.

Results: Patients ranged in age from 23 to 87 years (median 60 years). Thirty patients were men and 22 were women. ISUP nuclear grade was most commonly 3 (n= 29), followed by 2 (n=13) and 4 (n=10). Tumor size ranged from 0.6 cm to 24.9 cm. The AJCC pathology T categories included pT1a (n=19), pT1b (n=2), pT2a (n=3), pT3a

(n=16), pT3b (n=6), or pT4 (n=6). Twenty cases included lymph node(s), of which 55% (n=11) had metastases. The adrenal gland was included in 26 cases, of which 31% (n=8) were involved. The tumors were assigned to the following morphologic groups: eosinophilic cytoplasm (n=39); papillary architecture (n=5); clear cytoplasm (n=3); collecting duct-like (n=3); and sarcomatoid (n=2). Tumors were assessed for a variety of histologic features, including: calcifications (n=10); low volume clear cytoplasm (n=10); cystic spaces (n=12); "chicken-wire" vasculature (n=9); cytoplasmic hyaline globules (n=2); infiltrative borders (n=12); multinucleate giant cells (n=3); necrosis (n=12); perinuclear haloes (n=6); pigment (n=25); thick-walled blood vessels (n=4); tubules (n=35); and cytoplasmic vacuoles (n=18).

Conclusions: Overall, RCCU is a term that encompasses tumors with a variety of morphologic features and a wide biologic spectrum. The most common source of difficulty was tumors composed of eosinophilic cells followed by tumors with papillary architecture. The tumors ranged from low nuclear grade (ISUP grade 2) and low stage (pT1a) to high grade (ISUP grade 4) and high stage (pT4) carcinomas.

1005 Prognostic and Predictive Significance of TSC1/2 in Urothelial Carcinoma of the Bladder (UCB)

Katherine Pinheiro, Aseeb Rehman, Chunlai Zuo, Sanaz Ainechi, Bhaskar VS Kallakury, Christine E Sheehan, Julia A Elvin, Jo-Anne Vergilio, James Suh, Shakti H Ramkissoon, Siraj M Ali, Alexa Schrock, Sumanta Pal, Hugh A Fisher, Badar Mian, Tipu Nazeer, David Fabrizio, Garrett Frampton, Caitlin Connelly, Vincent Miller, Philip Stephens, Laurie M Gay, Jeffrey Ross. Albany Med Col, Albany, NY; Georgetown University Hosp, Washington, DC; Foundation Med, Cambridge, MA.

Background: The tuberous sclerosis proteins, hamartin (TSC1) and tuberin (TSC2) co-form an intracellular tumor suppressor complex involved in the mTOR signaling pathway. In this study, we investigated the prognostic significance of TSC1/2 protein expression and the frequency of *TSC1/2* genomic alterations (GA) and high tumor mutation burden (TMB) in UCB.

Design: FFPE sections from 57 UCB were immunostained by an automated method (Ventana) using rabbit monoclonal tuberin/TSC2 (clone D93F12, Cell Signaling) and mouse monoclonal hamartin/TSC1 (clone 3A2, Abcam) antibodies. Cytoplasmic TSC2 (cTSC2) and TSC1 (cTSC1) immunoreactivity was scored based on stain intensity (weak, moderate, intense) and percent positivity (focal <= 10%, regional 11-50%, diffuse >50%). Results were correlated with clinicopathologic variables. In another cohort, DNA was extracted from 40 microns of FFPE specimens from 1,129 cases of relapsed, refractory and metastatic mUCB. Comprehensive genomic profiling (CGP) was performed using a hybrid-capture, adaptor ligation based next generation sequencing assay to a mean coverage depth of >600X. Tumor mutational burden (TMB) was calculated from a minimum of 1.11 Mb of sequenced DNA as previously described and reported as mutations/Mb.

Results: In the IHC cohort**,** cTSC2 was noted in 42 (74%) UCB. Moderate or diffuse overexpression was noted in 30 (53%) UCB and correlated with high tumor grade (p=0.004), advanced tumor stage (p=0.05), and overall survival (p=0.004). cTSC1 was noted in 27 (47%) UCB, but did not correlate with clinicopathologic variables. On multivariate analysis, advanced tumor stage (p=0.001) independently predicted shortened survival. In the mUBC cohort, 88 (7.8%) mUCB showed *TSC1* GA with a mean TMB of 14 mut/Mb and a median TMB of 9 mut/Mb. Of the 88 mUCB with *TSC1* GA, 44% had a TMB ≥ 10 and 22% had a TMB ≥ 20. 7 (0.6%). mUCB featured *TSC2* GA with a mean TMB of 8 mut/Mb and a median TMB of 3 mut/Mb. Of the 7 mUBC with *TSC2* GA, 38% had a TMB ≥ 10 mut/Mb and 29% had a TMB ≥ 20 mut/Mb. In 865 mUBC negative for *TSC1/2* GA, 31% had a TMB ≥ 10 mut/Mb and 9% had a TMB ≥ 20 mut/Mb.

Conclusions: Increased expression of TCS2 but not TSC1 correlates with high grade, advanced stage UCB and decreased survival. TSC1 but not TSC2 GA are frequent in mUBC and indicate potential for targeted therapy with MTOR pathway inhibitors. TSC1 and TSC2 GA appear to be more frequent in mUBC featuring high TMB which has been associated with enhanced responsiveness to immune checkpoint inhibitor therapy.

1006 Prevalence of *TERT* Promoter Mutations in Different Morphological Variants of Urothelial Carcinoma and in Basal and Non-Basal Urothelial Carcinoma

Dinesh Pradhan, Wayne Ernst, Stephanie Mercurio, Marina N Nikiforova, Rajiv Dhir, Somak Roy. UPMC, Pittsburgh, PA.

Background: Somatic activating point mutations in the promoter region of the *Telomerase reverse transcriptase (TERT)* gene are the most common genetic alterations in urothelial carcinoma (UC) of the bladder. Recent studies have described basal and non-basal subtypes of high grade UC (HGUC) that correlates with the presence (basal) or absence (non-basal) of expression of CK14 and CK5/6 by immunohistochemistry (IHC). The aim of this study was to evaluate the prevalence of *TERT* promoter mutations (TPM) in Basal and Non-basal subtypes and across morphological variants of UC.

Design: 48 cases of HGUC were profiled using IHC that included 2 basal markers (CK14 & CK5/6). The *TERT* promoter was amplified by PCR on extracted DNA using and interrogated for the hotspot mutation loci for g.1295228C>T (c.-124C>T; C228T) and g.1295250C>T (c.-146C>T; C250T) using bi-directional Sanger sequencing.

Results: Of the 48 cases, 11 (22.9%) and 37 (77.1%) cases were categorized as basal (CK5/6+ and CK14+) and non-basal (CK5/6- and CK14-) subtype, respectively. Although immunostaining was performed on all 48 cases, TPM could be interrogated in only 34 cases. TPM was positive in 7 (70%) basal and negative in 3 (30%) basal UCs. In the non-basal category, TPM was positive in 17 (70.8%) cases and negative in 7 (29.2%) cases. TPM was positive in all micropapillary, small cell and nested variants and was present at lesser frequency in plasmacytoid and squamous differentiation.

Urothelial Carcinoma Variants (# of cases)	TERT promoter mutations (34 cases)	Basal Phenotype (48 cases)
Micropapillary (8)	5/5 (100%)	0
Small Cell (7)	6/6 (100%)	0
Nested (1)	1/1(100%)	0
Plasmacytoid (4)	2/3(66.7%)	0
Papillary HGUC (2)	1/2 (50%)	0
Squamous Differentiation (16)	10/13 (77%)	11/16 (69%)
HGUC-NOS (10)	0/5 (0%)	0
Total (48)	25/34 (74%)	11/48 (23%)

Both C250T mutations were seen in UC with squamous differentiation. There was no significant difference in prevalence of TPM between basal and non-basal UCs. TPM C228T was observed in 23 (92%) cases (6 basal and 17 non-basal) while C250T was positive in only 2 (8%) cases (1 basal and 1 non-basal).

Conclusions: TPM was highly prevalent in micropapillary, small cell and nested variant and was less prevalent in UC with plasmacytoid and squamous differentiation. Most of the variants were non-basal, except UC with squamous differentiation which was predominantly revealing basal phenotype. Basal and non-basal status of UC does not correlate with TPM.

1007 Characteristics of Initial Prostate Biopsies That Predict Repeat Biopsy Upgrade to Gleason ≥7

Saranya Prathibha, Kashika Goyal, Debra L Zynger. The Ohio State University Medical Center, Columbus, OH.

Background: Extended prostate biopsies are standard of care for the diagnosis of prostatic carcinoma. Subsequent prostate needle core biopsies may be performed for a variety of indications. Knowledge of initial biopsy characteristics which indicate risk for progression on subsequent biopsies may have utility to guide therapeutic management.

Design: Pathology reports from prostate needle core biopsies performed between 2008-2013 were reviewed. Patients with at least 1 subsequent biopsy were identified. Cases were categorized by worst initial diagnosis. Gleason ≤6 carcinoma was further classified as significant or insignificant with insignificant defined as: ≤2 cores with carcinoma, each container with ≤50% carcinoma, and unilateral carcinoma.

Results: Of 1,853 prostate biopsies, 264 men underwent repeat biopsies (median interval 20 months). Initial biopsies were diagnosed as: carcinoma 46%, HGPIN/ASAP 5%, ASAP 7%, HGPIN 6%, and negative 36%. Gleason ≤6 insignificant carcinoma, HGPIN and/or ASAP, and negative biopsies had a similar rate of Gleason ≥7 carcinoma in the repeat biopsy (16%, 16%, 14%; p=0.9). Gleason ≤6 insignificant carcinoma had less frequent carcinoma diagnoses on repeat biopsy versus Gleason ≤6 significant carcinoma (72%, 91%; p=0.04). Initial biopsy diagnoses of Gleason ≤6 significant carcinoma had a higher rate of Gleason ≥7 on repeat biopsy compared to initial biopsies of Gleason ≤6 insignificant carcinoma (38%, 16%; p=0.01). Using only core number to stratify initial diagnoses of Gleason ≤6, 1 core compared to >1 core positive had a similar rate of carcinoma on repeat biopsy (74%, 84%; p=0.3) but the >1 core group upgraded to Gleason ≥7 more frequently (33%, 15%; p=0.04).

	Follow-up Diagnosis			
Initial Biopsy Diagnosis	Gleason ≥7	Gleason ≤6 Significant Carcinoma	Gleason ≤6 Insignificant Carcinoma	All Other Diagnoses
Gleason ≥7 (n=11)	64%	9%	0%	27%
Gleason ≤6 Significant Carcinoma (n=34)	38%	26%	26%	9%
Gleason ≤6 Insignificant Carcinoma (n=76)	16%	25%	32%	28%
ASAP and/or HGPIN (n=49)	16%	6%	20%	57%
Negative (n=94)	14%	4%	14%	68%

Conclusions: An initial biopsy diagnosed as Gleason ≤6 insignificant carcinoma, ASAP and/or HGPIN, or negative had a similar rate of Gleason ≥7 carcinoma upon subsequent biopsy while Gleason ≤6 significant carcinoma carried a higher risk. These findings support the continued stratification of Gleason ≤6 insignificant from Gleason ≤6 significant carcinoma for treatment decisions.

1008 Amphicrine Carcinoma: Expanding the Spectrum of Neuroendocrine Tumors of the Prostate

Susan Prendeville, Issam Al-Bozom, Eva Comperat, Joan Sweet, Andrew J Evans, Mohammad Ben-Gasheer, Ozgur Mete, Theodorus van der Kwast, Michelle R Downes. University Health Network, Toronto, ON, Canada; Hamad Medical Corporation, Doha, Qatar; Hôpital Tenon, Paris, France; Sunnybrook Health Sciences Centre, Toronto, ON, Canada.

Background: The current WHO classification categorizes high grade neuroendocrine (NE) carcinomas of the prostate into small cell and large cell types. A distinct form of NE carcinoma demonstrating synchronous dual exocrine and NE differentiation, termed amphicrine carcinoma, is recognized within the broader classification of NE tumors of the gastrointestinal tract. In this preliminary study we describe a series of prostatic amphicrine carcinomas which display an aggressive clinical phenotype and represent an under-recognized entity based on contemporary morphologic classification.

Design: Cases of high grade prostatic carcinoma (PCa) demonstrating dual positivity for exocrine (PSA, androgen receptor [AR]) and NE (chromogranin, synaptophysin) immunohistochemical (IHC) markers were prospectively collected from 4 academic institutions (2015-2016). Slides were reviewed by 2 pathologists.

Results: 5 cases were identified. Clinical features are outlined in table 1. All 5 patients had metastatic disease; 4 at initial presentation. Microscopically the tumors demonstrated a solid/nested growth pattern composed of cells with vesicular chromatin, macronucleoli and amphophilic cytoplasm. Compared with conventional high grade PCa, the tumor cells displayed greater nuclear pleomorphism and brisk mitotic activity (up to 29/10 HPF). Morphologic features of small cell/large cell NE carcinoma were absent. All tumors demonstrated IHC positivity for PSA and AR and diffuse positivity for at least one NE marker.

	CASE				
	1	2	3	4	5
Age	64	75	66	88	74
Sample site	Bone	Lymph node	Bladder	Bladder	Bone
PSA (ng/ml)	992	347	46	38	200
Hormone therapy prior to biopsy	N	N	Y	Y	Y

Conclusions: Our series highlights an unusual and potentially under-recognized variant of PCa exhibiting dual exocrine and NE differentiation (amphicrine carcinoma). Morphologic clues distinct from conventional high grade PCa include greater nuclear pleomorphism and prominent mitotic activity. Our findings are in line with a previously reported case of highly aggressive PCa which demonstrated a dual luminal-neuroendocrine molecular phenotype based on next-generation sequencing. Classification of this entity within the spectrum of NE tumors of the prostate may facilitate increased recognition and appropriate clinical management of these aggressive carcinomas.

Reference: Wu C et al. J Pathol.2012;227:53-61

1009 Overexpression of the Long Non-Coding RNA SChLAP1 in Prostate Cancer: Morphologic Distribution and Association with Intraductal and Cribriform Carcinoma

Susan Prendeville, Winnie Lo, Melania Pintille, Robert Bristow, Theodorus van der Kwast. University Health Network, Toronto, ON, Canada; Princess Margaret Cancer Centre, Toronto, ON, Canada.

Background: Recent studies have identified overexpression of the long noncoding RNA SChLAP1 using in situ hybridization (ISH) as a marker of aggressive prostate cancer (PCa). Morphologic correlates of SChLAP1 overexpression, including it's association with adverse histologic features of intraductal/cribriform carcinoma (IDC/CR) and it's tissue distribution have not been studied. The aims of this study were: 1) correlate ISH expression with IDC/CR status 2) determine the distribution of SChLAP1 expression within benign and malignant prostate tissue 3) correlate SChLAP1 expression using ISH and RNA microarray analysis.

Design: The study cohort comprised 76 patients with intermediate risk PCa treated with radical prostatectomy (RP). 2 pathologists determined IDC/CR status. SChLAP1 ISH was performed on representative RP tumor tissue from all cases using tissue microarrays (3 cores per patient; total 228) and also on selected RP whole sections (n=38) encompassing a spectrum of benign and malignant prostate tissue. ISH was scored using published criteria (0 - 400). To assess concordance between SChLAP1 ISH and gene expression, RNA microarray analysis was performed using frozen tissue from 50 cases.

Results: 42 cases were IDC/CR+(55%) while 34 were IDC/CR-(45%). IDC/CR+ status was associated with increased SChLAP1 signals with median ISH value of 18.22 for IDC/CR+ cases vs 0 for IDC/CR- cases (p=<0.0001). There was good correlation between SChLAP1 expression using ISH and microarray analyses (Spearman 0.636;Pearson 0.672). Increased SChLAP1 signals were observed within invasive tumor and adjacent high grade prostatic intraepithelial neoplasia (HPIN), but were not seen in HPIN lesions distant from tumor or any benign glands. Notably, whole section ISH analysis revealed marked heterogeneity in SChLAP1 expression with localised foci of increased signals observed within invasive tumor and adjacent HPIN, without evidence of homogeneous diffuse overexpression in any case.

Conclusions: IDC/CR+ status at RP is associated with increased expression of SChLAP1. In addition to invasive cancer, increased SChLAP1 signals were often observed in adjacent HPIN lesions, and further study is warranted to determine the biologic mechanisms responsible for this distribution of expression. While ISH showed good concordance with microarray analysis, marked heterogeneity of SChLAP1 expression within individual tumors may limit its utility as a tissue based biomarker of aggressive disease.

1010 Paratesticular Rhabdomyosarcoma: An 18-Year Review of 32 Cases

David Priemer, Shaoxiong Chen, Guang Q Xiao, Thomas M Ulbright, Muhammad Idrees. Indiana University, Indianapolis, IN; University of Southern California, Los Angeles, CA.

Background: Primary paratesticular(PT) tumors are rare but diverse, with about half of soft tissue origin. A large subset of PT soft tissue malignancies are rhabdomyosarcomas(RMS), however large-scale data for these lesions are limited. Herein we present the clinical and pathologic characteristics of PT RMS in orchiectomy specimens at our institutions.

Design: We searched our computerized databases from 1998 to 2016 for PT RMS diagnosed in orchiectomy specimens. Available slides(19 cases) and all pathology reports were reviewed and patient information gathered from computerized charts.

Results: 32 patients were identified(**Table**). Mean and median ages were 19.1 and 17.0 years, respectively, with 12 adults(range: 18-77 years; median: 21.0) and 20 children(range: 1-17 years; median: 14.5). 21 were Caucasian, 4 African-American and 7 unknown. The average ages of not otherwise specified(NOS) embryonal, spindled embryonal, alveolar, and pleomorphic subtypes were 15.9, 13.4, 19.5, and 70 years, respectively. The only tumor which occurred exclusively in a single age group was pleomorphic RMS(adults). Metastasis either at presentation or after orchiectomy occurred in 54% of cases(6 adults, 7 children). Retroperitoneal lymph nodes were the most common site(11/13). Other sites included the lungs(4), the opposite testis(2), and bone(1). Follow-up in 24 cases was 1-174 months(mean 54). Only one patient(age 25, with alveolar RMS) died of disease(at 12 months).

Variables	Total cases	Adult cases	Child cases
Tumor laterality (n=31)			
Right	18 (58%)	7 (64%)	11 (55%)
Left	13 (42%)	4 (36%)	9 (45%)
Tumor size, stage (n=23)			
<5.0 cm, pT1b	5 (22%)	3 (30%)	2 (15%)
>5.0 cm, pT2b	18 (78%)	7 (70%)	11 (85%)
RMS subtype (n=32, 1 bilateral)			
Embryonal, NOS	23 (72%)	7 (58%)	16 (80%)
Embryonal, spindled	5 (16%)	2 (17%)	3 (15%)
Alveolar	2 (6%)	1 (8%)	1 (5%)
Pleomorphic	2 (6%)	2 (17%)	0
Secondary testicular involvement (n=32)			
Yes	11 (34%)	5 (42%)	6 (30%)
No	21 (66%)	7 (58%)	14 (70%)
Lymphovascular invasion (n=32)			
Yes	13 (41%)	6 (50%)	7 (35%)
No	19 (59%)	6 (50%)	13 (65%)

Conclusions: PT RMS occurs in young patients except for the pleomorphic type. It usually presents as a large mass(>5cm) at stage pT2b. The embryonal NOS category is the most common. Despite frequent lymphovascular invasion, testicular involvement and metastases, modern therapy allows survival of most patients. We found no differences between adult and pediatric cases with regard to patient demographics, pathologic characteristics, or tumor behavior.

1011 An Expanded Immunohistochemal Profile of Osteoclast-Rich Undifferentiated Carcinoma of the Urinary Tract

Salvatore Priore, Lauren E Schwartz, Jonathan I Epstein. University of Pennsylvania, Philadelphia, PA; Johns Hopkins University, Baltimore, MD.

Background: Osteoclast-rich undifferentiated carcinoma of the urinary tract (ORUCUT) is a rare tumor composed of ovoid or spindle shaped mononuclear cells with intermixed or focally clustered osteoclast-like giant cells. Due to its rarity the histogenesis of these tumors remains unclear. Previous immunohistochemical profiling (IHC) with antibodies to various keratins has suggested that the mononuclear cells in these tumors are of epithelial origin. Further, the near perfect association of these tumors with *in situ* or high-grade papillary urothelial carcinoma suggests a urothelial origin for these tumors. However, to our knowledge, no study to date has investigated the staining of these tumors for more specific urothelial markers – GATA3, uroplakin II and thrombomodulin.

Design: Historical records, including consultation cases, at two tertiary care hospitals were searched. 21 cases of ORUCUT were identified and reviewed (both H&E and available IHC). For cases in which IHC was not available, a single block from each case, which contained both mononuclear cells and osteoclast-like giant cells, was selected for immunohistochemistry.

Results: The average age at diagnosis was 73 years (range 55-85) with a male to female ratio of 7:1. The mononuclear cell population was positive(as defined by >5% positive cells) for GATA 3 in 95% (20/21) of cases. The majority (70%) of positive cases showed >50% of the mononuclear cells to be positive. Thrombomodulin staining was seen in 90% (19/21) of cases. In contrast to GATA3 staining, thrombomodulin staining tended to be patchy with the majority of cases showing positivity in 5-25% of mononuclear cells. Several cases (37%) showed more diffuse staining. The case which was negative for GATA3 showed patchy clusters of positive cells for thrombomodulin (>50% of total mononuclear cells). Three cases (3/21) were focally positive for AE1/3 in the area of the tumor closest to in situ urothelial carcinoma. No (0/21) cases stained positive for uroplakin. The osteoclast-like giant cells in all cases were negative for all four immunostains.

Conclusions: The finding in our study that the strong majority of the mononuclear cells in these tumors stain positive for GATA3 (95%) and thrombomodulin (85%) further supports a urothelial origin of these tumors. Further the lack of staining for all four markers in the osteoclast- like giant cells is consistent with prior reports that they are histiocytic in nature.

1012 Acquired Cystic Disease-Associated Renal Cell Carcinoma (ACD-RCC): A Multi-Institutional Study with Clinical Follow Up

Christopher Przybycin, Roni Cox, Angela Wu, Ankur Sangoi, Jesse K McKenney. Cleveland Clinic, Cleveland, OH; University of Arkansas for Medical Sciences, Little Rock, AR; El Camino Hospital, Mountain View, CA; University of Michigan Health System, Ann Arbor, MI.

Background: ACD-RCC, the most common kidney tumor in patients with end-stage renal disease (ESRD) and acquired cystic disease, was included as a distinct entity in the 2016 WHO classification of genitourinary tumors. Our aim was to describe the morphologic spectrum of these tumors in a series of cases with long term follow up.

Design: Nephrectomies containing the phrase "acquired cystic" diagnosed from 1980-2016 were retrieved from the pathology archives of contributing institutions, yielding 21 cases of ACD-RCC. Slides were reviewed and follow up obtained from the medical record and social security death index.
Results: Patients were 17 men and 4 women (mean age 52 years), all of whom had been dialyzed for ESRD. Mean length of dialysis before nephrectomy was 4.6 years. Primary kidney disease causing ESRD was known in 20 cases and included hypertension (10 cases), diabetes (3), focal segmental glomerulosclerosis (2), lupus or other glomerulonephritides (2), polycystic kidney disease (2), and HIV nephropathy (1). Mean tumor size was 2.0 cm; all tumors were ISUP grade 3, and 20/21 (95%) were stage pT1. No cases had rhabdoid/sarcomatoid features or necrosis. Multiple ACD-RCCs were seen in 7/21 (33%) patients, and 9/21 (43%) contained other RCC subtypes in the same and/or opposite kidney. While all cases had at least a focal sieve-like pattern, morphologic features varied widely, as summarized in Tables 1 and 2 below. Follow up was available in 18/21 (86%) patients, none of whom had metastases or died of disease (median 18 months, range 2-96 months).

Eosinophilic cytoplasm	Cytoplasmic clearing	Hemosiderin	Histiocytes	Psammoma bodies	Oxalate	Atypical cysts
21/21 (100%)	15/21 (71%)	18/21 (86%)	10/21 (48%)	10/21 (48%)	16/21 (76%)	11/21 (52%)

Sieve-like	Solid	Papillary	Cystic	Tubular
21/21 (100%)	5/21 (24%)	15/21 (71%)	20/21 (95%)	11/21 (52%)

Conclusions: Our study underscores the typically indolent prognosis of most ACD-RCCs that has been published so far and highlights their varied intratumoral morphology that can lead to diagnostic confusion.

1013 Sarcomatoid Carcinoma Associated with Small Cell Carcinoma of the Urinary Bladder

Yuly Ramirez, Jonathan I Epstein. Johns Hopkins Hospital, Baltimore, MD.
Background: Although it is recognized that small cell carcinoma (SCC) can be a component of sarcomatoid carcinoma of the urinary bladder, a systematic study of this association has not been performed.
Design: From 2001 to 2016, we identified 39 patients with sarcomatoid carcinoma of the bladder and coexisting SCC. In 28 cases to date, we were able to retrieve slides from outside institutions with clinical data on 22 patients.
Results: The average age at diagnosis was 72 years (51-89y) with 68% men.

SCC, UC	13 (46.4%)
SCC, sarcoma, UC, adenocarcinoma	7 (25%)
SCC, sarcoma	3 (10.7%)
SCC, sarcoma, UC, squamous cell carcinoma	2 (7.1%)
SCC, sarcoma, adenocarcinoma	1 (3.5%)
SCC, sarcoma, adenocarcinoma, squamous cell carcinoma	1 (3.5%)
SCC, sarcoma, UC, adenocarcinoma, squamous cell carcinoma	1 (3.5%)

In 26 cases (92.8%), the sarcoma component had nonspecific malignant spindle cells, 4 cases (14%) chondrosarcoma, 2 cases (7%) myxoid sarcoma, 1 case (3.5%) osteosarcoma, and 1 case (3.5%) rhabdomyosarcoma.The predominant component in 11 cases (39%) was SCC, in 6 cases urothelial carcinioma (UC) (21%), 3 cases (10%) sarcoma and 8 cases (29%) showed equal amounts of sarcoma and SCC. There were 3 morphological groups: group 1 [18/28 (64%)] showed a gradual transition from SCC to the other components; group 2 [5/28 (18%) had an abrupt transition from SCC to the other components; and in group 3 [5/28 (18%)], the SCC was separate from the other components. In Group 1, 12 (66%) cases SCC showed a gradual transition to sarcoma, 3 (17%) to UC, and 3 (17%) to several of the following components including squamous cell carcinoma, UC, and sarcoma. Mortality was not different between the three groups: 7/18 (39%) in Group 1; 2/5 (40%) in Group 2, and 2/5 (40%) in the Group 3. The average time between diagnosis and death was 9 months for all groups.
Conclusions: SCC is not a rare component of sarcomatoid carcinoma of the bladder. The multitude of different components in these tumors is further evidence of the remarkable ability of UC in the bladder to show divergent differentiation. Morphologically, a unique feature was the gradual transition between SCC and other elements including sarcoma. In future studies, a molecular comparison between the various elements in these cases will be performed. Despite the presence of a SCC component, the prognosis does not seem worse than usual sarcomatoid carcinoma of the bladder. Greater recognition of this entity with chemotherapy targeted to the various histological elements may impact prognosis.

1014 3D Light-Sheet Microscopy Improves the Accuracy of Grading Prostate Cancer by Distinguishing Pattern 3 Glands from Poorly Formed Pattern 4 Glands

Nicholas P Reder, Adam K Glaser, Erin McCarty, Ye Chen, Jonathan TC Liu, Lawrence True. University of Washington Medical Center, Seattle, WA; University of Washington, Seattle, WA.
Background: Patients with low grade prostate cancer are offered active surveillance while patients with a higher grade cancer are candidates for intent-to-cure therapy, i.e. radical prostatectomy or radiation therapy. However, there is variability among pathologists in differentiating Gleason score 6 from Gleason score 7 carcinoma. This variability is most frequent in distinguishing the poorly formed gland variant of Gleason pattern 4 from tangential sections of Gleason pattern 3 glands (PMID: 21679996). We hypothesized that visualizing cancers in 3D would aid pathologists in making this distinction.
Design: Ex vivo core needle biopsies (n=4) taken from radical prostatectomies were clarified and stained with nuclear (DRAQ5) and cytoplasmic (eosin) fluorescent stains. Slide-free non-destructive imaging of the biopsies was performed using a custom-built light-sheet microscope (LSM). The images were reconstructed and false-colored to simulate H&E-staining. Regions of interest (ROI, n=9) highlighting areas of benign prostate glands, Gleason pattern 3, and Gleason pattern 4 were selected for further examination in 3D. MatLab and ImageJ were used for image processing, and Imaris for 3D visualization.
Results: Needle biopsies were imaged comprehensively in 3D within 3 minutes. Approximately 400 optical sections, spaced 1 micron apart in the z-axis, were examined for each core. Benign prostate glands coalesced to form larger glands and ducts throughout the z-stack. Regions of interest with the poorly formed gland variant of Gleason pattern 4 were proven to be tangential sections of Gleason pattern 3 cancer glands by scrolling through 1 micron optical sections in the z-axis. Gleason pattern 3 glands form continuous, highly convoluted tubules rather than separated, individual glands.
Conclusions: This is the most complete examination of prostate core needle biopsies to-date. Examination of prostate cancer 3D histoarchitecture yields more precise grading than conventional grading of 2D sections. Most importantly, tangentially sectioned Gleason pattern 3 glands can be distinguished from the poorly formed gland variant of Gleason pattern 4. This finding raises the question of whether poorly formed pattern 4 glands are a sectioning artifact of pattern 3 glands or a discrete morphologic entity. Further studies are needed to fully characterize all grades of prostate cancer and to discover novel 3D morphologies.

1015 Comprehensive Genomic Profiling of Small Cell Neuroendocrine Carcinoma of the Urinary Bladder

Aseeb Rehman, Julia A Elvin, Jo-Anne Vergilio, James Suh, Shakti H Ramkissoon, Siraj M Ali, Alexa Schrock, Sumanta Pal, Hugh A Fisher, Badar Mian, Tipu Nazeer, David Fabrizio, Garrett Frampton, Vincent Miller, Philip Stephens, Laurie M Gay, Jeffrey Ross. Albany Med Col, Albany, NY; Foundation Med, Boston, MA; City of Hope, Duarte, CA.
Background: Small cell neuroendocrine carcinoma of the bladder (SCCB) is a rare, but aggressive form of genitourinary cancer that can arise de novo or in conjunction with a high grade urothelial carcinoma (UCB).
Design: DNA was extracted from 40 µ of FFPE tissues from 29 cases of relapsed and metastatic SCCB and 1,113 UCB. Comprehensive genomic profiling (CGP) was performed using a hybrid-capture, adaptor ligation based next generation sequencing assay to a mean coverage depth of >503X. Tumor mutational burden (TMB) was calculated from a minimum of 1.11 Mb of sequenced DNA as and reported as mutations/Mb. The results were analyzed for all classes of genomic alterations (GA), including base substitutions, insertions and deletions (short variants; SV), fusions, and copy number changes including amplifications (amp) and homozygous deletions.
Results: The diagnosis of all 29 (100%) SCCB cases was confirmed on routine histology and featured positive IHC staining for either chromogranin, synaptophysin or both. The 29 SCCB patients had a mean age of 68.1 years (range 49-90 years), and 25 (86%) were male. All (100%) of the SCCB cases were considered to be high grade tumors. At the time of CGP, 3 (10%) SCCB were Stage III, and 26 (90%) were stage IV. The primary SCCB was used for sequencing in 14 (48%) of cases, and a metastasis sample was used in 15 (52%). The 29 SCCB featured 2.86 GA/case.

GA	UCB (1,113 cases)	SCCB (29 Cases)	Significance
TP53	56%	90%	P=0.0002
RB1	20%	83%	P<0.0001
TERT	66%	62%	NS
FGFR3	19%	0%	P=0.006
ERBB2	15%	3%	NS
TMB> 10/>20	31%/9%	28%/7%	NS

The genomics of SCCB differed significantly from UCB with 26 (90%) of SCCB featuring *TP53* GA and 24 (83%) with *RB1* GA (Table). The most frequent clinically relevant GA in SCCB were *RICTOR* amp (21%) and *PIK3CA* (10%), *BRCA1*, *HGF*, *FBXW7* and *CCND2* SV (7% each). The relatively high TMB in SCCB (7% TMB > 20 mut/Mb and 28% TMB > 10 mut/Mb) is similar to that seen in UCB. No SCCB cases were MSI-high. *ERBB2* and *FGFR1* GA frequencies (both 3%) in SCCB were lower than in similarly studied UCB.
Conclusions: Although SCCB shares likely origin in urothelium, it differs in genomic landscape from UCB in having higher frequencies of *TP53* and *RB1* GA and lower frequencies of *FGFR3* and *ERBB2* GA. However, like UCB, SCCB shares the presence of multiple GA associated with potential responses to targeted therapies and high TMB associated with response to immune checkpoint inhibitor therapy.

1016 Influence of Chronic Inflammation on Bcl2 and PCNA Expression in Prostate Needle Biopsy Specimens

Qinghu Ren, Michael Glover, Shardul Soni, Gregory T MacLennan, Sanjay Gupta. University Hospitals Cleveland Medical Center, Cleveland, OH; Case Western Reserve University, Cleveland, OH.
Background: The relationship between inflammation and cancer has been established in some forms of human malignancies; however, its role in prostate cancer remains unclear. The purpose of this study was to investigate a possible association between chronic inflammation and the development of epithelial neoplasia in the prostate.
Design: Needle biopsy specimens were obtained from patients with serum PSA levels >4 ng/ml, evaluated for morphologic findings, immunostained for Bcl2 and proliferation cell nuclear antigen (PCNA). Bcl2 is a survival protein that appears to lie at a nodal point

in pathways involved in cell survival, carcinogenesis, and development of therapeutic resistance in certain cancers. Similarly, PCNA is a critical protein for DNA replication, repair of DNA damage, chromatin structure maintenance, chromosome segregation and cell-cycle progression. We examined the relationship between these two proteins in prostate tissues with and without chronic inflammation, as well as tissues with and without evidence of neoplastic changes.

Results: Of the 106 needle biopsies examined, 18% shows atrophy with inflammation. Proliferative inflammatory atrophy (PIA)/ post atrophic hyperplasia (PAH) were observed in 42%, high-grade prostatic intraepithelial neoplasia (PIN) in 8%, prostatic adenocarcinoma in 11%, and 2% had atypical acinar proliferation suspicious for malignancy. Thirty six specimens were stained for Bcl2 and PCNA. Bcl2 was expressed widely in both inflammatory (38%) and epithelial tissue (77%), however more intense expression was observed in the areas of chronic inflammation, predominantly in infiltrating immune cells. The highest proliferation index was observed in the epithelium of high-grade PIN (8.1%) and cancer (17.6%). An inverse correlation in the expression of Bcl2 and PCNA was observed in the epithelium.

A strong positive association between inflammation and Bcl2 expression was observed ($r = 0.88$) suggesting that cell survival increases with the increasing inflammation. We observe a negative association ($r = -0.197$) between inflammation and proliferation, suggesting that prolonged inflammation facilitates the initiation of normal prostate epithelial cells through increased survival which gains independence to proliferate and progress to malignancy.

Conclusions: The results suggest that Bcl2 alters the phenotype of these particular epithelial cells and gain them neoplastic characteristics, leading to a likely precursor that may later develop into PIN and cancer.

1017 Novel Histological Finding: Adipose Tissue Is Prevalent within Penile Tunica Albuginea and Corpora Cavernosa. An Anatomical Study of 63 Specimens and Considerations for Cancer Invasion

Ingrid M Rodriguez, Martin Cuevas, Arturo Silvero, Sofia Cañete-Portillo, Diego F Sanchez, Jose Barreto, Antonio Cubilla. Instituto de Patología e Investigación, Asunción, Paraguay; Facultad de Ciencias Médicas - Universidad Nacional de Asunción, Asunción, Paraguay; Instituto de Previsión Social, Asunción, Paraguay.

Background: Adipose tissue, along with arteries, veins and peripheral nerves are normal constituents of mesenchymal tissues encasing corpora cavernosa at the level of penile shaft, variously designated as penile fascia or Bucks fascia. To our knowledge the presence of fat has not been previously reported within the corpora cavernosa.

Design: One or 2 transversal histological sections at the level of the surgical margin at the shaft of 63 consecutive partial penectomy specimens for squamous cell carcinoma were evaluated.

Results: From outer to inner tissues 3 anatomical levels were identified: 1**. Outer fascia** composed of a loose fibrovascular mesenchyme containing some nerve branches. Adipose tissue was present in the majority of the cases. 2. The **Tunica Albuginea**, a thick and dense fibroelastic band of tissue separating the outer fascia from erectile tissues of corpora cavernosa. Adipose tissue within the albuginea was present in 21 specimens (19%). 3. Erectile tissues of **Corpora cavernosa:** besides the typical erectile tissues, adipose tissue was present in 33 cases (52%). The fatty tissue was focal or multifocal and scant and peripherally located at the junction of the tunica albuginea with the corpora. In some cases, it was associated with small amounts of fibrous tissue, small vessels and nerves.

Conclusions: It is possible that adipose tissue, along with small nutritional vessels and nerves perforates from the fascia through the Tunica Albuginea to reach the corpora. In previous examination of the local routes of cancer spread we found this pathway to be one of the mechanisms of cancer invading penile corpora from penile fascia.

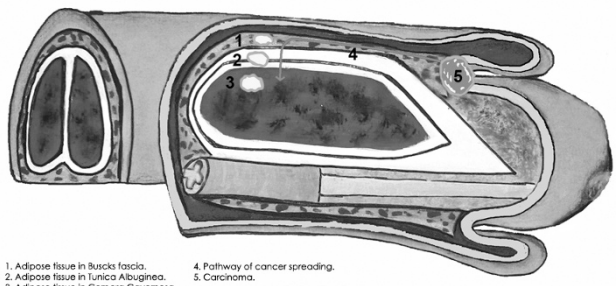

1018 *Tert* Promoter Mutation Status in PUNLMP of the Urinary Bladder

Maria Del Carmen Rodriguez Pena, Aline C Tregnago, Marie-Lisa Eich, Simeon Springer, Yuxuan Wang, Diana Taheri, Dilek Ertoy, Kazutoshi Fujita, Stephania M Bezerra, Isabela W Cunha, Trinity J Bivalacqua, Nickolas Papadopoulos, Ken Kinzler, Bert Vogelstein, George J Netto. Johns Hopkins University, Baltimore, MD; Hacettepe University, Ankara, Turkey; Osaka University, Osaka, Japan; AC Camargo Cancer Center, Sao Paulo, Brazil.

Background: Our group and others have previously demonstrated the presence of *TERT* promoter mutations (*TERT-mut*) in 60-80% of urothelial carcinomas and some of their histologic variants. These mutations have been found in both non-invasive and invasive urothelial tumors and have been detected in corresponding urine specimens, making them attractive candidates for early detection and surveillance. In the current study, we sought to determine the rate of *TERT-mut* in *de novo* papillary urothelial neoplasms of low malignant potential (PUNLMP) of the urinary bladder.

Design: The surgical pathology database at The Johns Hopkins Hospital was searched for all in-house bladder neoplasms diagnosed as PUNLMP between 1998 and 2013. 127 cases were identified. After reviewing the electronic medical records, 30 *de novo* PUNLMP cases were found and included in the study. All histologic slides were reviewed to confirm the diagnosis and select a representative tumor section for mutational analysis. The tumor areas were cored with a sterile 16-gauge needle. After DNA purification, samples were analyzed with Safe-SeqS, a sequencing error reduction technology which better discriminates genuine *TERT-mut* from artefactual sequencing variants introduced during the sequencing process. PCR products were purified with AMPure and sequenced on a MiSeq instrument. Findings were correlated with recurrence and progression of disease.

Results: We found *TERT*-mut in 4/5 (90%) of cases with completed mutational analysis. Sequencing data on the remaining 25 PUNLMP cases is being finalized. Three of the 4 *TERT-mut* positive tumors had a "g.1295228C>T" alteration with the remaining tumor demonstrating "g.1295250C>T".

Recurrence was encountered in three of 5 cases. Two of them demonstrated grade progression to non-invasive papillary low grade urothelial carcinoma (LGTCC), with the third case recurring as PUNLMP. All three tumors with recurrence, including those which progressed, were *TER-mut* positive.

Conclusions: Similar to our previously demonstrated high rate of *TERT-mut* in CIS and low and high grade non-invasive papillary urothelial carcinomas, a high proportion of primary *de novo* PUNLMP appear to harbor *TERT-mut*. The findings could support the proposed utility of *TERT-mut* assesment in urine samples as a biomarker for early detection of bladder neoplasms.

1019 Immunohistochemical Assessment of Basal and Luminal Markers in Non-Muscle Invasive Urothelial Carcinoma of Bladder (NMIBC)

Maria Del Carmen Rodriguez Pena, Aline C Tregnago, Alcides Chaux, Diana Taheri, Walaa Borhan, Marie-Lisa Eich, Hirofumi Nonogaki, Rajni Sharma, M Katayoon Rezaei, George J Netto. Johns Hopkins University, Baltimore, MD; Universidad del Norte, Asuncion, Paraguay; George Washington University, Washington, DC.

Background: The Cancer Genome Atlas (TCGA) collaboration has identified two intrinsic subtypes (basal and luminal) in urothelial bladder carcinoma. However, the study was limited to muscle invasive bladder cancer (MIBC). Subsequent studies suggested a limited panel of immunohistochemical markers could be used to assign basal vs luminal phenotype in MIBC with potential prognostic role. In this study we assess the applicability of the proposed phenotype classification in non-muscle invasive bladder cancer (NMIBC).

Design: Three TMAs were constructed from 165 TURB specimens of 52 bladder cancer patients treated at one of author's institution (1998-2008). Follow up data on recurrence, grade or stage progression were obtained. Immunohistochemistry was performed using automated Ventana System for markers indicative of luminal (GATA3, CK20, ER, uroplakin, HER2/neu) and basal phenotype (CK5/6 and CD44). The extent, intensity and pattern of expression were evaluated for all markers by 3 urologic pathologists. HER2/neu was assessed using the breast and stomach scoring systems.

Results: By univariate analysis, using mean extent of expression as a cut off, higher proportion (83%; p=0.002) of tumors with stage progression demonstrated high CK5/6 expression. 15/143 (10.4%) of tumors with high CK5/6 expression demonstrated a higher stage on subsequent biopsy compared to 3/176 (1.7%) of those with low CK5/6. Higher proportion of tumors with stage progression had low levels of CK20 (75%;p=0.03) and CD44 (66%;p=0.009).

Regarding recurrence, higher proportion of tumors with recurrence had low expression levels of CK5/6 (64%), CD44 (53%) and ER (91%) and high HER2/neu expression (53%) ($p \leq 0.002$). There was no association between the rate of expression of any of the markers and grade progression upon recurrence.

Conclusions: Our findings suggest that both high CK5/6 and low CK20 expression are associated with higher likelihood of stage progression in NMIBC. Further analysis of potential role of basal and luminal markers, individually or in combination, in the prognostication of NMIBC in the context of known clinicopathologic parameters is needed.

1020 Programmed Death-Ligand 1 Expression Correlates with No Downstaging After Platinum Therapy in Muscle-Invasive Bladder Cancer

Shira Ronen, Christopher Hartley, Kenneth Iczkowski. Medical College of Wisconsin, Milwaukee, WI.

Background: Platinum (Pt)-based neoadjuvant chemotherapy (NAC) is the standard of care for muscle-invasive bladder cancer (MIBC). However, at least half of patients do not respond to NAC. Non-responders are subject to the adverse effects of Pt, with delay in definitive treatment. Programmed death-ligand 1 (PD-L1) plays a major role in immune evasion of tumor cells. Whether expression of PD-L1 may influence Pt sensitivity in MIBC has not been previously studied.

Design: We identified matched paraffin-embedded tissue from pre-NAC transurethral resection of bladder tumor (TURBT) and post-NAC radical cystectomy specimens in 47 patients with MIBC who received Pt-based NAC. Tumor and adjacent normal tissues (≥3 cores each on tissue microarray) were stained with PD-L1 clone E1L3N (1:200, Cell Signaling). PD-L1 expression was determined through immunohistochemistry by two pathologists blinded to the outcome (0 = undetectable; 1+ = barely detectable; 2+ = moderate; and 3+ = intense staining). Pathologic response was defined as either down-staging to non-MIBC (≤ pT1N0M0) or complete pathologic response (pT0).

Pathologic outcome was compared between PD-L1 expression groups. Univariate logistic regression was performed to correlate PD-L1 staining in TURBT and cystectomy tumor cells with the presence of T2 or higher cancer at cystectomy.

Results: PD-L1 positivity in the tumor of cystectomy specimens significantly correlated with lack of downstaging of T2 cancer after Pt (p=0.02; OR=12; CI: 1.35-106.1). The lack of a trend with TURBT specimens was attributed to sampling limitation. No other significant correlations were noted inlcuding PD-L1 expression in the inflammatory cells, age, or race.

	Cystectomy Stage		Univariate Analysis		
Clinicopathologic Feature	Tis and T1	T2 or higher	P value	Odds Ratio	95% CI
Resection Tumor Cells PD-L1 (+)	1/14 (7%)	12/25 (48%)	0.02	12	1.4-106.1
TURBT Tumor Cells PD-L1 (+)	7/11 (64%)	6/22 (27%)	0.051	0.21	0.04-1.01

Small numbers of PD-L1 positive cases precluded multivariate analysis.

Conclusions: This is the first study demonstrating a correlation between tumor PD-L1 expression and pathologic outcome in Pt-treated MIBC. Although PD-L1 examination has been studied in conjunction with of response to PD-L1 inhibitors, our study shows that it may also predict standard chemotherapy response. Thus, PD-L1 expression may be a biomarker for high stage cancer after Pt therapy.

1021 Primary Renal Synovial Sarcomas: Morphological, Immunohistochemical, and Molecular Genetic Findings

Laurel Rose, Liang Cheng, David Grignon, Rong Fan, Shaoxiong Chen. Indiana University, Indianapolis, IN.

Background: Synovial sarcoma is a high-grade spindle cell sarcoma of uncertain line of differentiation that rarely involves the kidney. Use of immunohistochemical stains is helpful in making the diagnosis and molecular testing for the chromosomal translocation t(X;18)(p11.2;q11.2) has been shown to be specific for this entity. Prompted by a case of renal synovial sarcoma with supporting immunohistochemical stains and trisomy 18 detected by FISH we set out to investigate the morphological, immunohistochemical, and molecular genetic findings in primary renal synovial sarcoma.

Design: Nine cases of primary renal synovial sarcoma were identified by searching the pathology database at Indiana University Health from January 2000 to April 2016. Immunohistochemical stains including TLE1, BCL-2, EMA, AE1/AE3, S100, and PAX8, as well as molecular testing using break-apart FISH probes for the *SS18 (SYT)* gene were performed on all cases.

Results: The nine cases included five males and four females ranging in age from 15 to 55 years (mean, 36.2 y). These cases included 7 monophasic synovial sarcomas, 1 biphasic synovial sarcoma, and 1 poorly differentiated synovial sarcoma. In addition, microscopic features included very high mitotic count, hemangiopericytomatous vascular pattern, and calcifications. All 9 cases were positive for TLE1 and BCL-2 (100%). Three cases showed positivity for EMA (33%). Three cases showed positivity for AE1/AE3 (33%). One case showed positivity for S100 (11%). Two cases showed tumor cell positivity with PAX8 (22%), one with strong and diffuse staining and the other with focal staining. FISH testing identified an *SS18* gene rearrangement in 7 cases (78%). One case showed both *SS18* gene rearrangement and polysomy 18. One showed only trisomy 18.

Conclusions: Primary synovial sarcomas of the kidney are rare and the diagnosis can be rendered by histological examination with supporting immunohistochemical stains. In this study, 100% of synovial sarcomas stain positively with both TLE1 and BCL-2. A smaller percentage of cases show positivity with EMA and AE1/AE3. Interestingly, two cases are positive for PAX8. The *SS18 (SYT)* gene rearragement is present in most cases and useful for confirming the diagnosis. However, a negative test does not rule out the diagnosis. While not as common, other chromosomal alterations, such as polysomy 18, may support the diagnosis.

1022 Characterization of Driver Mutations in Hybrid Renal Oncocytic Tumors

Roberto Ruiz-Cordero, Priya Rao, Pheroze Tamboli, Rajesh Singh, Mark J Routbort, Kanishka Sircar. MD Anderson Cancer Center, Houston, TX.

Background: Hybrid oncocytic tumors (HOT) of the kidney represent a poorly understood clinicopathologic entity with histologic features that overlap with various subtypes of renal cell carcinoma (RCC), including benign (oncocytoma) and malignant (chromophobe RCC; SDHB RCC) renal tumors. Since the characterization of HOT and their separation from the foregoing entities are clinically important, we performed next generation sequencing of HOT to look for significant gene mutations that may improve our molecular understanding of these hybrid tumors.

Design: DNA was extracted from mapped frozen HOT and normal kidney controls, after review by three genitourinary pathologists. Targeted gene sequencing of the entire coding regions of 261 cancer related genes was performed using Illumina (San Diego, CA) compatible indexed libraries prepared using the KAPA library preparation kit. Libraries were multiplexed, 20 libraries per pool for capture, and combined post capture for sequencing in one HiSeq3000 lane using 100 base pair, paired end sequencing with a high depth of coverage per sample (read depth > 400X).

Results: High-quality DNA with a median concentration of 62.4ng/ul (16.6-131.2) was sequenced from 13 paired tumor-normal HOT samples belonging to 11 patients (age: 64 years, median (28-82); male (83%)). The median tumor size was 4.2 cm (1.5-8.5 cm) and tumor purity was at least 60% in all cases. All patients are alive and have not developed metastases. Mutations in cancer related genes were detected in 4 of 13 cases (30%), including *SMARC4* (1)*, AXIN1*(1)*, COL2A1*(1)*,* and *ATM*(1). However, mitochondrial DNA mutations were found in 9 of 13 cases (70%) involving the following genes: *MT-ND1*(4), *MT-ND2*(1)*, MT-ND4*(2)*, MT-ND5*(3)*, MT-CO3*(1), and *MT-CYB*(1). Three cases with predominant chromophobe RCC morphology (> 90%) did not show any mutations. Interestingly, oncocytoma rich areas showed different mutations than chromophobe rich areas in two tumors belonging to one patient: a *COL2A1* mutation was observed in the oncocytoma area and no mutations were present in the chromophobe RCC area.

Conclusions: Hybrid oncocytic tumors of the kidney show male predominance and a significant number of mitochondrial DNA mutations in genes responsible for respiratory defects, similar to those found by the TCGA group on oncocytomas and chromophobe RCCs. Our mutational analysis further suggests that mitochondrial mutations could be driver events in these types of tumors.

1023 Acquired Cystic Disease-Associated Renal Cell Carcinoma: A Whole Exome Sequencing Pilot Study

Faisal Saeed, Francesca Khani, Weihua Huang, Changhong Yin, Brian Robinson, John T Fallon, Minghao Zhong. New York Medical College at Westchester Medical Center, Valhalla, NY; Weill Cornell Medical College, New York, NY.

Background: Acquired cystic disease-associated renal cell carcinoma (ACD-RCC) has been recognized as a distinct entity by the World Health Organization (WHO). This tumor has unique clinical and morphological features. In contrast to other common types of RCC, such as clear cell renal cell carcinoma (CCRCC) and papillary renal cell carcinoma (PRCC), genetic alterations in ACD-RCC have not been well established. The purpose of this study was to comprehensively evaluate the molecular features of ACD-RCC by next generation sequencing in a pilot study.

Design: Three cases of ACD-RCC from our institutions were identified and reviewed by genitourinary pathologists. The diagnosis was primarily based on morphological features in accordance with the histopathologic features described in the WHO. Macrodissection was used in some cases to ensure that at least 20% of the cells were neoplastic. Genomic DNA was extracted from formalin-fixed paraffin-embedded (FFPE) tissues by Qiagen AllPrep DNA/RNA Kit. The isolated genomic DNA was subject to targeted sequencing by using Illumina Exome Enrichment & Sequencing Kits. We used Illumina MiSeq system for paired-end (151 bp × 2) sequencing and Illumina on-instrument MiSeq Reporter to generate the variant call format (VCF) files through BWA alignment/mapping and somatic variant caller. By using Illumina VariantStudio, we performed variant filtering, annotation and interpretation with various sources of variant databases. We focused on variants in most frequently mutated genes associated with clear cell RCC and papillary RCC.

Results: The whole exome sequencing (WES) generated data had a mean coverage > 50× and 20,000-30,000 single nucleotide variants (SNV) for each of the three cases. The most common mutations associated with CCRCC and PRCC were not found in these cases. However, mutations *COL6A6* and *MAGEC1*, which are seen in less than 5% of CCRCC, were found in two cases of ACD-RCC. Additionally, *EMR3, ATF7IP2,* and *FBN2* mutations which were less frequently associated with CCRCC, were also found in a single ACD-RCC case.

Conclusions: This study is the first reported comprehensive molecular evaluation for ACD-RCC. The data demonstrated that ACD-RCC had distinct features from those of CCRCC or PRCC. Interestingly, the recurrent mutations identified in two of these ACD-RCC cases, *COL6A6* and *MAGEC1*, are seen infrequently in CCRCC. Sequencing of additional cases is underway.

1024 Papillary Renal Cell Carcinoma Histological, Immunophenotypical and Molecular Characterization; New Classification System

Rola Saleeb, Fadi Brimo, Fabio Rotondo, Mina Farag, Pamela Plant, George M Yousef. St. Michael's Hospital, Li Ka Shing Knowledge Institute, Toronto, ON, Canada; University of Toronto, Toronto, ON, Canada; McGill University Health Center, Montreal, QC, Canada.

Background: Papillary Renal Cell Carcinoma (PRCC) has two histological subtypes. A number of PRCC cases (~ 50%), fail to meet all morphological criteria for either type, hence are best characterized as PRCC not otherwise specified (NOS). There are yet no reliable markers to resolve the PRCC NOS category. That in turn reflects the clinical dilemma of how to manage these patients.

Design: PRCC patient cohort of 115 cases was selected for the study. Cases were subtyped histologically into PRCC types 1, 2 and NOS. Potentially distinguishing markers ABCC2, CA9, GATA3, SAll4, and BCL2 selected from our previous genomic analysis, were assessed by immunohistochemistry (IHC). A total of 24 cases were further selected for molecular analysis using miRNA expression and copy number variation (CNV). Univariate and multivariate survival analysis were performed using Log rank test and cox proportionate hazards.

Results: ABCC2, CA9 and GATA3 exhibited distinct staining patterns between the two classic PRCC subtypes; and classified many of the PRCC NOS (45%) cases. Moreover, immunomarkers revealed a third distinct subtype of PRCC (35% of the PRCC cohort). Molecular testing using miRNA expression and CNV analysis confirmed the presence of three distinct molecular signatures corresponding to the 3 subtypes. On univariate analysis DFS was significantly enhanced in the type1 versus 2& 3 (p value 0.047). PRCC subtyping retained significance on multivariate analysis (p value 0.025, HR:6, 95% CI 1.25 to 32.2).

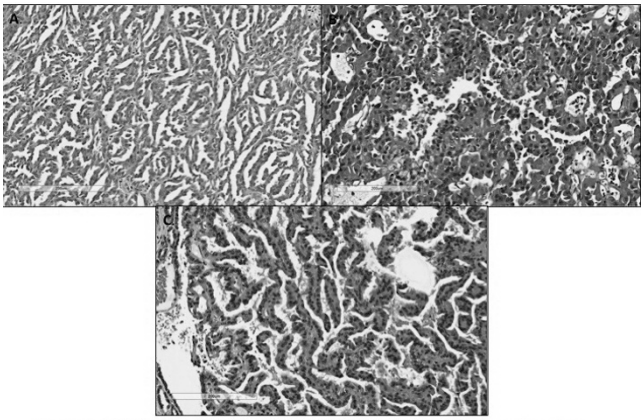

Figure: A. PRCC type 1, B. PRCC type 2, C.PRCC type 3. (PRCC subtypes confirmed as distinct entities on molecular analysis

Conclusions: We propose a new classification system of PRCC integrating morphological, immunophenotypical, and molecular analysis. Our classification reveals a 3rd PRCC subtype that was not previously described. This subtype has overlapping morphology of with PRCC types 1 and 2, hence would be subtyped as PRCC NOS in the current classification. Molecularly PRCC3 has a distinct signature and clinically it behaves similar to PRCC type 2. The new classification stratifies PRCC patients into clinically relevant subgroups and has significant future implications on their management.

1025 Comparison of Targeted and Non-Targeted RNA-seq for Translocation RCC in FFPE Tissue

Christian Salib, Weihua Huang, Konstantin Volyanskyy, Liying Han, Larisa Debelenko, Nevenka Dimitrova, John T Fallon, Minghao Zhong. Westchester Medical Center/ New York Medical College, Valhalla, NY; Philips Research North America, Briarcliff Manor, NY.

Background: *TFE3*, *TFEB* and *ALK* translocations have been associated with renal cell carcinoma (RCC). Traditional molecular and genetic methods could be used to detect the translocation with certain limitations. Next generation sequencing has recently been employed for detecting translocation. Here, we aim to compare targeted and non-targeted RNA-seq for detecting translocations in translocation RCC FFPE tissue.

Design: RCC with *TFE3* (4), *TFEB* (1) and *ALK* (1) translocations (all proven by FISH or cytogenetics) were collected for this study. For non-targeted RNA-seq, the total RNA was extracted from FFPE tissue using the AllPrep DNA/RNA FFPE. 100 ng RNA was applied for sequencing library preparation using the TruSeq RNA Access Library Prep Kit as per the manufacturer's protocol. Paired-end sequencing (75 bp×2) was performed using the MiSeq Reagent V3 Kit (150 cycles) and the MiSeq sequencing system. STAR algorithm was employed for detection of any potential fusions. For targeted RNA-seq, we used Archer® FusionPlex® Solid Tumor Kit, which uses an Anchored Multiplex PCR™-based enrichment method and can detect fusions associated with >50 genes.

Results: 1) Both targeted and non-targeted RNA-seq failed to detect *TFEB* translocation. 2) *ALK* translocation was successfully detected by targeted RNA-seq, but not by non-targeted RNA-seq. 3) Both targeted and non-targeted RNA-seq identified 2 out of 4 cases of *TFE3* translocation.

Conclusions: 1) Both targeted and non-targeted RNA-seq can detect gene fusions with some limitation: TFEB translocation partner gene alpha is an intronless gene, which makes this fusion undetectable by RNA based tests. 2) Targeted RNA-seq is more sensitive for the detection of low expression fusion genes, such as ALK translocation. 3) Non-targeted RNA-seq requires more demand for bioinformatics support.

1026 Pathologic Features of Renal Carcinoma Following Anti-PD1 Therapy. A Clinicopathologic Analysis of 12 Cases

Rashmi Samdani, Priya Rao. The University of Texas MD Anderson Cancer Center, Houston, TX.

Background: The advent of immunotherapy and approval of immune checkpoint inhibitors such as anti PD1 antibody nivolumab by FDA in 2015 for treatment of clear cell renal cell carcinoma (CCRCC) has refined treatment paradigm of advanced RCC. Our study highlights the histopathologic features encountered in these postimmunotherapy cases.

Design: We retrieved 12 cases of CCRCC from the electronic files of MD Anderson Cancer Center of patients enrolled in a pre-surgery clinical trial who were randomized upfront to immunotherapy for 3 mos following biopsy confirmation of clear cell histology.

Results: Age at diagnosis ranged 55-79 yrs (mean 63.3). Pretherapy tumor size on imaging ranged 5-20 cm (mean 9.9 cm); post therapy gross size ranged 3.5-19.5cm (mean 9.4cm). Mean follow up period was 6 mos. All patients are alive with metastases (AWD). One tumor showed focal (<5%) sarcomatoid histology. Therapy related changes such as fibrosis, hyalinization, necrosis and dense intra and peri-tumoral lymphocytic infiltrate were observed in all cases. Post therapy response was variable; 4 cases revealed 80% tumor necrosis with no apparent decrease in tumor size on post therapy imaging. Case 2 increased in size on post therapy imaging raising clinical concern for tumor progression, however showed an excellent pathologic response with only 30% of viable tumor.

Case No.	Age	Pre Rx Tumor size (cm)	Post Rx Tumor size (cm)	Pathologic stage	% viable tumor
1	78	7.5	8.5	ypT3aNxM1	60
2	79	8.7	10.2	ypT3aN0Mx	30
3	62	6.2	4.3	ypT3aNxMx	40
4	56	13	11.5	ypT3bN1	70
5	55	12.5	11.8	ypT3Nx	40
6	46	7.5	7.1	ypT3aN0Mx	20
7	61	12.1	13	ypT3aNxM1	80
8	70	7.6	7.6	ypT3aNxMx	60
9	68	11.1	10.5	ypT4N0Mx	20
10	60	8.7	6	ypT1bN0M1	10
11	68	20	19.5	ypT3aN0	5
12	53	5	3.5	ypT3N0	20

Conclusions: - Ours is first study in literature documenting histologic features in post immunotherapy (anti PDL1) treated CCRCC.

-Despite no apparent change in post treatment tumor size on imaging, most tumors showed an excellent response to immunotherapy, underscoring need for thorough histologic examination to assess exact tumor burden.

-One case exhibited "pseudoprogression" where activation of immune cells with a dense peritumoral infiltrate mimicked progression on imaging studies

-Importantly, in metastases where tumor growth might initially outpace the activation of immune cells showing initial progression followed by response, histologic evaluation may be of help.

1027 Regional Metastasis and Outcome in HPV-Related vs Non-HPV-Related Histological Subtypes of Penile Squamous Cell Carcinoma

Diego F Sanchez, Fernando Soares, Gustavo C Guimaraes, Isabela W Cunha, Sofia Cañete-Portillo, Arturo Silvero, Martin Cuevas, Ingrid M Rodriguez, Antonio Cubilla. Instituto de Patología e Investigación, Asunción, Paraguay; Facultad de Ciencias Médicas - Universidad Nacional de Asunción, Asunción, Paraguay; AC Camargo Cancer Center, Sao Paulo, Brazil; Instituto de Previsión Social, Asunción, Paraguay.

Background: Studies indicate that patients with HPV-related carcinomas of the head and neck and vulva have a better prognosis than tumors unrelated to the virus. The WHO classification of penile carcinoma separates histological subtypes of squamous cell carcinoma into HPV- and non-HPV-related. The purpose of this study was to compare prognosis in both groups of penile cancer patients.

Design: Cases were diagnosed and reviewed at the Hospital do Cancer AC Camargo Cancer Center in Sao Paulo Brazil during the period from May 1953 to March 2006. From a group of 375 surgically treated patients with penile cancers 318 were selected by subtype on the base of their known positive or negative relation to HPV. Mixed and unclassified neoplasms were excluded. In the HPV-related group were warty (condylomatous), basaloid and warty-basaloid carcinomas (41 cases). In the non-HPV-related group were usual, verrucous, papillary, pseudohyperplastic, pseudoglandular, sarcomatoid and adenosquamous carcinomas (277 cases). Nodal dissection materials were available in 136 cases. Follow up ranged from 1 to 453 months (Average: 107.9). The rates of inguinal nodal metastases and patients' outcome were compared in HPV-related and non-HPV-related groups of cases. Kruskal-Wallis and Fisher's exact test were used for general statistical analysis. Kaplan-Meier curve with log-rank test was applied to survival analysis.

Results: Incidence of inguinal nodal metastasis was similar in both groups (51% vs. 58%, P = 0.629). Cancer related death was also similar in HPV- and non-HPV-related neoplasms (15% vs. 18%, P = 0.826).

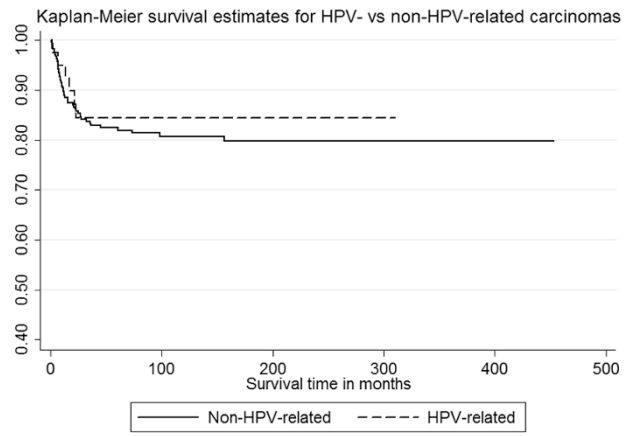

Conclusions: Different to other anatomical sites, we found no prognostic differences in this outcome comparison of HPV-related and non-HPV-related subtypes of penile squamous cell carcinomas.

1028 Comparison of Pathologic and Outcome Features of Classical vs. Mixed (Hybrid) Verrucous Carcinoma (VC) of Penis. A Study of 59 Cases

Diego F Sanchez, Fernando Soares, Isabel Alvarado-Cabrero, Gustavo C Guimaraes, Isabela W Cunha, Diana Piedras, Adriana Rodríguez-Gómez, Sofía Cañete-Portillo, Arturo Silvero, Martin Cuevas, Ingrid M Rodriguez, Antonio Cubilla. Instituto de Patología e Investigación, Asunción, Paraguay; Facultad de Ciencias Médicas - Universidad Nacional de Asunción, Asunción, Paraguay; AC Camargo Cancer Center, Sao Paulo, Brazil; Hospital de Oncología, Centro Médico Nacional Siglo XXI, Instituto Mexicano del Seguro Social, Mexico City, Mexico; Instituto de Previsión Social, Asunción, Paraguay.

Background: Classic verrucous carcinoma (VC) is a rare penile neoplasm which need to be differentiated from the mixed hybrid variant. We found no studies comparing features and outcome of these tumors.

Design: Clinical and pathological materials from the archives of the AC Camargo Cancer Center, Sao Paulo (44 cases) and the Hospital de Oncología, CMN, IMSS, Mexico (15 cases) were evaluated. Partial (42 cases) and total (17 cases) penectomy specimens and nodal dissection materials (23 cases) were available. Kruskal-Wallis and Fisher's exact test were used for statistical analysis.

Results: Patients' age (mean: 60 and 59 year) was similar in classic and hybrid tumors. Pathologically, classic VC had a broadly based delineated limit with the stroma whereas hybrid VC, in addition to the invariable presence of classic features, had an irregular invasive front, undistinguishable from usual squamous cell carcinoma. All Classic VCs were highly differentiated grade I tumors. In hybrid VCs a full spectrum of grades from I (47%), II (40%) to III (13%) were present. Classic VC were significantly thinner than hybrid VCs (5.5 vs 11.6 mm, p = 0.0001). Compromise of corpora cavernosa (CC) was noted in a classic irregular invasive pattern in 40% of hybrid tumors. CC was involved in fewer classical VCs (17%) but it kept the broadly based tumor front. Lymphovascular (0 vs. 13%, P<0.02) and perineural invasion (3% vs. 17%, P = 0.06) were unusual but more common in hybrid tumors. Differentiated PeIN was present in the majority of both tumors. Lichen sclerosus was equally found in classic and hybrid tumors (31 vs 23%, p =0.710). Inguinal metastases were absent in classic VC and present in 2 of 16 patients with hybrid carcinomas. None of the classic VC patients died from disease whereas 1 patient with hybrid VC died from metastatic disease. Another 2 patients with hybrid VC were alive but with metastatic disease at time of last follow up.

Conclusions: A comparison of classic and hybrid VCs disclosed that the latter are tumors with higher grade, thicker, invade deeper into penile anatomical levels and although rarely, had a potential for nodal metastasis, tumor dissemination and patients' death.

1029 Geographic Comparison of Histological Subtypes and Outcome of Surgically Treated Penile Squamous Cell Carcinoma (SCC) Patients from Mexico and Brazil. A Study of 411 Cases

Diego F Sanchez, Fernando Soares, Isabel Alvarado-Cabrero, Gustavo C Guimaraes, Isabela W Cunha, Diana Piedras, Adriana Rodríguez-Gómez, Sofía Cañete-Portillo, Arturo Silvero, Martin Cuevas, Ingrid M Rodriguez, Antonio Cubilla. Instituto de Patología e Investigación, Asunción, Paraguay; Universidad Nacional de Asunción, Asunción, Paraguay; AC Camargo Cancer Center, São Paulo, Brazil; CMN Siglo XXI, IMSS, Mexico City, Mexico.

Background: There is a wide geographic variation in the prevalence of penile SCC comparing northern and southern countries. A hypothetical explanation may be the variation in SCC subtypes related to HPV. This study aim was to compare the prevalence of penile SCC subtypes and patients' outcome in 2 countries from North and South America

Design: 298 cases from Brazil and 113 from Mexico were reviewed. SCC were classified in usual, papillary NOS, verrucous classical, verrucous hybrid, and sarcomatoid (non-HPV-related) and basaloid, warty and warty-basaloid (HPV-related, WHO 2016) All patients had partial or total penectomy. Nodal dissections were available in 226 cases. Follow up ranged from 1–453 in Brazilian, and 10–82 months in Mexican series. Kruskal-Wallis, Fisher's exact test, and Kaplan-Meier curve with log-rank test were used

Results: Brazilian patients were younger than Mexican (55 vs 62 years). Sarcomatoid, basaloid, and warty were more frequent in the Mexican cases, whereas usual and verrucous predominate in Brazilian series (P=0.0005). There was no difference between HPV- and Non-HPV-related subtypes by country (P=0.067). Tumors from Mexican patients had deeper invasion, higher grade and rates of vascular and perineural invasion. The rate of nodal metastases was similar (42 vs 52%, P=0.178) but tumor specific death was higher (42 vs 18%, P<0.0005) in Mexican cases. Tumor related death by subtypes was similar for most subtypes except for usual (41 vs 21%, P=0.003) and basaloid (88 vs 23%, P=0.008) SCC, with higher rates in the Mexican series.

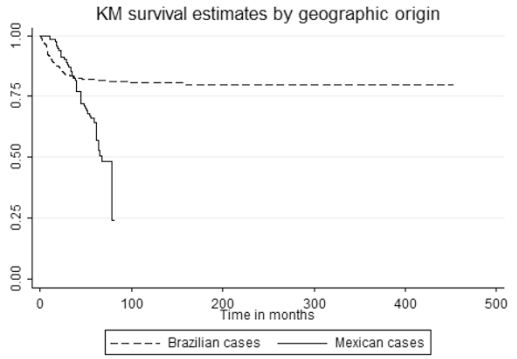

Log-rank test: P<0.00005

Conclusions: The distribution of penile SCC subtypes was different but not significant comparing HPV- vs. non-HPV-related subtypes. Mexican tumors series showed pathological aggressive features and a higher death rate perhaps due to more advanced stages at diagnosis. Usual and basaloid carcinomas had a higher mortality in Mexican cases and the cause is unknown. Geographic variation in the prevalence of penile SCC was related to specific subtypes more than to HPV-related tumors

1030 Expression of OCT4 in Small Cell Carcinoma of the Urinary Bladder

Ronda Sanders, Enrique Rodriguez-Zarco, Paula S Espinal, Andre Pinto, Ana Vallejo-Benítez, Merce Jorda. University of Miami Miller School of Medicine, Jackson Memorial Hospital and Sylvester Comprehensive Cancer Center, Miami, FL; Virgen de la Macarena Hospital, Seville, Spain.

Background: Small cell carcinoma of the urinary bladder (SmCCB) accounts for less than 1% of malignant bladder tumours, but is however associated to a dismal prognosis. Some studies have shown that targeting pluripotency transcription factors such as OCT4 may have therapeutic potential. This study aims to explore the expression of OCT4 by immunohistochemistry in SmCCB.

Design: We retrospectively studied 30 cases of SmCCB diagnosed between 2001 and 2015, obtained from University of Miami and Jackson Memorial Hospitals, Miami, Florida and Virgen de la Macarena Hospital, Seville, Spain. Immunohistochemistry (IHC) for OCT4 was performed in conjunction with known SmCCB neuroendocrine markers: synaptophysin chromogranin and CD56. A positive reaction for OCT4 was considered when nuclear staining was present. Analysis of immunohistochemical results (percentage and intensity of staining) was performed by light microscopy using a semi-quantitative method. We used a four-tier system: 0, 1 (1–33%), 2 (34–66%) and 3 (67–100%); Intensity was also graded using a four-tier system: 0 (no staining), 1 (weak), 2 (moderate) and 3 (strong).

Results: Thirteen of 30 cases (43.3%) of SmCCB expressed OCT4 by IHC. Percentage of staining was distributed as follows: 7/13 (53.9%) were classified as 1, 5/13 (38.5%) as 2, and 1/13 (7.6%) as 3. Intensity of staining was distributed as follows: 2/13 (15.4%) were classified as 1, 7/13 (53.8%) as 2 and 4/13 (30.8%) as 3. All cases demonstrated some degree of positivity for the known aforementioned SmCCB neuroendocrine markers.

Conclusions: OCT4 is expressed in a significant percentage of SmCCB. Although additional studies are needed in order to further elucidate clinical significance of this findings. OCT4 may be a potential marker for targeted therapy in SmCCB.

1031 Genetic Heterogeneity in Clear Cell and Papillary Renal Cell Carcinomas with Sarcomatoid Features

Joseph Sanfrancesco, John N Eble, Mingsheng Wang, Shaobo Zhang, David Grignon, Muhammad Idrees, Erik Kouba, Liang Cheng. Indiana University, Indianapolis, IN.

Background: Recurrent hallmark chromosomal abnormalities in clear cell and papillary renal cell carcinoma (CCRCC and PRCC) have been identified for quite some time; however, intra- and intertumoral concordance of these abnormalities in the setting of sarcomatoid differentiation has not been extensively studied.

Design: We analyzed 49 cases of CCRCC (n=43) or PRCC (n=6) with sarcomatoid transformation. Additionally 7 of these cases had metastatic diseases. Three separate tumor foci with classic CCRCC and PRCC morphologies and three separate tumor foci with sarcomatoid features were selected in each case for dual color interphase fluorescence in situ hybridization analysis. Metastatic lesions were also analyzed.

Results: In the CCRCC cohort, hallmark chromosome 3p deletion was identified in 65% of cases (28/43). Concordance between intratumoral foci was 93% (40/43). Complete concordance between clear cell and sarcomatoid morphologies was identified in 93% of cases (40/43). Hallmark 3p deletion was present in all CCRCC metastases (5/5) and was concordant with the primary CCRCC tumor in 80% (4/5). In the PRCC cohort, trisomy 7 and 17 was identified in all six cases (6/6). Complete trisomy 7/17 concordance between intratumoral foci was 83% (5/6). Trisomy 7 and 17 were identified in all metastatic PRCC samples with 100% concordance with the primary tumor.

Conclusions: In CCRCC and PRCC with sarcomatoid differentiation, our findings demonstrate high concordance of hallmark chromosomal alterations between both intratumoral foci as well as metastatic disease, though a small portion of cases showed intratumoral heterogeneity.

1032 A Comparative Study of pT3 versus pT2 Testicular Germ Cell Tumors, Including Evaluation of Lymphovascular Invasion (LVI) in the Spermatic Cord

Joseph Sanfrancesco, Karen Trevino, Adeboye Osunkoya, Guang Q Xiao, Chia-Sui Kao, Jennifer Gordetsky, Pamela Unger, Thomas M Ulbright, Muhammad Idrees. Indiana University, Indianapolis, IN; Emory University, Atlanta, GA; University of Southern California, Los Angeles, CA; UAB, Birmingham, AL; Stanford University, Stanford, CA; Lenox Hill, New York, NY.

Background: The American Joint Committee on Cancer (AJCC 2010) stages germ cell tumor (GCT) invasion into the spermatic cord, regardless of LVI, as pT3. Such invasion historically implies a worse prognosis than LVI alone (pT2), but there are few supporting data. We studied pT3 GCTs to assess their clinical stage (CS) at presentation compared to pT2 cases with and without cord LVI.

Design: 100 cases of pT3 testicular GCTs with stromal invasion of the spermatic cord from 2007-16 were identified. Pathologic, radiographic, and clinical findings were reviewed and compared to those of 70 pT2 cases, 25 of which had LVI in the spermatic cord.

Results: The mean age of pT3 cases was 32.1 yrs and mean follow up was 31 mos (range 2 – 204). Pure tumors were embryonal carcinoma (14), seminoma (11), yolk

sac tumor (2), and teratoma (2), with the remainder (71) mixed GCTs. LVI occurred in 85, with 44% of these having concurrent LVI in the cord. A positive cord margin occurred in 39, 14 of which consisted only of LVI at the margin. Metastases were found by radiographic evaluation at presentation in 85% (CSII-41%; CSIII-44%) with 12% of pT3 cases having M1b disease. In comparison, 56% (39/70) of pT2 cases were CSII/III ($p=2.3x10^{-5}$), including 64% with cord LVI (p=0.017). There was no significant difference in pT2 cases with and without cord LVI (p=0.30). 89 pT3 patients had post-orchiectomy chemotherapy; 61 underwent retroperitoneal lymph node dissections and 20% had clinical recurrence, with pathologic confirmation in 60% (12/20). Six pT3 patients (6%) died of disease progression and 4 of treatment complications. In comparison, 3 pT2 patients (4%) died of disease.

Conclusions: Our findings support that seminomatous and non-seminomatous GCTs with spermatic cord invasion (pT3) have a greater frequency of advanced CS at presentation compared to pT2 cases, regardless of cord LVI. Prior studies have postulated that LVI of the spermatic cord (classified as pT2 by AJCC 2010) may be similar to pT3 lesions; our study supports that pT2 tumors with LVI of the cord are correctly, and most appropriately, staged as pT2.

1033 Acquired Cystic Disease-Associated Renal Cell Carcinoma: A Single Institutional Morphologic and Immunohistochemical Study

Joseph Sanfrancesco, Hiroyuki Hayashi, Muhammad Idrees, Liang Cheng, John N Eble, David Grignon. Indiana University, Indianapolis, IN; Fukuoka University, Fukuoka, Japan.

Background: Acquired cystic disease-associated renal cell carcinoma (ACD-RCC) is a distinct, yet rare, renal neoplasm arising in patients with end-stage kidney disease with associated ACD, most often in the setting of long-term hemodialysis treatment. We looked to evaluate the histopathologic spectrum in these tumors as well as their immunophenotypic staining patterns.

Design: We identified patients with end-stage kidney disease status post partial or total nephrectomy from 1990 until 2014. Sixteen ACD-RCC tumors were found arising in 14 patients. A retrospective systematic review of morphologic features as well as immunohistochemical staining was performed on all cases.

Results: Of the 16 tumors identified, 100% had intratumoral oxalate deposition meeting our minimal criteria for a diagnosis of ACD-RCC. Tumors ranged in size from 0.5 to 3.5 cm. Prominent nucleoli and abundant eosinophilic cytoplasm were identified in all tumors (16/16). A sieve-like pattern was present in 13 cases (81%). Less common morphologic features included prominent papillary architecture (6/16), tumor arising out of cyst walls (5/16), and marked secondary changes including hemorrhage and fibrosis (7/16). Psammoma bodies (2/16), tumor cell hobnailing (1/16), and focal chromophobe-like morphology (1/16) were rare features. No clear cell change or tubulocystic growth pattern was seen. Immunophenotypic findings showed positive immunoreactivity for cytokeratin AE1/3 (15/15), CD10 (15/16), AMACR [p504s] (14/16), and PAX8 (10/11). Staining for cytokeratin 7 (2/16) and vimentin (3/15) was seen in a minority of cases. Staining for CK20, 34BE12, Ckit (CD117), and GATA3 was negative. Succinate dehydrogenase B was retained in all 16 (100%) tumors. Positive staining with Hale's colloidal iron was seen in 4 cases (25%) and was typically focal.

Conclusions: Overall, our study highlights the variable morphologic features of ACD-RCC as well a unique and relatively consistent immunophenotypic pattern. While the setting of acquired cystic disease is associated with an increased risk of neoplasia, ACD-RCC remains a distinct diagnostic entity from other sporadic-type renal cell carcinomas that can also arise in this clinical setting.

1034 Loss of LINE-1 Expression Could Help to Differentiate High Grade Malignancies of the Urothelium from Low Grade and Benign Conditions

Angela Sanguino Ramirez, Thu Tran, Alex Forrest-Hay, Kathleen Cieply, Sheldon Bastacky, Rajiv Dhir. University of Pittsburgh, Pittsburgh, PA; Thermo Fisher Scientific, Santa Clara, CA.

Background: Long interspersed element-1 (LINE-1) are abundant retrotransposomes in the human genome that are active during embryogenesis and silenced in somatic cells. In recent years, LINE-1 aberrant activation by hypomethylation has been linked with carcinogenesis. We investigated the expression of LINE-1 in benign and neoplastic urothelium.

Design: Formalin-fixed paraffin embedded tissue were stained with In situ hybridization (ISH) using a LINE-1 RNA probe using the QuantiGene® ViewRNA technology (Affymetrix, Santa Clara, CA) and scored as follows: weak, lower staining intensity of tumor cells compared to stromal cells; moderate/strong, similar or higher staining intensity of tumor cells with respect to stroma.

Results: A total of 54 bladder cases were examined: 10 cases of reactive urothelium, 10 cases of dysplasia, 13 cases of low grade urothelial carcinoma (LG-UC), 10 cases of high grade urothelial carcinoma (HG-UC) and 11 cases of carcinoma in situ (CIS)/invasive carcinoma. We found that loss of LINE-1 expression is more likely to be associated with high grade urothelial carcinoma (2/10 cases (20%)) and CIS/invasive carcinoma (1/11 cases (9%)). In contrast, benign reactive atypia (7/10 cases (70%)), dysplasia (7/10 cases (70%)) and low grade urothelial carcinoma (7//13 cases (54%)) appear to preserve the expression of LINE-1.

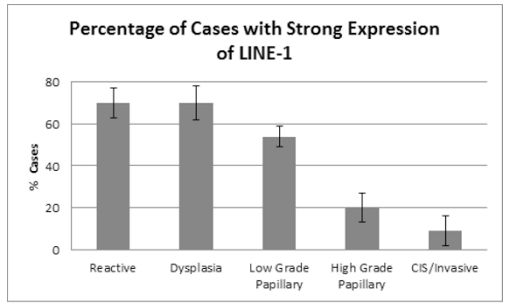

Conclusions: Based on our knowledge, we are the first group to investigate the correlation of LINE-1 expression and urothelial carcinoma. Our findings suggest that LINE-1 expression is suppressed in high grade urothelial malignancies and could be used as ancillary test in diagnostic challenging cases, such as differentiating between carcinoma in situ and urothelial dysplasia. However, futures studies are needed to confirm these results.

1035 Lymphovascular Invasion in Seminoma Revisited – A Potential Overstaging Pitfall

Aylin Sar, Kiril Trpkov, Asli Yilmaz. University of Calgary, Calgary, AB, Canada.

Background: Identification of lymphovascular invasion (LVI) can be problematic in testicular seminoma compared to nonseminomatous germ cell tumors. Presence of LVI results in pathologic stage upgrade to pT2 in the TNM system. Minimal diagnostic criteria for LVI are also not well defined, which increases the risk of LVI overdiagnosis with potential use of unnecessary adjuvant therapy in patients with organ-confined disease.

Design: We reviewed the slides and the clinical data for all patients diagnosed as pure seminoma with LVI on radical orchiectomy from 2000 to 2016 in our institution. Presence of LVI was reassessed on original H&E slides. LVI was defined as presence of compact neoplastic cell clusters in endothelial–lined spaces, conforming to the shape of the vascular space, with or without attachment to the endothelium. Extent of LVI was defined as focal (1-5 foci), established (5-10 foci) and extensive (>10 foci). The following features were also evaluated: tumor size, necrosis, invasion into rete testis, epididymis, hilar soft tissues and spermatic cord. Clinical stage at presentation and follow-up data were also obtained.

Results: We identified 48 patients reported positive for LVI in 441 patients with pure seminoma. On review, 7 (15%) were considered LVI overcalls and LVI was confirmed in 40 (9%) patients with seminoma (slides were unavailable in one case). The most common LVI overcall was due to carryover ('butter') artefact. In seminomas with LVI, the mean tumor size was 6.2cm (range: 2.4 to 18). Rete testis invasion was found in 92%, hilar invasion in 68%, tumor necrosis in 67%, epididymis invasion in 25% and spermatic cord invasion in 5% cases. LVI was focal in 65%, established in 12% and extensive in 23% cases. LVI was most commonly found in the hilum (70%). At presentation, 76% of patients with LVI were clinical stage I and 26% had advanced stage (II/III). Clinical stage I patients with LVI had relapse rate of 24%. Overall, metastatic disease (either initial or relapse) was found in 38% of patients with pure seminoma and LVI. When stratified by extent of LVI, metastatic outcome was identified in 50% of cases in the established/extensive LVI group compared to 31% in the focal LVI group.

Conclusions: LVI can be overcalled in seminoma, leading to overstaging. A conservative approach with strict criteria must be applied to prevent overtreatment, particularly in patients with clinical stage I. LVI was most commonly found in the hilar region and was invariably associated with rete testis invasion. Patients who showed more extensive, rather than focal LVI, demonstrated a more frequent metastatic disease.

1036 Predictors of Metastatic Disease in Testicular Seminoma: Clinicopathologic Study of 406 Cases

Aylin Sar, Kiril Trpkov, Tina Cheng, Asli Yilmaz. University of Calgary and Calgary Laboratory Services, Calgary, AB, Canada; Tom Baker Cancer Centre, Calgary, AB, Canada.

Background: The significance of histologic predictors of metastatic disease in testicular seminoma is not well studied. For example, tumor size and rete testis invasion are not considered in the 7th TNM edition.

Design: We studied 406 testicular seminomas, collected in our center between 1999 and 2015. We evaluated the clinical stage at presentation, age, tumor size, tumor necrosis, vascular invasion and invasion into following structures - rete testis, hilar soft tissue, epididymis, tunica vaginalis and spermatic cord. Histologic parameters were correlated with metastatic disease at presentation and at relapse. Univariate and multivariate logistic regression analyses were performed to explore potential risk factors for metastasis.

Results: Overall, 91% of patients presented with clinical stage I and 9% presented with stage II/III. Mean patient age was 38 years (range, 17 - 99). Mean tumor size was 3.9 cm (range, 0.5 - 18). Vascular invasion was found in 9% of cases. Rete testis invasion and hilar invasion were seen in 58% and 24% cases, respectively. Tumor necrosis was present in 36% cases. Tumor invaded into the epididymis in 5%, spermatic cord in 2% and tunica vaginalis in 3% of cases. Disease-free survival was 97%, during a mean follow-up of 70 months (range, 1-192). On multivariate analysis, metastatic disease at presentation was associated with tumor size (p=0.004) and vascular invasion (p=0.037) (rete testis, p=0.083). For clinical stage I patients, the relapse rate was 8%. Rete testis invasion was the only histologic parameter significantly associated with relapse (p=0.047). Vascular invasion was the only indipendent predictor of metastatic disease overall (either initial or as relapse) (p=0.030).

Conclusions: In patients with seminoma, tumor size and vascular invasion were significantly associated with metastasis at presentation. Rete testis invasion was the only predictor of relapse in stage I patients. Vascular invasion was the only histologic parameter associated with metastatic disease overall (either initial or as relapse). Invasion into epididymis, spermatic cord and tunica vaginalis were uncommonly found in seminoma.

1037 Pathologic Features and Long Term Clinical Follow Up of Treatment-Naïve Non Invasive Papillary Urothelial Neoplasms of the Urinary Bladder

Judy Sarungbam, Qiang Li, Hikmat Al-Ahmadie, Ying-Bei Chen, Samson W Fine, Sahussapont J Sirintrapun, Anuradha Gopalan, Satish K Tickoo, Guido Dalbagni, Victor E Reuter. MMC, Bronx, NY; MSKCC, NY, NY.

Background: Non-invasive papillary urothelial neoplasms(PUN) show high recurrence rates;a subset of which progresses to higher grade or invasive disease. Per WHO 2016, papillary urothelial neoplasm of low malignant potential(PUNLMP), low grade and high grade carcinoma show 4%, 10% and 25% rates of progression to invasive disease, respectively. Our inability to predict progression commits these patients to lifelong surveillance at a high financial and psychological cost. We report a large series of first-time diagnosed, treatment-naïve patients undergoing biopsy/TURBT for non-invasive PUN of the bladder and with the longest follow-up reported in literature.

Design: Treatment-naïve patients undergoing biopsy/TURBT for non-invasive PUN (Ta) between 1990 and 2008 diagnosed and treated at a tertiary care center were identified. Clinical details were collected from a prospectively maintained bladder cancer data-base. Detailed histopathological analysis was performed for multiple histological parameters and were graded using the 2004 WHO/1998 ISUP classification. The cases were also assessed for recurrence, and progression, defined as invasion into or beyond lamina propria.

Results: 264 patients were identified (68 F, 196 M), with a mean age of 68 years (range:31–90) and a median follow-up of 98 months(range:1-262). Loss of polarity, nuclear membrane irregularity, coarse chromatin, nucleoli, mitosis, location of mitotic figures and apoptotic bodies were significantly associated with histologic grade ($p < 0.005$). Results on follow-up are tabulated. The 5 year progression free survival was significantly associated with grade (p=0.01).

	Papilloma	PUNLMP	Low grade	High grade
	N/%	N/%	N/%	N/%
Total(264)	4/1.5	16/6	182/69	62/23.5
Recurrence(overall)	0/0	7/43.8	99/54.4	38/61.3
Recurrence(as HG)	0/0	1/6.3	36/19.4	
Progression to T1	0/0	0/0	10/5.5	5/8.1
Progression to T2	0/0	0/0	2/1.1	4/6.5
Progression to T1/T2	0/0	0/0	12/6.6	8/12.9

Conclusions: 1. This large series with long term clinical follow-up validates the clinical utility of the 2004 WHO/1998 ISUP classification for papillary urothelial neoplasms.
2. Other than papilloma, all papillary urothelial neoplasms show high incidence of recurrence.
3. In patients presenting with non-invasive papillary disease, progression is rare and most often seen in high grade tumors .
4. The histologic grade at initial presentation significantly correlates with progression free survival.

1038 Molecular Characterization of Tubulocystic Carcinoma of the Kidney

Judy Sarungbam, Rohit Mehra, Scott A Tomlins, Steven C Smith, Hikmat Al-Ahmadie, Anuradha Gopalan, Sahussapont J Sirintrapun, Samson W Fine, Mahul B Amin, Victor E Reuter, Yingbei Chen, Satish K Tickoo. MSKCC, NY, NY; UMICH, Ann Arbor, MI; UTHSC, Memphis, TN; MMC, Bronx, NY; VCU, Richmond, VA.

Background: Limited molecular studies are available on renal tubulocystic carcinoma (TC). Studies have variably reported copy number changes or no changes in chromosomes 7 and 17, and some publications have even suggested it is potentially related to papillary renal cell carcinoma. More recently, TC with poorly differentiated foci has been described to often show mutations in Fumarate Hydratase(*FH*). No comprehensive molecular characterization of pure TC has been reported. We therefore studied pure TC using targeted next generation sequencing.

Design: 7 cases of pure TC were studied for clinicopathologic features. Immunohistochemical stains were performed for FH, 2SC, CK7, 34bE12, CD10 and racemase. Molecular analyses were performed by 2 different platforms using targeted next-generation sequencing(hybridization capture-based and multiplex PCR-based).

Results: The clinicopathologic features are tabulated. All 7 cases showed copy number alterations (CNA) in the form of loss of chromosome 9 and gain of chromosome 17. Two tumors showed truncating mutations in *KMT2C*(a histone modifying gene), 2 harbored alterations in p53/Rb tumor suppressor pathway (R337H mutation of *TP53* in 1 case and *MDM2* and *CDK4* amplification in another), and 1 had a known oncogenic mutation of *PMS2* (DNA mismatch repair gene). None of the cases showed mutations in *FH*,*VHL*, *TSC1/2* or *MET* genes.

	Cases (N=7)
Age (year/mean)	39-79 (63)
Size (cm/median)	1.4 - 10.5 (4.2)
Stage	pT1 (6/7); pT3a (1/7)
Metastasis	None (0/7)
Gross Well circumscribed (7/7) Multicystic/ gelatinous/microcystic (7/7) Renal vascular invasion (None (0/7)	
Microscopic examination Encapsulation (0/7) Circumscription: Complete (6/7), Infiltration of sinus fat (1/7) 100% tubulocystic areas (7/7) Papillary /Solid/Cribriform areas (0/7) Prominent nucleoli (7/7) Perinucleolar halo (0/7)	
Immunohistochemistry 2SC (cytoplasmic and nuclear), negative (7/7) FH, retained (diffuse) (7/7) CK7/34bE12, positive (patchy) (7/7) CD10/Racemase, positive (focal) (7/7)	

Conclusions: 1. Recurrent alterations of *KMT2C* and p53/Rb tumor suppressor pathway are present in tubulocystic carcinoma (TC).
2. CNAs in the form of loss of chromosome 9 and gain of chromosome 17 are present in all TC.
3. *FH* mutations are not seen in usual TC, in contrast to TC with poorly differentiated foci which is a frequent morphologic pattern of FH-deficient RCC.
3. Unlike TC with poorly differentiated areas, most TCs are well circumscribed, with no metastases at presentation.

1039 Different Performances of Three Anti-PAX8 Monoclonal Antibodies

Tomoyo Sasaki, Zhiming Liao, Hui Zhang, Cleo Lee, Julia Ma, Weiwei Cai, Lina Liu, Dennis Wang, Joe Couto, Yifei Zhu. Spring Bioscience, Pleasanton, CA.

Background: PAX8 is a transcriptional factor that is widely expressed in renal, ovarian and thyroid cancers. Immunohistochemical (IHC) analyses of PAX8 can provide useful information for differential diagnosis of renal, ovarian and thyroid cancers. However, it is reported that some of the commercial anti-PAX8 antibodies can cross-react with PAX5 due to their high sequence homology between these two proteins and may cause false positivity in B-cell lymphoma and pancreatic cancers.

Design: A new rabbit monoclonal antibody (clone SP348) was generated using a unique sequence of human PAX8 for immunogen and recombinant technology. The performance of clone SP348 was compared to two commercially available mouse monoclonal anti-human PAX8 antibodies - clone MRQ-50 from Cell Marque and clone BC12 from Biocare Medical. The immunohistochemical performance of all three antibodies was assessed on a variety of human normal and tumor tissues that included 177 renal cell carcinoma cases. The specificity of the antibodies was evaluated by Western Blots using PAX1, 2, 3, 4, 5, 6, 7, 8 and 9 transfected cell lysates.

Results: All three PAX8 antibodies stained nuclei of normal kidney, renal cell carcinoma, normal thyroid and normal fallopian tube. In addition, MRQ-50 also stained B-cells in tonsil, B-cell lymphoma and pancreatic islet cells that were negative when SP348 and BC12 were used. The PAX8 positive rates varied among different renal carcinomas. They were 78.0%, 62.4% and 24.8% respectively for clones SP348, MRQ-50 and BC12 for clear cell carcinoma (n=109); 93.3%, 86.7% and 26.7% for granular cell carcinoma (n=15); 36.7%, 23.3% and 10.0% for transitional cell carcinoma (n=30); 93.3%, 86.7% and 20.0% for papillary renal cell carcinoma (n=15); and 50.0%, 50.0% and 12.5% for chromophobe renal cell carcinoma (n=8). The IHC results showed clone SP348 exhibited greater sensitivity than clones MRQ-50 and BC12 in renal cell carcinomas. Western blotting showed that clone SP348 only detected PAX8; but BC12 detected PAX8 and an unknown protein in PAX4 transfected cell lysates; while MRQ-50 detected PAX8, PAX5, and multiple proteins in PAX2 and PAX9 transfected cell lysates. This suggests that SP348 is more specific than both MRQ-50 and BC12.

Conclusions: IHC and Western Blots results from this study indicate that rabbit monoclonal anti-human PAX8 antibody clone SP348 is more specific and more sensitive than clones MRQ-50 and BC12.

1040 The Incidence of Intraductal Carcinoma of the Prostate Is Higher in Peripheral Zone Cancer Than in Transition Zone Cancer in Japanese Radical Prostatectomy Cohort

Shun Sato, Hiroyuki Takahashi, Takashi Yorozu, Takahiro Kimura, Masahiro Ikegami. The Jikei University School of Medicine, Tokyo, Japan.

Background: We have reported clinicopathological characteristics of transition zone (TZ)/anterior (ANT) cancer at the previous USCAP annual meetings. The frequency of TZ/ANT cancer was strikingly higher in Japanese patients, and TZ/ANT cancer had different clinicopathological characteristics of earlier pT stage and lower Gleason score (GS), compared to peripheral zone (PZ)/posterior (POST) cancer. The term intraductal carcinoma of the prostate (IDC-P) was proposed as intraductal progression of established invasive cancer rather than precursor lesion, and many studies have shown that IDC-P is associated with adverse outcome. In this aspect, we performed further research to show relationship between IDC-P and cancer location.

Design: A total of 211 radical prostatectomy specimens were utilized. The cases were divided into TZ or PZ cancer by its zonal origin; into ANT, POST or no dominancy (ND) cancer by the predominant location of tumor. The criteria proposed by Guo and Epstein

were adopted for the identification of IDC-P. Immunohistochemistry was performed to identify basal cell if necessary. Incidence of IDC-P was compared between TZ/ANT cancers and PZ/POST cancers, subsequently analyzed by tumor volume, GS or pT stage.
Results: IDC-P was detected in 76 cases (36.0%) among all cases. The number of cases with IDC-P in each category is shown in table 1. Incidence of IDC-P was significantly higher in PZ/POST cancers than in TZ/ANT cancers (p<0.0001/<0.0001). Especially, the higher incidence was shown in higher grade (GS 7 and above) and advanced stage (pT3) categories.

	TZ	PZ	p-value	ANT	POST	p-value
All cases	18/88	57/122	<0.0001	14/88	40/75	<0.0001
Tumor volume (cm3)						
<4.0	9/54	24/74	0.0647	8/60	15/40	0.0073
≥4.0	9/34	33/48	0.0003	6/28	25/35	0.0001
Gleason score						
6	0/14	1/12	0.9373	0/14	1/6	0.6543
7	9/59	30/82	0.0073	8/61	17/47	0.0060
8-10	9/15	26/28	0.0143	6/13	22/22	0.0003
pT stage						
pT2	6/55	13/60	0.1387	6/60	5/26	0.2957
pT3	12/33	44/62	0.0019	8/28	35/49	0.0004

Conclusions: Current research has suggested that cancer location is one of the most significant predictive factors of IDC-P, and TZ/ANT cancer have unique characteristics compared to PZ/POST cancer. Further studies to analyze the nature of TZ/ANT cancer are required.

1041 Treatment Choices in Patients Undergoing Multiparametric MRI/Ultrasound Fusion Biopsy Compared to Standard Biopsy

Benjamin Saylor, Soroush Rais-Bahrami, Jeffrey Nix, Jennifer Gordetsky. The University of Alabama at Birmingham, Birmingham, AL.
Background: Studies have shown that multiparametric magnetic resonance imaging (MRI)/Ultrasound (US) fusion-guided prostate biopsy detects more clinically-significant prostate cancers compared to standard biopsy alone. This new technology could impact patient management in selection of active surveillance vs definitive treatment. Our study assesses treatment choices in patients who underwent MRI/US fusion-guided prostate biopsy compared to patients who underwent standard biopsy.
Design: We reviewed our prospectively maintained prostate biopsy database, evaluating men who underwent MRI/US fusion-guided prostate biopsy since 2014. In addition, we retrospectively assessed patients who underwent standard 12-core biopsy over the same time period. Patient demographics and pathologic findings were reviewed. The highest Grade Group per case was considered for analysis.
Results: Follow-up was available on 133 patients who underwent MRI/US biopsy and 215 patients who underwent standard biopsy. Patients in the MRI group were older (64.5±7.2 vs 62.7±7.5, p=0.02). There was no difference in pre-biopsy PSA (10.1±10.0 vs 12.9±20.5, p=0.11) or Grade Groups (p=0.11) between the two cohorts. Patients in the MRI group were more likely to have had a previous prostate biopsy. Overall, more patients in the MRI group choose active surveillance compared to the standard group (49.6% versus 24.2%, p<0.0001). When stratifying by Grade Group, this finding held true independently for Grade Groups 1 and 2 (p=0.02 and p=0.005, respectively).

Treatment Choices by Grade Group				
		MRI/US Biopsy	Standard Biopsy	p-value
Grade Group 1	Active Surveillance	54 (88.5)	45 (73.8)	0.02
	Treatment	7 (11.5)	16 (26.2)	
Grade Group 2	Active Surveillance	10 (27.0)	6 (7.4)	0.005
	Treatment	27 (73.0)	75 (92.6)	
Grade Group 3	Active Surveillance	2 (12.5)	1 (3.7)	0.26
	Treatment	14 (87.5)	27 (96.4)	
Grade Group 4	Active Surveillance	0 (0)	0 (0)	1
	Treatment	10 (100)	23 (100)	
Grade Group 5	Active Surveillance	0 (0)	0 (0)	1
	Treatment	9 (100)	22 (100)	

Radiation and prostatectomy were chosen equally in the MRI group (24.8% vs 23.3%). In the standard group, more patients chose radiation over prostatectomy (47.2% vs 24.4%, p<0.0001).
Conclusions: Patients who undergo MRI/US fusion-guided prostate biopsy are more likely to choose active surveillance for Grade Groups 1 and 2 tumors.

1042 The Pathology of Death from Germ Cell and Testicular Neoplasia. Review from a Large Tertiary Center

Glenda Scandura, Wendy Ansell, Michelle Greenwood, Jonathan Shamash, Daniel Berney. Queen Mary University, London, United Kingdom.
Background: Unlike most solid tumors, germ cell tumors (GCT) are usually cured by multidisciplinary treatment. The supraregional centralisation in the UK of all GCTs and other tesicular tumors means many men with advanced disease are treated at our center including central pathology review. We investigated the pathology and causes of death at our tertiary referral centre for testicular tumors and non gonadal GCTs to review whether the initial and/or recurrent pathology might reveal men at high risk of death from disease and potentially requiring alternative treatments.
Design: The database at Bartshealth NHS trust was interrogated between 2003 and 2015 including a search of pathology and clinical databases to reveal the initial pathology and marker levels including tumor type and stage as well as any recurrences. This was correlated with treatments given and survival data as well as cause of death.
Results: 1221 cases were reviewed. 51 men died from their disease (DOD) (4.1%) and 6 (0.3%) died from other causes. These included road traffic accident, suicide, hepatitis C, renal failure, vascular disease and a second malignancy (glioma).
The DODs included 38 GCTs and 13 non-germ cell tumors. The 13 non germ cell tumours included 1 Leydig cell tumour, 2 Sertoli cell tumours and 10 lymphomas. Of the GCT cases, 24 were primary testicular GCTs and 14 were extratesticular primaries (10 mediastinal). All the extra testicular cases, were non seminomatous GCT. Of the testicular case,s 18 were non-seminomatous GCTs and 6 were seminoma.
10 cases overall were treated on raised markers without primary pathology. Pathology at presentation of the remainder included 5 seminomas and 33 non seminomas. 6/23 (26%) of primary testicular GCTs showed later transformation to rhabdomyosarcoma (3), PNET (2) or in one case a leukaemia of proven germ cell derivation by isochromosome 12p investigation. On review of clinical records, all of these cases had metastatic or extragonal disease at presentation. The mean age at presentation of men who died was 45.7 compared to 35.0 for all men.
Conclusions: There were no deaths in this study from primary testicular GCTs which were localised at presentation. Adverse prognostic factors included a non-testicular primary, non-germ cell malignancy, increasing age and somatic transformation. Although referral of relapsed cases from other areas means that there may be bias towards high risk cases, current treatments are more than sufficient for clinically localised GCTs. High risk men with non germ cell tumors or extragonadal primaries may require more treatment at diagnosis.

1043 Metastatic Renal Cell Carcinoma Presenting as a Solitary Subcentimeter Gastroesophageal Mucosal Polyp: Report of 5 Cases

Mohanad Shaar, Cynthia Guy, Shannon McCall, Diana Cardona, Xuefeng Zhang. Duke University Medical Center, Durham, NC.
Background: Metastatic renal cell carcinoma (RCC) involving the gastroesophageal (GE) mucosa is very rare. The majority of reported metastatic RCC in the stomach or esophagus exhibited characteristic endoscopic appearance of "volcano-like" ulcers. There are few case reports of GE metastasis of RCC presenting as small polyps. In this study, we systemically analyzed the clinicopathological features of metastatic RCC with endoscopic appearance of subcentimeter GE mucosal polyps.
Design: The pathology database from Duke University Medical Center was searched from 1990 to 2015 for surgical specimens of metastatic RCC involving the stomach or esophagus. Patients' demographics and the clinicopathological characteristics of the tumor were analyzed.
Results: Five cases of metastatic RCC as a mucosal polyp less than 10 mm were identified, as summarized in Table1.

Case (Year)	Age/ Gender	Polyp location, size (mm)	Years after primary RCC diagnosis	Primary RCC size cm	Other mets (Year of diagnosis)	Follow up
1 (2015)	59/M	Gastric fundus, 4	6	10	Lung, pancreas, liver (2012)	Alive (8 months to date)
2 (2012)	72/M	Esophagus, 4	14	N/A	Gallbladder (2012); Lung (2006)	Death (2013)
3 (2010)	80/M	GE junction, 10	12	N/A	Leg soft tissue (2005); Lung (2003)	Death (2011)
4 (2009)	79/M	Stomach, 7	1	10	Liver, pancreas (2009)	Not available after 2010
5 (1998)	68/F	Gastric fundus, 10	10	3	Lung, mesentery (1998)	Death (2000)

The endoscopy was performed due to GERD symptoms (2 cases) or for GI bleeding (3 cases). In 4 patients, the GE polyp was solitary. The metastatic RCC presented as a gastric polyp and multiple erosions in 1 patient (case 5). All the RCCs were clear cell type. In 3 cases, the GE metastasis occurred more than 10 years after RCC being diagnosis. All patients also had metastasis in other sites.
Conclusions: We presented 5 cases of metastatic RCC involving the stomach or the esophagus with endoscopic appearance of a solitary subcentimeter GE mucosal polyp. This is a rare presentation of metastatic RCC, and may potentially be overlooked by endoscopists and pathologists, especially when the history of RCC is remote or not provided. If not clinically anticipated, the histology of clear cell RCC may resemble that of mucosal xanthomas. It is important to raise awareness of this potential diagnostic pitfall and expand the differential diagnosis for GE mucosal polyps with clear cell morphology.

1044 Variant Histologies Are Common in Urinary Tract Cancers with Positive Polyomavirus (SV40) Antigen Immunohistochemistry

Alpa B Shah, Nilesh S Gupta, Sean R Williamson. Henry Ford Hospital, Detroit, MI.
Background: BK polyomavirus identified using SV40 antigen immunohistochemistry is increasingly recognized in association with urogenital tract cancers, particularly bladder cancer in immunocompromised patients. Whether the virus has an oncogenic or passenger role remains debated.

Design: Cases were retrieved from institutional archives of urinary tract cancers with SV40 positive immunohistochemistry, performed either for presence of viral cytopathic effect or known immunocompromised state. Histologic, clinicopathologic, and immunohistochemical findings were studied.

Results: Ten tumors were identified and evaluated for SV40, five of which were positive (Figure 1: Summary). Two tumors included micropapillary variant urothelial carcinoma, of which one was detected in a pelvic lymph node metastasis. One tumor demonstrated a mixture of urothelial carcinoma with small tubules and plasmacytoid variant urothelial carcinoma (Figure 2A; Figure 2B: SV40+). Another tumor occurred in an allograft kidney, explanted after transplant failure due to BK nephropathy. This tumor overgrew the kidney and manifested as a poorly-differentiated carcinoma with only PAX8 positivity, leaving the differential diagnosis between collecting duct and urothelial carcinoma unresolved (Figure 2C). One patient had history of epidermolysis bullosa and multiple tumors, including squamous carcinoma of the skin and vaginal intraepithelial neoplasia, whose urinary bladder tumor demonstrated viral cytopathic effect in a papillary noninvasive neoplasm (Figure 2D).

Case	Transplant Organ	Tumor Location	SV40	GATA-3	P63	Other	Histology	Invasion
1	None	Bladder	+	N/A	N/A	N/A	Papillary	pTa
2	Lung	Bladder	+	+	N/A	N/A	Small tubular pattern, plasmacytoid	pT2
3	Kidney	Bladder	+	+	+	N/A	Adenocarcinoma in situ, invasive micropapillary variant	pT1
4	Heart	Lymph node	+	+	-	N/A	Micropapillary variant	pTXM1
5	Kidney	Explant kidney	+	-	-	PAX8+	Poorly differentiated carcinoma in cords and nests with scattered pleomorphic bizarre giant cells	pT3a

Conclusions: SV40 positivity is enriched in urinary tract cancers from immunocompromised patients, and may have predilection for variant histologies. Unique findings in our series include positivity in a lymph node metastasis, supporting the presence of BK virus even in metastatic sites. One case showed viral cytopathic effect and presence of BK virus in a papillary noninvasive tumor occurring in a patient with epidermolysis bullosa.

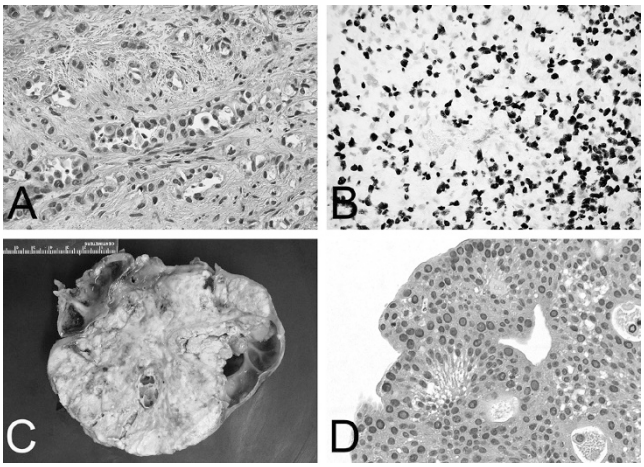

1045 Impact of the Case Pathologist on Prostate Needle Core Biopsy Diagnosis within a Single Institution

Mit D Shah, Saranya Prathibha, Anil Parwani, Debra L Zynger. The Ohio State University Medical Center, Columbus, OH.

Background: As prostate needle core biopsies are the gold standard for diagnosing prostatic adenocarcinoma, it is paramount that the diagnostic process is accurate and precise. There are abundant studies describing diagnostic interobserver variability in prostate biopsy diagnosis, yet quality assurance literature analyzing the impact of individual pathologists within the same practice is limited. We sought to determine whether pathologists at a single, tertiary care institution vary in diagnostic practice patterns within prostate needle core biopsies.

Design: A retrospective search for prostate needle core biopsies performed at our institution from 2008-2013 was conducted. Reports were evaluated for case pathologist, worst diagnosis per case, and highest Gleason grade for cases containing prostatic adenocarcinoma. A blinded review of selected cases was performed by 2 fellowship-trained genitourinary pathologists to assess for accuracy of Gleason grade. Statistical analyses were performed using the Pearson χ^2 test, standardized Pearson residuals, K-sample equality-of-medians test, and a one-way ANOVA.

Results: The cohort included 1,777 prostate biopsies diagnosed by 9 pathologists. Diagnostic reporting varied significantly between pathologists (non-neoplastic 24-48%, HGPIN/ASAP 5-20%, adenocarcinoma 46-56%; $p < 0.001$). Two pathologists had lower rates of non-neoplastic cases than expected for the cohort (24%, SPR = -3.0; 30%, SPR = -5.6), while 1 pathologist had a higher rate (48%, SPR = 5.7), despite no significant differences in patient age or serum PSA between groups. Gleason grade for cases diagnosed as adenocarcinoma varied significantly between pathologists (Gleason score ≤6, 35-49%; Gleason score 3+4=7, 21-40%; Gleason score 4+3=7, 7-30%; Gleason score 8, 5-12%; Gleason score ≥9, 0-13%; $p < 0.001$). Gleason score 4+3=7 contained the greatest degree of variation between pathologists. A blinded review of cases with Gleason score 4+3=7 from the farthest outlying pathologist revealed discrepant Gleason scores in 45% of cases (9/20) with 15% having a higher score and 30% having a lower score. Two cases differed by more than 1 grade group (3+3=6 and 4+5=9 upon review).

Conclusions: The case pathologist significantly impacted prostate needle core biopsy diagnosis and Gleason score. Institutions should be aware that there may be significant variation in practice patterns among individual pathologists within a single practice. Comparing data between individual pathologists from routine clinical practice may help identify errors and reduce diagnostic variability.

1046 Atypical Intraductal Proliferation and Intraductal Carcinoma of the Prostate on Core Needle Biopsy: A Comparative Clinicopathological and Molecular Study with Proposal to Expand Morphological Spectrum of Intraductal Carcinoma

Rajal B Shah, Jiyoon Yoon, Gang Liu, Wei Tian. Miraca Life Sciences Research Institute, Irving, TX; University of Toledo, Toledo, OH.

Background: Atypical intraductal proliferation (AIP) of the prostate is characterized usually by a loose cribriform proliferation, with greater architectural complexity and/or nuclear atypia than high-grade prostate intraepithelial neoplasia (HGPIN), however with insufficient morphological features for diagnosis of intraductal carcinoma (IDC-P). The clinical significance and morphological spectrum of AIP on core needle biopsy (NBX) are not well understood.

Design: Clinicopathological and molecular characteristics (ERG overexpression and PTEN loss) of AIP in relation to IDC-P±AIP and invasive prostate adenocarcinoma (PCa) were examined in 1480 consecutive NBXs. IDC-P and AIP were classified based on morphological features with aid of basal cell markers.

Results: Total 84 (5.6%) cases met criteria for AIP and/or IDC-P: AIP (n=36, 2.4%), IDC-P (n=19, 1.3%), and IDC-P coexisting with AIP (n=29, 2%). Invasive PCa was present in 95% cases of AIP and 100% cases of IDC-P±AIP. The mean number of glands and mean largest gland diameter for IDC-P and AIP was 11.7 (range 1-51) and 7.6 (range 2-27) and 0.75 MM (range 0.2-1.8) and 0.59 MM (range 0.2-1.1) respectively. For AIP, loose cribriform architecture ± branching was commonest morphological presentation (89%) followed by micropapillary (28%), tufting (16%), papillary (13%) and flat pattern (2%). IDC-P±AIP associated invasive PCa were more likely to have higher Gleason score (≥ 4+3) than AIP associated invasive PCa (77% vs. 44%, P= 0.0013). Other clinical features including age at presentation, preoperative PSA, clinical stage and tumor volume were not significantly different. Within AIP group, ERG and PTEN status were identical to adjacent invasive PCa in 93% and 82% of cases respectively. Within IDC-P+AIP group, ERG and PTEN status was identical among IDC-P, AIP and invasive PCa in 93% and 82% of cases respectively. PTEN loss was frequently heterogeneous in invasive PCa and localized adjacent to AIP or IDC-P.

	AIP (%)	IDC-P (%)	IDC-P + AIP (%)	INVASIVE PCa (%)
ERG	39	60	50	46
PTEN LOSS (PARTIAL OR COMPLETE)	70	60	78	64

Conclusions: AIP and IDC-P are morphological continuum, representing intraductal spread of underlying invasive PCa. Patients with only AIP need immediate repeat biopsy to rule out clinically significant PCa. Finally, AIP frequently shows broad morphology including non-cribriform architecture.

1047 Utility of Immunohistochemistry for Classification into Luminal and Basal Urothelial Bladder Carcinoma and Clinical Significance

Carolina Silva Morera, Anna Scavuzzo, Miguel Angel Jimenez, Guadalupe Moncada, David Cantu de Leon, Lourdes Pena, Julia Mendoza Perez, Delia Perez Montiel. Instituto Nacional de Cancerologia, Mexico City, Mexico.

Background: Molecular classification of high grade urothelial carcinoma of the bladder (BC) includes two different subtypes: luminal (LS) and basal-like (BL). Based on immunohistochemistry, BL had a molecular signature expressing high levels of keratin (CK) 5/6 and 14. In addition, others studies added the expression of additional markers such as GATA3 and FOXA1 to distinguish LS. The purpose of this study was to evaluate if the expression of these makers could be associated to recurrence or progression of the disease.

Design: A total of 57 formalin-fixed paraffin-embedded (FFPE) BC cases with at least a 2-y follow-up were included. Immunohistochemistry for CK5/6, 14, GATA3 and FOXA1 was evaluated in FFPE using complete histological sections (to evaluated heterogenous and invasion areas). Morphologic features such as type of growth, infiltrative pattern, histologic subtype and desmoplastic reaction were evaluated. Immunoreaction was scored and stratified as positive or negative. For analysis of continuos variables t-student was used. Categorical data were analyzed using X^2 test or Fisher´s exact test when appropriate. Logistic regression model was intended for the multivariate analysis.

Results: LS occurred in 47 cases (82.4%), pure BL in 1 (1.7%) and 9 cases (15.7%) showed heterogeneous areas where the tumor area was GATA3 and FOXA1-positive in 95 to 80%, CK5/6 and CK14 was positive 5-20%. The presence of CK14 was more frequently expressed in invasive and poorly differentiated areas. Progression was seen in 27% of LS patients versus 60% of basal-like areas patients (p=0.049), regardless of the clinical stage. Even though histologic characteristics were statistically significant in the univariate analysis, they could not be identified as independent factors for progression of disease in the multivariate analysis. There was no correlation of recurrence with histological or immunohistochemical subtypes. Additionally, 40% of patients with BL areas were treated with chemo-radiotherapy against 9% of the LS.

Conclusions: The expression immunohistochemical markers is heterogeneous with different proportions of luminal and basal-like subtypes. Furthermore, tumours with

basal-like areas were associated with progression of the disease, but not with the recurrence. Future research to elucidate the biology underlying this association is warranted.

1048 Evaluation of Tumor Morphologies at Radical Prostatectomy in High Risk Gleason Score ≥9 Prostate Cancer Diagnosed at TRUS-Guided Biopsy

Jordan Sim, Nicola Schieda, Susan J Robertson, Rodney H Breau, Chris Morash, Eric C Belanger, Trevor A Flood. The Ottawa Hospital, Ottawa, ON, Canada; University of Ottawa, Ottawa, ON, Canada.

Background: Selected patients with Gleason score (GS) ≥9 prostate cancer (PCa) detected on TRUS-guided biopsies may be considered for radical prostatectomy (RP). Intraductal carcinoma (IDC), ductal carcinoma (DC), and cribriform architecture (CA) are morphologies that are associated with aggressive biologic behaviour. This study assesses Gleason pattern 5 morphologies and other non-pattern 5 morphologies detected on RP in high risk tumors to predict adverse features including: ≥pT3 disease, positive margins, lymph-vascular invasion (LVI), lymph node involvement (LNI) and biochemical recurrence (BCR).

Design: A database search for men with GS ≥9 PCa diagnosed on TRUS-guided biopsy that underwent RP between January 2004 and July 2016 identified 62 patients. Thirteen patients who received neoadjuvant therapy were excluded. RP specimens were reviewed for the following morphologies by two blinded GU pathologists: sheets, single cells, single file arrangement, solid cylinders, comedonecrosis, IDC, DC, and CA. Age, PSA, and clinical stage were also recorded. Adverse outcomes (stage ≥pT3, LVI, LNI and BCR) were retrieved from the medical records. Data were compared using independent t-tests and chi-square.

Results: Mean age and PSA were 64.0±6.9 years and 15.2±17.0 ng/mL, respectively. Of the clinical variables evaluated, only PSA was associated with LNI (p=0.04). There was no difference compared to all other outcomes (p>0.05). The prevalence of the morphologies was: 100% (49/49) single cells, 94% (46/49) CA, 90% (44/49) single file, 78% (38/49) IDC, 51% (25/49) comedonecrosis, 47% (23/49) sheets, 43% (21/49) DC, and 33% (16/49) solid cylinders. IDC and comedonecrosis were both associated with LVI (p=0.04 and p=0.01, respectively) and ≥pT3 disease (p<0.001 and p=0.004, respectively). IDC was additionally associated with positive margins (p=0.03) and BCR (p=0.03) while comedonecrosis was also associated with LNI (p=0.04). CA was associated with ≥pT3 disease (p=0.007). The other features demonstrated no association to any adverse outcome (p>0.05).

Conclusions: IDC was significantly associated with adverse features including: ≥pT3 disease, LVI, positive margins and BCR. CA was seen in the majority of tumors and was associated with ≥pT3 disease. Although not considered Gleason pattern 5 morphologies, our results show that IDC and CA are associated with adverse features in the setting of high risk PCa.

1049 Programmed Death-Ligand 1 (PD-L1) Expression in Upper Tract Urothelial Carcinoma

Stephanie Skala, Tzu-Ying Liu, Aaron M Udager, Alon Z Weizer, Jeffrey S Montgomery, Ganesh S Palapattu, Javed Siddiqui, Xuhong Cao, Kristina Fields, Ahmed E Abugharib, Moaaz Soliman, Khaled S Hafez, David Miller, Cheryl T Lee, Ajjai Alva, Arul M Chinnaiyan, Todd M Morgan, Daniel E Spratt, Hui Jiang, Rohit Mehra. University of Michigan, Ann Arbor, MI.

Background: Urothelial carcinoma (UC) is the most common malignancy of the urinary tract. Upper tract (renal pelvis and ureter) urothelial carcinomas (UTUC) account for approximately 5% of UC but a significant subset are invasive. Locally-advanced (AJCC stage pT2 or higher) UTUC have poor long-term survival; five-year cancer-specific survival is <50% for pT2/pT3 tumors and <10% for pT4 tumors. Although the U.S. Food and Drug Administration (FDA) recently approved the PD-L1 inhibitor atezolizumab for treatment of advanced bladder UC, PD-L1 expression in UTUC is not yet well-studied.

Design: UTUC cases from 1997-2016 were retrospectively identified from the surgical pathology database at a single large academic institution. The cohort included 149 cases: 27 low-grade and 24 high-grade pTa, 29 pT1, 24 pT2, 38 pT3, and 7 pT4. PD-L1 immunohistochemistry (IHC) was performed on representative whole tumor sections using anti-PD-L1 primary antibody clone 5H1. PD-L1 expression was evaluated using a previously established cutoff for positivity (≥5% membranous staining). Association between PD-L1 IHC expression and clinicopathologic parameters was examined by Fisher's exact test; the effect of PD-L1 expression on cancer-specific mortality was assessed using the log-rank method and Cox proportional hazard ratios.

Results: Approximately one-third (32.7%) of invasive primary UTUC and 23.5% of primary UTUC were positive for PD-L1 expression. Positive PD-L1 expression was associated with high histologic grade, high pathologic stage, angiolymphatic invasion, and regional lymph node metastasis. The odds of having an invasive component were 7.76 times higher when PD-L1 expression was present (95% CI: 2.24-26.82, p=0.0002). Cancer-specific survival was not significantly associated with PD-L1 expression.

Conclusions: Previous studies have shown PD-L1 expression in approximately 17% of invasive primary bladder UC, and the U.S. FDA recently approved a PD-L1 inhibitor for treatment of bladder UC. Approximately one-third of primary invasive UTUC in our cohort demonstrated positive PD-L1 expression. Given the low utilization of neoadjuvant therapy in UTUC and the critical need for non-nephrotoxic agents in both the neoadjuvant and adjuvant settings, checkpoint inhibition may yield a substantial benefit for patients with UTUC.

1050 Application of Clinical-Grade FISH Assays for Identification of MiT Family Translocation-Associated Renal Cell Carcinoma (t-RCC): Clinicopathologic Characteristics and Report of 20 Genetically Confirmed Cases, Including *TFEB*-Amplified Renal Cell Carcinoma

Stephanie Skala, Aaron M Udager, Yang Zhang, Carrie Landau, Saravana Dhanasekaran, Diane Roulston, Lina Shao, Javed Siddiqui, Xuhong Cao, Steven C Smith, Jesse K McKenney, Jeffrey L Myers, Arul M Chinnaiyan, Hong Xiao, Scott A Tomlins, Rohit Mehra. University of Michigan, Ann Arbor, MI; Virginia Commonwealth University, Richmond, VA; Cleveland Clinic, Cleveland, OH.

Background: *TFE3* and *TFEB* gene rearrangements define a subset of renal cell carcinoma (t-RCC). Recently, *TFEB*-amplified RCCs have also been described (PMID: 27565001). We present our experience with application of clinical fluorescence *in situ* hybridization (FISH) assays for detection of *TFE3* and *TFEB* gene aberrations.

Design: 60 consecutive consultation and in-house RCC cases submitted to the genitourinary FISH service at a large academic institution due to suspicion for t-RCC were prospectively collected. CLIA-grade dual-color break-apart FISH assays were performed on formalin-fixed, paraffin-embedded sections to detect *TFE3* and *TFEB* aberrations. Morphologic and clinical features were assessed and correlated with FISH results.

Results: Patient age at RCC diagnosis was 12-85 years, with only two patients <18 years old. 20 (33%) tumors showed genomic *TFE3* or *TFEB* aberrations, including *TFE3* rearrangement (14), *TFEB* rearrangement (2), and *TFEB* amplification (4). RCCs with *TFE3* rearrangement demonstrated a spectrum of morphologic features either consistent with t-RCC or overlapping with clear cell, oncocytic, papillary, or unclassified RCC. Notably, 4 out of 5 (80%) high-grade RCCs with some features of clear cell papillary RCC demonstrated *TFE3* rearrangement. Both *TFEB*-rearranged RCCs demonstrated dual cell populations with clear and eosinophilic cytoplasm and entrapped benign renal tubules, features previously reported with this aberration. One case showed a smaller cell population surrounding basement membrane material. One in-house *TFEB*-amplified RCC was poorly differentiated with immunohistochemical expression of PAX-8, pancytokeratin, and Melan-A. The other *TFEB*-amplified RCCs demonstrated either oncocytic or clear cell features, with only one case showing the classic biphasic morphology of *TFEB*-rearranged RCC.

Conclusions: Clinical-grade *TFE3* and *TFEB* FISH assays are helpful for genetic confirmation of t-RCC, facilitating accurate diagnosis and potential clinical trial enrollment. RCCs with *TFE3* and *TFEB* aberrations demonstrate a wide morphologic spectrum, highlighting the need for judicious use of *TFE3* and/or *TFEB* FISH in routine clinical practice. Based on our experience, *TFEB* amplification may be more common than *TFEB* rearrangement, a finding that needs to be independently validated in subsequent studies.

1051 Immunohistochemical Analysis of the Unfolded Protein Response in Urothelial Carcinoma

James Solomon, Mariah Z Leivo, Jeffrey J Rodvold, Maurizio Zanetti, Jonathan H Lin, Donna Hansel. Univ of California, San Diego, San Diego, CA.

Background: The unfolded protein response (UPR) is a response to stress in the endoplasmic reticulum related to unfolded or misfolded proteins. Under unstressed circumstances, the protein GRP78 is bound to and inhibits PERK, IRE1, and ATF6, the initiators of each of the three arms of the UPR. However, when unfolded or misfolded proteins accumulate, GRP78 binds to the unfolded regions, dissociating from PERK, IRE1, and ATF6, allowing for downstream signaling. When activated, signaling pathways along the three separate arms cause the cell to halt protein translation, target misfolded proteins for degradation, and increase expression of protein folding chaperones. In addition, ATF6 upregulates expression of GRP78 in a feedback loop. The UPR has been shown to be altered in many types of human cancers. It is thought to enhance cancer cell survival, promote metastasis, increase resistance to chemotherapy, and is associated with poor outcomes. Both the expression of GRP78 in urothelial carcinoma (UC) and its correlation with histologic subtypes and clinicopathologic staging are unknown.

Design: Tissue microarrays for a series of 89 conventional UCs, 21 micropapillary UCs, and 35 primary squamous cell carcinomas (SCC) of the bladder were stained with an anti-GRP78 antibody (C50B12 clone, Cell Signaling). Percentage of carcinoma cells with absent, weak, moderate, and strong staining was assessed to determine H-score. Kaplan-Meier and chi-square testing was used for statistical analysis.

Results: Using publicly available datasets, genomic amplification of ATF6 is seen in up to 20% of UC, but alterations affecting the PERK and IRE1 arms occur in only 4% and 5%, respectively, and often overlap with ATF6 alterations. In our cohort, elevated GRP78 immunoexpression, a well-defined biomarker for ATF6 activation, was seen in 42% of conventional UC, 43% of micropapillary UC, and 51% of SCC cases (p = 0.6). The mean H-score was higher in cases of conventional UC with metastases compared to those without (181 vs. 157, p=0.23), but H-score was not related to recurrence-free or overall survival, even when stratifying by presence of lymph node metastases, morphology, or history of chemotherapy. Micropapillary UC showed an average H-score of 165 and SCC of 181.

Conclusions: Genomic alterations affect the ATF6 branch of the UPR in approximately 20% of UC, and there appears to be upregulation of the UPR by immunostaining for GRP78 in a substantial subset of tumors. Increased expression may be related to lymph node status, and additional studies to examine the biological effects of UPR upregulation in UC are warranted.

1644 Immunoprofiling of Renal Cell Carcinoma with Rhabdoid Features Identifies Potential Targets for Adjuvant Treatment by Antibody Drug Conjugates

Buer Song, John E Tomaszewski, Wilfrido D Mojica. University at Buffalo, Buffalo, NY.

Background: Adult renal cell carcinoma with rhabdoid features (RCCR) is an aggressive neoplasm with a poor prognosis and a higher likelihood to metastasize relative to conventional clear cell renal cell carcinoma (CCRCC). Current treatment options to prevent recurrence or treat metastatic disease after surgical resection are limited. Immunotherapeutics, in the form of antibody drug conjugates (ADC), represent a mechanism whereby toxic agents can be delivered via a monoclonal antibody to targeted tumor cells and offer an alternative option for adjuvant therapy. This option is gaining in appeal because of its directed nature and the growing library of ADCs in development and reaching the clinic. Ideal targets are tumors whose cells demonstrate overexpression of specific plasma membrane proteins (PMbP). This study was undertaken to identify if any possible PMbP target candidates exist in RCCR from a limited panel of antibodies.

Design: Four cases of RCCR were identified from the archival files of the Department of Pathology at the University of Buffalo. The rhabdoid component in these cases ranged from 25% to > 95% (semi-quantitative measurements done manually by pathologists) with a background of CCRCC. The rhabdoid tumor cells possessed a voluminous, pink cytoplasm, some with eosinophilic inclusions, and vesicular nuclei with prominent nucleoli. Immunohistochemistry using antibodies to 5 plasma membrane proteins (L1-CAM, CDH2, AXL, Trop-2 and PTK-7) was performed on sections of tumor with rhabdoid elements. ADCs to these PMbP are either currently in development or have been recently FDA approved.

Results: Diffuse staining in a majority of tumor cells with membranous accentuation was noted for CDH2 in all four cases. Similar membranous staining was noted with the antibody to AXL, but in a more localized/ regional pattern. L1CAM was focally positive in a membranous fashion in one case. No staining was noted with either PTK7 or Trop2.

Conclusions: Based on the findings in this study, RCCR appears to be a candidate for treatment with a combinatorial regimen of ADC's directed to CDH2, AXL, and to a lesser extend L1CAM, in the adjuvant setting to help prevent recurrence or treat metastatic disease.

1052 Total Prostate-Specific Antigen (tPSA) Outperformed Free PSA Percentage (fPSA%) in Detecting High-Grade Prostate Cancer (PCa) and PCa in Patients Older Than 60 Years of Age

Tong Sun, Kristine Cornejo, MRabie Al-Turkmani, Lokinedi Rao. University of Massachusetts Medical School, Worcester, MA.

Background: The PSA based PCa screening remains a controversial topic. Several worldwide trials resulted in a consensus against PSA screening for men of all ages few years ago to eliminate overdiagnosis. However, subsequent data suggests abandoning screening would result in a doubling of patients presenting
with metastatic disease and a significant increase in PCa related death. Although multiple new biomarkers such as PSA isoform p2PSA and PCA3 have been reported, which may improve diagnostic accuracy, tPSA levels along with tPSA% still remain the most widely-used screening markers for PCa in clinical practice. Personalizing tPSA and fPSA% screening and means to identify high-grade PCa is critically needed.

Design: A total of 853 patients who received 6 or 12 core prostate biopsies between 01/2011 and 08/2016 were included in the study and the tPSA and fPSA% were evaluated. The levels of tPSA and fPSA% were measured by Beckman-Coulter Access Immunoassay. The highest tPSA and lowest fPSA% levels within the prior 2 years of the biopsies were scrutinized.

Results: The tPSA and fPSA% levels differed significantly between men with and without PCa (AUC: 0.602 and 0.664). The tPSA levels increased steadily with age in men with and without PCa. Intriguingly, only tPSA levels in patients older than 60 years showed a significant difference between men with and without PCa. No difference in tPSA levels was observed in patients younger than 60 years. Further analysis in patients with biopsy-proven PCa revealed tPSA but not fPSA% demonstrated a strong association between levels and Gleason grade. Median tPSA levels of patients with pathologic Gleason 6 PCa is 5.8 (95%CI 5.0 -6.8), while the median tPSA with Gleason 4+3 PCa is 10.9 (95%CI 8.9 -12.7) and the median tPSA with Gleason 8 or higher PCa is 11.4 (95%CI 6.5 -14.7, $P = 0.0001$). With a level of tPSA > 20ng/mL, the likelihood ratio for detecting PCa with pathologic Gleason score ≥8 is 6.43, with 95% specificity and 30% sensitivity.

Conclusions: Both tPSA and fPSA% have significant predictive values in PCa screening. The tPSA levels with the highest predictive value for PCa were achieved in patients older than 60 years in our cohort. Our data suggests it is necessary to have separate reference ranges for different age groups when using tPSA for PCa screening. Furthermore, a higher level of tPSA, such as 20 ng/mL rather than the widely adopted screening cutoffs (i.e. 4.0 or 10.0 ng/mL) is significantly associated with a high-grade PCa.

1053 Different Patterns of PD-1 and PD-L1 Expression in Histologic Subtypes of Renal Cell Carcinoma (RCC) – Analysis of Data from the Cancer Genome Atlas (TCGA) Kidney Projects

Yue Sun, Hikmat Al-Ahmadie, Anuradha Gopalan, Samson W Fine, Sahussapont J Sirintrapun, Satish K Tickoo, Victor E Reuter, Ying-Bei Chen. Memorial Sloan Kettering Cancer Center, New York, NY.

Background: Recent clinical trials demonstrate therapeutic benefit of Nivolumab, a PD-1 checkpoint inhibitor, in patients with advanced clear cell RCC. PD-L1 and PD-L2 are the only known ligands for PD-1. Although PD-L1 expression has been associated with improved outcomes with Nivolumab treatment in metastatic melanoma and some lung cancers, its role in predicting treatment benefit of anti-PD-1 therapy in RCC is unclear. Only limited data is available regarding the expression and associations of PD-L1, PD-1 and other potential targets of immunotherapy in various RCC subtypes.

Design: Using publically available normalized mRNA expression data from 673 primary RCC tumors included in 3 TCGA kidney cancer projects [446 clear cell (ccRCC), 66 chromophobe (chRCC), and 161 papillary (pRCC)], we analyzed associations between PD-1 and PD-L1 gene expression and their relationships with other genes representing targets for immunotherapy.

Results: PD-1 expression, presumably mainly on tumor infiltrating lymphocytes (TILs), showed significantly different levels among the 3 histologic subtypes studied, with ccRCC as the highest and chRCC the lowest. In ccRCC, PD-1 expression also showed significant differences between stages (1 v. 2/3 v. 4), with stage 4 showing the highest level of expression. In comparison, PD-L1 expression was not significantly different between histologic types or stages. Importantly, there was no correlation between PD-L1 and PD-1 expression observed in chRCC or pRCC, and only a weak correlation in ccRCC (r=0.23, Pearson). In contrast, across all 3 histologic types, strong correlations were found between PD-1 expression and markers for TILs (e.g. CD3) or other immune checkpoints such as CTLA-4 or PD-L2. Immunohistochemical studies to validate these findings are ongoing.

Conclusions: PD-1 and PD-L1 expression exhibits different patterns in three common subtypes of RCC, and there is a lack of correlation between PD-1 and PD-L1 expression particularly in pRCC and chRCC. Our analysis suggests that PD-1 expression or TILs may be evaluated as predictive markers of anti-PD-1 immunotherapy in RCC.

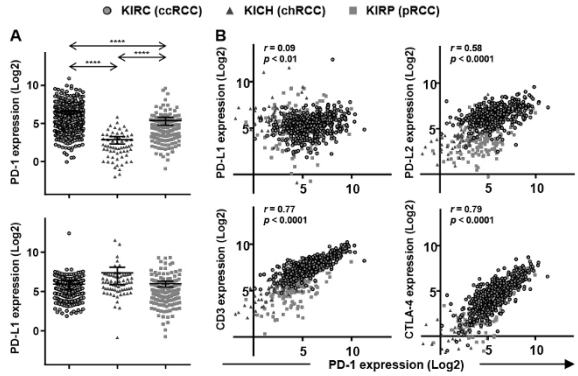

Figure 1. (**A**) mRNA expression of PD-L1 and PD-1 in TCGA clear cell (ccRCC), chromophobe (chRCC), and papillary (pRCC) projects. **** p<0.0001. (**B**) Correlations between mRNA expression (normalized) of PD-1 (X axis) and PD-L1, CD3, CTLA-4, and PD-L2 (Y axis).

1054 Low-Grade Spindle Cell Proliferation in Clear Cell Renal Cell Carcinoma Is Unlikely an Initial Step in Sarcomatoid Differentiation

Ozlem Tanas Isikci, Huiying He, Petr Grossmann, Reza Alaghehbandan, Monika Ulamec, Fredrik Petersson, Delia Perez Montiel, Kvetoslava Michalova, Kristyna Pivovarcikova, Ondrej Ondic, Bohuslava Saskova, Pavla Rotterova, Milan Hora, Michal Michal, Ondrej Hes. Ankara Education and Research Hospital, Ankara, Turkey; Peking University, Science Center, Beijing, China; Charles University, Medical Faculty and University Hospital, Plzen, Czech Republic; Faculty of Medicine, University of British Columbia, Vancouver, Canada; Clinical Hospital Center, Medical Faculty, Zagreb, Croatia; National University Health system, Singapore, Singapore; Institute Nacional de Cancerologia, Mexico City, Mexico.

Background: Spindle cell proliferation (SCP) within clear cell renal cell carcinoma (CRCC) is usually considered as sarcomatoid differentiation. Low-grade (LG) SCP in CRCC is an uncommon phenomenon which can pose diagnostic challenges. The aim of this study was to describe morphologic, immunohistochemical and molecular characteristics of CRCCs with LG-SCP.

Design: 11 cases of CRCC with LG-SCP were retrieved from 19500 renal tumors in our registry. 10 cases of typical sarcomatoid CRCC were included as control group. Morphologic and immunohistochemical characteristics of epithelial mesenchymal transition (EMT) were assessed. *VHL* gene abnormalities were analyzed.

Results: Of 11 CRCCs with LG-SCP, there were 5 males, 5 females, and in case the gender was unknown. Median age was 67 years (range 60-81 years). Mean tumor size was 7.1 cm (range 1.7-12 cm). Follow up was available in 9 cases (mean 44.78 months), with no aggressive behavior. LG-SCP constituted 5-80% of tumor volume (mean 32.3 %), while the remaining of the tumor volume was consistent with "conventional" CRCC. The immunohistochemical profile of LG-SCP was consistent with "conventional" CRCC. Compared to sarcomatoid CRCC, some EMT markers showed alteration in LG-SCP, including reduced expression of N-Cadherin and Zeb1 as well as increased expression of E-cadherin. No significant differences in EMT markers between LG-SCP and "conventional" CRCC component were found. Abnormalities in *VHL* gene were found in 6/11 cases.

Conclusions: CRCC with LG-SCP showed comparable immunohistochemical and molecular characteristics to those seen in "conventional" CRCC. Immunohistochemical analysis of EMT markers showed that LG-SCP did not differ from "conventional" CRCC. LG-SCP is a part of morphologic heterogeneity which may not be considered as an initial stage of sarcomatoid differentiation.

1055 Small Cell Carcinoma of the Bladder (SCCB): Role of Multimodality Management and Genomic Predictors of Response

Min Yuen Teo, Xueli Hao, Neil Desai, Semra Olgac, Anuradha Gopalan, Ying-Bei Chen, Samson W Fine, Sahussapont J Sirintrapun, Dean F Bajorin, Jonathan E Rosenberg, Bernard H Bochner, Guido Dalbagni, Barry S Taylor, Michael F Berger, David Solit, Satish K Tickoo, Victor E Reuter, Gopa Iyer, Hikmat Al-Ahmadie. Memorial Sloan Kettering Cancer Center, New York, NY; Virginia Mason Medical Center, Seattle, WA.

Background: SCCB is a rare and aggressive neoplasm. We reviewed our center's experience in a large cohort of SCCB. We also identified potential genomic markers of chemo-response/resistance in this aggressive tumor.

Design: SCCB cases were identified and reviewed for confirmation and detailed histologic evaluation. A subset of tumors was sequenced with the MSK-IMPACT assay (covering >279 genes, PMID: 25801821). Clinical stage and treatment response were correlated with recurrence-free (RFS) and overall survival (OS). Distribution of somatic alterations was compared between responders (≤ypT1N0) and nonresponders.

Results: Between 1985 and 2015, 152 SCCB were identified. Median age was 67 years (range: 47 – 93). 42 patients (28%) presented with metastasis (M1), and 103 (68%) did not (M0); and no clinical data for 7 patients. Of M0 patients, 80 underwent cystectomy (RC); 50 of them received neoadjuvant chemotherapy (NAC), 7 received adjuvant chemotherapy and 9 received definitive chemoradiation. Of M1 patients, 39 received chemotherapy. OS for subgroups is listed below.

Table 1. Clinical Outcome of SCCB		Median OS (mos)	12-month OS	24-month OS
M0 (n=103)	All (n=103)	44.7	73%	56%
	Chemotherapy only (n=14)	8.1	15%	15%
	Chemoradiation (n=9)	NR	89%	89%
	RC only (n=23)	17.3	59%	33%
	NAC + RC (n=50)	NR	88%	68%
	Adjuvant Chemotherapy (n=7)	238.8	57%	57%
M1 (n=42)	Chemotherapy only (n=39)	10.2	36%	16%

Of 50 NAC patients, pT0N0 and ≤pT1N0 rates were 38% and 48%, respectively. Responders had superior median RFS (NR vs 12.6 mos, HR 0.18 p<0.01) and OS (NR vs. 23.8 mos, HR 0.16 p<0.01). The amount of neuroendocrine component in tumor did not correlate with outcome for NAC or M1 patients. Genomic data were available for 31 of 50 NAC patients (62%). Responders were enriched with mutations in *ERBB2* (33% vs. 0%, p=0.02), PI3K pathway (*PIK3CA*, *PTEN*, *AKT1*, *TSC1*, *TSC2*) (40% vs. 6%, p=0.04) and histone acetyltransferases (60% vs. 25%, p=0.07). Of 22/31 tumors sequenced with larger 341-gene set, *ERCC2* and *RBM10* mutations were mutually exclusively enriched in responders (54% vs. 11%, p=0.07) and nonresponders (44% vs. 0%), respectively.

Conclusions: In non-metastatic SCCB, chemotherapy plus RC or in conjunction with radiotherapy improves survival. Patient outcomes are independent of the amount of neuroendocrine component. Alterations in *ERBB2*, *ERCC2* and PI3K pathway are associated with response to chemotherapy but only *RBM10* mutation was enriched among non-responders.

1056 Comprehensive Determination of Prostate Tumor ETS Gene Status in Clinical Samples Using the CLIA Decipher® Assay

Alba FC Torres, Mohammed Alshalalfa, Scott A Tomlins, Nicholas G Erho, Ewan A Gibb, Jijumon Chelliserry, Lony Lim, Lucia LC Lam, Elai Davicioni, Kasra Yousefi, Angelo M De Marzo, Ashley E Ross, George J Netto, Edward M Schaeffer, Tamara L Lotan. Johns Hopkins School of Medicine, Baltimore, MD; GenomeDx Biosciences, Vancouver, BC, Canada; University of Michigan, Ann Arbor, MI; Northwestern University, Chicago, IL.

Background: Gene fusions involving *ETS* oncogene family are the most common somatic genomic rearrangements in prostate cancer and define a molecularly distinct tumor subset. Though *ERG* is the most commonly rearranged *ETS* family member leading to its over-expression, rearrangements and over-expression of ETV1, ETV4 or ETV5 also occur and are generally mutually exclusive. Here, we report on the validation of the CLIA-certified Decipher® prostate cancer classifier assay, a clinical-grade gene expression microarray assay, to detect all four common *ETS* gene alterations, enabling accurate molecular classification FFPE prostate tumors.

Design: Benchmarking against ERG immunohistochemistry (IHC) and ETV1, 4 and 5 RNA *in situ* hybridization (RISH), we demonstrate the accuracy, precision, and reproducibility of Human Exon Array ETS classification models using 456 FFPE prostate tumor samples at radical prostatectomy (RP). We then apply these models to classify prospective samples (n=4,545) from the Decipher GRID® transcriptome database.

Results: The m-ERG model achieved an AUC of 95% (93-98%), with 93% sensitivity and 98% specificity to predict IHC status across 456 RP samples. The ETV1, ETV4 and ETV5 models achieved AUCs of 98%, 88%, and 99%, respectively. The models had 100% robustness for ETS status calls and model scores were highly correlated using 11 samples with 10 replicates each across different operators, batches and reagent lots. Based on these models, 41.5% of the prospective RP cohort samples (n=4,036) were predicted to be ERG+, 6.3% ETV1+, 1% ETV4+, and 0.4% were ETV5+. In prospective biopsy samples (n= 509), 41.2% were ERG+, 8.6% ETV1+, and 0.4% ETV4+ and 0% ETV5+. Interestingly, tumors with higher Decipher® risk status were more likely to be ERG+ in the prospective RP cohort (p=0.04) and more likely to be ETV+ in the prospective biopsy cohort (p=0.01) compared to those with lower Decipher® risk status.

Conclusions: These results support the utility of microarray-based ETS status prediction models as part of a clinically adopted genomic test pipeline for streamlined and accurate molecular classification of prostate tumors.

1057 Gene Expression Meta-Signature Identifies INSM1 Expression and YAP1 Loss as Markers of Neuroendocrine Prostate Cancer

Alba FC Torres, Harrison Tsai, Lisa M Rooper, William H Westra, Tamara L Lotan. Johns Hopkins School of Medicine, Baltimore, MD.

Background: Neuroendocrine prostate cancer (NEPC) is rare historically but may be increasing in prevalence as patients potentially develop resistance to contemporary anti-androgen treatment. Diagnosis can be straightforward when classic morphological features are accompanied by a prototypical immunohistochemistry profile, however there is increasing recognition of disease heterogeneity and hybrid phenotypes with high grade prostatic adenocarcinoma (AdCa). To identify markers to distinguish NEPC from AdCa, we used outlier analysis to develop a 69 gene meta-signature of NEPC tumors (versus AdCa) using public gene expression data from 6 microarray datasets. INSM1 was among the top genes up-regulated and YAP1 was among the top genes down-regulated in NEPC relative to AdCa. Here, we tested whether immunohistochemistry (IHC) assays for INSM1 and YAP1 protein distinguish NEPC from AdCa.

Design: The YAP1 and INSM1 IHC assays were developed in a CLIA-accredited laboratory using the YAP1 (EP1674Y) and INSM1 (A-8) monoclonal antibodies on the Ventana Benchmark immunostaining system. Prostatic AdCa and NEPC cell lines and murine TRAMP tumor tissues were used for validation. A previously described cohort of 35 cases of formalin fixed paraffin embedded (FFPE) NEPC (almost all diagnosed based on morphology as prostatic small cell carcinoma) and 68 cases of high grade prostatic AdCa were immunostained for YAP1 and INSM1 on tissue microarrays (TMAs). Loss of YAP1 was defined as focal or homogeneous loss of nuclear and cytoplasmic protein expression. Expression of INSM1 was defined as any nuclear positivity.

Results: Compared to gold-standard morphology, YAP1 protein loss was 89% sensitive for detection of NEPC, identifying 31/35 cases correctly. Intact YAP1 immunostaining was 79% (54/68) specific for adenocarcinoma. INSM1 protein expression was 77% sensitive for detection of NEPC, identifying 27/35 cases correctly. Absence of INSM1 immunostaining was 91% (62/68) specific for adenocarcinoma. In FFPE prostate tumors, the positive predictive value (PPV) of combined YAP1 loss and INSM1 protein expression for NEPC was 90% (27/30), while the negative predictive value of YAP1 expression and absence of INSM1 expression for AdCa was 93% (51/55). In contrast, the PPV of chromogranin and/or synaptophysin expression for NEPC was 46% (32/69).

Conclusions: YAP1 and INSM1 are complementary immunohistochemical markers useful for distinguishing NEPC from high grade prostatic adenocarcinoma.

1058 Genomic Alterations in Primary Bladder Adenocarcinoma and Urachal Adenocarcinoma

Antoun Toubaji, Emmet J Jordan, Neil Desai, Anuradha Gopalan, Ying-Bei Chen, Samson W Fine, Sahussapont J Sirintrapun, Satish K Tickoo, Bernard H Bochner, Guido Dalbagni, Eugene K Cha, Dean F Bajorin, Jonathan E Rosenberg, Barry S Taylor, Michael F Berger, Victor E Reuter, David Solit, Gopa Iyer, Hikmat Al-Ahmadie. Memorial Sloan Kettering Cancer Center, New York, NY.

Background: Primary adenocarcinoma of the urinary bladder is rare and can present either as a pure primary bladder adenocarcinoma (PBA) or a urachal adenocarcinoma (UA). No standard of care treatment currently exists for either variant. To define the genetic landscape of alterations which characterize bladder and urachal adenocarcinoma, we used a targeted exon capture and next generation sequencing assay to interrogate the mutation and copy number status of 379 oncogenes and tumor suppressor genes commonly altered in cancer within a cohort of PBA and UA.

Design: Tumor samples and matching normal DNA were sequenced from PBA (n=9) and UA (n=22). Somatic alterations including copy number alterations and mutations were assessed. Clinicopathological data were also recorded.

Results: Patient and tumor characteristics are listed below.

Table 1. Clinical and genetic features of primary bladder adenocarcinoma (PBA) and urachal adenocarcinoma (UA)			
		PBA (n=9)	UA (n=22)
Gender	Male	6	14
	Female	3	8
Race/Ethnicity	Caucasian	7	21
	African American	2	1
Neoadjuvant chemotherapy		3	2
Cystectomy	Partial	1	19
	Radical	8	3
Mutation Profile	TP53	7	17
	KRAS	3	7
	GNAS	1	4
	ERBB2	1	3 (2 mutations, 1 amplification)
	EGFR	1	1 (amplification)
	APC	1	0

The mutation profiles of PBA and UA were similar. *TP53* mutations were commonly present in both tumor types in 77% of cases. Compared to urothelial carcinoma, alterations in chromatin modifying genes were rare in either PBA or UA (1 *ARID1A* mutation in each of PBA and UA and 1 *CREBBP* mutation in another UA).

Conclusions: Significant overlap exists in the genomic profiles of PBA and UA which are similar to those seen in colorectal adenocarcinoma and are distinct from those found in urothelial carcinoma. Multiple alterations are predicted to result in upregulation of the MAPK pathway including *KRAS* and *GNAS* hotspot mutations, and targeting this pathway represents a potential novel therapeutic strategy in the treatment of PBA and UA.

1059 DPC4 Expression Status in Upper Tract Urothelial Carcinoma (UTUC)

Aline C Tregnago, Maria Del Carmen Rodriguez Pena, James A Miller, Isabela W Cunha, Stephania M Bezerra, Hirofumi Nonogaki, Rajni Sharma, Kazutoshi Fujita, George J Netto. Johns Hopkins University, Baltimore, MD; Osaka University, Osaka, Japan; AC Camargo Cancer Center, Sao Paulo, Brazil.

Background: The *Smad4/deleted in pancreatic cancer 4* (*DPC4*) gene controls growth suppression through the transforming growth factor beta signaling pathway. DPC4 loss has been documented in several solid tumors including bladder cancer (12-35%). Given known biologic differences among upper and lower urinary tract urothelial carcinoma, we assessed expression status of DPC4 in UTUC.

Design: The cohort includes 99 primary UTUCs who underwent radical nephroureterectomy between 1997 and 2011 at one author's institution. Two tissue microarrays were constructed with spotted triplicate tumor and paired benign tissue. Immunohistochemistry for DPC4 (Clone B8, Santa Cruz) was performed. Only cases with documented positive reactivity in paired benign tissue were considered informative. Any positivity in a tumor spot indicated at least focal tumor expression, and tumors with positivity in all three spots were classified as diffusely positive. Findings were correlated with clinicopathological features.

Results: Of the 99 patients, 60 (61%) were men. Average age at diagnosis was 70 (48-99) years. 37 patients were ≤pT1 stage, and 62 were ≥pT2 stage (8 pT2, 48 pT3, and 6 pT4). LVI was present in 59 cases. 12% had lymph node metastasis and 4% had distant metastasis. DPC4 staining was evaluable in 90 tumors and non-informative (no positive internal control) in remaining 9 cases. DPC4 was diffusely positive in 23 (26%), focal in 13 (14%) and negative in 54 (60%) tumors. There was no statistically significant association between DPC4 expression status and gender, tumor grade, pT stage, presence of metastasis or LVI.

Conclusions: Our study is the first to evaluate the immunohistochemical expression of DPC4 in UTUC. DPC4 showed considerably lower expression in UTUC than bladder cancer. The finding should be confirmed on whole slide sections given the inherent under-representation of TMA sampling. Furthermore, evidence of *DPC4* gene alterations in UTUC at the molecular level is needed.

1060 Immunohistochemical Characterization of Basal and Luminal Phenotypes in Muscle Invasive Bladder Urothelial Carcinomas (MIBC) Treated with Neoadjuvant Chemotherapy (NAC)

Aline C Tregnago, Maria Del Carmen Rodriguez Pena, Marie-Lisa Eich, Diana Taheri, Hirofumi Nonogaki, Rajni Sharma, David McConkey, Trinity J Bivalacqua, George J Netto, Alexander Baras. Johns Hopkins University, Baltimore, MD.

Background: MIBC patients who respond to cisplatin based NAC, defined as stage <ypT2 at cystectomy, exhibit a high 5 year cancer specific survival (CSS) of up to 90%. In contrast, non-responders (stage ≥ypT2 at cystectomy) exhibit a worse CSS (30–40%) than cystectomy alone, highlighting the need for predictors of NAC response. Recent MIBC studies have identified a gene expression based taxonomy (basal versus luminal phenotypes) similar to that of breast cancer. We evaluated the role of such a classification using immunohistochemical stains in a NAC cohort of MIBC.

Design: Pre-treatment tissues from a cohort of 71 NAC treated MIBC patients at our institution between 2000 and 2013 were incorporated in tissue microarray and stained for CK5/6 and GATA3 (Ventana Medical Systems, AZ). Cases were assigned as luminal or basal phenotype based on the extent (70% cut off) of tumor cells with ≥2+ staining intensity, Figure 1A. We limited our analysis of CSS to the 40 patient who were able to tolerate ≥2 doses of NAC to avoid the confounding effect of patients who were not adequately dosed.

Results: As expected, there was an inverse association for CK5/6 and GATA3: 77% (43/56) of strong GATA3 cases exhibited weak/negative CK5/6 staining, most consistent with the luminal phenotype, and 73% (11/15) of the GATA3 weak/negative cases exhibited strong CK5/6, most consistent with the basal phenotype (Fisher's exact p-value 0.0003). Interestingly there was a ~ 2 fold enrichment of basal the phenotype in cases with residual MIBC following NAC, Figure 1B.

Conclusions: Our results suggest a differential responsiveness to NAC for MIBC based on assignment of basal and luminal phenotypes. The current findings should be further evaluated taking *P53* gene expression status into account, given previous suggestion of chemotherapy resistance in *P53* intact (p53-Like) MIBC. Furthermore, comparison to IHC luminal/basal MIBC phenotypes in our cohort of cystectomy only treated patients is ongoing to help discern the prognostic vs predictive role of this classification for NAC.

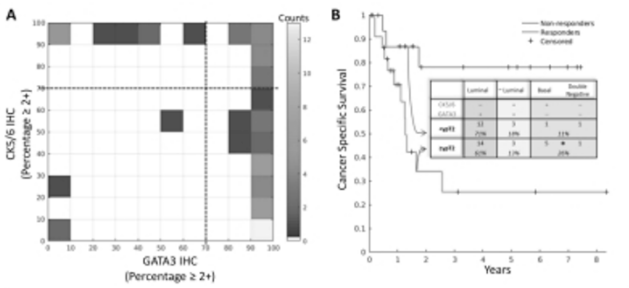

Figure 1. IHC assessment of basal and luminal phenotypes in MIBC treated with cisplatin neoadjuvant chemotherapy. (**A**) IHC scoring of the percentage of cells with ≥ 2+ intensity staining for CK5/6 and GATA3 are shown. The dotted lines represent the 70% threshold used for each stain. (**B**) The composition of NAC responders (<ypT2) and non-responders (>=ypT2) with respect to basal and luminal phenotypes is shown. A ~ 2 fold increase in the basal phenotype is observed in cases with residual MIBC at cystectomy following neoadjuvant cisplatin chemotherapy.

1061 Glucocorticoid Receptor Expression Is Increased in Primary Recurrent Prostate Cancer, Castration Resistant Localized and Metastatic Disease

Maria Tretiakova, Lawrence True, Bruce Montgomery, Mary-Ellen Taplin, Peter S Nelson. University of Washington, Seattle, WA; Harvard Medical School, Boston, MA.

Background: Androgen receptor (AR) and glucocorticoid receptor (GR) signaling pathways are intimately related, so inhibition of AR may induce GR upregulation and explain prostate cancer (PC) resistance to androgen deprivation therapies. One postulated mechanism of resistance to drugs targeting the AR is GR binding to a subset of AR regulated genes with consequent transcription activation. Since the GR status in PC is largely unknown, we assessed GR expression in hormonally naïve primary PC with known outcomes, intermediate- to high-risk PC post-neoadjuvant therapy with enzalutamide (ENZ), and castration-resistant PC metastases (mCRPC).

Design: Immunohistochemistry was performed using the N-terminus mouse monoclonal antibody (Leica, clone 4H2) on tissue microarrays and conventional sections. Slides contained 122 primary non-treated PCs with paired benign tissue, ENZ treated primary PC (n=47), and mCRPC (n=45). Each TMA case was represented in triplicate, scored for nuclear intensity and % positivity.

Results: Of 122 non-treated primary PC, 32 expressed GR (26%); 90 did not (74%). More cases with biochemical recurrence (BCR) following radical prostatectomy (34%) expressed GR compared to those without BCR (19%) (p=0.02). GR expression was strong/diffuse in 65% of recurrent PC vs. 25% of non-recurrent PC. Of localized tumors treated with ENZ, 81% expressed GR and diffuse GR expression directly correlated with higher residual cancer cellularity and volume. Of 45 mCRPC tumors 33% were GR positive: 67% strongly, 90% in bone. GR expression in mCRPC correlated with prior Abiraterone/ENZ treatment ($p<0.05$), but not with AR loss. Epithelial and stromal GR expression was present in 93% of prostate controls (n=169): 72% cases with strong nuclear reactivity.

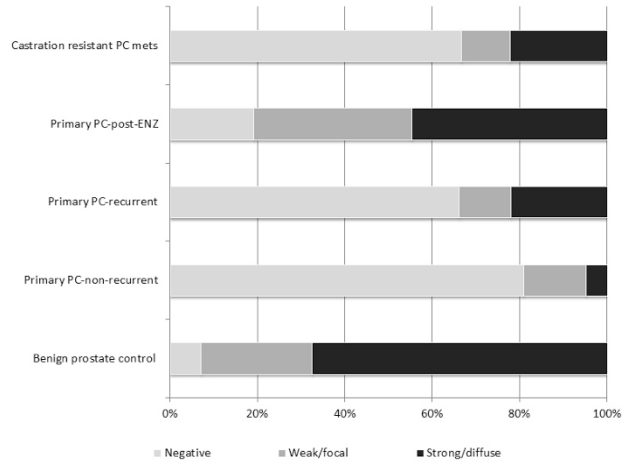

Conclusions: GR staining was present in a higher proportion of cases and higher expression levels in hormonally naïve recurrent PCs versus non-recurrent PCs. The highest levels of GR were in localized PC following AR-directed therapy. Residual tumor burden was highest in these cases. Our findings suggest that GR could be a prognostic marker in untreated localized PC and could contribute to AR resistance in localized or metastatic CRPC.

1062 Comparison of 4 PD-L1 Antibodies in 560 Kidney, Bladder and Prostate Cancers

Maria Tretiakova, Regan Fulton, Masha Kocherginsky, Nicole Andeen, Lawrence True, Allen M Gown. University of Washington, Seattle, WA; PhenoPath, Seattle, WA; Northwestern University, Chicago, IL.

Background: PD-L1 expression in melanoma and lung cancer is associated with tumor aggressiveness and clinical response to FDA approved anti-PD-L1 therapy. In genitourinary (GU) cancers the significance of PD-L1 expression is uncertain. The wide range of reported PD-L1 prevalence in GU tumors and the lack of correlation with clinical outcomes and immunotherapy response might be attributed to methodological differences of the immunohistochemical reagents and procedures. We characterized PD-L1 expression in 560 GU cancers using a panel of 4 PD-L1 antibodies: 3 FDA-approved immunoassays (22C3 for Pembrolizumab, 28.8 for Nivolumab, SP142 for Atezolizumab), and a commonly used clone EIL3N.

Design: Tissue microarrays of GU cancers included clear cell renal cell carcinoma (CCRCC) (103 primary, 25 metastatic), 64 papillary RCC, 145 primary urothelial carcinomas (UC), with 84 matched LN metastases and 12 distant metastasis, and 127 primary prostate cancers (PC), (63 recurrent, 64 non-recurrent). TMA sections were stained with 4 PD-L1 monoclonal antibodies following manufacturer guidelines: 2 anti-extracellular domains (22C3 & 28.8) and 2 against intracellular epitopes (E1L3N & SP142).

Results: Expression of PD-L1 was detected in 6 RCC cases (3.1%) by at least 2 antibodies, 1 PC (0.8%) by all 4 antibodies, and in 36 UC (15%) by at least 3 antibodies. Tumor heterogeneity in PD-L1 expression (negative vs positive, low vs high) was present in 3 RCC (50%) and 12 UC (33%) cases. In positive UC cases, high PD-L1 expression (>50% cells) was detected in 44% primary and 46% metastases. PD-L1 sensitivity (% positive cases, combined score) ranked from highest to lowest as follows: clone 28.8,

22C3, E1L3N and SP142. Analysis of all UC cores (n=621) showed 93.6-96% pairwise agreement between 4 antibodies. Pairwise concordance correlation coefficients for were also high, ranging from 0.79 (CI 95% 0.76-0.82) for 22C3 vs SP142 to 0.91 (CI 95% 0.9-0.92) for 28.8 vs E1L3N.

PD-L1 Clone	N	22C3	28.8	E1L3N	SP142
Drug		KEYTRUDA	OPDIVO	NA	TECENTRIQ
Primary and met RCC	192	5 (2.6%)	7 (3.6%)	4 (2.1%)	1 (0.5%)
Primary and met UC	241	36 (14.9%)	42 (17.4%)	33 (13.7%)	29 (12%)
Primary PC	127	1 (0.8%)	1 (0.8%)	1 (0.8%)	1 (0.8%)
TOTAL	560	42 (7.5%)	50 (9%)	38 (6.8%)	31 (5.5%)

Conclusions: PD-L1 expression prevalence is low in prostate and kidney cancers (0.8-3.6%), and higher in bladder cancer (12-17.4%), with similar detection levels in primary and metastatic cases. Despite some heterogeneity in staining, the overall results are highly concordant.

1063 Pathologic Factors Predicting Higher Clinical Stage in Testicular Seminomas: A Proposal for Upstaging Based on Rete Testis or Hilar Soft Tissue Invasion

Karen Trevino, Alaleh Esmaeili Shandiz, Thomas M Ulbright, Muhammad Idrees. Indiana University School of Medicine, Indianapolis, IN.

Background: Testicular germ cell tumors require accurate staging for effective management. 20% of seminomas are metastatic at presentation while the remaining are clinical stage I, requiring only orchiectomy and surveillance. Rete testis and hilar soft tissue invasion incur a higher risk of metastasis and recurrence in clinical stage I seminomas. However, there remains confusion about the significance of pagetoid rete involvement and the relative importance of rete invasion versus hilar soft tissue invasion.

Design: We reviewed slides and clinical data of 144 pure testicular seminomas and recorded patient age, tumor size, lymphovascular invasion (LVI) and rete testis, hilar soft tissue, epididymis, spermatic cord, tunica albuginea, and tunica vaginalis involvement. Direct rete testis stromal and epididymal invasion versus pagetoid spread was specifically recorded. A univariate and multivariate analysis was performed comparing clinical stage I to higher clinical stage patients (stage II and III) in reference to these factors.

Results: We found that tumor size (p=0.02), LVI (p=0.02), rete testis invasion (p=0.01), epididymal invasion (p=0.02), spermatic cord invasion (p=0.047), and hilar soft tissue invasion (p=0.04) were significant predictors of higher clinical stage. Pagetoid spread was not a significant predictor of higher clinical stage (p=0.47). When cases with pagetoid spread but lacking rete stromal invasion were included in the rete testis invasion subgroup, there was no significant difference between the clinical stage I and II/III groups (0.072). There was no statistical difference in clinical stage between patients with rete testis invasion or hilar soft tissue invasion (pT1) versus patients with lymphovascular invasion (pT2) (p=0.92, 0.68 respectively). Rete testis invasion and hilar soft tissue invasion were both predictive of higher clinical stage, but rete testis invasion had a higher odds ratio (3.13 versus 2.52).

Conclusions: Direct rete testis stromal and epididymal invasion but not pagetoid spread predict advanced disease at diagnosis. Our data suggest that rete testis invasion and hilar soft tissue invasion relate to higher clinical stage similar to LVI, with rete testis invasion as a stronger predictor than hilar soft tissue. We propose to report these cases as pT2 in TNM pathologic staging. This study is the largest cohort of pure seminomas examining pathologic features indicative of higher clinical stage and supports tumor upstaging based on stromal invasion of rete testis, epididymis and hilar soft tissue.

1064 Cribriform/Intraductal Carcinoma, a Candidate Predictor of Response to Neoadjuvant Treatment with Novel Androgen Inhibitors in Localized High Risk Prostate Cancer

Patricia Troncoso, Elsa Li-Ning-Tapia, John W Davis, Xuemei Wang, Ina Prokhorova, Louis Pisters, Curtis Pettaway, Eleni Efstathiou. The University of Texas MD Anderson Cancer Center, Houston, TX.

Background: Novel androgen signaling inhibitors are currently being evaluated in the neoadjuvant setting in localized high risk prostate cancer (LHRPC). Treated prostate cancer is morphologically heterogeneous and therapy-induced changes preclude the use of the Gleason grading system. A morphology-based predictor of outcome may facilitate therapy development in LHRPC, a therapeutically unmet need.

Design: We applied an established morphologic grouping of treated prostate cancer (*Eur Urol. 2010 June:57[6]: 1030-8*), to the radical prostatectomy specimens from patients (pts) with LHRPC who were randomized (2:1 ratio) to receive 3 months of either abiraterone acetate (AA) and luteinizing hormone-releasing hormone agonist (LHRHa) or LHRHa prior to prostatectomy. The post-therapy groups are defined by the presence or absence of tumor with cribriform architecture (Crib) and/or intraductal carcinoma (Crib/IDC).

Results: Patients' pretreatment characteristics were similar between the two treatment arms (AA: 44 pts, LHRHa: 21 pts). The distribution of the pathologic stage (≤ypT2N0 AA: 48%, LHRHa: 33%, p= 0.66) and the morphologic groups (Crib/IDC present: AA= 48%, LHRHa=67%, p= 0.19) were comparable between the two arms. Crib/IDC tumors had a significantly higher percentage of high pathologic stage (>ypT2N0: Crib/IDC present/absent: 80%/30% p<0.0001), a greater median tumor volume (Crib/IDC present/absent: 2.22cc/0.2cc p<0.008) and a higher relapse rate at ≥4 years follow up (Crib/IDC present/absent: 68%/27% p= 0.001) than tumors without Crib/IDC. On multivariate analysis the presence of Crib/IDC and tumor volume were stronger predictors of relapse than pathologic stage. Presence of Crib/IDC in the pretreatment biopsy was significantly associated with post-therapy Crib/IDC tumors (73% of biopsies with Crib/IDC had Crib/IDC tumors vs 26% when Crib/IDC absent, p= 0.0001).

Conclusions: The presence of residual tumor with Crib/IDC carcinoma is a predictor of relapse in the setting of androgen signaling inhibition including novel inhibitors. Our results support the use of Crib/IDC to characterize treated prostate cancer. Further validation is planned in a prospective neoadjuvant study.

1065 Biphasic Papillary Renal Cell Carcinoma Is a Rare and Distinct Morphologic Variant – Clinicopathologic Study of 24 Novel Cases

Kiril Trpkov, Daniel Athanazio, Cristina Magi-Galluzzi, Helene Yilmaz, David Clouston, Abbas Agaimy, Sean R Williamson, Fadi Brimo, Jose I Lopez, Monika Ulamec, Nathalie Rioux-Leclercq, Maysoun Kassem, Nilesh S Gupta, Samir Al Bashir, Arndt Hartmann, Asli Yilmaz, Ondřej Hes. University of Calgary, Calgary, Canada; Cleveland Clinic, Cleveland, OH; Tissupath, Australia; Erlangen University Hospital, Germany; Henry Ford Hospital, Detroit, MI; McGill University, Montreal, Canada; Cruces University Hospital, Spain; Clinical Center, Zagreb, Croatia; CHU Pontchaillou, Rennes, France; Charles University, Pilsen, Czech Republic.

Background: Biphasic squamoid alveolar renal cell carcinoma (RCC) was recently proposed as a distinct subtype of papillary RCC by Hes et al (Am J Surg Pathol 2016;40:664-75). Two cases were recently reported in allografts. We sought to further characterize and validate this entity through broad multi-institutional collaboration.

Design: We identified 24 cases by searching multiple institutional archives, using the criteria outlined by Hes et al. The tumors showed two cell populations - larger eosinophilic cells with abundant cytoplasm and higher grade nuclei, clustered in aggregates of variable size, surrounded by smaller amphophilic cells with scanty cytoplasm. Emperipolesis was uniformly found. We performed case review with immunohistochemical (IHC) evaluation and follow-up (F/U) data were collected.

Results: All 24 tumors were found in native kidneys. Male-to-female ratio was 1.9:1, with median age of 55 y (range 39-78). Median tumor size was 2 cm (mean 2.6, range 0.9-6.5). Multifocality was found in 8/21 (38%) cases (3 NA): multifocal biphasic RCC (1), papillary RCC (2), clear cell RCC (3), low-grade urothelial carcinoma (1) and Birt-Hogg-Dube syndrome (1). On microscopy, all tumors showed typical biphasic morphology that varied broadly (range 5-100%; median 60%); emperipolesis was found in all cases. Stage pT1a was found in 18 patients, pT1b in 3, and 1 patient each had pT3a and pT3b (2 NA). Uniform IHC positivity was found for: PAX-8, CK7, AMACR, EMA, vimentin and cyclin D1 (only in larger cells). Negative IHC included: CA9, C-kit, GATA3, WT1, CK5/6 and CK20. Variable IHC reactivity was found for CD10 and 34βE12. FISH showed chr +7, +17 in 2 evaluated cases. F/U was available for 20 patients (median 28 mo, range 1-244); 16 were alive with no disease, 1 was alive with recurrent tumor and 1 died of disease (2 died of other causes). Estimated incidence was ≤1% of all papillary RCC.

Conclusions: Biphasic papillary RCC is a rare and distinct variant of papillary RCC. It shows the IHC profile of papillary RCC, with larger cells reactive for cyclin D1. In the largest study to date we found frequent multifocality and although a majority of tumors were low stage and indolent, some showed adverse behaviour.

1066 Histological Patterns of Ductal Adenocarcinoma of Prostate Correlates with Mutations in DNA Repair Genes and May Aid in Selecting the Type of Systemic Therapy for Castration-Resistant Prostate Carcinoma

Lawrence True, Roman Gulati, Jane Lange, Maria Tretiakova, Funda Vakar-Lopez, Peter Humphrey, Lars Egevad, Ondrej Hes, Tatjana Antic, Heather H Cheng, Bruce Montgomery, Peter Nelson, Eric Q Konnick, Michael Schweizer, Colin Pritchard. University of Washington, Seattle, WA; Yale University, New Haven, CT; Karolinska Institute, Stockholm, Sweden; Fred Hutchinson Cancer Center, Seattle, WA; University of Chicago, Chicago, IL; Charles University, Plzeň, Czech Republic.

Background: Ductal adenocarcinoma (DAC) is an aggressive type of prostate carcinoma (PCa). Mutations in homologous recombination DNA repair genes (HR) and mismatch repair genes (MMR) are more common in DAC than in PCa. Based on current classifications of PCa, DAC can manifest as four different histological patterns – papillary, cribriform, solid, and gland-like. We hypothesized that mutations in DNA repair genes are associated with specific histological patterns of DAC.

Design: Blocks and slides of 10 sequentially accessioned cases of primary prostate carcinoma which had a DAC component were retrieved. Digitized images of H&E sections of the DAC component were evaluated independently by 7 GU pathologists and categorized by predominant histological DAC pattern. Inter-pathologist variance in categorization was assessed by Fleiss's kappa statistic. The ductal component of the 10 cancers was microdissected from formalin-fixed, paraffin-embedded blocks and sequenced using targeted gene panel sequencing on a custom array of > 200 genes. Correlation between the histological pattern of DAC selected by the majority of pathologists and HR gene mutations was assessed.

Results: Pathologist agreement in categorizing DACs by pattern was modest (k=0.18). One of 4 cases with cribriform DAC had an HR gene alteration (a *BRCA2* mutation). Four of the 10 cases had MMR gene changes. The MMR gene changes did not correlate with any histological pattern of DAC. Of the 10 cases, one was not regarded as DAC by 4 of 7 pathologists. Otherwise agreement among pathologists in pattern of DCA was good, better than by chance.

Conclusions: The reported frequency of HR and MMR gene changes in primary PCa is low (estimated at <5%). Our finding of an HR gene alteration in 1 of 4 cribriform DACs is of potential clinical importance, since prostate carcinomas which have progressed to a castration resistant state and have HR mutations appear to be sensitive to cytotoxic chemotherapy. MMR mutations may also have clinical significance as these cancers

may be sensitive to immunotherapy. Our study also found that concordance of GU pathologists in distinguishing different patterns of DAC is low enough to warrant clarification of criteria for categorization of DAC by histological pattern.

1067 More Than 10 Needle Biopsy Cores Are Needed for the Presence of Intraductal Carcinoma of the Prostate to Be a Prognostic Factor of Cancer-Specific and Overall Survival in Prostate Cancer Patients with Distant Metastasis

Toyonori Tsuzuki, Masashi Kato, Kyosuke Kimura, Ryo Ishida, Akihiro Hirakawa, Fumie Kinoshita, Naoto Sassa, Akitoshi Fukatsu, Tohru Kimura, Ryohei Hattori, Momokazu Gotoh. Aichi Medical University Hospital, Nagakute, Japan; Nagoya University Hospital, Nagoya, Japan; National Hospital Organization Nagoya Medical Center, Nagoya, Japan; Japanese Red Cross Nagoya Daini Hospital, Nagoya, Japan; Komaki City Hospital, Komaki, Japan; Chukyo Hospital, Nagoya, Japan; Japanese Red Cross Nagoya Daiichi Hospital, Nagoya, Japan.

Background: The presence of intraductal carcinoma of the prostate (IDC-P) is an adverse prognostic factor for both cancer-specific survival (CSS) and overall survival (OS) in prostate cancer patients with distant metastasis at presentation. However, it is unclear how many needle biopsy cores are needed to predict the CSS and OS precisely. Herein, we aimed to evaluate the appropriate core number in needle biopsies for IDC-P to be an adverse prognostic parameter for CSS and OS in prostate cancer patients with distant metastasis.

Design: We retrospectively evaluated 150 prostate cancer patients who presented with distant metastasis between 2002 and 2012, and reviewed the slides prepared from prostate needle biopsy specimens. Data on the submitted core number, patient age, performance status, clinical T stage, serum prostate-specific antigen, alkaline phosphatase, hemoglobin, albumin, biopsy Gleason score (> 8 vs. ≤ 8), and the presence of Gleason pattern 5 were analyzed. The patient characteristics were analyzed using Fisher's exact test. Fine & Gray and multivariate Cox proportional hazard regression models were developed to predict the CSS and OS in each group.

Results: The median age of the patients was 73 years (range, 47–90 years). The median follow-up period was 36 months (range, 3–120 months). IDC-P component was detected in 103 (64.8%) patients. Eighty-two and 6 patients died of the disease and of other causes, respectively. We divided the patients into three groups according to the number of examined cores; Group A (≤5 cores, 27 patients), Group B (6–9 cores, 67 patients), and Group C (≥10 cores, 56 patients). In the Fine & Gray analysis, IDC-P was significantly associated with CSS only in Group C (p=0.0024; hazard ratio, 5.962). Similarly, in the multivariate analysis, IDC-P was significantly associated with OS only in Group C (p=0.0014; hazard ratio, 8.523).

Conclusions: More than 10 needle biopsy cores are needed for the presence of IDC-P to be a prognostic parameter for CSS and OS in prostate cancer patients with distant metastasis at presentation.

1068 Clinicopathologic Characteristics of Patients with Very Low-Risk (PI-RADS 1 or 2) Lesions by Multiparametric Prostate Magnetic Resonance Imaging

Aaron Udager, Joel Friedman, Nicole Curci, John Wei, Chandy Ellimoottil, Rohit Mehra, Scott A Tomlins, Jeffrey S Montgomery, Matthew Davenport, Angela Wu, Lakshmi P Kunju. University of Michigan Health System, Ann Arbor, MI.

Background: Multiparametric prostate magnetic resonance imaging (mpMRI) utilizing the PI-RADS classification system attempts to identify clinically-significant [Gleason score (GS) 7 or higher] prostate cancer (PCa), with PI-RADS 1 or 2 typically corresponding to very low risk of clinically-significant PCa. In this study, we analyzed the clinicopathologic characteristics of patients undergoing prostate core biopsy (PBx) with PI-RADS 1 or 2 lesions.

Design: All patients at a single large academic institution who had at most PI-RAD 1 or 2 lesions on mpMRI between 1/1/15 and 6/30/16 and underwent pre- or post-MRI PBx were retrospectively identified. All cases of clinically-significant PCa were re-reviewed by study pathologists to confirm pathologic findings; clinicopathologic data from all other cases was obtained from pathology reports and electronic medical records.

Results: 276 patients with PI-RADS 1 or 2 lesions were identified, of which 98 (35.5%) had either pre- (60) or post-MRI (38) in-house PBx. Six (6.1%) patients showed GS7 PCa (3 pre- and 3 post-MRI), including 2 with GS4+3=7 tumors. For the remaining patients, the most recent PBx findings included: GS6 PCa (22 pre- and 13 post-MRI); atypical glands (3 pre- and 2 post-MRI); high-grade prostatic intraepithelial neoplasia (5 pre- and 4 post-MRI); or, benign (27 pre- and 16 post-MRI). For patients with GS7 PCa, the median number of involved cores was 1 (range = 1-3), the median number of total cores was 20 (range = 12-30), the median % involvement of a single core was 12.5 (range = 5-25), and the median % Gleason pattern 4 was 30 (range = 5-90); types of Gleason pattern 4 included: poorly-formed glands only (4), cribriform glands only (1), or poorly-formed and cribriform glands (1). One GS7 tumor occurred in the post-radiation (XRT) setting, and one showed aberrant p63 expression; follow-up for patients with GS7 PCa included primary XRT (1), salvage XRT (1), and active surveillance (AS; 4). Nearly all patients (>90%) with GS6 PCa opted for AS; one patient underwent radical prostatectomy (pT2a GS6 PCa), and one patient was lost to follow-up.

Conclusions: The majority (58.2%) of patients with PI-RADS 1 or 2 lesions by mpMRI do not have detectable PCa on core biopsy, however, a small subset (6.1%) harbor GS7 PCa. Although long-term follow-up data are needed, PCa patients with PI-RADS 1 or 2 lesions by mpMRI appear to represent a very low-risk cohort that may be amenable to AS in the majority of cases.

1069 Squamous Cell Carcinoma (SqCC) of the Urinary Bladder: A Clinicopathologic and Molecular Study with PD-L1 Immunohistochemistry (IHC) Correlation

Aaron Udager, Daniel H Hovelson, Andrew S McDaniel, Simpa S Salami, Javed Siddiqui, Xuhong Cao, Daniel E Spratt, Ganesh S Palapattu, Alon Z Weizer, Khaled S Hafez, Jeffrey S Montgomery, Arul M Chinnaiyan, Ajjai Alva, Scott A Tomlins, Rohit Mehra. University of Michigan Health System, Ann Arbor, MI.

Background: SqCC is an uncommon subtype of bladder cancer, particularly in the United States, where it accounts for less than 5% of malignant bladder tumors. In contrast to conventional urothelial carcinoma (UC), the clinicopathologic and molecular characteristics of bladder SqCC remain relatively understudied; in addition, while conventional UC is known to express PD-L1 in approximately 20 percent of cases, PD-L1 expression in bladder SqCC has not been previously explored.

Design: All cases of pure bladder SqCC diagnosed at a single large academic institution between 1998 and 2012 were retrospectively identified and reviewed to confirm the diagnosis. Representative formalin-fixed paraffin-embedded tissue was selected from each case for PD-L1 IHC (clone 5H1) and targeted next-generation DNA profiling using the Oncomine Comprehensive Assay and an Ion Torrent Proton sequencer. PD-L1 staining in tumor cells was assessed semi-quantitatively via concurrent review by two study pathologists (cutoff for PD-L1 positivity ≥5% membranous staining). Molecular alterations were identified from aligned sequencing reads via an established bioinformatics pipeline. Clinicopathologic information for all cases was obtained from the electronic medical record.

Results: Overall, 18 unique bladder SqCC cases were available for the purposes of this study. Sequencing data was available for 15 tumors and demonstrated a total of 123 molecular alterations (median per tumor = 8; range = 2-15); the top 5 recurrent mutated genes were *TP53*, *NOTCH1*, *CDKN2A*, *ATM*, and *PIK3CA*, and the top 5 recurrent copy number alterations were *CDKN2A* (loss), *EGFR* (gain), *FGFR1* (gain), *MDM2* (gain), and *TERT* (gain). PD-L1 IHC showed positive expression in 11 (61%) tumors (median % tumor cells staining = 20; range = 10-60). There were no significant associations between PD-L1 expression and examined clinicopathologic parameters, however, PD-L1 positivity was negatively correlated with the presence of one or more *TP53* mutations (r = -0.564; P = 0.029) and showed a trend toward positive correlation with the presence of a *PIK3CA* mutation (r = 0.426; P = 0.113) and copy number loss of *CDKN2A* (r = 0.492; P = 0.062).

Conclusions: Bladder SqCC harbor recurrent molecular alterations, including frequent targetable mutations in *PIK3CA*, and the majority of tumors express PD-L1. These data, in particular positive PD-L1 expression in the majority of cases, suggest new therapeutic possibilities for bladder SqCC, including a possible role for immunotherapy.

1070 Molecular Tumour Grading and Classification of Non Muscle Invasive Bladder Cancer Based on Whole Transcriptome Analysis

Theodorus van der Kwast, Alexandre R Zlotta, Jess Shen, Iryna Shnitsar, Aidan P Noon, Eduardo A Cabeza, Haiyan Jiang, Cynthia Kuk, Ruoyu Ni, Balram Sukhu, Kin Chan, Annette Erlich, Morgan Roupret, Thomas Seisen, Eva Comperat, Joan Sweet, Girish S Kulkarni, Neil E Fleshner, Azar Azad, Jeffrey L Wrana. University Health Network, Toronto, ON, Canada; Mount Sinai Hospital, Toronto, ON, Canada; University of Sheffield, Sheffield, United Kingdom; Groupe Hospitalier La Pitié-Salpêtière, Université Pierre et Marie Curie, Paris, France; University of Toronto, Toronto, ON, Canada.

Background: Non muscle invasive bladder cancer (NMIBC) has a highly variable clinical behaviour not adequately predicted by its histological grade and clinical parameters. Some are indolent; others quickly progress to muscle-invasive bladder cancer (MIBC). The discrepancy between phenotype and genotype is compounded further by interobserver variability in pathological grading.

Design: Whole transcriptomic (WT) analysis of 184 bladder tumours (164 NMIBC and 20 MIBC or metastatic) was performed from FFPE tissues incorporating messenger RNA expression, splice variants, gene fusion and mutation detection. In NMIBC, we used a discovery (n=40) and 2 validation cohorts (n= 40 and 84). These data were integrated and tested for correlations with both pathological grading and clinical outcomes. Conventional pathological grading for both WHO 1973 (grade 1, 2 and 3) and 2004 (low grade-LG vs high grade-HG) classifications was reviewed by 3 different expert uro-pathologists and kappa statistic for interobserver variability was calculated.

Results: Assessment of histological grade by 3 expert pathologists resulted in an interobserver variability kappa of 0.40 for 1973 WHO grading whereas it reached 0.78 for the 2004 classification. Unsupervised clustering of data from RNA sequencing revealed classification of three robust-non-overlapping molecular subtypes of NMIBC termed Grade Related Index (GRI) 1, GRI 2 and GRI 3. GRI 1 comprised of almost exclusively LG tumours, while GRI 3 clustered with HG MIBC tumours. The AUC for WT at predicting grade was 0.98 for the discovery cohort. Most discrepant cases based on pathologist grading clustered in molecular subtype GRI 2.

Conclusions: WT sequencing data delineated three molecular classes of NMIBC compared to conventional histologic grading. WT analysis could be integrated to a new WHO classification.

1646 Identification of Altered Genes and Pathways in Tumor versus Normal Tissue from Renal Cell Carcinoma Gene Expression TCGA Data Sets

Konstantin Volyanskyy, Minghao Zhong, John T Fallon, Nevenka Dimitrova. Intellispace Genomics Philips, Hawthorne, NY; Westchester Medical Center, Valhalla, NY.

Background: In cancer research, one of the most important topics is to identify driving factors for disease progression across various histological and molecular subtypes. In recent cancer studies, it has become increasingly challenging to deal with big amounts of genomics data and to identify patterns due to highly complex gene interaction pathways

and continuous multi-level changes with disease progression. Unsupervised machine learning tools are needed to quantitatively and more accurately describe a patient's tumor subtype and its driving factors.
Design: We used Level III RNASeq gene expression data from 20531 genes in 889 tumor samples of RCC across three major subtypes – clear cell renal cell carcinoma (ccRCC), papillary renal cell carcinoma (pRCC), chromophobe carcinoma (chRCC), and 129 normal samples from The Cancer Genome Atlas (TCGA) anddeveloped an unsupervised computational framework for molecular sub-subtype identification.
Results: We identified genes significantly up- and down-regulated in tumor compared to normal in each of the subtypes. The highest ranked up-regulated genes by expression in ccRCC vs. normal are CA9, CDCA2, EGLN3, and down-regulated are IRX1, UST, EGF, BIK, CTSH. We observed that aldosterone-regulated sodium channels, ion channel transport, and rhesus glycoproteins mediating ammonium transport pathways can play a significant role in distinguishing ccRCC vs. normal.
In pRCC tumor vs. normal the highest ranked up-regulated genes by expression are LIG1, GPX1, ACAP3, PUS1, HOXA1 and down-regulated are STC1, ANK2, WLS, SYT9, SOX5. We observed that pentose phosphate pathway, TNF signaling, fatty acid metabolism, MAPK signaling, regulation of insulin-like growth factor transport pathways can play a significant role in distinguishing pRCC vs. normal.
In chRCC tumor vs. normal the highest ranked up-regulated genes by expression are ARAP1, HCN2, IDH3A, and down-regulated are ABP1, HDGF, GYG2, IRX1, FOXJ1. We observed that glycosphingolipid biosynthesis, and potassium transport channels pathways can play a significant role in distinguishing chRCC vs. normal.
Conclusions: In this study, we identified gene expression profiles and associated pathways for distinguishing each RCC subtype from normal tissue. We observed known as well as novel genes. The top ranking pathways recap the well-known and biology. With further investigations, the genes that we ranked higher could be potential therapeutic targets, however, more research is needed to confirm this.

1071 Small Cell Carcinoma of the Urinary Bladder: A Clinicopathologic Analysis of 81 Cases

Gang Wang, Li Xiao, Miao Zhang, Bogdan Czerniak, Charles Guo. UT MD Anderson Cancer Center, Houston, TX.
Background: Small cell carcinoma (SmCC) is an uncommon malignancy in the urinary bladder. We studied a large series of bladder SmCC in comparison with conventional urothelial carcinoma (UC) at similar stages.
Design: We identified 81 patients with bladder SmCC from our pathology database. Histologic slides were reviewed for pathologic analysis, and clinical data were collected from the medical records. The outcomes of patients with SmCC were compared with those of patients with UC (n=82) at similar stages.
Results: SmCC patients included 69 men and 12 women, with a mean age of 68 years (range, 34–90 years). Most patients presented with hematuria (n=72**).** SmCC was pure in 27 patients and mixed with other histologic types in 54 patients. The most common mixed components were invasive UC (n=32) and UC in situ (n=26). Other components included glandular (n=14), micropapillary (n=4), sarcomatoid (n=4), and squamous (n=3) differentiation. The tumors invaded the lamina propria (n=5), muscularis propria (n=55), perivesical fat (n=20), and pelvic wall (n=1). Lymphovascular invasion was identified in 23 patients, and lymph node metastasis was present in 17 patients. Immunohistochemical studies showed that SmCCs were positive for synaptophysin **(**41/56), chromogranin (26/55), CD56 (39/41), pancytokeratins (8/9), and CK7 (9/19) and were negative for GATA3 (0/8) and CK20 (0/17). Clinical follow-up was available for 77 patients. The median survival for patients with pT2 disease was 66 months and significantly better than those with pT3 disease (12 months) (p=0.0046). Median survivals were not available for patients with pT1 or pT4 disease due to the limited number of cases. The outcome of SmCC was compared with that of UC (n=82) at similar stages. At pT2 the median survival time for SmCC was not significantly different from that of conventional UC (p=0.3799), but at pT3 the median survival time for SmCC (12 months) was significantly shorter than that of conventional UC (24 months) (p=0.0077).
Conclusions: The majority of SmCC are mixed with UC and other histologic types. When identified at an early stage, SmCC does not have a significantly different prognosis from conventional UC. However, the presence of SmCC at an advanced stage is associated with a significantly worse prognosis than UC.

1072 Gleason Score 7 and 8 Prostate Cancer with Cribriform Morphology Diagnosed in Prostate Biopsy Is More Likely to Have Seminal Vesicle Invasion and Pelvic Lymph Node Metastasis in Radical Prostatectomy

Ying Wang, Fang-Ming Deng, Hongying Huang, Peng Lee, Jonathan Melamed, Ming Zhou. New York University Langone Medical Center, New York, NY.
Background: Prostate carcinoma (PCa) Gleason pattern (GP) 4 has 4 morphological subpatterns (ill-formed, fused, glomeruloid and cribriform). Whether these subpatterns are prognostically similar is unclear. Several recent studies of radical prostatectomy (RP) found that cribriform morphology is associated with worse outcome than other GP4 subpatterns. We investigated whether cribriform GP 4 subpattern in prostate biopsy is also associated with more aggressive disease.
Design: We routinely document the GP 4 subpatterns in biopsy reports for PCa that contain a GP 4 component, including cases with Gleason score (GS) 3+4, 4+3 and 4+4. This study cohort includes cases with subsequent RP. RP pathologic features, including GS upgrading from biopsy, pT stage, seminal vesicle (SV) invasion, lymph node (LN) metastasis and dominant nodule (DN) size, were compared between cases with and without cribriform subpattern in prostate biopsies.
Results: 18 cases with cribriform subpattern and 36 without cribriform subpattern ("non-cribriform" including poorly formed, fused and glomerulation) were studied. There was no age difference between the two groups (64.12±1.73 years in crifriform group vs. 63.53±1.08 years in non-cribriform group, p=0.77).The GS distribution between the two groups was not significantly different, with GS 3+4, 4+3 and 4+4 in 5, 11, 2 cases in cribriform group and 19, 14, 3 in non-cribriform group (p=0.28). GS upgrading in RP was similar between the 2 groups (5/18 in cribriform group and 4/36 in non-cribriform group, p=0.25). The DN size was similar (20.39±1.80 mm in cribriform group vs. 18.17±1.07 mm in non-cribriform group, p=0.32). The number of cases with pT2 and pT3a in RP was also similar (11/18 and 4/18 in cribriform group vs 25/36 and 11/36 in non-cribriform group, p=0.52). However, cribriform group is more likely than non-cribriform group to have SV invasion (3/18 vs 0/36, p=0.01) and pelvic lymph node metastasis (2/18 vs 0/36, p=0.038).
Conclusions: GS 7 and 8 PCa with cribriform morphology is more likely to have SV invasion and LN metastasis than those cases with the same GS but without cribriform morphology, suggesting subpattern of GP4 in prostate biopsy may provide additional prognostic information.

1073 MRI-Targeted Prostate Biopsy Detects More Cribriform Prostate Carcinoma Than Standard Sextant Prostate Biopsy

Ying Wang, Fang-Ming Deng, Hongying Huang, Peng Lee, Jonathan Melamed, Ming Zhou. New York University Langone Medical Center, New York, NY.
Background: Prostate carcinoma (PCa) Gleason pattern (GP) 4 has 4 morphological subpatterns (ill-formed, fused, glomeruloid and cribriform). Whether these subpatterns are prognostically similar is unclear. Several recent studies of radical prostatectomy found that cribriform pattern is associated with worse outcome than other subpatterns. MRI-targeted biopsy (TBx) has been shown to detect more aggressive PCa than standard sextant biopsy (SBx). We studied the detection of cribriform PCa by SBx and TBx.
Design: We routinely document the GP 4 subpatterns in biopsy reports for PCa that contains a GP 4 component, including cases with Gleason score (GS) 3+4, 4+3 and 4+4. We compared the detection rate of cribriform PCa by 12-core SBx and TBx and compared the cancer volume in the biopsies (highest percentage of cancer involvement of any core and overall cancer percentage in total biopsy cores) in biopsies with and without cribriform morphology.
Results: 119 cases with GS 7 and GS 8 PCa were studied, including 114 with SBx, 85 with TBx and 80 with both SBx and TBx performed in the same case. 40 (33.6%) cases had cribriform pattern (cribriform group) and 79 had non-cribriform patterns (including poorly formed and/or fused and/or glomerulation, non-cribriform group). Patient age and GS distribution in both groups was similar. The highest % of cancer involvement of any core was significantly higher in cribriform group than in non-cribriform group in both SBx (71.5%±4.5 vs. 51.4%±2.7, p=0.0003) and TBx (72.3%±4.0 vs 52.8%±3.4, p=0.0013). The overall % of cancer involvement in total cores was significantly higher in cribriform group than in non-cribriform group in both SBx (17.4%±2.1 vs. 11.5%±1.1, p=0.013) and TBx (50.7%±5.0 vs 31.9%±2.7, p=0.0005). Cribriform pattern was detected in 26/80 cases with both SBx and TBx. In these 26 cases, cribriform pattern was detected in 13 by SBx and 23 by TBx (p=0.002). Number of cores with cribriform/total biopsy cores was significantly higher in TBx biopsy than SBx (0.30±0.06 vs 0.05±0.02, p=0.0002). Number of cores with cribriform/total cancer core(s) was also significantly higher in TBx than SBx (0.38±0.06 vs 0.17±0.04, p=0.002).
Conclusions: Cribriform PCa is associated with higher cancer volume in prostate biopsies. TBx detects significantly more cribriform PCa than SBx, supporting that MRI targeted biopsy detects more aggressive PCa.

1074 Morphologic Variants of Bladder Cancer and Markers of Molecular Subtype

Joshua I Warrick, Matthew Kaag, Jay Raman, Wilson Chan, Truc Tran, Sudhir Kunchala, David J DeGraff, Guoli Chen. Penn State University College of Medicine, Hershey, PA.
Background: Squamous, micropapillary, nested, and plasmacytoid are clinically important variant histomorphologies (VH) of bladder cancer. Squamous VH is enriched in the "basal" expression subtype of bladder cancer, while micropapillary has a "luminal" expression signature. We set out to study markers of luminal and basal subtype in these VH and their associated conventional urothelial carcinomas (UC) in a consecutive series, and to determine if these VH patterns are mutually exclusive.
Design: Microscope slides from a consecutive series of cystectomy cases were reviewed (n=309 cases, all for bladder cancer, 2001-2014) for the presence of invasive conventional UC and invasive carcinoma with squamous, micropapillary, nested, and plasmacytoid VH. Immunohistochemistry for FOXA1 (luminal marker) and CK14 (basal marker) was performed on identified cancers, and expression graded semi-quantitatively.
Results: Of the 309 cases, 269 had invasive bladder cancer, with 53 squamous, 27 micropapillary, 7 nested, and 8 plasmacytoid VH; 49% of cases with VH had an associated conventional UC. Squamous VH had greater CK14 expression, and lower FOXA1 expression, than micropapillary, nested, and plasmacytoid VH (all $p<0.05$, Wilcoxon). There were no significant differences in CK14 or FOXA1 expression among micropapillary, nested, and plasmacytoid VH (all $p>0.1$, Wilcoxon). Conventional UC associated with micropapillary VH had higher FOXA1 expression than conventional UC associated with squamous VH (p=0.0017, Wilcoxon). Squamous VH had higher CK14 expression than its associated conventional UC (p=0.014, Wilcoxon, paired). Squamous VH was largely mutually exclusive of micropapillary VH, which approached statistical significance (p=0.067, Fisher test).
Conclusions: Micropapillary VH and its associated conventional UC tend to be luminal, while squamous VH and associated conventional UC tend to be basal. Combined with the mutual exclusivity of squamous and micropapillary VH (trending to statistical significance), the findings suggest fundamental biological differences in the cancers from which these VH arise. That CK14 expression was higher in squamous VH than its associated conventional UC suggests CK14 is more a marker of squamous differentiation than basal subtype. Though few nested and plasmacytoid VH were identified, the findings suggest these VH may have a luminal subtype.

1075 PLZF Is a Novel Sensitive and Specific Diagnostic Marker for Metastatic and Extragonadal Primary Yolk Sac Tumor

Christina Wei, David Priemer, Muhammad Idrees, Manju Aron, Qi Yang, Loralee McMahon, Guang Q Xiao. USC, Los Angeles, CA; Indiana U, Indianapolis, IN; U Rochester, Rochester, NY.

Background: Yolk sac tumors (YST) have a diverse morphology that may simulate somatic carcinoma (SC). Without a testis primary, metastatic or extragonadal primary YST can be confused with SC, particularly adenocarcinoma. Accurate distinction between these entities is crucial because they have very different treatment and prognostic implications. Current YST markers are neither sensitive nor specific for YST. In addition, in posttreatment setting, their expressions can be diminished or lost. Promyelocytic leukemia zinc finger (PLZF), a transcription repressor, plays an important role in spermatogenesis. We have previously shown PLZF is a robust marker for primary testicular YST. In this study, we investigated its utility in identifying metastatic and extragonadal YST.

Design: A total of 32 metastatic YST-containing germ cell tumors (GCT) and 5 extragonadal primary YST were retrieved from the archives of two academic institutions. The details of tumor locations and compositions are described in Table 1. Non-YST component of metastatic mixed GCT as well as 45 SC from various sources were evaluated. Among the 32 metastatic YST, 7 cases are recurrent YST after chemotherapy. Only nuclear reactivity with PLZF was considered positive. Immunoreactivity was graded as <1% (negative; 0), 1-25% (focal; 1+), 25%-50% (moderate; 2+), and >50% (diffuse; 3+).

	# of cases	Composition of GCT	Location	PLZF Positivity
Primary GCT				
≥ 50% YST in GCT	5	YST (4/5) TT, YST (1/5)	Retroperitoneum (2/5) Mediastinum (1/5) Liver (1/5) Bladder (1/5)	3+ (5/5; 100%)
Metastatic GCT, no chemotherapy				
< 50% YST in GCT	6	TT, EC, YST (3/6) TT, YST (3/6)	Periarotic LN (4/6) Retroperitoneal LN (2/6)	3+ (1/6; 17%) 2+ (3/6; 50%) 1+ (2/6; 33%)
≥50% YST in GCT	19	YST (14/19) TT, YST (3/19) TT, EC, YST (1/19) EC,YST (1/19)	Periaortic LN (6/19) Retroperitoneal LN (5/19) Mediastinal LN (4/19) Abdomen (2/19) Lung (1/19) Pelvic LN (1/19)	3+ (8/19; 42%) 2+ (4/19; 21%) 1+ (4/19; 21%) 0 (3/19; 16%)
Metastatic GCT, postchemotherapy				
< 50% YST in GCT	2	TT,YST (2/2)	Periarotic LN (1/2) Renal vein (1/2)	3+ (1/2; 50%) 1+ (1/2; 50%)
≥50% YST in GCT	5	YST (2/5) TT,YST (1/5) TT, EC, YST (1/5) EC, YST (1/5)	Retroperitoneal LN (2/5) Mediastinal LN (1/5) Periaortic LN (1/5) Pelvic LN (1/5)	3+ (2/5; 40%) 2+ (2/5; 40%) 0 (1/5; 20%)
Somatic carcinoma				
Hepatocellular carcinoma	4			0 (4/4; 100%)
Cholangiocarcinoma	5			0 (5/5; 100%)
Pancreatic adenocarcinoma	6			0 (6/6; 100%)
Gastric adenocarcinoma	4			0 (4/4; 100%)
Colorectal adenocarcinoma	5			0 (5/5; 100%)
Lung adenocarcinoma	21			0 (21/21; 100%)

Abbreviations: GCT = germ cell tumor; YST = yolk sac tumors; EC = embryonal carcinoma; TT = teratoma; LN = lymph node

Results: Twenty-nine (29/32; 91%) metastatic YST and all 5 primary extragonadal YST (5/5; 100%) were positively reactive with PLZF, with 70% of cases exhibiting >25% cell staining. Six of 7 (6/7; 89%) postchemotherapy metastatic YST were positive for PLZF, with 71% of cases exhibiting >25% cell staining. All non-YST components in 17 cases of mixed metastatic GCT were negative for PLZF. All 45 somatic adenocarcinoma in this series were negative for PLZF. The receiver operating characteristic curve (area under the curve=0.944) for nuclear PLZF expression accurately discriminated YST from SC with 89% sensitivity and 100% specificity.

Conclusions: PLZF is highly sensitive and specific in identification of metastatic YST and extragonadal primary YST. PLZF is a useful diagnostic marker to differentiate YST from SC and non-YST germ cell components in metastatic mixed GCTs.

1076 Symmetrical Dominant Prostatic Carcinomas Are Higher Grade yet Less Likely to Recur After Radical Prostatectomy Compared to Non-Symmetrical Prostate Carcinomas

Grant Williams, William R Gesztes, Huai-Ching Kuo, Jennifer Cullen, Inger L Rosner, Shiv K Srivastava, Allen Burke, Isabell Sesterhenn. Uniformed Services University of the Health Sciences, Bethesda, MD; Center for Prostate Disease Research, Rockville, MD; Joint Pathology Center, Silver Spring, MD.

Background: Although it is known that prostatic carcinomas are usually multiple, it is not well appreciated that they may be symmetric and of nearly equal size. The pathologic features and outcome of such tumors have not been studied.

Design: 1150 prostatic carcinomas were studied retrospectively from a cohort of military patients followed as part of an ongoing study. Each prostate was entirely sectioned from whole mounts according to protocol. Coronal location (anterior, lateral, posterior) and axial location (base, mid, apex) were noted and tumor volume quantitated. Pattern grade (Grade group) was assessed according to WHO 2016 criteria, and nuclear grade by WHO 2002 criteria. Codominant symmetrical tumors (CST) were on opposite sides (R v. L), did not cross the midline, and were in the same coronal and axial location. Non-codominant symmetrical tumors (NCST) met the same criteria, but were of different size (one >2X the volume of the other), one being the dominant tumor. CST and NCST were compared to carcinomas with non-symmetric dominant tumors (NSDT).

Results: There were 97 CST (8.4%) 115 NCST (10.0%) and 938 NSDT (81.6%). 67% of CST and 65% of NCST were located posterolaterally, compared to 38% of NSDT (p<.0001). CST had a mean nuclear grade of 1.89 ± .05, compared to 1.82 ± .05 for NCST, and 1.75 ± .02 for prostates with NSDT. Mean GG was 3.17 ± .13 for CST, 2.99 ± .12 for NCST, and 2.77 ± .05 for NSDT (p=.007). However, BCR occurred in 13% of CST, 20% of NCST, and 26% of NSDT. Kaplan Meier analysis showed the difference to be statistically significant (p=.008).

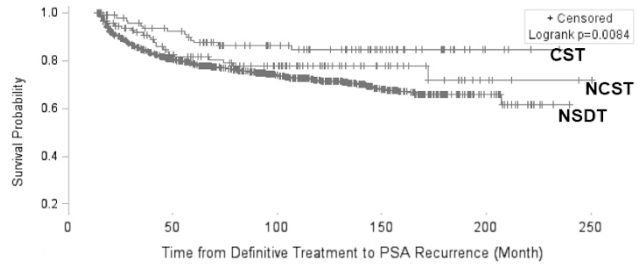

Conclusions: Symmetrical dominant tumors represent nearly 20% of prostate cancer, are usually posterolateral, are associated with a higher histologic grade, but with a better prognosis than NDST.

1077 Renal Cell Tumors with an Entrapped Papillary Component: Evidence for a Tumor-in-Tumor Collision Phenomenon

Sean R Williamson, Liang Cheng, Ramya Gadde, Matthew J Wasco, Nilesh S Gupta, Merce Jorda, Oleksandr N Kryvenko. Henry Ford Health System, Detroit, MI; Indiana University, Indianapolis, IN; St Joseph Mercy Hospital, Ann Arbor, MI; University of Miami, Miami, FL.

Background: Renal tumors with mixed morphology resembling multiple recognized renal cell carcinoma (RCC) subtypes are regarded as unclassified RCC. However, we have encountered occasional cases in which a papillary lesion (tubulopapillary hyperplasia, adenoma or RCC) appears entrapped within a larger, different tumor.

Design: We retrieved 13 renal tumors containing a papillary lesion admixed with another tumor histology. These areas were studied with immunohistochemistry (CK7, AMACR, KIT, CA-IX, vimentin, CD10, and colloidal iron).

Results: "Host" tumors were oncocytoma (n=7, Fig), chromophobe RCC (n=3), clear cell RCC (n=2), and 1 borderline oncocytoma-chromophobe tumor. The papillary component ranged from 1 to 10 mm, including 9 papillary adenomas and 3 papillary RCCs (based on cytologic atypia or size). One was an oncocytoma within a cyst (2.0 cm) with papillary hyperplasia of the cyst lining. Papillary lesions were typically diffusely CK7 positive (12/13), in contrast to oncocytoma clear cell RCCs which were CK7-negative or focally positive. AMACR exhibited greater intensity in the papillary lesions (8/10). KIT was negative in the papillary lesions and 2 clear cell RCCs and positive in 11/11 oncocytomas and chromophobe RCCs.

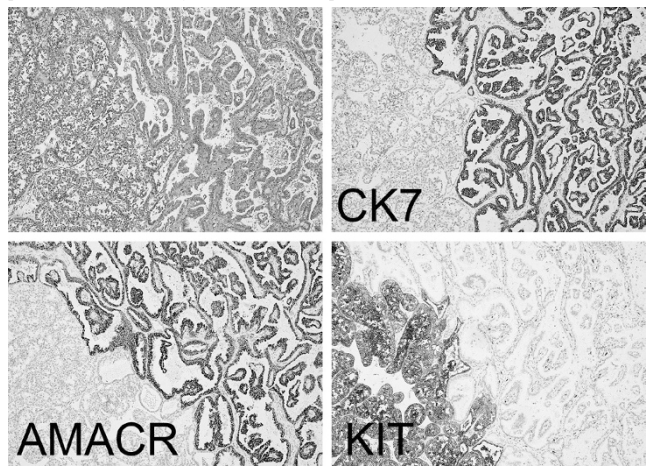

CA-IX was negative in 1 papillary lesion in a "host" clear cell RCC showing diffuse positivity. One tumor was interpreted as a single clear cell RCC with a component mimicking papillary RCC, in light of positive CA-IX and similar CK7 and AMACR in both components.

Conclusions: Entrapment of a papillary renal cell lesion within another tumor is an uncommon phenomenon with predilection for oncocytoma and chromophobe RCC. This may be related to the limited tumor pseudocapsule in these tumors and tendency to entrap benign tubules. Although mixed morphology of two distinct tumor types would warrant diagnosis of unclassified RCC, this scenario may represent a tumor-in-tumor collision phenomenon, for which diagnosing the two lesions separately may have major implications for staging and patient counseling (i.e. oncocytoma and papillary adenoma vs high-stage unclassified RCC).

1078 Monosomy 8 as a Surrogate for *TCEB1* Mutation in Renal Cell Tumors with Prominent Stroma

Sean R Williamson, Nallasivam Palanisamy. Henry Ford Health System, Detroit, MI.

Background: Recent evidence suggests that many, or perhaps all, *TCEB1* mutant renal cell carcinomas (RCCs) also exhibit loss of heterozygosity in the form of monosomy for chromosome 8. These tumors have been recognized to have some distinctive histologic features, including bands of fibrous stroma, leading some authors to speculate that a majority of tumors noted to have abundant stroma (particularly RCC with angioleiomyoma-like or smooth muscle-rich stroma) may represent this genetic entity.

Design: We studied a cohort of renal cell tumors with unusual features, emphasizing those with prominent stroma, using bacterial artificial chromosome-derived fluorescence

in situ hybridization (FISH) probes against the *TCEB1* locus and a chromosome enumeration probe for chromosome 8 (centromere). The cohort included 7 RCCs with angioleiomyoma-like stroma, 4 difficult to classify RCCs with prominent fibromuscular stroma, 5 low-stage clear cell RCCs with fibrous bands or increased CK7 positivity, and 7 tumors with borderline but imperfect features of clear cell papillary RCC.

Results: From the entire cohort (n=23), only a single tumor with borderline but imperfect features of clear cell papillary RCC (including positive CD10 staining and incomplete positivity for CK7) was found to have monosomy 8 by FISH. The remainder (n=22) demonstrated two signal pairs per nucleus.

Conclusions: Using monosomy 8 as a surrogate for the diagnosis of *TCEB1* mutant RCC, there remains a wide spectrum of renal cell tumors with prominent fibromuscular stroma that appears genetically distinct. RCC with angioleiomyoma-like (or smooth muscle-rich) stroma and *TCEB1* mutant RCC likely represent two distinct entities.

1079 Clinical Follow-Up of 37 Cases of Chromophobe Renal Cell Carcinoma with Vascular Invasion

Sara E Wobker, Christopher Przybycin, Jonathan I Epstein. University of North Carolina, Chapel Hill, NC; Cleveland Clinic, Cleveland, OH; Johns Hopkins Medical Institutions, Baltimore, MD.

Background: Chromophobe renal cell carcinoma (chRCC) has a favorable prognosis and generally presents as organ confined disease. Vascular invasion is common in other variants of renal cell carcinoma and portends a worse prognosis; however, the prevalence and significance of vascular invasion in chRCC is not well-understood.

Design: We retrospectively searched for cases of chRCC with vascular invasion mentioned in the report, which were diagnosed at 2 institutions between January 1, 2000 and December 31, 2015 with slides available for review, and obtained clinical follow-up. Presence of vascular invasion was confirmed by review of the slides.

Results: Of 609 cases of chRCC diagnosed between 2010-2015, 37 (6.2%) had vascular invasion. The patients included 19 men and 18 women with an average age of diagnosis of 55.5 years (range 35-80 years). Diagnostic specimens included 9 partial nephrectomies and 28 radical nephrectomies. Tumor size ranged from 2.2-21.0 cm (mean 10.4 cm). Nineteen of the cases had usual chromophobe cytology, without sarcomatoid or high grade features. Of the 18 cases with unusual features, 6 showed sarcomatoid features only, 8 had areas of high grade cytology exceeding the degree of atypia expected in chRCC without sarcomatoid features and 4 had both features. Positive margins were identified in 6 cases. Metastatic disease was present in 19 of the 37 cases with vascular invasion (45.9%). Clinical data was available on all cases identified with an average follow-up time of 49.4 months (range 1.0-168.0 months). Nine patients were dead at the time of last follow-up (24.3%), with 8 dead of disease and 1 dead of unknown causes. Of the 19 cases with usual chromophobe features and vascular invasion, only 1 died of metastatic disease to lung and liver. The remainder of deaths occurred in patients with sarcomatoid or high grade features.

Conclusions: The presence of vascular invasion in chRCC is often associated with other adverse features including sarcomatoid/high grade features and a high rate of metastasis. In our series of 37 cases, vascular invasion occurring in chRCC with usual cytologic features does not appear to significantly impact prognosis.

1080 Diagnostic Efficacy of 12 Core Systematic Prostate Biopsy versus Multiparametric MRI with Image Targeted Biopsy: A Retrospective Review of 133 Patients

Richard Wong, Donna Hansel, Ahmed Shabaik. University of California San Diego, San Diego, CA.

Background: Multiparametric magnetic resonance imaging with image targeted biopsy (mpMRI) is increasingly being adopted as a tool in the detection of prostate cancer. Current US guidelines for primary diagnosis biopsies recommends a 10-12 core systematic sampling of the prostate, however a critique of this method has been the diagnosis of clinically insignificant cancers. Studies comparing both methods have shown mixed results regarding the superiority of one method to the other. In this study we analyze one institutions experience comparing 12-core versus targeted biopsies within the same prostate of 133 patients.

Design: A retrospective review was performed on a series of patients who underwent mpMRI/transrectal ultrasound image-fusion guided biopsy of the prostate. Clinical, MRI, and tissue pathology data was reviewed and compared. Radiologists reported MRI studies using a modified PIRADS scoring system. Biopsies were performed by Urology surgeons using transrectal ultrasound and MRI image fusion technology. Image targeted biopsies were performed in addition to 12-core systematic sampling. All core biopsies were evaluated by experienced GU pathologists. Statistical significance was calculated with McNemar's Chi-Square Testing.

Results: 133 patients comprising a total of 1758 biopsy cores were reviewed. In this cohort 162 PIRADS scored lesions were identified. In patients where at least Gleason score 6 (3+3) prostatic adenocarcinoma was identified, 12-core sampling identified a higher Gleason score lesion 43% of the time within the same prostate. This trend was consistent across all stratifications of PIRADS scores. In targets assigned a PIRADS score of 3-5 (intermediate-high suspicion), targeted biopsy was positive for malignancy in 56% of patients. In the same patients 12-core sampling was positive for malignancy in 69% of patients. In targets with a PIRADS score of 4-5 there was no statistical difference in the ability to identify malignancy, 75% in PIRADS vs 73% in 12-core.

Conclusions: mpMRI with image targeted biopsy has been proposed as an alternative to 12-core systematic sampling. Analysis of biopsy cores from 133 patients assessed with both methods showed 12-core was a superior method of sampling in identifying any malignant lesion as well as higher grade lesions. Although this is contrary to some published studies, the variability in image fusion technology as well as the clinical department sampling the tissue, may account for differing conclusions in the literature.

1081 Identification of MicroRNA Signature for Aggressive Prostatic Adenocarcinoma

Huiqing Wu, Xiwei Wu, Jennifer Jin, Tommy Tong, Przemyslaw Twardowski, Arthur Li, Chao Guo, Yuping Li, Rebecca Nelson, Young Kim, Jinhui Wang, Bertram Yuh. City of Hope, Duarte, CA.

Background: Prostate cancer (PC) is the most common cancer diagnosed and 2nd most likely cause of cancer death in American men. While many men harbor tumors that are indolent even in the absence of therapy, others experience disease recurrence or/and metastasis which are difficult to predict reliably based on clinical manifestations, pathologic findings or other currently available laboratory tests. It is clinically critical to develop molecular biomarkers which can early differentiate patients with aggressive and indolent PC. These biomarkers may help to guide patients with aggressive PC for suitable clinical trials, and patients with indolent disease for alternative local treatment or watchful waiting to avoid unnecessary prostatectomy.

Design: (1) We used formalin-fixed paraffin-embedded (FFPE) tissue for the study. (2) We established a training cohort of indolent and aggressive PC specimens (n=38). We used a group of localized PCs with Gleason scores 6-8 (T2a-c, n=23) from prostatectomy specimens to represent the indolent disease, in which all the patients had been followed for at least 10 years with no metastasis/recurrence developed. We used metastatic PCs (M1, n=15) taken from distant metastatic organs to represent the aggressive disease. (3) We made an independent cohort of metastatic PC in regional lymph nodes (N1, n=20). (4) We performed small RNA deep sequencing of all 58 specimens. (5) We analyzed the miRNA expression in the training cohort specimens with univariate regression, leave-one-alone (LOA) and risk score method to build a miRNA signature for aggressive PC. (5) We examined the power of the signature using the independent cohort of metastatic PC in regional lymph nodes.

Results: (1) We identified miRNAs highly associated with PC metastasis. (2) We built a miRNA signature specifically for aggressive PC. This signature had a mathematic (risk score) formula weighed by the expression of miR-18a-5p, miR-37a-3p, miR-106b-5p, 130a-3p and 135a-5p with defined risk score cutoff to determine/predict the risk status of PC metastasis/recurrence (aggressive disease). (3) We tested the signature algorithm using the independent cohort of metastatic PC samples from regional lymph nodes and founded that the signature correctly predicted 19 out of 20 (19/20) cases to be aggressive PCs (sensitivity=95%).

Conclusions: We identified a 5-miRNA signature for aggressive PC. The signature is ready for further validation and may help for early identification of patients with aggressive PC in the near future.

1082 Clinicopathologic Correlation of Metastatic Prostatic Adenocarcinoma with Emphasizing Effects of Prognostic Grade, Extraprostatic Extension and Neoadjuvant/Adjuvant Therapy on the Onsets of Distant Metastasis

Bo Xu, Ramayee Periakaruppan, Jinrong Cheng, Yingdong Feng. Roswell Park Cancer Institute, Buffalo, NY; State University of New York at Buffalo, Buffalo, NY.

Background: Prostate adenocarcinoma is the most commonly diagnosed cancer and the second leading cause of cancer-related deaths in men in the United States. Most prostate cancer–related deaths are due to advanced disease, such as local spread and distant metastasis. In this study, we examine effects of prognostic grade, extraprostatic extension (EPE) status and neoadjuvant/adjuvant therapy on the onset of distant metastasis of prostatic adenocarcinoma.

Design: Seventy eight cases of metastatic prostatic adenocarcinoma were retrieved from pathology archive between 2005 and 2016. Patient history was reviewed from electronic medical record. Tumor Gleason scores from radical prostatectomy (RP) or biopsy specimen were converted to prognostic grade group (PGG). Time intervals between initial diagnosis and onset of distant metastasis were collected. Tukey's method, chi-square and t-tests were used to evaluate the association between each PGG group and time interval for development of distant metastasis, EPE status and therapy effects on time of intervals for onset of distant metastasis, respectively.

Results: Among 78 patients, there were 30 with local positive lymph nodes and 48 patients developed distant metastasis (bone, soft tissue, lung and liver). Within distant metastasis, 19 cases with EPE, 29 without EPE; 44 patients received neoadjuvan/adjuvant therapy and 4 without therapy. No case was assigned PGG I. The time interval of developing distant metastasis for PGG II is significantly longer than PGG III, IV and V (128 months vs, 61, 49 and 37 months, $p = 0.02$, 0.03 and 0.002 for each comparison group), whereas no statistic differences of time intervals were found between PGG III, IV and V ($p > 0.05$ for each comparison group). In addition, time intervals between EPE vs non-EPE groups and neoadjuvan/adjuvant therapy vs non-therapy groups did not show significant statistic differences ($p > 0.5$).

Conclusions: In this study, we demonstrated that PGG II patients have significant longer interval between initial diagnosis of prostatic adenocarcinoma and onset of distant metastasis comparing that of PGG III and higher groups. EPE status and neoadjuvan/adjuvant therapy have no significant effects on tintervals of developing distant metastasis.

1083 The Relationship Between Tobacco Smoking and Clinicopathologic Features of Bladder Urothelial Carcinoma with Emphasis on Variant Histology

Jianmin Xu, Giovanna Giannico, Peter E Clark, Omar Hameed, Lan L Gellert. Vanderbilt University Medical Center, Nashville, TN.

Background: It has been well established that tobacco smoking is among the common risk factors for bladder urothelial carcinoma (UC). However, there are limited data regarding the relationship between smoking and clinicopathologic variables of bladder carcinoma, specifically variant histology. In this study, we investigated the correlation between smoking and variables of bladder UC.

Design: We retrospectively identified 471 consecutive cystectomies performed at our institution from 2007 to 2011. Pathological features were reviewed by GU pathologist. Histologic variants were classified using strict diagnostic criteria as defined by the WHO. Clinical data were collected from electronic medical records. Statistical analysis was performed with STATA (v13.1).

Results: Of the 471 patients, 16% (77/471) were non-smokers and 84% (394/471) were smokers, including 33% (131/394) current smokers and 67% (263/394) former smokers. 34% (160/471) exhibited variant morphology. Overall, smoking was significantly associated with bladder cancer in men, with M:F ratio of 5.4 vs. 1.5 in smokers vs. non-smokers ($p<0.001$). 63% (247/394) of smokers had muscle invasive diseases compared to 51% (39/77) of nonsmokers, but the difference was not significant ($p=0.056$). No statistically significant correlation was identified between smoking and age ($p=0.1$), nodal metastasis ($p=0.97$) or variant histology ($p=0.79$). Breaking down by variant subtype (table1), micropapillary was significantly more common in smokers (29/30) ($p = 0.04$), although the difference was not statistically significant after controlling for pT stage in multivariate analysis ($p = 0.11$). No significant difference was identified in this cohort between former and current smokers regarding pT, nodal metastasis or variant histology.

Conclusions: Tobacco smoking is commonly associated with bladder UC in men. Tobacco smoking may have a stronger association with micropapillary variant compared to other histologic variants, although stage seems to be a contributing factor as well.

	Total	Non Smokers (%)	Smokers (%)	p
N	471	77 (16)	394 (84)	
Histologic Variant	160	27 (35)	133 (34)	0.79
Variant subtype				
Squamous	58	15 (26)	43 (74)	0.06
Micropapillary	30	1 (3)	29 (97)	0.04
Glandular	24	5 (21)	19 (79)	0.57
Sarcomatoid	22	3 (14)	19 (86)	0.99
Plasmacytoid	17	3 (18)	14 (82)	0.75
NE/small cell	7	0 (0)	7 (100)	0.61

1084 Urothelial Carcinoma In-Situ of the Bladder with Glandular Differentiation: Report of 92 Cases

Zhiming Yang, Jonathan I Epstein. The Johns Hopkins Hospital, Baltimore, MD.

Background: Urothelial carcinoma in-situ (CIS) of the bladder with glandular differentiation (CIS-GL) is a rare variant of CIS. Its histological features and prognosis have been reported in only a couple of prior series, which showed an association with concurrent small cell carcinoma and invasive urothelial carcinoma (UC).

Design: CIS-GL Only: We identified 27 cases of CIS-GL from the consult files of one of the authors from 2008 to 2015. No patient had a prior or co-existing invasive UC at the time of diagnosis. Mean patient age at diagnosis was 75.8 years (range: 64 to 89 y) and male-to-female ratio was 7:1. CIS-GL & Invasive Carcinoma: We also identified 65 additional cases with concurrent CIS-GL and invasive carcinoma.

Results: CIS-GL Only: Follow-up time ranged from 11 to 81 months (mean 38.7). One living patient refused to release her disease status and 2 cases were lost to follow-up. Of 24 cases with follow-up information, 13 (54.2%) had no evidence of disease at last follow-up. Treatment modality was typically induction and maintenance BCG and follow-up cystoscopy. 3 (12.5%) patients underwent radical cystectomy due to disease progression. 2 (8.3%) patients had recurrent CIS, and 1 (4.2%) had recurrent non-invasive low-grade papillary UC; these patients underwent TURB and BCG treatment. 2 (8.3%) patients died of metastatic UC, and 3 (12.5%) died of other causes or unknown causes. Of note, none of the patients developed small cell carcinoma. CIS-GL & Invasive Carcinoma: The invasive carcinoma was pure UC in 29/65 (45%) cases. In 13/66 (20%) cases, the invasive UC showed glandular differentiation. The next largest group was with co-existing small cell carcinoma in 8/66 (12%). A few cases each were seen of the following variants: plasmacytoid (4); sarcomatoid (3); signet ring (3); micropapillary (2); squamous (2); and signet ring with colloid features (1).

Conclusions: Patients with CIS-GL w/o invasive carcinoma are at significant risk for cancer progression and in a minority of cases at risk for death from bladder carcinoma, similar to usual CIS. Typically, subsequent invasive carcinoma is UC rather than adenocarcinoma. Similarly, the largest fraction of concurrent invasive carcinoma and CIS-GL is UC. However, this study for the first time demonstrates the wide spectrum of other variants that co-exist with CIS-GL including a sizeable minority of cases with invasive UC with glandular differentiation. Although there is a disproportionately high fraction of CIS-GL with co-existing small cell carcinoma, small cell carcinoma does not seem to develop following a diagosis of CIS-GL.

1085 Comparative Analysis of Histologic and Molecular Features of MRI-Visible and MRI-Invisible Gleason Score 3+4=7 Prostate Cancer

Helene Yilmaz, Andrei Purysko, Zaid Haddad, Mandeep Takhar, Kasra Yousefi, Nicholas G Erho, Beatrix Palmer-Arontsen, Elai Davicioni, Jesse K McKenney, Christopher Przybycin, Eric A Klein, Cristina Magi-Galluzzi. Douglass Hanly Moir Pathology, Sydney, Australia; Cleveland Clinic, Cleveland, OH; GenomeDx Biosciences, Vancouver, Canada; Glickman Urological Institute, Cleveland, OH.

Background: Multiparametric magnetic resonance imaging (MRI) is increasing used in pre-treatment prostate cancer (PCA) diagnosis. Prostate Imaging Reporting and Data System version 2 (PI–RADS)[PI] scoring indicates likelihood of carcinoma in lesions identified on MRI (PI 1-5, from extremely unlikely to extremely likely). As most Gleason score (GS) $\geq$ 4+3=7 PCAs are MRI-visible, we compared histologic and molecular features of 3+4=7 PCA identified on radical prostatectomy (RP).

Design: 32 GS 3+4=7 PCAs on RP were identified in 27 patients with paired MRI. MRIs were scored by a single radiologist and correlated with pathology findings annotated on RP maps reconstructed by a single uropathologist. Location, GS and pathologic stage was recorded. MRI categories were MRI-invisible (PI 1-2) and MRI-visible (PI 4-5); PI 3 lesions were excluded. Histological analysis included estimation of tumor volume, percent pattern 4, architectural patterns (cribriform, glomeruloid, fused, poorly formed glands), background and a semi-quantitative analysis of tumor stroma and glandular components. Twenty-five tumors were evaluated for gene expression and Decipher genomic classifier.

Results: 17 tumors were MRI-invisible, 15 MRI-visible. All MRI-invisible and 12 MRI-visible tumors were organ-confined. 94% of MRI-invisible lesions were in transition (TZ), 6% in peripheral zone (PZ); 60% of MRI-visible lesions were in TZ, 33% in PZ, 7% in anterior zone (**p=0.041**). MRI-visible tumors had larger volume (mean 1.4 vs 0.3 cm3, **p<0.001**), greater percent pattern 4 (mean 21.3 vs 13.2, **p= 0.047**) and more frequently glomeruloid and poorly formed glands (**p=0.033** and **p=0.018**, respectively), compared to MRI-invisible. There was significant difference in stroma-to-glandular ratio in MRI-visible vs MRI-invisible tumors. MRI-visible tumors (n=12) tended to cluster together based on differentially expressed genes and 25% were classified as high-risk for metastasis by Decipher genomic classifier, compared to 0% for MRI-invisible.

Conclusions: Our findings indicate that GS 3+4=7 MRI-visible and MRI-invisible PCAs are histologically distinct. Location, tumor volume, architectural pattern and stroma-to-glandular ratio may account for visibility of lesions seen on MRI. Only MRI-visible tumors were designated as "high-risk for metastasis" by genomic classifier.

1086 Fluorescent In Situ Hybridization Analysis of Sarcomatoid Carcinoma of the Prostate

Ramin Zargham, William R Sukov, John C Cheville, Rafael E Jimenez. Mayo Clinic, Rochester, MN.

Background: Sarcomatoid carcinoma of the prostate (SCP) is a rare form of prostate cancer known for its aggressive clinical course with diagnostic and treatment difficulties. The molecular mechanisms responsible of progression of adenocarcinomas (AC) to a sarcomatoid phenotype are incompletely understood. Numeric alterations of chromosome 10 and deletions of p53 have been implicated in sarcomatoid transformation of renal cell carcinomas. Chromosome 10 harbors members of integrin family of cell adhesion receptors, as well as the gene PTEN, associated with aggressive behavior in prostatic AC. We decided to investigate genomic alterations that can potentially participate in sarcomatoid phenotype, by utilizing fluorescent in situ hybridization (FISH).

Design: We identified six SCP from our files; all had a Gleason 9-10 epithelial component and a high grade pleomorphic spindle cell component. Mean age was 69 (range 40-85). 3 cases had a previous diagnosis of AC (time between the initial diagnosis of AC and the diagnosis of SCP ranged from 2 to 64 months), while 3 presented de novo as SCP. All patients died of disease between 4-13 months after the first biopsy-proven sarcomatoid change. FISH analysis was performed on paraffin-embedded tissue using centromeric probes for chromosomes copy number, a unique PTEN fluorescence in situ hybridization probe set that would detect as many structural variants as possible (see Mod Pathol 2016; 29:143–156), and a dual color FISH probe for p53 deletion analysis. 50 interphase nuclei for each case was scored by two technicians in a blinded manner. Results were compared to those of six Gleason 10 AC from age-matched patients (61-85 years old).

Results: 3/6 SCP cases demonstrated gain of chromosome 10 copy number. 4/6 SCP cases showed deletion of PTEN, and deletion of p53 was demonstrated in 3/6 SCP. The abnormalities were seen exclusively in SCP, being absent in all cases of the control group of AC.

Conclusions: Gain of chromosome 10 and p53 deletion are common findings in SCP, suggesting a possible role in the transformation from epithelial to sarcomatoid phenotype. The role of PTEN deletion in this phenomenon is less clear, as our control group had an unusual low prevalence of this abnormality. We are in the process of performing additional analysis using next generation sequencing and whole exome studies investigating possible genes involved in this transformation.

1087 Percentage of Germ Cell Tumor Components in Non-Seminomatous Germ Cell Tumor: Clinical Significance in Current Treatment Era

Miao Zhang, Hasan Samra, Shi-MIng Tu, Pheroze Tamboli. MD Anderson Cancer Center, Houston, TX; Medical College of Wisconsin, Milwaukee, WI.

Background: Current recommendations for germ cell tumor (GCT) reports include the percentage of different GCT components. Accurate evaluation of percentage of each component can be subjective, due to overlapping histological features of some components. The purpose of this study is to determine whether reporting percentage of GCT component is of clinical significance.

Design: We evaluated 587 consecutive patients with non-seminomatous GCT (NSGCT) treated at our center between 2000 and 2010. Tumors were evaluated for: percentage of Choriocarcinoma (C), Embryonal carcinoma (E), York sac tumor (Y), teratoma (T), seminoma (S); lymphovascular invasion, invasion of rete testis, epididymis, spermatic cord or tunica vaginalis. Follow-up information was obtained from medical records.

Results: The mean age at diagnosis was 28.5 years (15-56 years). Of 587 cases, pathological data was confirmed in 330 cases. Among stage I patients (n=171), there were pure E (n=24); pure Y (n=1); pure T (n=5); EYT (n=86); EYST (n=26); ES (n=20); ESY (n=9) cases. Among stage II patients (n=99), there were pure E (n=23); pure T (n=6); EYT (n=30); EYST (n=13); EY (n=13); SYT (n=2); ST (n=8); ESY (n=4) cases. Among stage III patients (n=60), there were pure C (n=3); pure Y (n=5); pure E (n=19); pure T (n=10); ES (n=3); ST (n=2); EYT (n=6); ESY (n=4), and EYST (n=8) cases. Clinically, stage I patients were observed with only 7 patients (4%) relapsed and 6 (3.5%) died of disease (ES, n=1; ESY, n=1; EYT, n=3; ESYT, n=2). Stage II patients had chemotherapy with 13 patients (13%) relapsed and 8 patients (8%) died of disease (EYT, n=4; SYT, n=1; ST, n=1; T, n=1; EY, n=1; ESY, n=1; ESYT, n=4). Stage III patients also had chemotherapy with 53 patients relapsed and 33 died of disease (EYST, n=8; EYT, n=6; Y, n=2; pure C, n=3; ESY, n=4; ECYT, n=2; ECT, n=1; CY, n=1; SY, n=1; ES, n=1). Statistical analysis showed no significant difference between the percentages of each GCT component and relapse/death (p=0.3).

Conclusions: In modern treatment era, patients with NSGCT are treated with surgery followed by surveillance and/or chemotherapy, depending on stage. With current treatment protocols, less than 10% of patients with stage I and II died of disease. In our series, the percentage of GCT component did not influence treatment/prognosis. Therefore, reporting GCT percentages may not be necessary for these tumors.

1088 Renal Cell Carcinoma with Hemangioblastoma-Like Features: A Clinicopathologic Study of 4 Cases

Ming Zhao, Xiaoming Qiu, Minghua Fan, Lianghong Teng, Dengfeng Cao. Zhejiang People's Hospital, Hangzhou, China; Fujian Longyan First Hospital, Longyan, China; Beijing Xuanwu Hospital, Beijing, China; Washington University School of Medicine, Saint Louis, MO.

Background: Renal cell carcinoma with hemangioblastoma-like features (RCC-HB-like) are very rare (only 3 cases reported). Here we present the clinicopathologic features of 4 such cases.

Design: Four RCC-HB-like cases were included. Patient age, gender, presentating symptoms, tumor laterality, tumor size, gross appearance and microscopic features were recorded. Immunohistochemical (IHC) stainings for AE1/AE3, CAM5.2, CK7,EMA, P504S, RCC, CD10, carobonic anhydrase IX (CA-IX), PAX2, PAX8, S100, and inhibin were performed.

Results: The mean age was 36 years (27 to 44 years, 3 females and 1 male). One patient presented with flank soarness/pain for 1 year and other three tumors were incidentally discovered (2 in left kdiney, 2 in right, 3 total and 1 partial nephrectomy). The mean tumor size is 3.0 cm (1.0 to 4.0 cm). Grossly the tumors are grey to brownish. Microscopically all 4 tumors show 2 distinct components. The 1st component (1-20%, mean 8%) is conventional RCC in which tumor cells are arranged in tubules and nests (4/4), small cysts (3/4) and papillary structures (focal in 2/4, complex in ¼). The tumor cells have clear or mixed clear and eosinophilic cytoplasm with ISUP nuclear grade 2 or 3. The 2nd component shows HB-like features with a solid growth pattern and a rich capillary network. The tumor cells are oval to short spindled with delicate to pale chromatin and occasional visible nucleoli and nuclear grooves. No mitotic activity is seen. Their moderate to abundant cytoplasm is pale to eosinophilic with intracytoplasmic vacuoles. The IHC profiles are summarized in table 1.

Marker	Conventional RCC area	HB-like area
CK-AE1/AE3	4/4 (100% cells)	4/4 (40-70%)
CAM5.2	4/4 (40-100% cells)	0/4
CK7	2/3 (100%)	0/3
EMA	3/4 (80-100%)	3/4 (2-5%)
P504S	1/3 (30%)	0/4
RCC	2/3 (5-100%)	3/3 (1-2%)
CD10	3/3 (90-100%)	3/3 (50-70%)
PAX2	3/3 (70-100%)	3/3 (40-60%)
PAX8	4/4 (90-100%)	4/4 (1-40%)
CA-IX	3/3 (90-100%)	3/3 (90-100%)
S100	0/4	4/4 (70-90%)
Inhibin	0/4	4/4 (15-90%)

Conclusions: The HB-like component is morphologically distinct from the conventional component. Besides retaining some IHC profile of RCC, it also acquires IHC profile of HB and may represent an intermediate step between RCC and HB. Its relationship with the conventional component awaits for further molecular analysis (ongoing).

1089 Prostate Neuroendocrine Tumors: Clinicopathological Study of 15 Cases with Emphasis on the Neuroendocrine Tumors of the "Intermemdiate Grade" and Overlapping Features

Yani Zhao, Fang-Ming Deng, Hongying Huang, Peng Lee, Jonathan Melamed, Ming Zhou, Ming Zhou. New York University Langone Medical Center, New York, NY.

Background: 2016 WHO classifies prostate neuroendocrine (NE) tumors as prostate carcinoma with NE differentiation, well-differentiated (carcinoid), small cell (SmCC) and large cell (LCC) neuroendocrine carcinomas. In contrast to the lung counterparts, intermediate grade (atypical carcinoid) is not recognized in prostate classification. We report the clinicopathological features of 15 prostate NE tumors and identified one tumor with intermediate morphology.

Design: We searched our surgical pathology file for prostate cases with diagnosis of SmCC, "NE carcinoma", "NE features or differentiation" and cases for which IHC for NE markers were performed from 2002 to August 2016. Cases were retrieved and reviewed for morphology, IHC stains, clinical and followup results. Classification was based on the 2016 WHO criteria. Tumors with mitosis 2-20/2mm^2 or Ki-67 index 20-50% were labeled as "intermediate grade" NE carcinoma (iNEC). Tumors with morphologic overlap between NE and acinar carcinoma were diagnosed as "PCa with overlapping features". Metastatic carcinoma to the prostate with NE differentiation was excluded.

Results: 15 prostate NE tumors were identified out of 5256 (0.29%) prostate cancer cases. There were 9, 1, 2 and 3 cases of SmCC, iNEC, Paneth cell-like NE differentiation and PCa with overlapping features. SmCC and iNEC patients were older than the other two groups (74.1 and 72.0 vs 66.0 and 67.7 years). 5/9 SmCC and 2/6 of other tumors had history of PCa with treatment. The iNEC tumor had a mitosis 3/mm^2 and Ki-67 labeling 15%, was positive for NE markers but negative for prostate markers. The patient was alive without disease 35 months after surgery. 3 tumors with overlapping features all had tumor cells showing cytological and nuclear features intermediate between acinar and NE carcinomas and expressed both prostate and NE markers.

Conclusions: Prostate NE tumors are rare and comprise a morphological spectrum. SmCC is most common. We also report a case of intermediate grade NEC and 3 tumors with overlapping features of acinar PCa and NEC. Our study suggests 2016 WHO classification of prostate NEC should be expanded to include these additional NEC entities.

1090 Gleason Score 3+4=7 Prostate Carcinomas Detected by MRI-Targeted Biopsies Contain Higher Percentage of Pattern 4 and Are Less Likely to Be Upgraded in Radical Prostatectomies

Yani Zhao, Fang-Ming Deng, Hongying Huang, Peng Lee, Jonathan Melamed, Ming Zhou. New York University Langone Medical Center, New York, NY.

Background: In Gleason score (GS) 7 prostate carcinoma (PCa), % of pattern 4 is an important prognostic factor and may also influence treatment decisions. Standard sextant (SBx) and MRI-targeted biopsies (TBx) have a similar cancer detection rate; however TBx detects more aggressive cancer. This study investigated whether GS 3+4=7 prostate carcinoma (PCa) detected by TBx may have a higher pattern 4 % and more likely to have a concordant GS in the radical prostatectomy (RP).

Design: We routinely document % of pattern 4 in prostate biopsy reports for PCa with GS3+4 and 4+3. We searched our surgical pathology file for prostate biopsies with GS 3+4 and 4+3 PCa with % pattern 4 documented. Biopsy results, including GS and % of pattern 4, were recorded. Subsequent RP, if performed, were retrieved for review of GS, pathologic stage, dominant tumor nodule size. GS upgrading is defined as higher RP GS than the highest GS in any biopsy cancer cores.

Results: 190 biopsies with both SBx and TBx were included in this study. PCa was detected by TBx in 170 (89.5%) and by SBX in 184 (96.8%). Significantly more GS 7 PCa was detected by TBx than by SBx (133/170 vs 115/184, p=0.002). The % pattern 4 in GS3+4 PCa detected by TBx was significantly higher (13.7$\pm$0.14% vs 10.5$\pm$0.13% by SBx, p=0.016). TBx detected significantly more cases with $\geq$5% pattern 4 than SBX (64/133 vs 23/115; p=0.001). 34 patients subsequently had RP. Fewer GS upgrading was observed when comparing TBx and RP GS (5/34 vs 14/34, p=0.029). SBx with $\leq$10% pattern 4 was more likely to have GS upgrading in RP than those with >10% pattern 4 (13/21 vs 1/13, p=0.002). SBx with $\leq$20% pattern 4 had a similar risk of GS upgrading in RP as those with >20% pattern 4 (13/26 vs 1/8, p=0.067). In TBx, neither these cutpoints were associated with RP GS upgrading.

Conclusions: TBx detects higher % pattern 4 in GS 3+4 PCa therefore more aggressive PCa. GS rendered on TBx is more concordant with the final RP GS. $\leq$10% pattern 4 in SBx is associated with GS upgrading in RP, suggesting a possibility of GS upgrading should be considered for a GS3+4 PCa with $\leq$10% pattern 4 diagnosed on SBx.

1091 Heterogeneity of Neuroendocrine Differentiation in Prostate Adenocarcinoma: A Study on Whole-Mount Radical Prostatectomy Specimens

Menglei Zhu, Wei Chen, Sanjay Gupta, Gregory T MacLennan. University Hospitals Cleveland Medical Center, Cleveland, OH; Case Western Reserve University, Cleveland, OH; University Hospitals Cleveland Medical Center, Cleveland, OH.

Background: Neuroendocrine differentiation (NED) has been recognized in prostatic adenocarcinomas, in addition to small cell neuroendocrine carcinomas and carcinoid tumors of the prostate. NED has been shown to increase in high-grade and high-stage prostate cancers. However, the prognostic value of NED in prostate adenocarcinoma is not well understood due to conflicting results in reported studies. Genomic and transcriptomic studies have suggested that there is intra-tumor heterogeneity of neuroendocrine differentiation in prostatic adenocarcinoma. We hypothesize that the heterogeneous nature of NED may contribute to the difficulty in predicting outcomes in morphologically similar prostate cancer specimens.

Design: Thirty-six radical prostatectomy cases with a diagnosis of prostatic adenocarcinoma were chosen from our archival specimens, including 18 patients who developed recurrent cancer after curative surgery, and 18 patients whose cancers did not recur during matched follow up times. NED was evaluated by performing immunohistochemistry (IHC) for Chromogranin A (CgA). 10 cancer areas are randomly selected on each whole mount section, and the CgA IHC staining intensity in these areas was graded as 0-5.

Results: Significant intra-tumoral heterogeneity of CgA staining intensity was observed, as illustrated in Figure 1A. The cumulative CgA scores from 10 areas were higher in specimens from patients whose cancers relapsed, as compared with specimens from patients whose cancers did not recur. Mean cumulative CgA score is 18.72 ± 2.78 in the relapsed group and 8.28 ± 1.44 in the remission group. (Figure 1B and C)

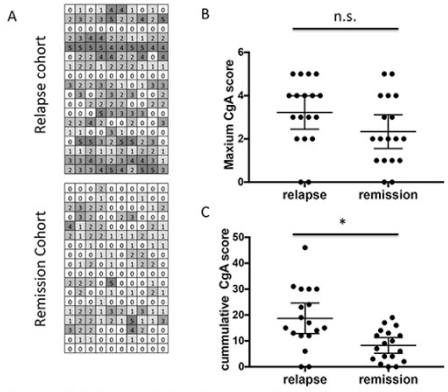

Figure 1: **A)** CpA scores of all specimens are illustrated as each row represents one specimen and each column represents one randomly selected area. **B)** Highest scores in each samples are plotted. **C)** Cumulative scores from 10 random areas are plotted. * P<0.05

Conclusions: This study reveals that intra-tumor heterogeneity of NED exists in prostate adenocarcinoma and influences the precise evaluation of NED in clinical samples. Though the data is not conclusive, we do observe a lower level of NED in patients with remission compared to patients with relapsed cancer by thorough evaluation of NED in prostate whole mount sections. This study potentially provides guidance to clinical usage of NED in prostate adenocarcinoma.

Gynecologic and Obstetric Pathology

1092 Ovarian Granulosa Cell Tumors: A Surveillance, Epidemiology and End Results (SEER) Data Review of Prognostic Clinicopathological Parameters in 1815 Patients

Eman Abdulfatah, Marcel T Ghanim, Oumaima Chaib, MHD Fayez Daaboul, Baraa Alosh, Khaleel I Al-Obaidy, Zaid Mahdi, Kinda Hayek, Sharif Sakr, Adnan R Munkarah, Sudeshna Bandyopadhyay, Rouba Ali-Fehmi. Wayne State University School of Medicine, Detroit, MI; Karmanos Cancer Center/Wayne State University, Detroit, MI; Henry Ford Health System, Detroit, MI.

Background: Ovarian granulosa cell tumors (GCTs) represent approximately 2-5% of all ovarian cancers. The prognostic indicators of GCT are still controversial. The aim of this study is to identify the clinico-pathological variables affecting prognosis and survival outcome in patients with GCT.

Design: SEER database was searched for patients diagnosed with Adult (AGCT) and Juvenile (JGCT) Granulosa Cell Tumors. Demographic characteristics and prognostic factors including age, race, marital status, FIGO stage, surgery, tumor size and lymphadenectomy were analyzed using Log-Rank, Cox regression and Kaplan-Meier survival analyses.

Results: 1794 and 21 patients were identified with AGCT and JGCT, respectively. Of all the AGCT patients, 1081 (60.2%) were surgically-unstaged while 395 (22%), 80 (4.5%), 158 (8.8%) and 80 (4.5%) were stages I, II, III and IV, respectively. Patients with AGCT > 50 years of age had better 10-year OS (85.3% vs. 63.8%, P <0.05)(HR2.4 ,P:0.003), whereas patients with JGCT had a 3-year OS of 63.4%. Surgically-staged I-II patients had better survival compared to non-staged and those with advanced stage III-IV (HR 10.6,P=0.0005) (10-year OS 93.8%, 69.9%, 49.4% respectively; P<0.05). No survival difference was noted between stage IA,IB and stage IC nor between Caucasians and African Americans. Patients with tumors greater than 5cm had significantly worse 10-year OS (98.1% vs 85.1%, P<0.05). Lymphadenectomy in AGCT was associated with significantly better OS (89.8% vs. 71.2%, P<0.05). Cox regression analysis revealed that older age (> 50 years), early stage and lymphadenectomy were independently associated with better OS (HR 0.41, 0.01, and 0.49; P<0.05 respectively). Clinically stage I (surgically-unstaged) patients had worse 10-year OS compared to those with surgical stage I (70.3 vs 89.3%, P<0.05).

Conclusions: Age, stage and lymphadenectomy were independent predictors of survival outcome in patients with ovarian granulosa cell tumor.

1093 Mucinous Differentiation Is Predictive of Improved Outcomes in Low Grade Endometrioid Carcinoma

Eman Abdulfatah, Sudeshna Bandyopadhyay, Oumaima Chaib, Andres A Roma, Denise Barbuto, Elizabeth Euscher, Bojana Djordjevic, Elizabeth E Frauenhoffer, Delia P Montiel, Anais Malpica, Elvio Silva, Rouba Ali-Fehmi. WSU, Detroit, MI; UC, San Diego, CA; CSMC, LA, CA; MDAnderson, Houston, TX; Ottawa, Ott, ON, Canada; Penn State, Hershey, PA; I N C, Mexico, Mexico.

Background: Endometrioid carcinoma(EC) is often associated with squamous or mucinous (MUC)differentiation(diff). The significance of MUC-diff in EC is yet to be determined. The aim of this study was to correlate the presence of MUC-diff with clinicopathologic features of a large multi-institutional cohort of low grade EC(LGEC) and its impact on clinical outcome.

Design: Retrospective review of LGEC(G1or2)(n=593) from 1991-2011 at 9 institutions was conducted to evaluate clinicopathologic parameters:age, tumor size, stage,depth and pattern of myometrial invasion(MI),necrosis,papillary architecture,squamous and MUC-diff,lymphovascular invasion(LVI),lymph node involvement and outcomes. MUC-diff was defined as ≥10% cells with intracellular mucin. Data was analyzed.

Results: Pts' median age was 61(22-91)yrs. MUC-diff was identified in 38%. Although pts with MUC-diff were significantly older(>60yrs) and their tumors showed more papillary architecture and MELF pattern of MI with lack of necrosis(P=0.001,P=0.001,P=0.020,P=0.005,respectively), they had a significantly lower recurrence rate (16% vs 23%, P=0.044). While tumors with only papillary showed poor prognosticators including tumor size > 6cm,advanced stage,deep MI,necrosis,MELF pattern and LVI(P=0.003,P=0.001,P=0.05,P=0.001,P=0.001 and P=0.001), combining both MUC and papillary features showed significantly lower recurrence rate(14% vs 23%,P=0.009). Although not significant, the presence of MELF in a separate analysis of patients with absence of MUC-diff showed worse outcome(mean DFI:122 vs 138 mths).

	Variable	MUCabsent N=366(%)*	MUCpresentN=227(%)*	P
Stage	I-II III-IV	239(65)127(35)	150(66)77(34)	0.859
MI	<50%≥50%	220(60)145(40)	129(57)97(43)	0.248
Necrosis	YesNo	142(39)223(61)	113(50)113(50)	0.005
Papillary	YesNo	201(55)164(45)	171(75)56(25)	0.001
MELF	YesNo	159(46)190(54)	123(56)98(44)	0.020
Squamous diff	YesNo	173(47)193(53)	118(52)109(48)	0.273
LVI	YesNo	178(49)187(51)	120(53)107(47)	0.353
LN	YesNo	88(24)278(76)	65(29)162(71)	0.247
Recurrence	YesNo	82(23)273(77)	36(16)188(84)	0.044
* Some missing data				

Conclusions: In this large series of LGEC, the presence of MUC-diff was associated with better outcomes despite the presence of poor prognostic factors including old age, papillary architecture and MELF pattern.

1094 Predictive Histologic Factors in Carcinosarcoma of the Uterus: A Multi-Institutional Study

Eman Abdulfatah, Leonardo Lordello, Muhammad Khurram, Kinda Hayek, Koen Van de Vijver, Lamia Fathallah, Sudeshna Bandyopadhyay, Rouba Ali-Fehmi, Esther Oliva. WSU, Detroit, MI; MGH, Boston, MA; St.J, Detroit, MI.

Background: Uterine carcinosarcomas (CSs) are rare aggressive biphasic neoplasms. While studies support that carcinomatous components predict outcome, others do not. The aim of this study is to evaluate the clinical and histopathological features of a large multi-institutional cohort of CSs.

Design: A retrospective review of CSs (n=196) from 1990 to 2012 at 3 institutions was conducted to analyze: histologic subtype, grade and % of carcinomatous and sarcomatous components, presence of homologous/heterologous elements, necrosis, depth of myometrial invasion (MI), and histologic components upon recurrence. Data was analyzed using Cox-regression and Kaplan-Meier survival analyses.

Results: Patients' age ranged from 34-95 (median 68) years, being more common >60 years. Median tumor size was 7.0 cm. Inner half MI was noted in 55%, LVI in 64%, adnexal involvement in 27.5% and lymph node (LN) metastasis in 27% of CSs. 40% of patients had stage I, 13% II, 30% III and 17% stage IV disease. Serous carcinoma was the predominant carcinomatous component (51%), whereas heterologous elements (64%), particularly rhabdomyoblastic differentiation (RMB)(71%) was the most common sarcomatous component. 36% & 66% of patients received adjuvant radiation or chemotherapy, respectively. Median disease free interval (DFI) and median overall survival(OS) were 11 and 16 months, respectively. Tumors ≥5cm, outer half MI, LVI, advanced stage and positive cytology were significantly associated with shorter DFI (P=0.039, P=0.001, P=0.015, P=0.001 and P=0.017, respectively) and worse 3-year OS(P=0.003, P=0.001, P=0.005, P=0.001 and P=0.028, respectively). Serous histology, and RMB had negative impact on 3-year OS(P=0.043 and P=0.046 respectively). In addition, sarcomatous histology upon recurrence and predominant sarcomatous component in primary tumor (≥50%) showed shorter DFI (P=0.009 and P=0.027, respectively). Cox regression analyses for DFI and 3-year OS are presented in Tables 1&2.

Table 1			
Variable		DFI HR (95% CI)	P value
Depth of MI	<50%≥50%	1 2.00 (1.01-4.01)	0.05
LN	NegativePositive	1 2.34 (1.11-4.95)	0.025
% Of sarcomatous component	<50%≥50%	1 2.45 (1.21-4.94)	0.012